Structure and function relationships of the carboxyl-tail of hClC-1, the voltage-gated skeletal muscle chloride channel

A thesis submitted to the University of South Australia
in fulfillment of the requirements for the degree

of

Masters of Applied Science (Biomedical Science)

By

Peony, Long-Yan FUNG

M.Phil., B.Sc. (Hons)

Sansom Institute
Division of Health Science
University of South Australia

2009

UNIVERSITY OF SOUTH AUSTRALIA
LIBRARY

TABLE OF CONTENTS

LIST OF FIGURES ..... **viii**

LIST OF TABLES ..... **xi**

LIST OF ABBREVIATIONS ..... **xii**

SUMMARY ..... **xiv**

DECLARATION ..... **xvi**

ACKNOWLEDGMENTS ..... **xvii**

CHAPTER ONE: LITERATURE REVIEW **1**

1.1 INTRODUCTION 1
1.2 ION CHANNELS 1
1.3 CHLORIDE CHANNELS: VOLTAGE-GATED CHLORIDE CHANNEL (CLC) 2
1.3.1 CLC family 2
1.3.2 The roles of CLC in human 4
1.4 STRUCTURAL PROPERTIES OF CLC 9
1.4.1 Investigation of CLC topology 9
1.4.2 Dimeric double-barreled structure 14
1.4.3 Pore-forming selectivity filter region 17
1.4.4 Gating 19
1.4.4.1 Protopore gate 21
1.4.4.2 Common gate 22
1.4.5 Proton coupled chloride transporter structure 24
1.5 CYTOPLASMIC C-TAIL OF MAMMALIAN CLC 24
1.5.1 Disease-causing mutations demonstrate the importance of the C-tail 25
1.5.2 CBS Domains 26
1.5.3 Crystal structure of CBS-containing protein 27
1.5.3.1 Crystal structure of bacterial inosine-5'-monophosphate dehydrogenase 28
1.5.3.2 Crystal structure of TM0935 from *Thermotoga maritime* 29
1.5.3.3 Crystal structure of the cytoplasmic C-tail of the ClC-0 31
1.5.4 Possible roles of CBS domains in various proteins 35
1.5.5 Proposed functional roles of the C-tail 35
1.5.5.1 Implications from the roles of CBS domain of other protein for the function of CLC family 35
1.5.5.1.1 CBS domains in CLC are not involved in oligomerisation 35

1.5.5.1.2 Cellular energy sensor 36
1.5.5.2 Interactions with regulatory proteins 37
1.5.5.3 Protein trafficking 37
1.5.5.4 Influence of the C-tail on functional properties of CLC 38
1.5.5.5 Mediating the common gate function 39
1.5.5.6 Conformational modification of CLC structure 39
1.5.6 Important sequence in the C-tail 40
1.6 PROJECT AIMS 42

CHAPTER TWO: GENERAL MATERIALS AND METHODS 47

2.1 INTRODUCTION 47
2.2 CHEMICALS AND WATER 47
2.3 CULTIVATION OF BACTERIA 47
2.3.1 Growth media 47
2.3.1.1 Luria-Bertani (LB) broth 48
2.3.1.2 LB agar 48
2.3.1 3 Ampicillin preparation 48
2.3.2 Bacterial strains 48
2.3.2.1 XL1-Blue *E.coli* strain 48
2.3.2.2 BL21(DE3) *E.coli* strain 49
2.4 INTRODUCTION OF PLASMID DNA INTO COMPETENT CELLS 49
2.4.1 Transformation of plasmid DNA to competent cells 50
2.5 EXTRACTION AND PURIFICATION OF DNA PLASMIDS 50
2.5.1 Alkaline lysis with SDS 51
2.5.2 QIAGEN® plasmid midi kit 52
2.5.3 QIAquick® gel extraction kit 53
2.6 DNA ANALYSIS 53
2.6.1 DNA agarose gel electrophoresis 53
2.6.1.1 DNA gel preparation 53
2.6.1.2 Gel casting and electrophoresis 54
2.6.1.3 DNA agarose gel staining and visualisation 54
2.6.2 Estimation of the molecular Size of DNA fragments 55
2.6.3 Determination of DNA concentration 55
2.7 DNA CLONING 55
2.7.1 Restriction enzyme digestion 55
2.7.2 DNA ligation 55
2.8 DNA SEQUENCING 56
2.8.1 DNA sequencing reactions 56
2.8.2 Purification of extension products 57

2.9 MUTANT DNA CONSTRUCTIONS....57
2.9.1 Primer synthesis and preparation....60
2.9.2 Site-directed mutagenesis....60
2.9.2.1 Primer design....60
2.9.2.2 Site-directed mutagenesis reaction mixture set up....60
2.9.2.3 Thermocycling conditions for site-directed mutagenesis....61
2.9.2.4 Digesting the amplified products by *Dpn* I restriction enzyme....61
2.10 PROTEIN CONCENTRATION DETERMINATION....62
2.10.1 Bicinchoninic acid (BCA) method....62
2.11 PROTEIN ANALYSIS....62
2.11.1 Polyacrylamide gel electrophoresis (PAGE)....62
2.11.2 Western blot....63
2.11.2.1 Target protein recognized by anti-C-tail antibody....63
2.11.3 Signal development of antibody recognized protein band on Western blot....64
2.11.3.1 Chromogenic detection....64
2.11.3.2 Enhanced chemiluminescence (ECL) detection....64
2.12 MAINTENANCE OF HUMAN EMBRYONIC KIDNEY (HEK) CELLS....64
2.12.1 General condition for cultivation of HEK cells....65
2.12.2 Revival of frozen HEK cells....65
2.12.3 Passaging the HEK cells....65
2.12.4 Freezing cells....66
2.12.5 Viable cell counts using trypan blue....66

CHAPTER THREE: ESTABLISHING A MAMMALIAN EXPRESSION SYSTEM FOR FUNCTIONAL COMPLEMENTATION EXPERIMENTS IN CLC-1....67

3.1 INTRODUCTION....67
3.2 EXPERIMENTAL PROCEDURES....69
3.2.1 Modification of the multi-cloning site of the pMIG....69
3.2.2 Introduction of a *Bam*HI site at the N-terminus of the $C_{721-988}$ peptides in pTLN....70
3.2.3 *Bam*HI restriction enzyme digestion....70
3.2.4 Cloning of the $C_{721-988}$ peptide into BEpMIG....71
3.2.5 Co-transfection of N_{1-720} and $C_{721-988}$ constructs in HEK cells....72
3.2.6 Electrophysiological study....74
3.2.6.1 Patch-clamping....74
3.2.6.2 Voltage steps protocols....74
3.2.6.3 Data analysis....77
3.3 RESULTS....80
3.3.1 Electrophysiological measurements on positive and negative controls....80

3.4 DISCUSSION 85
3.4.1 Establishing a mammalian expression system for split ClC-1 channel experiments 85

CHAPTER FOUR: IMPAIRED CHLORIDE CHANNEL FUNCTION, ASSOCIATED WITH MYOTONIA, RESTORED BY CO-EXPRESSION OF THE $C_{721-988}$ FRAGMENT WITH DISEASE-CAUSING NONSENSE MUTANTS OF HUMAN CLC-1 IN MAMMALIAN CELLS 88

4.1 INTRODUCTION 88
4.2 EXPERIMENTAL PROCEDURES 90
4.2.1 Construction of DNAs mimicking naturally-occurring C-terminal truncated mutants 90
4.2.1.1 Primers designed for mutant construction 90
4.2.1.2 Molecular method for construction of mutants 91
4.2.1.3 Cloning of mutants into the pCIneo 91
4.2.2 Co-transfection of with C-terminal truncated mutants with the $C_{721-988}$ construct 93
4.2.3 Electrophysiology 93
4.3 RESULTS 93
4.3.1. Electrophysiological study of C-terminal truncated mutants 93
4.3.2. Electrophysiological study of co-transfection of C-terminal truncated mutants with $C_{721-988}$ 95
4.4 DISCUSSION 100
4.4.1 Electrophysiological studies of nonsense mutants 100
4.4.2 Functional restoration of nonsense mutants by co-expressing with $C_{721-988}$ 102
4.4.3 Therapeutic potential 103

CHAPTER FIVE: ATTEMPTED FUNCTIONAL RESTORATION OF A C-TERMINAL TRUNCATED MUTANT BY SUPPLEMENTATION WITH SHORT C-TAIL FRAGMENTS 105

5.1 INTRODUCTION 105
5.2 EXPERIMENTAL PROCEDURES 107
5.2.1 Introduction of a *Bam*HI site at the N-terminus of the C-terminal peptides in pTLN 107
5.2.2 *Bam*HI restriction enzyme digestion 108
5.2.3 Cloning of C-terminal peptides into BEpMIG 108
5.2.4 DNA transfection in HEK cells 109
5.2.5 Detection of protein expression level of $C_{721-988}$ and $C_{863-988}$ by Western blotting 109

5.3 RESULTS 110
5.3.1 Electrophysiological measurements of N_{1-720} co-expressed separately with each of the C-terminal peptide constructs 110
5.3.2 Protein expression of the C-terminal peptides ($C_{721-988}$ and $C_{863-988}$) in HEK cells 112
5.4 DISCUSSION 113
5.4.1 Attempted functional supplementation of N_{1-720} with short C-terminal peptides 113

CHAPTER SIX: CHARACTERIZATION OF THREE NOVEL MYOTONIA-ASSOCIATED MISSENSE MUTATIONS IN THE C-TAIL REGION OF HUMAN CLC-1 VIA HETEROLOGOUS EXPRESSION 115

6.1 INTRODUCTION 115
6.2 EXPERIMENTAL PROCEDURES 117
6.2.1 Create missense mutations on human ClC-1 117
6.2.2 Cloning of C-tail missense mutants into the pCIneo 118
6.2.3 Transfection of C-tail missense mutants' DNA in HEK cells 118
6.2.4 Electrophysiology 119
6.3 RESULTS 119
6.3.1. Electrophysiological studies of missense mutants 119
6.4 DISCUSSION 125

CHAPTER SEVEN: PROTEIN EXPRESSION OF CARBOXYL-TAIL FRAGMENTS 127

7.1 INTRODUCTION 127
7.2 EXPERIMENTAL PROCEDURES 130
7.2.1 Construction of $C_{575-988}$/BEpMIG for electrophysiological studies 130
7.2.1.1 Construction of $C_{575-988}$ in BEpMIG 130
7.2.1.2 Mutant constructs transfected to HEK cells for electrophysiological studies 130
7.2.2 Construction of C-tail fragments for protein expression 130
7.2.2.1 Primers design for construction of C-tail fragments 131
7.2.2.2 PCR conditions for construction of C-tail fragments 132
7.2.2.3 Cloning of C-tail fragments into the protein expression vector 132
7.2.2.4 Verification of the resultant DNA with insert and correct DNA sequence. 133
7.2.3 Protein expression 133
7.2.3.1 Procedure for protein expression 133
7.2.3.2 Detection of target protein expression using 1 ml cell culture 134
7.2.4 Protein extraction 134

7.2.4.1 Extraction of protein from IPTG- induced cell pellets using the Native method for Thx-$C_{721-988}$ and Thx-$C_{575-988}$ protein....134
7.2.4.2 Extraction of protein from IPTG- induced cell pellets using the denaturing method for Thx-$C_{575-988}$ protein....135
7.2.5 Protein purification of Thx-$C_{721-988}$....135
7.2.6 Cleavage of Thx-tag from purified Thx-$C_{721-988}$ protein by proteases....135
7.2.7 Separation of Thx-tag and protease from $C_{721-988}$ fragment by Ni-NTA chromatography....136
7.2.8 Molecular weight determination of purified Thx-$C_{721-988}$ and $C_{721-988}$ using mass spectrometry....136
7.3 RESULTS....137
7.3.1 Electrophysiology recording of $C_{575-988}$ plus N_{1-720} co-transfected HEK cells .137
7.3.2 Construction of $C_{575-988}$ and $C_{721-988}$ cDNA for cloning into Thx/pET32a 138
7.3.3 Insert clones were verified by DNA sequencing....139
7.3.4 Detection of protein expression....139
7.3.4.1 Thx-$C_{721-988}$/pET32a expression....139
7.3.4.2 Thx-$C_{575-988}$/pET32a expression....140
7.3.5 Protein purification of $C_{721-988}$ peptide....142
7.3.6. Molecular weight determination of Thx-$C_{721-988}$....143
7.3.7 Purification of His-3C digested Thx-$C_{721-988}$ protein....143
7.3.8. Molecular weight determination of purified $C_{721-988}$....145
7.4 DISCUSSION....146
7.4.1 Protein expression....146
7.4.2 C-tail region selected for protein expression....147

CHAPTER EIGHT: GENERAL DISCUSSION AND FURTHER DIRECTIONS...150

8.1 GENERAL DISCUSSION....150
8.1.1 Split hClC-1 expression in HEK cells....150
8.1.2 Functional reconstitution of naturally-occurring nonsense mutants using supplement of C-tail peptide....151
8.1.3 Attempted functional restoration of C-tail truncated mutant by supplementation with short C-tail fragment....152
8.1.4 Characterization of three novel myotonia-associated missense mutations in the C-tail region of human ClC-1 via heterologous expression....153
8.1.5 Protein expression of C-tail peptide....154
8.2 FURTHER DIRECTIONS....156
8.2.1 Using animal model to strengthen the functional restoration hypothesis....156
8.2.2 Using fluorescence resonance energy transfer and site-directed mutagenesis to test for the CBS2 interaction hypothesis....157

8.2.3 Using peptide melting point analysis to determine the protein stability.....158
8.2.4 Allosteric effect on C-tail structure by nucleotides 159
8.2.5 Scale up the protein expression and purification steps for further investigation of the structure of C-tails 160

BIBLIOGRAPHY 161

APPENDIX A: Multiple sequence alignment of CLC 182

APPENDIX B: List of Suppliers, Distributors and Manufacturers.....189

APPENDIX C: Sequencing results of the recombinant DNAs in BEpMIG.....192

APPENDIX D: Methodology of constructing shortened $C_{863\text{-}888}$ peptide in pTLN 194

APPENDIX E: Sequencing results of missense mutants of hClC-1 197

APPENDIX F: Sequencing results of the C-tail cDNAs in Thx/pET32a.....200

APPENDIX G: Publications 201

LIST OF FIGURES

Figure 1.1 The percentage of sequence identity among mammalian CLC and ClC-0 3
Figure 1.2 Topological model of CLC finalized by Schmidt-Rose and Jentsch, 1997b (A) and Fahlke and colleagues, 1997 (B) 11
Figure 1.3 Topology model derived from bacterial CLC X-ray structure and the hydropathy and biochemical analysis of eukaryotic CLC 12
Figure 1.4 An interpreted model of ClC-0 single-channel trace after Hanke and Miller (1983) 15
Figure 1.5 Structure of the bacterial CLC viewed from the top of the extracellular side ... 16
Figure 1.6 The α-helical 3D structure of a monomer of bacterial CLC 17
Figure 1.7 Magnified region of the selectivity filter in closed (A) and open state (B) 19
Figure 1.8 Single current trace of hClC-1 elicited by whole-cell patch clamping 21
Figure 1.9 Localisation of nonsense and C-tail missense mutations 26
Figure 1.10 The topology of the cystathionine β-synthase (CBS) domains 27
Figure 1.11 Ribbon diagram of the IMPDH tetramer 29
Figure 1.12 Ribbon diagram of the TM0935 dimer 30
Figure 1.13 Sequence alignment of the C-tail domains of *T. marmorata* ClC-0 (TmClC-0) and human ClC-1 (hClC-1) 33
Figure 1.14 Ribbon diagram of the monomeric structure of the C-tail of ClC-0 34
Figure 1.15 Cartoon picture of the previously-defined 26 amino acid peptide 44

Figure 2.1 Overview of the site-directed mutagenesis method 59

Figure 3.1 Plasmid map of BEpMIG 70
Figure 3.2 Schematic diagrams of the cloning steps of $C_{721\text{-}988}$ fragment into BEpMIG vector 72
Figure 3.3 Voltage steps of activation protocol 76
Figure 3.4 Voltage steps of tail-1 protocol 76
Figure 3.5 Voltage steps of tail-2 Protocol 77
Figure 3.6 Example of current traces from hClC-1 in response to the tail-1 protocol 78
Figure 3.7 Example of current traces of hClC-1 response to the tail-2 protocol 78
Figure 3.8 Current traces measured from "no DNA" transfected HEK cell (A), BEpMIG transfected HEK cell (B), $N_{1\text{-}720}$/pCIneo+BEpMIG transfected HEK cell (C) and $C_{721\text{-}988}$/BEpMIG transfected HEK cell 80
Figure 3.9 Current traces in a whole cell patch of full-length hClC-1/pCIneo (A) and $N_{1\text{-}720}$/pCIneo + $C_{721\text{-}988}$/BEpMIG (B) co-transfected HEK cell evoked by the activation

protocol....81
Figure 3.10 Overall apparent open probability (P_o^o) of full-length WT hClC-1 and split channel construct (N_{1-720} + $C_{721-988}$)....82
Figure 3.11 Apparent open probability for common gate (P_o^c) of full-length WT hClC-1 and split channel construct (N_{1-720} + $C_{721-988}$)....83
Figure 3.12 Apparent open probability for the protopore gate (P_o^p) of full-length WT hClC-1 and split channel construct N_{1-720} + $C_{721-988}$....84

Figure 4.1 Schematic diagrams showing steps involved in sub-cloning the mutant constructs from pGEM-4Z into pCIneo vector....92
Figure 4.2 The current traces of the N_{1-716}, N_{1-806} and no DNA transfected HEK cells in response to the standard activation protocol....94
Figure 4.3 The current traces of the N_{1-871} construct and WT split channel N_{1-720} + $C_{721-988}$ co-transfected HEK cells in response to the standard activation protocol....95
Figure 4.4 Overall apparent open probability (P_o^o) of split and C-termnal truncated channels....96
Figure 4.5 Apparent open probability for common gate (P_o^c) of split and C-terminal truncated channels....97
Figure 4.6 Apparent open probability for protopore gate (P_o^p) of split and C-terminal truncated channels....98

Figure 5.1 Cartoon picture of the 26 amino acid peptide and the five proposed shorter peptides....106
Figure 5.2 Current traces of N_{1-720} co-transfected with the short peptides in HEK cells in response to the activation protocol....111
Figure 5.3 Western blot of $C_{721-988}$ and $C_{863-988}$ expressed protein in HEK cells....112

Figure 6.1 Approximate locations of the thirteen novel mutations on C-tail of human ClC-1....116
Figure 6.2 Current traces of WT hClC-1 and C-tail missense mutants....120
Figure 6.3 Overall apparent open probability for channel (P_o^o) of WT hClC-1 and C-tail missense mutants....121
Figure 6.4 Apparent open probability for common gate (P_o^c) of split and C-tail truncated channels....122
Figure 6.5 Apparent open probability for protopore gate (P_o^p) of WT hClC-1 and C-tail missense mutants....123

Figure 7.1 Current traces of normal appearance in a whole cell patch from a N_{1-720}/pCIneo + $C_{575-988}$/BEpMIG (A) and hClC-1/pCIneo(B) co-transfected HEK cell evoked by the standard activation protocol 137
Figure 7.2 $C_{575-988}$ cDNA (A) and $C_{721-988}$ cDNA (B) visualized by ethidium bromide staining on a 1.0% TAE agarose gel 139
Figure 7.3 SDS-PAGE analysis of Thx-$C_{721-988}$/pET32a protein expression 140
Figure 7.4 Western Blots result of Thx-$C_{721-988}$/pET32a expressed protein 140
Figure 7.5 SDS-PAGE (A) and Western blot (B) analysis of Thx-$C_{575-988}$/pET32a expressed protein 141
Figure 7.6 SDS-PAGE analysis of the solubility of Thx-$C_{575-988}$/pET32a expressed protein 141
Figure 7.7 Thx-$C_{721-988}$ protein was partially purified by adding a 150 mM imidazole washing step and the samples were analysed by SDS-PAGE 142
Figure 7.8 Mass spectrum of Thx-$C_{721-988}$ 143
Figure 7.9 SDS-PAGE analysis of Thx-$C_{721-988}$ proteins digested by His-3C 144
Figure 7.10 SDS-PAGE analysis of $C_{721-988}$ purification by Ni-NTA 144
Figure 7.11 Mass spectrum of $C_{721-988}$ 145

LIST OF TABLES

Table 3.1 List of DNAs used in six sets of DNA transfection reactions 73
Table 3.2 Summary of the Boltzmann parameters of overall, common and protopore gating of full-length WT hClC-1 and split channel construct ($N_{1\text{-}720}$ + $C_{721\text{-}988}$) 84

Table 4.1 Primer sequences for constructing naturally-occurring C-terminal truncated mutants 90
Table 4.2 List of DNAs used in six sets of DNA co-transfection experiments.....93
Table 4.3 Summary of the Boltzmann parameters of overall (A), common (B) and protopore (C) gating for the split and C-terminal truncated channels 99

Table 5.1 Primers for appending *Bam*HI sites onto the C-terminal peptide constructs inserted in pTLN vectors.....108

Table 6.1 Primer sequences for constructing thirteen missense mutants of hClC-1 117
Table 6.2 Summary of the Boltzmann parameters of overall (A), common (B) and protopore (C) gating for the WT hClC-1 and C-tail missense mutants 124

Table 7.1 Primers for construction of C-tail fragments 131
Table 7.2 Primer sequences of pET32a_fw, pET32a_rv and T7 pro_fw.....133

LIST OF ABBREVIATIONS

3'	3 prime
3C	PreScission
5'	5 prime
A	ampere(s)
Å	angstrom(s)
AdoMet	S-adenosyl-l-methionine
Approx.(~)	approximately
ADP	adenosine diphosphate
AMP	adenosine monophosphate
ATP	adenosine 5'-triphosphate
bp	base pair
BCA	bicinchoninic acid
BSA	bovine serum albumin
C-	carboxyl
°C	Celsius degrees
CBS	cystathionine beta-synthase
CBS1	cystathionine beta-synthase domain 1
CBS2	cystathionine beta-synthase domain 2
CD	circular dichroism
cDNA	complementary DNA
CFTR	cystic fibrosis transmembrane conductance regulator
CHO_K1	Chinese hamster ovary cells
CLC	voltage-gated chloride channel (for general idea of all of them)
CLCN1	ClC-1 chloride channel gene
ClC-	members of chloride channel usually with symbol or number to classify after hyphen
Co-CMA	cobalt-carboxylmethylaspartate
Cs	caesium
DAB	3,3'diaminobenzidine tetrahydrochloride
dATP	2'-deoxyadenine 5'-triphosphate
dCTP	2'-deoxycytosine 5'-triphosphate
dGTP	2'-deoxyguanine 5'-triphosphate
dITP	2'-deoxyinosine 5'-triphosphate
D-MEM	Dulbecco's modified eagle medium
D-MEM+	D-MEM supplemented with 0.1 mM non-essential amino acids, 4 mM L-glutamine, 10% (v/v) FBS
DMSO	dimethyl sulfoxide
DNA	deoxyribonucleic acid
DNase	deoxyribonuclease
dNTP	deoxynucleotide triphosphates
dsDNA	double-stranded DNA
DTT	dithiothreitol
dTTP	2'-deoxythymine 5'-triphosphate
dUTP	2'-deoxyuridine 5'-triphosphate
ECL	enhanced chemiluminescence
EGFP	enhanced green fluorescent protein

EtBr	ethidium bromide
FBS	fetal bovine serum
FCS	fetal calf serum
fs	frame shift
FRET	fluorescence resonance energy transfer
FUSA	SouthPath & Flinders Sequencing Facility
G	guanine
GABA	gamma-aminobutyric acid
GC	guanine-Cytosine
GFP	green fluorescent protein
GST	glutathione S-transferase
hClC-1	human ClC-1
HEK	human embryonic kidney
His	histidine
hsp	heat shock protein
IgG	immunoglobin G
IMAC	immobilized metal affinity chromatography
IMP	inosine monophosphate
IRES	internal ribosome entry site
IMPDH	inosine monophosphate dehydrogenase
IMVS	Institute of Medical and Veterinary Science
kb	kilobase
kDa	kilodalton
kHz	kilohertz
LB	Luria-Bertani
mant	*N*-methylanthraniloyl
mRNA	messenger RNA
MQ	milli-Q
Mw	molecular weight
MWCO	molecular weight cut off
MΩ	megaohms
N-	amino
Ni-NTA	nickel-nitrilotriacetic acid
PAGE	polyacrylamide gel electrophoresis
PBS	phosphate buffered saline
PBS-T	phosphate buffered saline with 0.05% (v/v) Tween-20
PCR	Polymerase chain reaction
PMSF	phenylmethylsulfonylfuoride
P_o	open probability
ppb	part per billion
pS	pico(10^{-9}) Siemens
psi	pound per square inch
rpm	revolution per min
Tween-20	polyoxyethelene sorbitan monolaurate
UV	ultraviolet
V	voltage
$V_{½}$	half maximum voltage
v/v	volume by volume
w/v	weight by volume
x g	gravity (9.8 m/s^2)

SUMMARY

Members of the mammalian voltage gated chloride channel (CLC) family have a particularly long cytoplasmic carboxyl-tail (C-tail) when compared with the prokaryotic CLCs. Two cystathionine β-synthase (CBS) motifs occur in the C-tail sequence. The X-ray structure of prokaryotic CLCs revealed that the double-barreled channel structure is formed by a subunit dimer of N-terminal membrane-resident regions. Truncation experiments performed on eukaryotic CLCs have shown, however, that channel dimers formed by subunits with only half of the C-tail region remaining are unable to conduct chloride current. Hence, the C-tail region is essential for normal channel function. Interestingly, the function of truncated channels can be restored by supplementation with the complementary missing fragment and by even shorter (sub-complementary) fragments with amino acids deleted at either, or both, termini. The shortest C-tail fragment so far known to be able to restore function to the mid-C-tail-truncated (at Ser 720) human skeletal muscle chloride channel, hClC-1, is Leu 863 to Arg 888, which has been identified in our laboratory recently.

In order to continue split channel experiments, without the *Xenopus* oocyte system, I established a mammalian split channel expression system with cultured human embryonic kidney (HEK) cells in the present work. Using the previously well-characterised split channel model of ClC-1, Met 1 to Ser 720 co-expressed with Gly 721 to Leu 988, I have demonstrated the success of the mammalian expression system. Unexpectedly, however, the shortened peptides, Leu 863 to Leu 988 and Leu 863 to Arg 888, were unable to rescue function as they did in the *Xenopus* oocyte co-expression system. This might suggest that there are intrinsic differences between the *Xenopus* oocyte and mammalian expression

system. Mammalian expression was, nevertheless, able to be used successfully to show that the Gly 721 to Leu 988 tail restored function to certain naturally-occurring nonsense mutations, Glu 717 Stop and Gln 807 Stop. Since CLC channels have the unique feature of being able to function as a split channel, gene delivery of the sequence of Gly 721 to Leu 988 (or even shorter sequences) might have potential for the treatment of myotonia congenita patients, particularly with the recessive phenotype, in the future.

In additional experiments, I have characterized three novel missense myotonia mutations, Arg 691 Ser, Glu 724 Ala and Val 851 Met, located in the C-tail region, by recording chloride currents from embryonic kidney cells transiently expressing mutant channels. The mutation at Val 851 is in a highly conserved residue among CLC family members and exhibited a shift of activation curve at a positive values which is common functional consequence of myotonia mutation. Arginine 691 and Glu 724 are not conserved residues and those mutants show similar characteristic to each other but not to Val 851 Met. In both, overall gating and common gate open probability are shifted to the left indicating that the common gate is more likely to be open at the resting potential. This is the opposite to what I would have expected for myotonia-inducing mutants.

In order to further study the C-tail structure, the bacterial expression system was used for protein production of the C-terminal fragments, Pro 575 to Leu 988 and Gly 721 to Leu 988. The former peptide contained the whole C-tail sequence and the latter contained about half of the C-tail sequence including CBS2. Both of the fragments were successfully expressed at high levels, however, the Pro 575 to Leu 988 peptide was mostly insoluble. The highly soluble Gly 721 to Leu 988 peptide was initially purified using two steps of metal-chelating chromatography and has been successfully purified Gly 721 to Leu 988 to homogeneity.

DECLARATION

I declare that this thesis does not incorporate without acknowledgment any material previously submitted for a degree or diploma in any university; and that to the best of my knowledge it does not contain any materials previously published or written by another person except where due reference is made in the text. I consent to this thesis being made available for photocopying and loan, once accepted for the award of the degree of ~~doctor of~~ MASTERS ~~Philosophy.~~



Peony LY FUNG
2009

ACKNOWLEDGMENTS

I am grateful to the following people. Without them, I would not have been able to finish my research degree and have a wonderful time in Australia.

My principal supervisor Professor Allan Bretag - for accepting me as his student, his brilliant ideas on chloride channel research, invaluable guidance, support and encouragement throughout my studies. Also I would like to express my gratitude to my co-supervisor Associate Professor Bernard Hughes for his enormous help with respect to my thesis writing, support and encouragement.

During the course of my studies, I have learnt a lot of valuable techniques. I am grateful to Dr. Grigori Rychkov and Associate Professor Michael Roberts for their knowledge, assistance, discussion and provision of the equipment to learn and do patch-clamping for my project. Also I would like to thank Dr. Christopher Bagley for his ideas, discussion and for enabling me to perform mass spectrometry analysis on my protein.

Also, there are important people I have met in the School who contributed their valuable time and thinking towards my studies and my living in Australia. "Thanks" may not be an adequate word to show my appreciations to them. I would like to especially thank Andrew Beck for his enormous help, assistance, support and encouragement in all dimensions during my years in Australia. Also, I would like to express my deep gratitude to my fellow research colleague, Jennie Cederholm, without her presence, company and sharing of my joy and sorrow, it would have been really hard for me to survive until now. Thanks also to Dr. Weiping Wu for her help and her warm family welcome in my first year in Adelaide, Dr.

Paul Bartley for his assistance and suggestions during my studies, Dr. Cobus Gerber and Graham Bull for their help and assistance that enabled me to finish my fluorescence experiments, Dr. Tom Litjens for his support, encouragement and suggestions, Frank Madaras for his ideas, comments and suggestion on my protein work and Linlin Ma for her cheerful chat.

Last but not least, I would like to thank my parents, my sister and her family, the supervisor of my previous research degree and his family for their support and encouragement during my studies in Australia.

CHAPTER ONE: LITERATURE REVIEW

1.1 INTRODUCTION

The main theme of my study is the structure and function of the carboxyl-tail (C- tail) of voltage-gated chloride ion channels (CLC channels). This literature review will, therefore, focus on members of this CLC family of proteins. A brief introduction to ion channels will be covered in Section 1.2. Members of the CLC family will be mentioned in Section 1.3. Structural properties of CLC will be described in Section 1.4 followed by a description of the research done on the C-tail of CLC which will be reviewed in Section 1.5. The last Section 1.6 is the project aims.

1.2 ION CHANNELS

Cells in the human body are bounded by a selectively permeable membrane. Membrane permeability properties ensure proper exchange processes for essential molecules inside and outside of the cells to maintain the normal cells' fluid and metabolite balance. Cellular membranes are largely composed of a phospholipid bilayer that is impermeable to most water-soluble molecules, ions and water. Thus, selective membrane transport proteins are necessary for mediating the passage of molecules. There are three major classes of transport proteins. They are ion channel proteins, transporters and ATP-powered pumps.

Ion channels provide a controllable communication link between the extracellular and intracellular sides of the membrane. There are two basic states in ion channels, open or closed. The control of the transitions between the states is called gating. In most living cells the cell interior is negatively charged with respect to the extracellular medium. Once the channels open, they allow facilitated diffusion of ions at a high rate of 10^7-10^8 ions/s

down their concentration or electrochemical gradient. Failure of ion channels can lead to a variety of human diseases (Hubner & Jentsch 2002; Kass 2005).

1.3 CHLORIDE CHANNELS: VOLTAGE-GATED CHLORIDE CHANNEL (CLC)

There is a wide variety of chloride channels located on the membrane surface of cells and organelles. There are three well-established types which are the CLC, the cystic fibrosis transmembrane conductance regulator (CFTR) and the glycine and the GABA receptors (Farrant & Cull-Candy 1993). More recently, a few new members have been described such as the volume-sensitive Cl^- channels (Nilius *et al.* 1996) and Ca^{2+}-activated Cl^- channels (Gandhi *et al.* 1998). They all contribute to different physiological functions and their opening mechanisms are triggered by different means such as by changing the membrane potential, binding of signaling molecules or stretching of the membrane. Mutations in their genes are associated with human diseases thus highlighting their importance. In this chapter, most of the information will focus on CLC including the members that have been recently classified as proton-coupled chloride transporters (Accardi & Miller 2004; Picollo & Pusch 2005; Scheel *et al.* 2005).

1.3.1 CLC family

Since the first CLC gene was cloned from the *Torpedo* fish electric organ (Jentsch, Steinmeyer & Schwarz 1990), nine mammalian members have been identified through homology cloning. The *Torpedo* chloride channel (ClC-0) was named as the initial member of this family of voltage-gated chloride channels. The nine mammalian chloride channels were numbered from 1 to 7 (ClC-1 to ClC-7) and in addition there are two highly conserved isoforms, with 90% sequence similarity named Ka and Kb in human (K1 and K2 in rat). The percentage of sequence homology of each of the mammalian CLC compared to ClC-0 and among the mammalian CLC is shown in Figure 1.1.

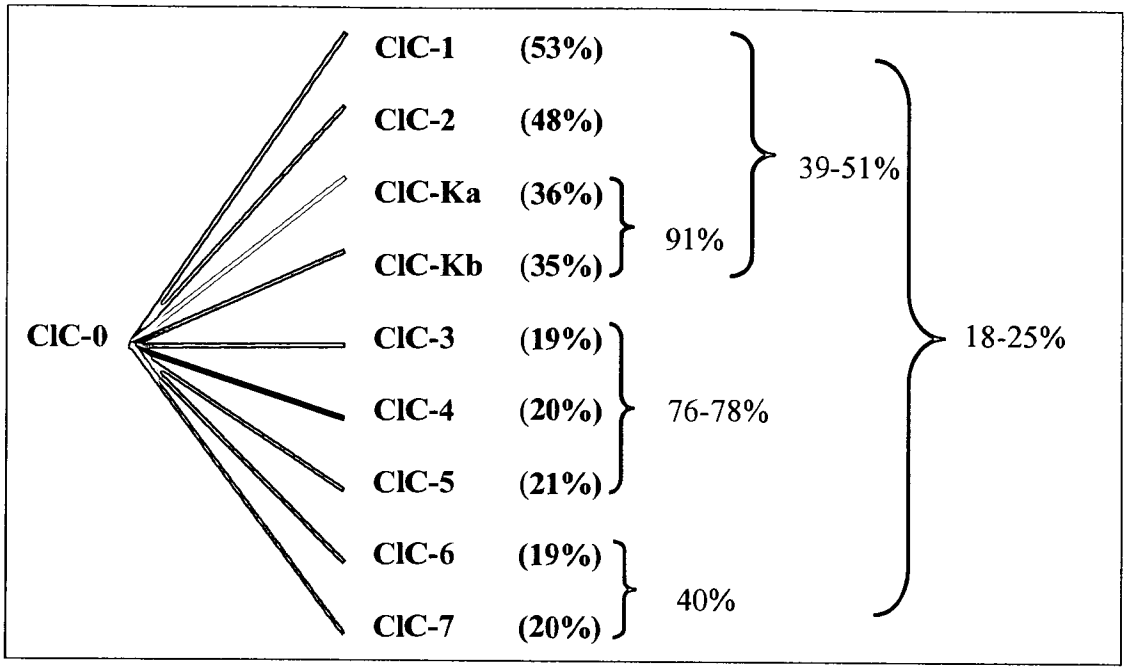

Figure 1.1 The percentage of sequence identity among mammalian CLC and ClC-0

The percentage of sequence identity of mammalian CLC to ClC-0 is indicated in the bracket on the right hand side of each ClC. The percentage of sequence identity among the mammalian ClC-1, -2, -Ka and -Kb is 39-51%; -Ka and -Kb is 91%; ClC-3, -4 and -5 is 76-78%; and ClC-6 and -7 is 40%. Overall sequence identity among all the mammalian CLC listed on the Table is about 18 to 25%.

The sequence homology of the mammalian CLC protein has been used for classifying the channels into three groups. Group I contained ClC-1, -2, -Ka and -Kb; group II contained ClC-3 to -5 and group III contained ClC-6 and -7. Recently, scientists have preferred to classify them by expression location, in plasma membrane (ClC-1, -2 and -K) or in intracellular membranes (ClC-3 to -7). This classification is not only by their expression location, but also by their Cl^- transporting characteristics. ClC-1, -2 and -K are absolutely Cl^- channels (Scheel *et al.* 2005) but ClC-4 and ClC-5 have been identified as proton-coupled chloride transporters (Picollo & Pusch 2005; Scheel *et al.* 2005). Despite there being no empirical evidence to say that all the intracellular membrane expressed CLC are transporters, the conserved glutamate residue (E203 at EcClC, Appendix A) for the

proton transporting pathway (Accardi *et al.* 2005) is found in all the intracellular membrane-expressed CLC which implies that they are more likely to be working as transporters rather than channels. As well as the big family of CLC found in mammalian tissue, this channel family view is being extended to almost all eukaryotic and prokaryotic species, including bacteria (Maduke, Pheasant & Miller 1999; Purdy & Wiener 2000; Iyer *et al.* 2002), yeast (Greene *et al.* 1993; Schwappach *et al.* 1998), *Caenorhabditis elegans* (Schriever *et al.* 1999), *Drosophila melanogaster* (Flores *et al.* 2006) and plants (Hechenberger *et al.* 1996; Lurin *et al.* 1996; Nakamura *et al.* 2006). Study of the homologous CLC of other species can also give insight into the structure and function of mammalian CLC.

1.3.2 The roles of CLC in human

ClC-1 is predominantly expressed in skeletal muscle (Steinmeyer, Ortland & Jentsch 1991). In skeletal muscle, Cl^- ions are responsible for about 70-80% of resting membrane conductance (Bretag 1987). This conductance is essential for membrane-potential stability. Chloride channel function can be disrupted by more than 80 mutations (Colding-Jørgensen 2005) occurring in its gene, *CLCN1*, in turn, causing muscle disease called myotonia congenita. It is a hereditary muscle disorder characterised by muscle stiffness after voluntary contraction due to an electrical instability of the muscle membrane itself, leading to series of repetitive action potentials following a single stimulus. Owing to the malfunction of ClC-1, muscle is not able to produce enough stabilizing conductance to repolarise fully after an action potential. This will give sodium channels enough time to recover from inactivation and lead to a train of action potentials after a single stimulus. This is the cause of myotonic runs that occur in the myotonia patient. There are two forms of non-dystrophic myotonia. Autosomal dominant myotonia (Thomsen's disease) reported by a Danish physician Thomsen in 1876 and autosomal recessive myotonia (Becker's

disease) found by Becker in 1971. In dominant myotonia congenita, mutations generally only occur in one allele, and symptoms are similar to the recessive ones but more benign (Koch *et al.* 1992). There is no single representative mutation causing myotonia. Mutations that cause malfunction can be found throughout the gene. The electrophysiological characteristics of ClC-1 have been studied by expression in heterologous systems such as *Xenopus* oocytes, mammalian cells and insect cells. Inwardly rectifying currents induced at positive voltages are nearly linear in the physiological voltage range. Currents are activated by depolarisation, have $Cl^- > I^-$ ion selectivity and are sensitive to extra- and intracellular pH (Fahlke *et al.* 1996; Rychkov *et al.* 1996; Rychkov *et al.* 1997). Two gating mechanisms (fast and common) and channel open probability are affected by voltage (Accardi & Pusch 2000) , Cl^- and pH (Rychkov *et al.* 1996). Low single-channel conductance (1 pS) has been revealed from ClC-1 expressed in HEK293 cells by noise analysis (Pusch, Steinmeyer & Jentsch 1994).

ClC-2 is broadly expressed in many tissues such as the brain, intestine, kidney, stomach, salivary glands and heart tissue (Thiemann *et al.* 1992; Duan *et al.* 2000; Jentsch *et al.* 2002). The channels are activated by non-physiologically strong hyperpolarisation, extracellular hypotonicity (Grunder *et al.* 1992), acidic extracellular pH (Jordt & Jentsch 1997) and intracellular chloride (Jordt & Jentsch 1997; Ramjeesingh *et al.* 2006). ClC-2 channels show an inwardly rectifying current, have low conductance ~2.8 pS (Weinreich & Jentsch 2001; Ramjeesingh *et al.* 2006) and an ion selectivity $Cl^- > I^-$ (Furukawa *et al.* 1998; Schwiebert *et al.* 1998). The channels have diverse roles from transepithelial fluid transport, cell volume regulation to neuronal chloride homeostasis regulation. Extensive site-directed mutagenesis studies identified an N-terminal stretch (L21-R38) in ClC-2 which is essential for activation by cell swelling and voltage changing. This domain is position independent, as it can be transplanted to the C-terminus without loss of function

(Grunder *et al.* 1992). Studies with the ClC-2 knock out mouse revealed testicular and retinal degeneration, that were attributed to the defects in transepithelial transport across Sertoli cells and the retinal pigmented epithelium (Bosl *et al.* 2001). Mutations occurring in ClC-2 have been suggested to be involved in human epilepsy (Haug *et al.* 2003). Actin cytoskeleton (Ahmed *et al.* 2000), phosphatase-1(Furukawa *et al.* 2002), retrograde motor dynein (Dhani *et al.* 2003), Nedd4-2 (Palmada *et al.* 2004) and heat shock proteins, hsp70 and hsp90 (Hinzpeter *et al.* 2006), have been found to interact with ClC-2 for functional regulation.

Two highly homologous channels, ClC-Ka and ClC-Kb in humans, are predominantly expressed in the kidney and the inner ear (Uchida *et al.* 1993; Kieferle *et al.* 1994; Estévez *et al.* 2001). Their proper function requires them to associate with a β-subunit called barttin for their transport to the plasma membrane (Estévez *et al.* 2001; Waldegger *et al.* 2002; Scholl *et al.* 2006) and modulation of the permeation and gating process (Scholl *et al.* 2006). Recently, ClC-K1 has been found to have partial function without co-expression with barttin but needs to associate with barttin to achieve full function (Scholl *et al.* 2006). Upon co-expression of ClC-Ka or ClC-Kb with barttin, Cl^- currents that are dependent on voltage and extracellular pH can be elicited (Estévez *et al.* 2001). Mutations in the gene of ClC-Kb causes Bartter's syndrome, a disease associated with severe renal salt loss (Simon *et al.* 1997). Knock out ClC-K1 mice (corresponding to ClC-Ka in humans) leads to renal water loss (Matsumura *et al.* 1999). Absence of barttin leads to deafness and renal salt loss (Birkenhager *et al.* 2001). Barttin carries a PY motif (Estévez *et al.* 2001). Nedd4-2 interacts with barttin through the PY motif and down-regulates the ClC-Ka/barttin function (Embark *et al.* 2004).

ClC-3 is expressed mainly on synaptic vesicles and endosomes (Stobrawa *et al.* 2001; Li,

X *et al.* 2002). The knock out ClC-3 mouse model leads to blindness (Stobrawa *et al.* 2001) and a severe neurodegeneration (Stobrawa *et al.* 2001; Dickerson *et al.* 2002; Yoshikawa *et al.* 2002). ClC-3, ClC-4 and ClC-5 are extremely outwardly rectifying channels with no obvious Cl^--dependent gating relaxations in the time range of ≥5 ms (Steinmeyer *et al.* 1995; Friedrich, Breiderhoff & Jentsch 1999; Li, X *et al.* 2000; Vanoye & George 2002). Outwardly rectifying ClC-3 was inhibited by phorbol ester, an activator of protein kinase C (Kawasaki *et al.* 1994). Also, this channel has been suggested as being a protein responsible for native volume sensitive outwardly rectifying anion channels (Duan *et al.* 1997). Results to the contrary have also been reported (Stobrawa *et al.* 2001; Arreola *et al.* 2002; Yamamoto-Mizuma *et al.* 2004).

ClC-4 and -5 have recently been identified as proton-coupled chloride transporters (Picollo & Pusch 2005; Scheel *et al.* 2005). ClC-4 is strongly expressed in liver and brain, but also in heart, muscle, kidney and spleen (Jentsch *et al.* 1995). Human ClC-4 expressed in mammalian cells shows a small conductance around 2-3 pS, and is a strongly outward-rectifying Cl^- channel. The channel only activates at depolarising potentials. Channel open probability is reduced by acidic external pH and displays $SCN^- >> NO_3^- >> Cl^- > Br^- \sim I^- >>$ aspartate conductance sequence. It requires intracellular ATP for stable channel function (Vanoye & George 2002).

ClC-5 is predominantly expressed in the proximal tubule of the kidney (Sakamoto *et al.* 1996; Gunther *et al.* 1998). It is a strongly outwardly rectifying channel and has the conductivity sequence of $NO_3^- > Cl^- > Br^- \sim I^- >>$ glutamate$^-$ (Steinmeyer *et al.* 1995). Mutations occurring in the gene of ClC-5, *CLCN5,* cause Dent's disease and are associated with loss of proteins into the urine. Dent's disease is an X-linked renal tubular disorder characterised by low molecular weight proteinuria, hypercalciuria, nephrocalcinosis,

kidney stones and renal failure (Wrong, Norden & Feest 1994). The knock out of ClC-5 in mice has revealed impairment of endocytosis of protein and fluid-phase endocytosis (Piwon *et al.* 2000; Wang *et al.* 2000; Gunther, Piwon & Jentsch 2003).ClC-5 has a role in neutralization of the electric current of the H^+-ATPase, without which, the voltage across the endosomal membrane would inhibit H^+-pumping and limit endosomal acidification (Devuyst *et al.* 1999). Interactions of cofilin (Hryciw *et al.* 2003), Nedd4 and Nedd4-2 (Hryciw *et al.* 2004) with ClC-5 have been suggested to be essential for the role of albumin uptake in the proximal tubule.

The third group of CLC channels is composed of ClC-6 and ClC-7. They are dominantly expressed in membranes of intracellular organelles (Buyse *et al.* 1998). No functional electrophysiology data have been obtained yet.

There are four ClC-6 isoforms (ClC-6a, -6b, -6c and -6d). ClC-6a is a 97 kDa protein encoding 869 amino acids. ClC-6b to -6d are C-tail truncated splice variants (Eggermont *et al.* 1997). *CLCN6* is located on the same chromosome (16p13) as *CLCNK*. Gene expression can be detected in brain, testes, muscle, kidney, thymus and pancreas (Brandt & Jentsch 1995; Eggermont *et al.* 1997). Since ClC-6 is an intracellularly expressed CLC (Buyse *et al.* 1998), so far no functional characterisation has been able to be obtained by expression in *Xenopus* oocytes (Brandt & Jentsch 1995) and mammalian cells (Buyse *et al.* 1998).

ClC-7 is an 89 kDa protein with 45% sequence homology to ClC-6 (Brandt & Jentsch 1995). It is expressed in lysosomes and the late endosomes. The knock out ClC-7 mouse model leads to osteopetrosis and retinal degeneration (Kornak *et al.* 2001). Mutations in the gene of ClC-7, *CLCN7,* causes malignant autosomal recessive osteopetrosis (Kornak *et*

al. 2001), intermediate autosomal recessive osteopetrosis (Campos-Xavier *et al.* 2005), the second type of autosomal dominant osteopetrosis (Cleiren *et al.* 2001) and lysosomal storage phenotype associated neurodegeneration (Kasper *et al.* 2005) in humans and mice. Recently, a membrane protein, Ostm1, was found to be required for trafficking of ClC-7 from the ER to lysosomes (Lange *et al.* 2006). Although ClC-7 can reach its destination without Ostm1, the stability of ClC-7 depends on its association with Ostm1. Mutations in the Ostm1 gene cause severe osteopetrosis (Chalhoub *et al.* 2003).

1.4 Structural properties of CLC

After the review of mammalian CLC family, in this section structural information of CLC will be provided.

1.4.1 Investigation of CLC topology

The first topological model of CLC was predicted by Kyte-Doolittle hydropathy analysis based on the complete cDNA sequence of ClC-0 (Jentsch, Steinmeyer & Schwarz 1990). Thirteen hydrophobic domains termed as D1 to D13 and a cytoplasmic N-terminus were predicted. At that time, there was indecision between two arrangements of the last hydrophobic domain (D13), whether it spanned the membrane or not. Based on *in vitro* glycosylation scanning, protease protection assays, cysteine scanning of ClC-1 (Schmidt-Rose & Jentsch 1997b) and a C-terminal domain transplantation experiment of ClC-2 (Grunder *et al.* 1992), the C-tail after D12, including D13, was empirically arranged as being located in the cytosol. In addition, a pair of cystathionine β-synthase (CBS) domains have been found in the cytoplasmic C-tail (Bateman 1997) and D13 is embedded within the second CBS domain (CBS2). An extracellular location of the connection loop between D8 and D9 was confirmed by locating a glycosylation site (365 in ClC-0; 430 in ClC-1) (Koch *et al.* 1992; Kieferle *et al.* 1994; Middleton, Pheasant & Miller 1994)

although this site is absent in ClC-6 (Brandt & Jentsch 1995). Moreover, as the connection loop between D8-D9 is extracellular, there should be an even number of membrane-resident domains before D8 to fit all the criteria that were obtained empirically. The weakly hydrophobic and not well conserved D4 domain was then suggested not to span the membrane region but rather to be located extracellularly since the C-terminus of D3 and the linker between the D4-D5 were able to be accessed from the exterior (Schmidt-Rose & Jentsch 1997b) (Figure 1.2A). On the other hand, D4 was also suggested as a pore forming segment and cysteine scanning data suggested that D4 should be located in the membrane-resident region (Fahlke *et al.* 1997c). The topology proposed by Fahlke and colleagues (Fahlke *et al.* 1997c) is shown in Figure 1.2B. Despite the location of D4-D5 loop being probed again by inserting specific epitopes and employing immunofluorescent staining, the localisation could not be confirmed (Kuchenbecker *et al.* 2001).

The percentage of sequence homology between bacterial and mammalian CLC is around 15-10% and they have similar hydropathy plots (Purdy & Wiener 2000). The most dramatic difference between them is in the length of cytoplasmic C-tail. Mammalian CLC have an extensive C-tail region. This region has been shown to have an important effect on the normal channel function and more information will be provided in Section 1.5. Finally, a new topology model (Figure 1.3) was deduced from X- ray crystal structure of bacterial CLC (Dutzler *et al.* 2002) combined with the topology information of mammalian CLC that had been deduced empirically. Additional length of the C-tail is inserted in this model.

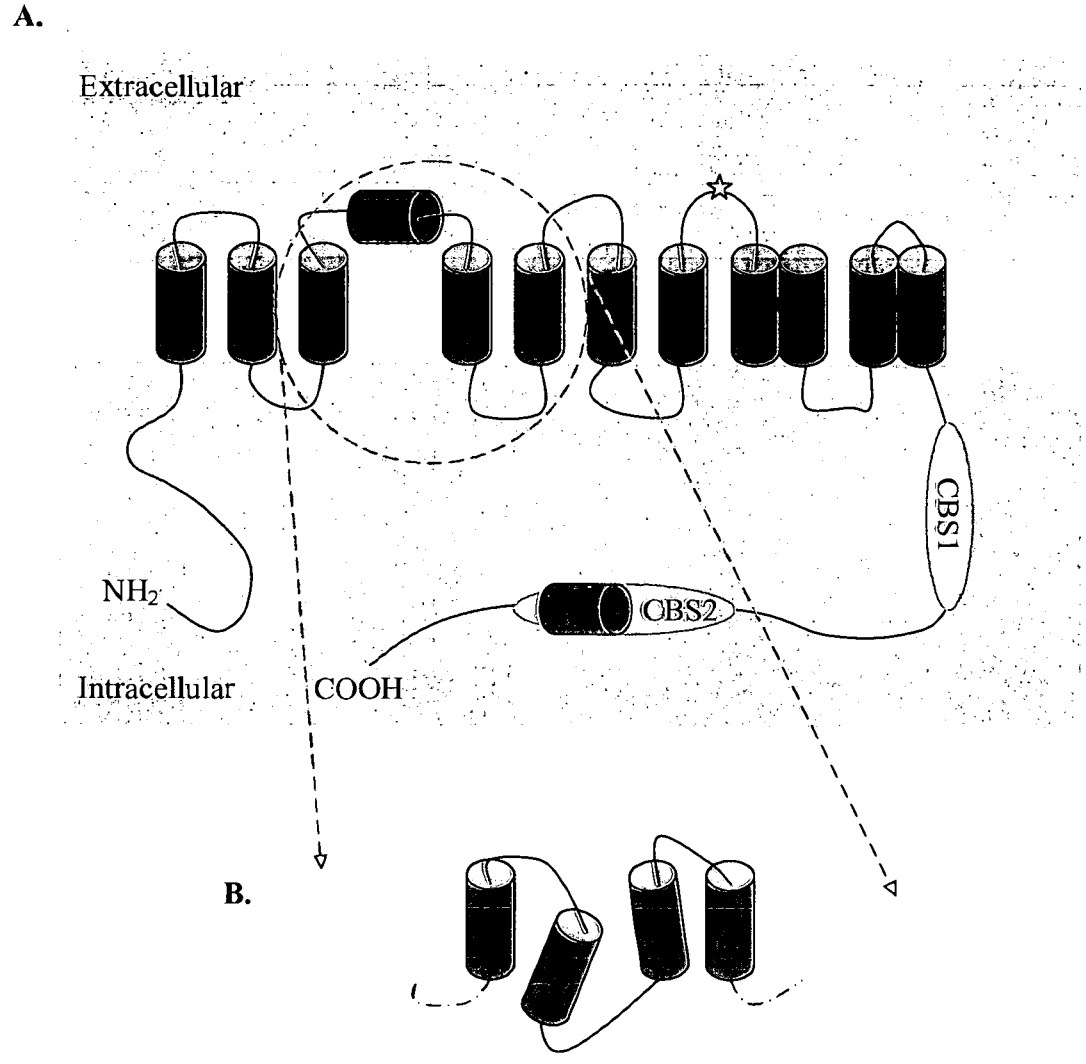

Figure 1.2 Topological model of CLC finalized by Schmidt-Rose and Jentsch, 1997b (A) and Fahlke and colleagues, 1997 (B)

(A) The thirteen hydrophobic stretches are represented by the bright green cylinders and labeled with domain numbers. The N- and C-tails are located intracellularly (pink area). The C-tail contained two CBS domains (purple oval) and the last hydrophobic stretch (D13). The red star sign represents the glycosylation site. The orange dashed line circles the area that is the controversial region, depending on whether D4 is located in the extracellular space (A) or spans the membrane (B).

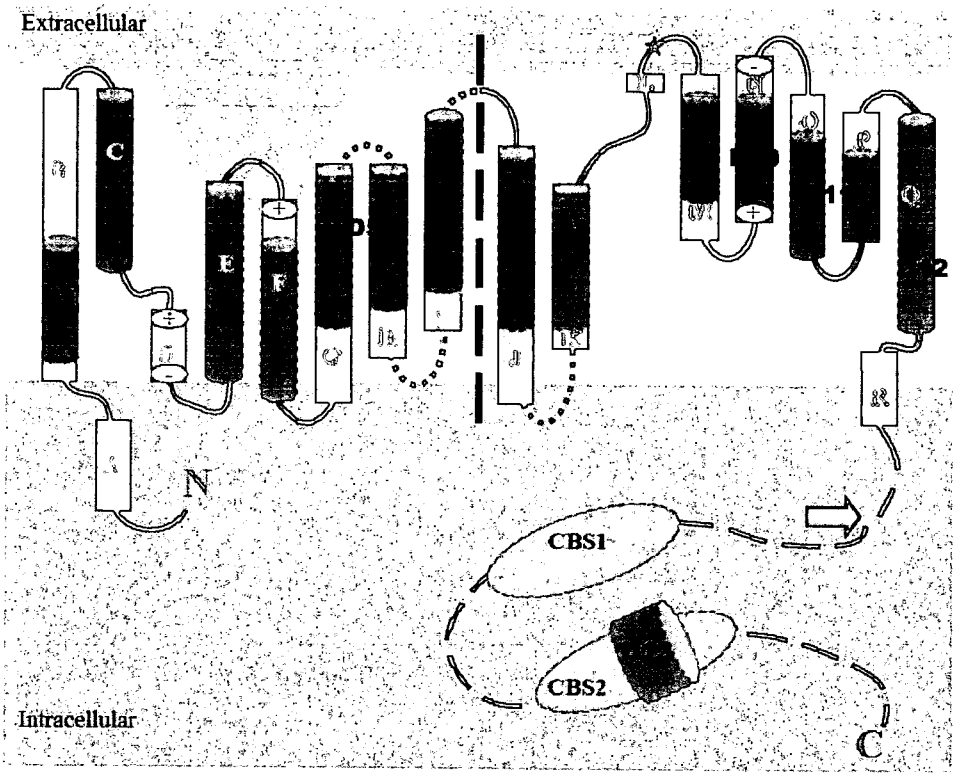

Figure 1.3 Topology model derived from bacterial CLC X-ray structure and the hydropathy and biochemical analysis of eukaryotic CLC

The bright green cylinders are the corresponding membrane-resident domains predicted by hydropathy analysis. The blue dashed line divides the topology structure into two halves. The N-terminal half includes helices B-J (lime coloured) and the C-terminal half includes helices I to Q (aqua coloured). They are structurally related. The connection helix linkers in solid lines have been identified via their localisation (light turquoise is extracellular; pink is intracellular) empirically, otherwise they are shown by the dotted line instead. The red colour outlined star indicates the glycosylation site. The R helix protrudes from the membrane-resident region (yellow area) to intracellular (pink area) and the extensive long C-tail of eukaryotic CLC (started from the violet dashed line) continued from the end of the C-tail of bacterial CLC (indicated by an arrow). The C-tail of eukaryotic CLC includes two CBS domains (purple oval) and D13 embedded in the second CBS domain. The helix dipole charges are highlighted on three alpha helices (D, F and N), which contribute their positively charged end along with the N-terminus of the R helix (in red colour) to stabilize halide ions in the ion-conduction pore.

According to the bacterial CLC structure, a subunit contains eighteen α-helices named A-R (Dutzler *et al.* 2002) which agreed with the estimated high α-helix content of bacterial CLC (Purdy & Wiener 2000). Alpha-helices A and R are located intracellularly so the cytoplasmic N- and C- terminal regions are consistent with the empirically deduced CLC topology (Schmidt-Rose & Jentsch 1997b). The structure can be divided into two halves. The N-terminal half of the polypeptide including helices B to I is structurally similar to the C-terminal half, which contains helices J to Q but their orientation is opposite in the membrane and they run anti-parallel within the membrane. This internal inverted repeat pattern has been found in different membrane proteins functionally related as channels or transporters and may be a product of protein evolution (Pornillos & Chang 2006). The membrane-resident α-helices within the bacterial CLC subunit are tilted and variable in length. This may be the reason why it was hard to define the localisation and boundaries of the predicted hydrophobic domains and the connection loops. In this topology structure, we can see that D4 spanned the membrane region which was suggested to be part of the pore forming segment and should have spanned the membrane (Fahlke *et al.* 1997c). D5 is composed of two α-helices (G and H) which helps to reconcile the problem encountered in interpreting the number of membrane-resident domains before D8 and the localisation of D4 (Schmidt-Rose & Jentsch 1997b). The broad hydrophobic stretches from D9-D12 actually are composed of five α- helices (M to Q) rather than four. In fact, Jentsch and colleagues had suggested that this broad stretch should have an odd number of membrane-resident domains (Jentsch *et al.* 1995). A recent study of membrane domain boundaries of rat ClC-2 used purified protein reconstituted in lipid bilayers and trypsin digestion to determine the intracellular region and membrane embedded domain (Ramjeesingh *et al.* 2006). The sequences of the domains were confirmed by mass spectrometry. In this study, the end of the N-tail was defined at residue R92 equivalent to R86 in hClC-2 and K113 in hClC-1 (Appendix A) which is before the B-helix and the

beginning of C-tail was proposed to be around R564-K567 equivalent to R558-K561 in hClC-2 and Q583-K586 in hClC-1 (Appendix A) which is halfway through R-helix. The extracellular linkers are E-F, L-M, N-O and intracellular linkers are A-B, D-E, F-G. Linkers embedded inside the membrane are C-D, K-L, M-N and O-P (Ramjeesingh *et al.* 2006). In fact, these studies further support the application of bacterial CLC topology to mammalian CLC (Ramjeesingh *et al.* 2006).

1.4.2 Dimeric double-barreled structure

The double-barreled structure of CLC was first proposed following experiments with *Torpedo Californica* electroplax chloride channel (ClC-0), which showed the barrel to have three substates of conductance using lipid-bilayer reconstitution experiments and single channel recording (Hanke & Miller 1983). An interpretation of a single channel recording result (Hanke & Miller 1983) is shown in Figure 1.4. The three levels were designated as D (Down), M (Middle) and U (Up) and with conductance 0 pS, 10 pS and 20 pS, respectively. Hanke and Miller interpreted this behaviour in terms of a double-barreled structure composed of two identical pores and gated independently. When both of the gates are in an open state (U), maximum conductance (20 pS) was obtained otherwise half of maximum conductance (10 pS) was observed when a single channel was opened (M). When both pores closed (D), no conductance (0 pS) can be observed.

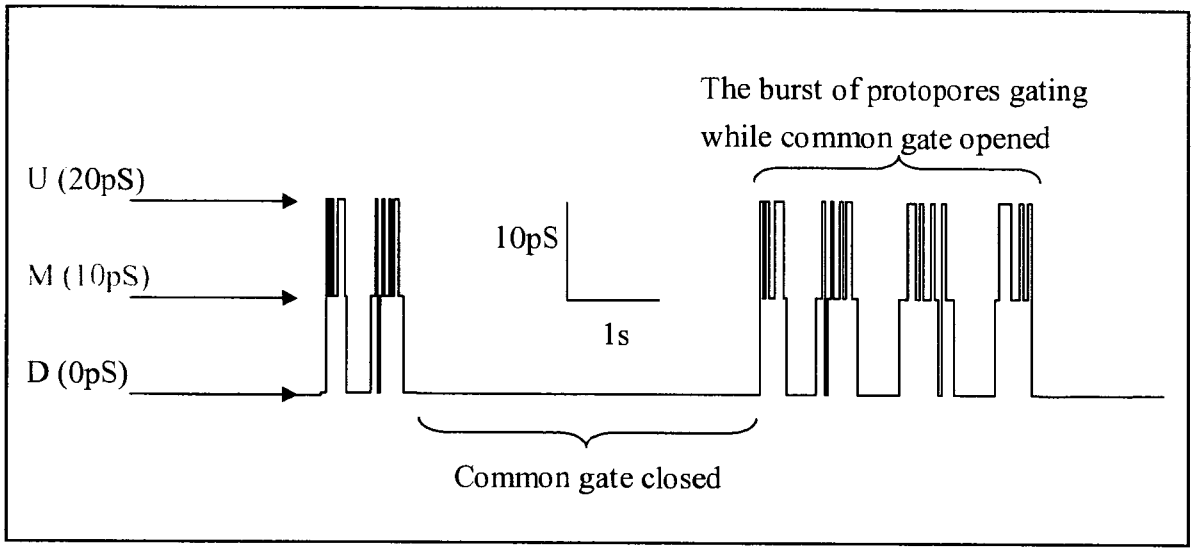

Figure 1.4 An interpreted model of ClC-0 single-channel trace after Hanke and Miller (1983)

Three levels of conductance are shown. Level D represents 0 pS conductance level with either both protopore gates or the common gate closed. Level M represents 10 pS single pore conduction level with one protopore gate closed while the common gate is opened. Level U represents double pore conduction level with both protopore gates opened while the common gate is opened. The time constants for common gating are in the range of seconds and protopore gating in the range of milliseconds. The double exponential decay of whole-cell, ensemble currents can then be explained in terms of this single channel behaviour as shown in Figure 1.8.

After 20 years, an initial 6.5 Å bacterial CLC X-ray structure was published (Mindell *et al.* 2001), which suggested a double-barreled structure for a homologous member of CLC. CLC is a dimer (Middleton, Pheasant & Miller 1994; Ludewig, Pusch & Jentsch 1996; Middleton, Pheasant & Miller 1996; Mindell *et al.* 2001; Dutzler *et al.* 2002) and each pore is formed by a single subunit (Mindell *et al.* 2001; Dutzler *et al.* 2002). This view is supported by experiments involving wild-type/mutant hybrids, recovery of wild-type conductance by two step methanethiosulphonate reagent modification and individual

conductance levels of wild-type/mutant concatamers (Ludewig, Pusch & Jentsch 1996; Middleton, Pheasant & Miller 1996). According to the second 3 Å bacterial CLC X-ray structure (Dutzler *et al.* 2002), the protein has a rhombus like structure (Figure 1.5) when viewed from the top of the extracellular side that is composed of two triangle shaped monomers which interact. Each monomer is composed of 18 α- helices (A-R) and they are wrapped around the ion permeation pathway (Figure 1.6) (Mindell *et al.* 2001; Dutzler *et al.* 2002).



Figure 1.5 Structure of the bacterial CLC viewed from the top of the extracellular side

Each monomer is shown with a different colour (red/blue) and the Cl^- ion in the selectivity filter is represented as a green sphere (Dutzler *et al.* 2002).

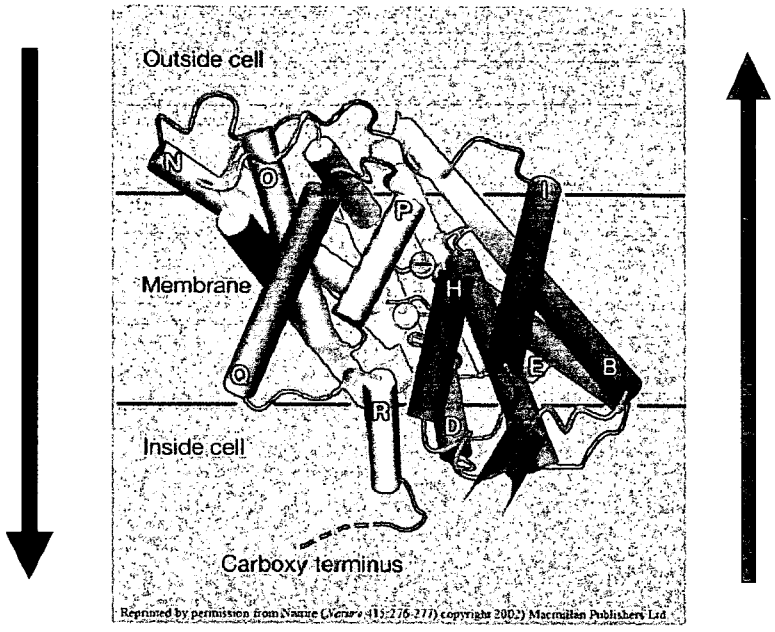

Figure 1.6 The α-helical 3D structure of a monomer of bacterial CLC

The two halves of the monomer are coloured in blue and green. They span the membrane region in antiparallel direction as shown by the arrows. Regions involved in the interaction with chloride ions are coloured as red (Dutzler *et al.* 2002).

1.4.3 Pore-forming selectivity filter region

Structurally, the bacterial CLC resembles double hourglass-like funnels. Wider openings face the extracellular and intracellular sides and a middle narrow region accommodates the ions, this narrow construction acting as an anion selectivity filter (Gouaux & Mackinnon 2005). CLC are specific for small monovalent anions such as Cl^-, Br^-, I^-, NO^{3-}, SCN^- (Fahlke 2001) and exclude the larger anions such as $H_2PO_4^-$ and SO_4^{2-}, the narrowed neck tunnel accounting for this. The selectivity filter does not distinguish between Cl^- and Br^- with high fidelity (Accardi *et al.* 2004) and is able to facilitate NO_3^- transport in plants (Geelen *et al.* 2000). Since Cl^- is the most abundant anion in organisms, strong interanionic selectivity is not required. Cations, on the other hand, are excluded by positive charge repulsion. There are four α-helices (D, F, N and R) (Figure 1.3) contributing helix dipole

positive charges from their N-terminus to expel cations and stabilize Cl^- ions inside the pore. Several sequences in the N-terminal membrane-spanning helices are highly conserved among the CLC channel family (Ludewig, Pusch & Jentsch 1996; Purdy & Wiener 2000; Dutzler *et al.* 2002) and have been suggested to act as pore-forming sequences (Fahlke *et al.* 1997c; Fahlke 2001) including for a highly conserved tyrosine residue (Tyr445) found in the N-terminal end of α-helix R. These sequences are GSGIP from helix D (Fahlke *et al.* 2001), G(K/R)(E/V)GP from helix F, and GXFXP from helix N (Appendix A). A 2.5 Å resolution bacterial CLC X-ray structure (Dutzler, Campbell & MacKinnon 2003) provided further information about the pore-forming region. It revealed that multiple ions occupy the region. Two halide ions occupy the channel when it is in the closed state and three halide ions occupy it in the open state. The positions occupied by halides are designated as S_{ext}, S_{cen} and S_{int} for external, central and internal sites, respectively (Figure 1.7). In the closed state, only S_{cen} and S_{int} were filled with ions and the S_{ext} site was blocked by a glutamate carboxyl group (E148) (Figure 1.7A). This glutamate carboxyl group is located between the ends of α-helices N and F. In the open state, the glutamate carboxyl group swings out and S_{ext} site can be occupied by an ion sandwiched between α-helices N and F and stabilized by hydrogen bonding (Figure 1.7B). The mechanism of glutamate side chain movement will be discussed in Section 1.4.4. The ion in the S_{cen} site is dehydrated and coordinated by main chain amide nitrogen atoms from the N-terminal end of α-helix N, the hydroxyl group of S107 (helix D) and Y455 (helix R). Mutation of the residue corresponding to S107, S123T in ClC-0, has been shown to reduce Cl^- conductance, affecting the rectification during depolarisation, changing the kinetics of gating and reducing the ion selectivity (Ludewig, Pusch & Jentsch 1996). The second ion in the S_{int} is coordinated on one side by main chain amide nitrogen atoms from the N-terminal end of α-helix D and on the other side it is exposed to the interior vestibule (Dutzler, Campbell & MacKinnon 2003). In addition, using an energy calculating program

called continuum dielectric approximation, a low affinity Cl^- binding site (S_{ext}*) was proposed on the top of the S_{ext} site for facilitating the binding of extracellular Cl^- ion to the S_{ext} site once the glutamate side chain has been removed from it (Faraldo-Gomez & Roux 2004).

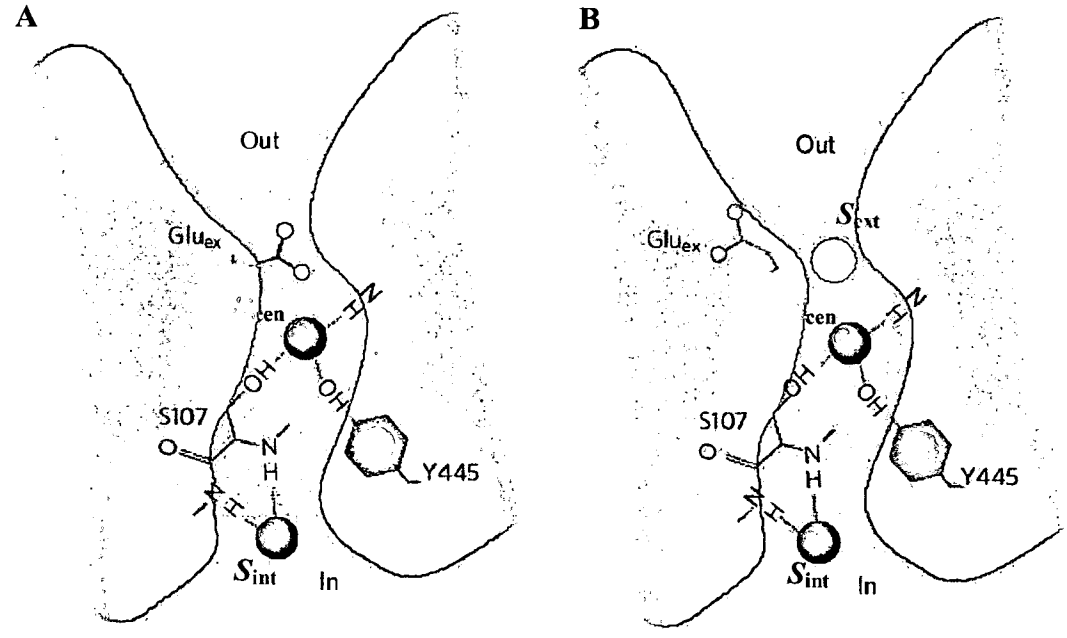

Figure 1.7 Magnified region of the selectivity filter in closed (A) and open state (B) In the closed state (A), two ions (green spheres) were found in the conduction pore tunnel. One located in the entry of internal mouth (S_{int}) stabilized by S107 and the second one located in the middle of the channel conduction pore (S_{cen}). The extracellular mouth (S_{ext}) is blocked by the side chain (red) of E148. In the open state (B), an additional ion (pink) was found located in the position of the side chain of E148 since it was flipped out and opened the channel to the extracellular vestibule. Diagram modified from Miller publication (Miller, C 2006).

1.4.4 Gating

According to the single channel recording of ClC-0 (Figure 1.4), there was up and middle bursting behaviour interrupting the zero conduction state (down) on a time scale of seconds (Hanke & Miller 1983). At that time, the authors suggested that ClC-0 was gated by two mechanisms, the first a fast gate, now also called the protopore gate, that was found in the

bursting mode on a time scale of milliseconds, the second a slow gate, now also called the common gate (throughout this thesis, I have used the term of "common gate" to represent the slow gate and "protopore gate" to represent fast gate), operating on a time scale of seconds. Protopore gating closes the conduction pores individually and independently, explaining why three levels of conductance could be found randomly and in a binomial distribution. Common gating closes both conduction pores simultaneously. The closed common gate is represented by the long-lasting zero conductance state in the single-channel recording (Figure 1.4). In ClC-0, protopore gating is activated by depolarisation, but the common gate is activated by hyperpolarisation. ClC-1 and ClC-2 have also been identified as having two gating mechanisms (Accardi & Pusch 2000; Aromataris *et al.* 2001; Zuniga *et al.* 2004). The time scales of the common and protopore gating of ClC-1 are both in the millisecond range with only a three-fold difference between them (Chen, TY 2005). A single current trace obtained from whole-cell patch clamping is shown in Figure 1.8 to show how the time constants contributed from the common and protopore gates of ClC-1 can be estimated using slope values. Both gates in ClC-1 are activated by depolarisation (Accardi & Pusch 2000), whereas, in ClC-2 they are activated by hyperpolarisation (Zuniga *et al.* 2004). The fast and common gating processes in ClC-2 are coupled rather than being independent as in ClC-0 (Zuniga *et al.* 2004). These gating processes are affected by voltage, pH and Cl^- concentration (Chen, TY 2005).

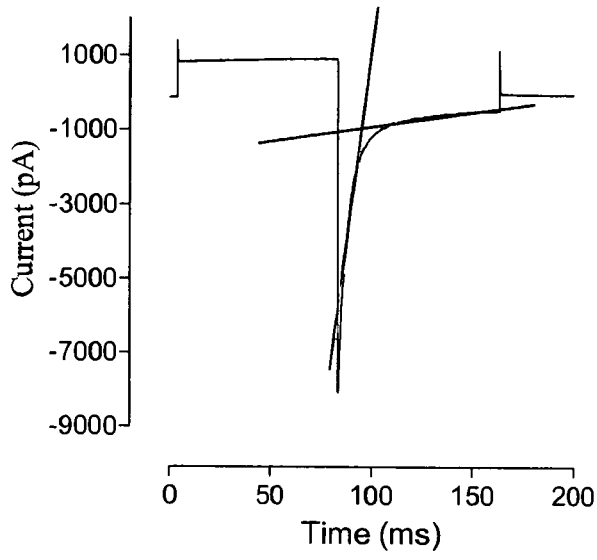

Figure 1.8 Single current trace of hClC-1 elicited by whole-cell patch clamping

The current trace (black line) is in response to a -140 mV test pulse for 80ms after a 40 mV conditioning pulse for 80ms. Using two component exponential analysis, time constants for the protopore gate and common gate can be determined as 4 ms and 26 ms, respectively. In a simplified view of the time constant relationship between these two gates, we can visualise the two time constants from the slope of the bi-exponential curve. The slope of red line represents time constant for protopore gating and slope of green line represents time constant for common gating.

1.4.4.1 Protopore gate

Opening of the protopore gate is favoured by low pH (Hanke & Miller 1983; Chen, MF & Chen 2001; Rychkov *et al.* 2001), high Cl^- in the extracellular solution (Hanke & Miller 1983; Pusch *et al.* 1995; Chen, TY & Miller 1996; Chen, MF & Chen 2001; Rychkov *et al.* 2001) and depolarising voltage (Chen, TY 2005). A glutamate side chain (E148) has been observed in the 3.0 Å bacterial CLC X-ray structure (Dutzler *et al.* 2002) blocking the extracellular vestibule of the ion-permeation pore. It was suggested that E148 might play the protopore gating role in the ion-permeation pathway (Dutzler *et al.* 2002). In order to

get a clear picture of this, Dutzler, Campbell and MacKinnon (2003) compared the 2.5 Å resolution bacterial CLC X-ray structure of wild-type, E148A and E148Q. In addition, corresponding mutations of E166A and E166Q (E166 of ClC-0 = E148 of EcClC) were introduced in ClC-0 for electrophysiological study. Mutants were expressed in *Xenopus* oocytes. The results showed that the protopore gate appears to stay open when the glutamate is mutated. Thus, E148A and E148Q were believed to represent an open state structure and were observed to have three halides occupying S_{ext}, S_{cen} and S_{int} sites (Figure 1.7B). The wild-type structure has been proposed as a gating closed state structure. It showed two halides ions occupying the S_{cen} and S_{int} sites (Figure 1.7A). On the other hand, the open state mutant can be mimicked by wild-type in an acidic extracellular pH (Dutzler, Campbell & MacKinnon 2003). Thus, one of the mechanisms for swinging the carboxyl side chain of glutamate out of the pore was suggested by protonation. In the unprotonated state, the glutamate carboxyl group blocks the S_{ext} site. By contrast, in the protonated state, the glutamate carboxyl group swings out and opens up the S_{ext} site for ion binding. Other workers have provided evidence that extracellular pH influences the rate of channel opening (Chen, MF & Chen 2001). In this study, the authors emphasize that the glutamate carboxyl side chain is special for protopore gate control since each pore contains its own glutamate residue and the conformational change within an individual pore is small and local. The small conformational change associated with gating in one pore is unlikely to influence gating in the other, thus suggesting that this only affects the individual protopore gate but not the common gate (Dutzler, Campbell & MacKinnon 2003).

1.4.4.2 Common gate

When compared to the protopore gate, the common gate has been much less studied. Also, from the bacterial CLC structure, there is no indication of the structural basis for the common gating process. Nevertheless, the common gate has been shown to be affected by

extracellular and intracellular (Pusch *et al.* 1999) chloride concentration and tends to open in high concentrations of Cl^- but shows an enhanced inactivation state with reduction of extracellular Cl^- concentration (Pusch *et al.* 1999). Increasing temperature (Pusch, Ludewig & Jentsch 1997) and binding of Zn^{2+} also favour the closing of the common gate (Chen, TY 1998). Common gating of ClC-0 is a highly temperature sensitive process (Q_{10}~40) which suggested that a large conformational change in the channel structure might be involved (Pusch, Ludewig & Jentsch 1997). In spite of the temperature dependence of common gating in ClC-1 (Q_{10}~4) (Bennetts *et al.* 2001) and ClC-2 (Q_{10}~4.1) (Zuniga *et al.* 2004) being lower than in ClC-0, conformational changes are still supported in the mechanism of the common gating process although a rather more complicated rearrangement must occur in ClC-0 than in ClC-1 and ClC-2. Mutation of C212 of ClC-0 (C212S and C212A) has been found to reduce the sensitivity of the channel to Zn^{2+} inhibition and eliminates the common gating process (Lin, Lin & Chen 1999) but this cysteine is only otherwise conserved in ClC-1 and ClC-2. Corresponding mutations in ClC-1 (C277S) (Accardi, Ferrera & Pusch 2001) strongly affected common gating but also had a mild effect on the protopore gate. On the other hand, the same mutations in ClC-2 (C256A) affect both fast and common gating to a similar extent (Zuniga *et al.* 2004). Since common gating involves opening and closing of both pores simultaneously, communication between subunits has been proposed (Dutzler, Campbell & MacKinnon 2003; Dhani & Bear 2006). Mutations that alter common gating have been found in the dimer interface (Saviane, Conti & Pusch 1999; Estévez & Jentsch 2002; Duffield *et al.* 2003; Wu, F *et al.* 2003). On the other hand, mutations in the C-tail (Fong, Rehfeldt & Jentsch 1998; Estévez *et al.* 2004; Wu, W *et al.* 2006) also affect common gating properties suggesting a role of the C-tail in mediating the common gating function (Section 1.5.5.5).

1.4.5 Proton coupled chloride transporter structure

The X-ray structure of bacterial CLC has provided considerable information on the likely structure of the mammalian CLC. However, functional characterisation of the bacterial CLC revealed that it is a proton coupled chloride transporter rather than a chloride channel (Accardi *et al.* 2004; Accardi & Miller 2004) leading to a profound review of transporter properties in CLC members. At the moment, at least two members of the mammalian CLC (ClC-4 and ClC-5) have been identified as proton coupled chloride transporters (Picollo & Pusch 2005) and a CLC member of the plant, *Arabidopsis thaliana* ClCa (AtClCa), has been identified as a proton coupled nitrate transporter (De Angeli *et al.* 2006). EcClC plays an important role in bacterial resistance to extreme acidity (Iyer *et al.* 2002). E148 in EcClC has a mediating effect of transporting H^+ from the external solution to the protein interior (Accardi & Miller 2004). An intracellular side amino acid (E203) was proposed to participate in the proton transfer pathway by shuttling protons to and from the protein interior. Mutation of this residue to a neutral amino acid completely and particularly abolishes all proton transport. Combination mutations, E148A/E203Q, abolish H^+ transport and display pH-independent Cl^- transport at its maximal rate (Accardi *et al.* 2005). Interestingly, E203Q is highly conserved among the transporter group of CLC, ClC-3 to 7 (Appendix A), but is replaced by valine in ClC-0, -1 and -K. Collectively, these results support the view that intracellular membrane-expressed CLC have a transporter role (Miller, C 2006).

1.5 Cytoplasmic C-tail of mammalian CLC

The following sections refer to the CLC C-tail. Based on the topology model (Figure 1.3) of CLC, the cytoplasmic C-tail is defined to begin about halfway through the R-helix. It includes two CBS domains and one hydrophobic stretch (D13) determined by hydropathy analysis (Jentsch, Steinmeyer & Schwarz 1990). It is variable in length among the

mammalian CLC, the longest tail being found in ClC-1 composed of 403 amino acids.

1.5.1 Disease-causing mutations demonstrate the importance of the C-tail

Various functional roles of the C-tail have been proposed but the precise physiological significance remains to be elucidated. Experiments conducted in the myotonic goat identified a single nucleotide mutation in ClC-1 (equivalent to A885P in human ClC-1) that caused the symptoms of myotonia with reduced chloride conductance and shifted the open channel probability to a more positive value (Beck, Fahlke & George 1996). Subsequently, other disease-causing mutations in mammalian CLC were described in the C-tail which further demonstrated its importance. To date, the C-tail of human ClC-1 has been found to contain six missense mutations, while there are at least 20 nonsense mutations for the protein (Figure 1.9) that cause both dominant and recessive myotonia phenotypes in humans (Colding-Jørgensen 2005). In ClC-7, there are at least 7 mutations located in the C-tail causing osteopetrosis (Cleiren *et al.* 2001; Campos-Xavier *et al.* 2005). There is also a newly found mutation occurring in ClC-2 (G715E) causing idiopathic generalized epilepsies (Haug *et al.* 2003) and a few missense and nonsense mutations found in the C-tail of ClC-5 causing Dent's disease (Lloyd *et al.* 1997a; Lloyd *et al.* 1997b) and the C-tail of ClC-Kb causing Bartter's syndrome (Konrad *et al.* 2000).

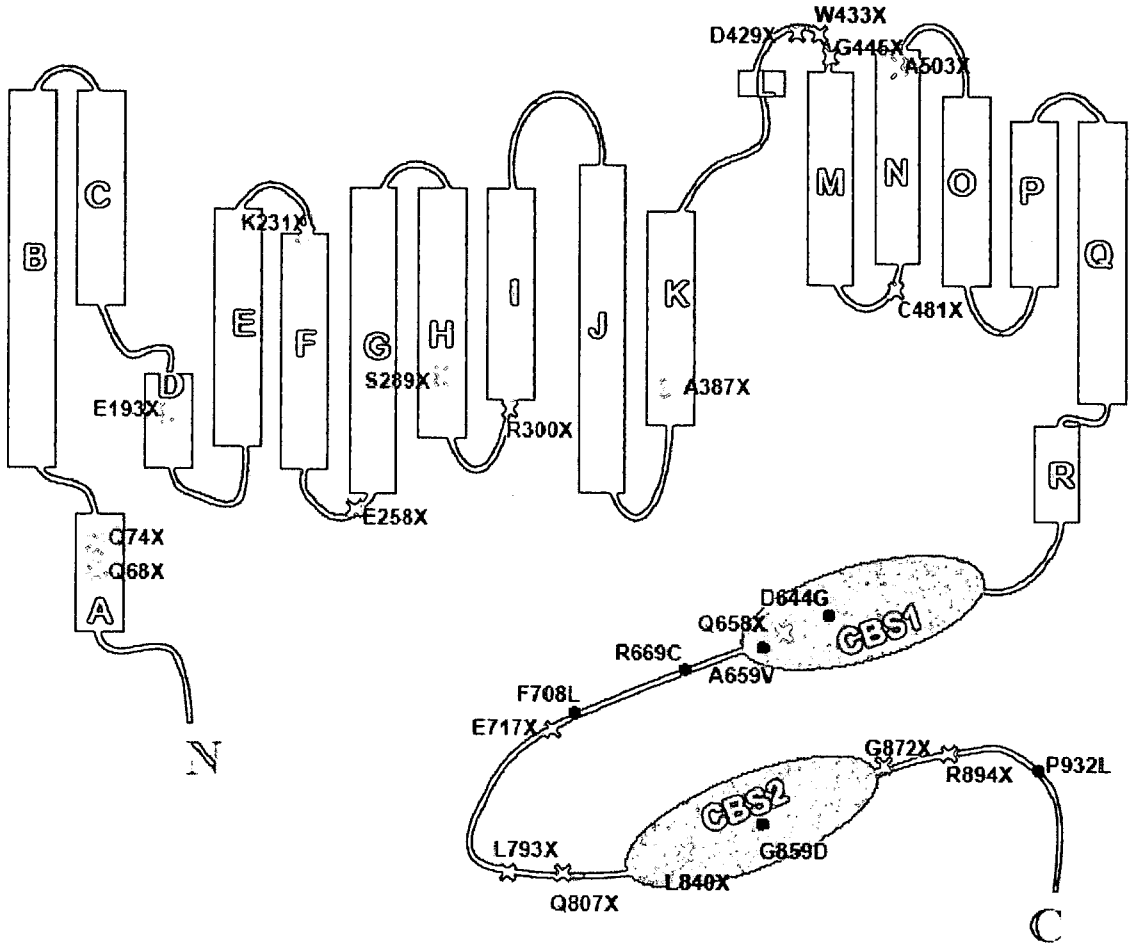

Figure 1.9 Localisation of nonsense and C-tail missense mutations

The approximate position of each nonsense mutation (indicated by a red cross) and missense mutation (indicated by a blue dot) is shown in the topology model corresponding to the Figure 1.3.

1.5.2 CBS Domains

Cystathionine β-synthase (CBS) domains were found by Alex Bateman (Bateman 1997) during the characterisation of the genome sequence of *Methanococcus jannaschii*. They are comprised of a conserved protein motif named after the enzyme cystathionine β-synthase that has a pair of CBS structural motifs at its C-terminal region. The general structure of this motif is composed of three β strands and two α helical regions in the sequence $\beta_1-\alpha_1-\beta_2-\beta_3-\alpha_2$ (Sintchak *et al.* 1996; Zhang, R *et al.* 1999; Miller, MD *et al.* 2004) as in Figure 1.10, however, the first β-strand (β_1) is not well defined in some proteins (Ignoul &

Eggermont 2005). It usually occurs in pairs, sometimes called Bateman domains (Kemp 2004), or as four tandem copies in a structure. Two copies of the CBS motif are found in eukaryotic CLCs. In fact, a wide range of proteins have been identified with this motif and it usually occurs in their C-tail (cytoplasmic) half. They include 5'AMP-activated protein kinase, inosine monophosphate dehydrogenase (IMPDH) and ABC transporters (Bateman 1997; Ignoul & Eggermont 2005). Their importance has been highlighted by disease causing mutations (Ignoul & Eggermont 2005). Mutations occur in the cystathionine β-synthase enzyme that cause homocystinuria (Shan *et al.* 2001), in the γ2 subunit of AMP-activated protein kinase that causes cardiac conductance problems similar to Wolff-Parkinson-White syndrome, in IMPDH-1 causing retinitis pigmentosa (Kennan *et al.* 2002) and, in the Hampshire pig γ3 causing skeletal muscle glycogen storage disease (Milan *et al.* 2000; Kemp 2004; Scott *et al.* 2004; Ignoul & Eggermont 2005).

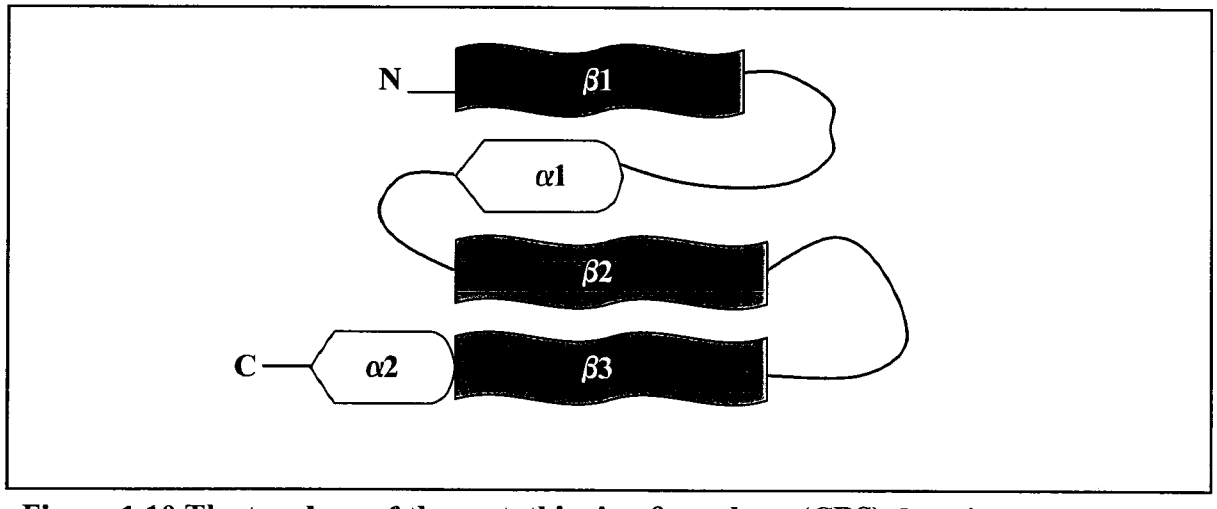

Figure 1.10 The topology of the cystathionine β-synthase (CBS) domains

It is composed of three beta strands (β1, β2 and β3) in blue and two alpha helices structures (α1 and α2) in yellow.

1.5.3 Crystal structure of CBS-containing protein

CBS domains occupy about one third of the sequence of the C-tail of eukaryotic CLC. This

structure may provide an important backbone of the C-tail of CLC.

1.5.3.1 Crystal structure of bacterial inosine-5'-monophosphate dehydrogenase

The first complete CBS structure was determined from the crystal structure of *Streptococcus pyogenes* (Sp) IMPDH (Zhang, R *et al.* 1999) that is shown as a tetramer (Figure 1.11). Each IMPDH monomer is composed of two domains, a TIM barrel domain (eight-stranded α /β barrel structure) that comprises the catalytic framework forming the interior core of the active tetrameric enzyme and a Bateman domain formed by a pair of CBS motifs projecting outward from the corners of the square. The two CBS motifs of the Bateman domain are associated in an antiparallel arrangement. The interface surface contains β-sheet structures formed by β2 and β3 from each CBS motif. The α-helices (α1 and α2) posited exterior. A distinct hydrophobic core is formed from this structural arrangement. The core may function as a potential binding site for regulatory molecules (Zhang, R *et al.* 1999) such as of ATP, a single molecule of which has been found bound per Bateman domain in IMPDH (Scott *et al.* 2004). There is no interaction among the Bateman domains from each monomer and such interaction was proposed not to be involved in the catalytic activity (Zhou *et al.* 1997).

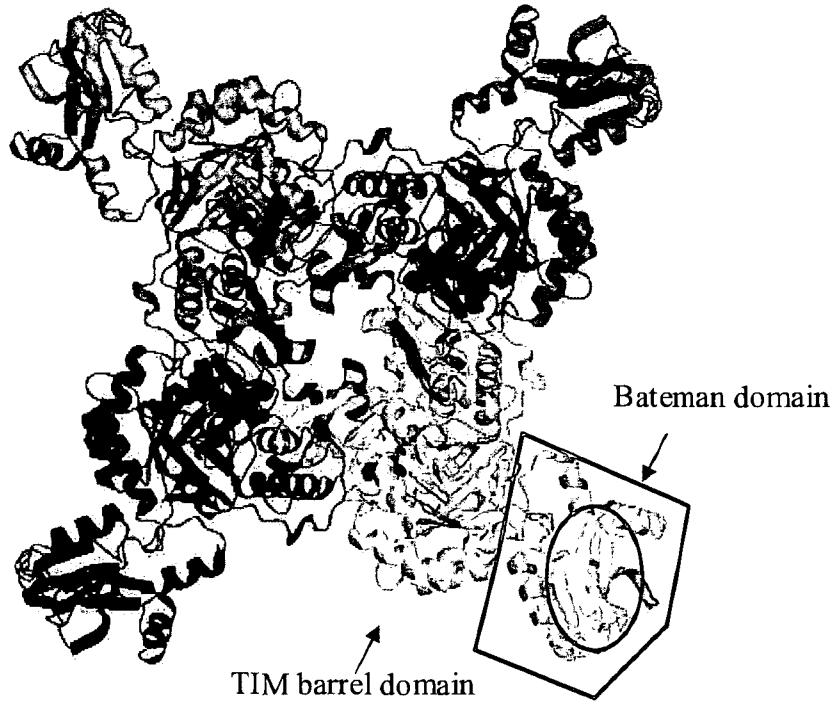

Figure 1.11 Ribbon diagram of the IMPDH tetramer

Each subunit is shown in a different colour. The protein is composed of the TIM barrel domain (catalytic domain) and Bateman domain (outlined in red polygon) that is composed of a pair of CBS motifs. The β-sheets formed by β2-β3 of each CBS motif are circled in a green oval. Diagram modified from Zhang and colleagues publication (Zhang, R *et al.* 1999).

1.5.3.2 Crystal structure of TM0935 from *Thermotoga maritime*

The first associated Bateman domain structure was obtained from TM0935, a CBS-containing protein from *Thermotoga maritime*. It is a dimer in its biologically active form. The monomeric structure of TM0935 is composed of five β-strands (two from CBS1 and three from CBS2) and six α-helices (each CBS domain contributing three helical

structures). Although there is no significant sequence similarity between TM0935 and the Bateman domain of IMPDH, the only structural differences are shifts of helix position of CBS1 and a 15 amino acid insertion after the second helix structure of CBS2 in TM0935. The X-ray structure showed that the dimeric association is formed through interactions of the helix structure of the CBS domains (Figure 1.12). Helix 1 of CBS1 interacts with helix 2 of CBS2 of the other monomer, and vice versa.

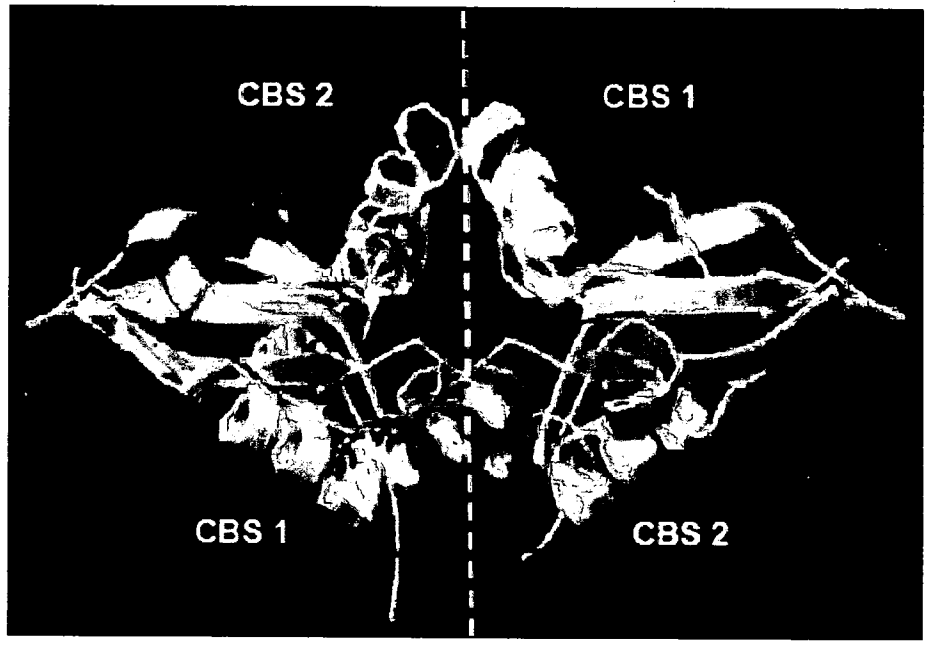

Figure 1.12 Ribbon diagram of the TM0935 dimer

Two subunits are separated by a red dashed line in the interface surface where they are associated by the helical structure of the CBS domains. The helical structures from CBS1 of one subunit interact with CBS2 of the other subunit. Diagram is modified from the resource obtained from protein data bank (www.rcsb.org/pdb).

1.5.3.3 Crystal structure of the cytoplasmic C-tail of the ClC-0

The third CBS-containing protein structure actually comes from CLC family, the C-tail of *T. marmorata* (Tm) ClC-0 (Meyer & Dutzler 2006). Sequence similarity comparison between the C-tail region of hClC-1 and TmClC-0 is shown in Figure 1.13. The C-tail sequence of TmClC-0 (299 amino acids) is shorter than hClC-1 (403 amino acids). They have 45% sequence similarity. The major difference can be found in the interlinker sequence between CBS1 and CBS2 and the rather short distal sequence after CBS2 of ClC-0. TmClC-0 C-tail X-ray structure does not include the whole of the cytoplasmic sequence. It represents only parts of the sequence after the predicted R-helix to five amino acids following CBS2. The X-ray structure (Figure 1.14) of the two CBS domains shows that it is in agreement with that of the previous mentioned CBS domain-containing proteins (Zhang, R *et al.* 1999; Miller, MD *et al.* 2004) in Section 1.5.3.1 and 1.5.3.2. There is tight interaction between the two domains via the β sheet formed by β strands 2 and 3 with a disordered linker connecting them. The structure is well defined within the two CBS domains and a portion of linker region before CBS2 (Figure 1.13) but the other part of the linker sequence shows an unorganised structure. This disordered arrangement has also been mentioned in the X-ray structure of Chinese hamster (*Cricetulus griseus*) IMPDH (Sintchak *et al.* 1996). A study of the purified C-tail of ClC-3 using near-UV CD spectra, differential scanning calorimetry and the DisEMBL program (a computational tool for prediction of disordered/unstructured regions within a protein sequence and is freely available via a web interface, http://dis.embl.de) further supports the view that this region contains a disordered segment leading to a partially folded structure (Li, SJ *et al.* 2006) . The C-tail crystal structure of ClC-0 only showed a monomeric arrangement rather than the dimeric structure of EcClC. The authors argued that this might due to a high salt effect during crystallization (Meyer & Dutzler 2006). By performing gel filtration and analytical

ultracentrifugation, the authors then demonstrated that the structure tended to form dimers in solution but these results contradicted those of similar studies on the C-tail of ClC-3 which showed monomeric structure using gel filtration and sedimentation equilibrium analysis (Li, SJ *et al.* 2006). Thus, whether the C-tail domain is dimeric or monomeric is still to be determined. Nonetheless, the dimeric structure has been proposed based on protein modeling with reference to the crystal structure of TM0935 (Miller, MD *et al.* 2004), assuming the dimerisation interaction involves helices α1 and α2 of the four CBS domains. In 2007, Dutzler has demonstrated that the crystallized C-tail structure of ClC-Ka has a similar dimer interaction to that of ClC-0 and ClC-5 (Markovic & Dutzler 2007). Using equilibrium dialysis, high micromolar range concentrations of ATP, ADP and AMP were detected bound with the C-tail of human ClC-5 (Meyer *et al.* 2007).ATP-binding has been found in C-tails of ClC-2 and ClC–5 (Scott *et al.* 2004; Wellhauser *et al.* 2006). Using homology modeling and nucleotide docking, a possible ATP binding site has been located in the C-tail of ClC-1 (Bennetts *et al.* 2005). In contrast, experiments involving equilibrium dialysis and incubation of crystallized ClC-0 C-tail with 10 mM ATP did not show any ATP-binding (Meyer & Dutzler 2006). Also, Zifarelli and Pusch (Zifarelli & Pusch 2008) could not find any direct influence of intracellular ATP up to a concentration of 10mM on ClC-1 regulation. Alternatively, Zhang et al. (Zhang, XD, Tseng & Chen 2008) suggest that sensitivity of ClC-1 to ATP depends on its redox state. Thus, the ATP-binding in muscle type CLC is still an enigma. Although there is now a crystal structure for the C-tail of ClC-0, this is still unable to explain its function, how this region interacts with N-terminal membrane-resident domain and how this affects channel function. In the following section, the functional roles of CBS domains in other proteins will be mentioned and whether these functions can be applied to the C-tail in CLC will be discussed.

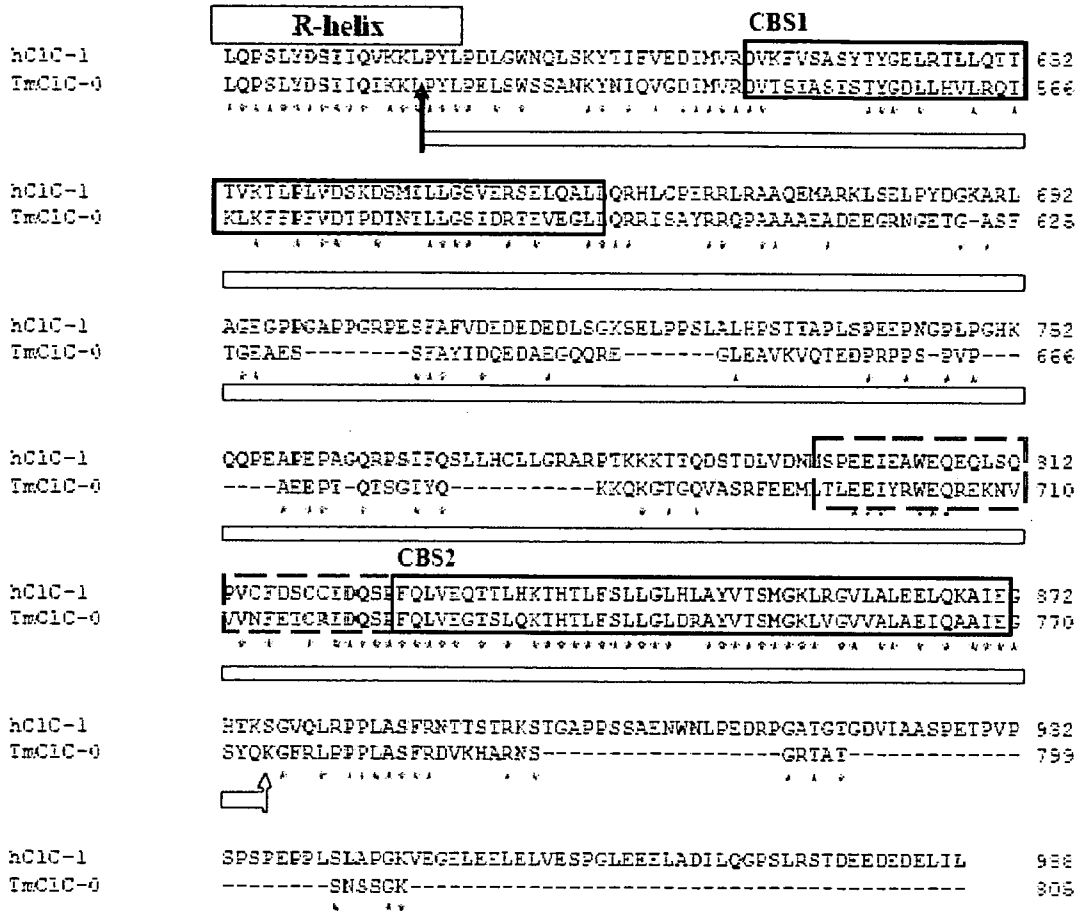

Figure 1.13 Sequence alignment of the C-tail domains of *T. marmorata* ClC-0 (TmClC-0) and human ClC-1 (hClC-1)

The coding sequence of the crystallized C-tail of TmClC-0 is on the top of the orange lines. The purple and pink arrows indicate the 3' and 5' ends, respectively. The partial R-helix sequence is underneath a green block and the portion of linker helix sequence shown with ordered structure has been enclosed in grey-dashed line. The sequences of CBS1and CBS2 have been enclosed in blue and green rectangles, respectively. Asterisks (*) indicate identical residues in the two sequences.

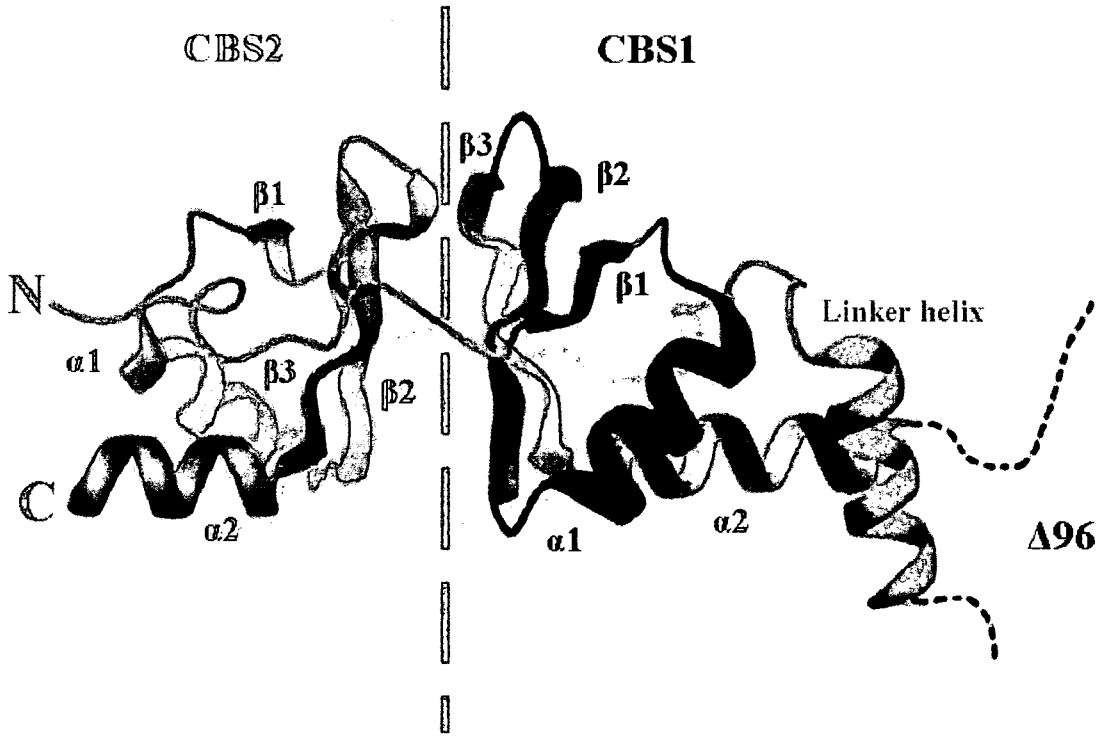

Figure 1.14 Ribbon diagram of the monomeric structure of the C-tail of ClC-0

The structure is divided into two halves by a green dashed line. The right hand side shows CBS1 with the linker helix structure while the left hand side shows CBS2. The interface surface is composed of β-sheets formed from β-strands (β2 and β3) of each CBS domain. The disordered structure of the 96 amino acid interlinker sequence is represented by the incomplete grey dashed line on the right hand side of the diagram. The linker helix is represented by a grey spiral. Diagram modified from Meyer and Dutzler publication (Meyer & Dutzler 2006).

1.5.4 Possible roles of CBS domains in various proteins

Understanding the function of CBS domains in other proteins might give hints about role of CBS in CLC, in fact, diverse roles have been suggested. CBS domains in human CBS enzymes operate as autoinhibitory domains (Janosik *et al.* 2001). They were found to bind *S*-adenosyl-L-methionine (AdoMet) (Scott *et al.* 2004) and sense its thermal denaturation, in turn, inducing a conformational change to displace the domain from its site of inhibition (Janosik *et al.* 2001). It also affects the multimeric nature of the enzyme. The homotetrameric structures of human and yeast CBS enzyme became homodimeric when the CBS domain was removed (Kery, Poneleit & Kraus 1998; Jhee, McPhie & Miles 2000; Meier *et al.* 2001). While the CBS domains of human CBS enzyme have been found to interact with AdoMet, the CBS domains from AMP-activated protein kinase were found to bind AMP or ATP and both IMPDH-2 and the chloride channel ClC-2 were found to bind ATP. This suggested that tandem pairs of CBS domains act as sensors of cellular energy status (Scott *et al.* 2004). Recently, a study of the CBS domains of the osmoregulatory ABC transporter, OpuA, demonstrated sensing ability for the membrane surface charge and the internal ionic strength that influences transporter activity by an on/off electrostatic switching mechanism (Biemans-Oldehinkel, Mahmood & Poolman 2006).

1.5.5 Proposed functional roles of the C-tail

1.5.5.1 Implications from the roles of CBS domain of other protein for the function of CLC family

1.5.5.1.1 CBS domains in CLC are not involved in oligomerisation

CBS domains have an effect on the oligomeric status of the CBS enzyme. However, this functional feature is not essential for CLC, since the bacterial CLC homologue structure showed that it is predominantly in the dimeric form without CBS domains. Thus, CBS

domains of eukaryotic CLC are more likely to be for other functions, as discussed below, rather than for dimerisation.

1.5.5.1.2 Cellular energy sensor

On the other hand, the role of cellular energy sensor by the CBS domains (Scott *et al.* 2004) has been suggested for CLC. Some ion channels have been shown to be sensitive to ATP such as the ATP-sensitive potassium channel (Vanoye *et al.* 2002) and the structurally unrelated chloride channel CFTR that have two ATP-binding sites to control their function (Ko & Pedersen 1995), but it is difficult to predict a role for ATP in the CLC family. ATP was required for full activity of ClC-4 and prevented the run-down phenomenon during activity measurement (Vanoye & George 2002). Subsequently, the C-tail of ClC-2 expressed as a GST fusion protein was found to bind one molecule of ATP per molecule of GST fused ClC-2 C-tail (Scott *et al.* 2004). In idiopathic generalized epilepsies a mutation in ClC-2 C-tail, G715E, has been suggested to reduce the ATP binding affinity (Haug *et al.* 2003). Bennetts and colleagues have shown that a high concentration of ATP (5 mM) inhibits ClC-1 activity by shifting the voltage-gating to a more positive potential and affects the voltage dependence of common gating (Bennetts *et al.* 2005). Further experiments suggested that ADP, AMP and ATP have a similar effect but not IMP. Thus, they believed that under anaerobic conditions, the inhibition of ClC-1 would be relieved. In turn, this effect would increase ClC-1 activity and reduce muscle excitability during the process of fatigue (Bennetts *et al.* 2005). Recently, a purified C-tail protein of ClC-5 has been found to interact with ATP by assaying the direct binding of ^{32}P-ATP (Wellhauser *et al.* 2006). The interaction does not involve ATP hydrolysis but improves the thermal stability of the structure by enhancing the melting temperature. It might have similar action to the CBS domain in the human CBS enzyme to sense thermal denaturation (Janosik *et al.* 2001).

1.5.5.2 Interactions with regulatory proteins

A proline-rich motif is found in the interlinker sequence of the ClC-5 CBS domains suggesting that this motif interacts with the E3 ubiquitin ligase, Nedd4-2, or the Nedd4-like protein WWP2 (Schwake, Friedrich & Jentsch 2001; Hryciw *et al.* 2004). Cofilin, a cytoskeletal protein, also has been reported to interact with ClC-5 via its C-tail (Hryciw *et al.* 2003). A splice variant of ClC-3 called ClC-3B has a slightly longer carboxyl-terminal sequence. This additional sequence is able to make up a PDZ (PSD95/Dlg/ZO-1) domain-binding motif in the C-tail. EBP50 (ERM-binding phosphoprotein 50) and GOPC (Golgi-associated PDZ and coiled-coil motif-containing protein) have been identified as binding candidates of the motif (Ogura *et al.* 2002). A few different proteins have been found to interact with members of CLC to regulate channel function. Whether the interaction occurs at the C-tail is to be investigated (Dhani & Bear 2006).

1.5.5.3 Protein trafficking

ClC-5 belongs to a branch other than muscle type CLC. It shares about 23% homology with ClC-1. Three naturally-occurring mutations, R648X, R704X and 695delCfs removing all or part of the CBS2 of ClC-5 (associated with Dent's disease) were transiently transfected in CHO-K1 cells. These truncated mutants have been found to be located mainly at an intracellular, perinuclear localisation but absent from the plasma membrane where wild-type ClC-5 is normally expressed. Thus, truncation of the second CBS domain was suggested to cause disruption of trafficking of the N-terminal membrane-resident domain to the plasma membrane and no functional expression (Carr, Simmons & Sayer 2003). Also, studies of yeast CLC by alanine scanning mutagenesis, showed that 5 amino acids (FVTID) from the N-tail and 25 amino acids located in the C-tail were essential for trafficking to the Golgi apparatus for proper function (Schwappach *et al.* 1998). Other

studies of the protein trafficking role of the C-tail of ClC-1 using co-immunoprecipitation following expression of an HA tagged N-terminal fragment and myc-C tagged C-terminal fragment of ClC-1, suggested that the N-terminal membrane-resident part was not able to show surface expression without co-expression with the C-terminal fragment (Estévez *et al.* 2004). However, Hebeisen and coworkers (Hebeisen *et al.* 2004) used confocal imaging observing the expression of truncation mutants fused with fluorescent protein to demonstrate that truncation mutants could insert themselves into the surface membrane without the association of the C-tail region. Thus, there appears to be no clear conclusion on the role of C-tail in protein trafficking.

1.5.5.4 Influence of the C-tail on functional properties of CLC

A naturally-occurring mutation in the myotonic goat, A885P, has been shown to influence voltage-dependent gating by shifting the channel opening probability curve to more positive voltage values (Beck, Fahlke & George 1996). Corresponding to the myotonic goat mutation, A783P, introduced into ClC-0 has shown a significant gating alteration. Channel inactivation behaviour at hyperpolarised potential was altered to activation (Maduke, Williams & Miller 1998). An amino acid residue K519 of ClC-0 is the initial residue of the defined C-tail. Its mutation to glutamate (K519E) affects conduction, gating and halide selectivity (Pusch *et al.* 1995). The single-pore conductance is sensitive to the charge at this position (Middleton, Pheasant & Miller 1996). Substitution of a neutral residue reduces the conductance to half. Substitution of a negative residue lowers the conductance further (Middleton, Pheasant & Miller 1996). A C-tail truncated mutant in *C.elegans* CLC demonstrated altered voltage-dependent gating, pH and Cl^- sensitivity. It also modified channel inhibition by Zn^{2+} binding, prevented ATP-depletion-induced activation and reducing volume sensitivity (Denton *et al.* 2006).

1.5.5.5 Mediating the common gate function

Four mutations, H838A, H835R, A862E/K and E865K, introduced into CBS2 of hClC-1 caused changes in voltage-dependence and one of these mutants with an especially strong effect, H835R, has shown a dominant effect when co-expressed with wild-type, implying an effect on the common gate. Two conserved mutations H736A and E763K (equivalent to H838A and E865K of hClC-1) introduced into ClC-0, reduced the sensitivity to Zn^{2+} inhibition and have a dominant effect when co-expressed with wild-type, further supporting the view that C-tail mutations in CBS2 have effects on common gating (Estévez *et al.* 2004). In an alanine scan, E865A mutations in hClC-1 particularly reduced common gate closing probability at negative potentials (Wu, W *et al.* 2006). In other studies, when the C-tail of ClC-0 was deleted and replaced with the corresponding region from ClC-2, no common gating was observed (Fong, Rehfeldt & Jentsch 1998). Interestingly, when a portion of carboxyl region (D13) was replaced with corresponding ClC-2, common gating could be retained but it was altered (Fong, Rehfeldt & Jentsch 1998). According to this result, interactions of appropriate regions of the C-tail with N-terminal membrane-resident region are of importance for common gate formation. Structural rearrangement in the C-tail during common gate opening and closing have been observed using fluorescence resonance energy transfer (FRET) methods (Bykova *et al.* 2006).

1.5.5.6 Conformational modification of CLC structure

Differences in methanethiosulphonate reagent modification rate of K231C, which is located beside the glutamate residue (E232), predicted a component of protopore gate in the full-length ClC-1 and C-tail truncated mutants, R894X and K875X, implying that the C-tail has a modifying effect on the pore-forming region assisting the normal gating process (Hebeisen & Fahlke 2005). In addition, by using AlexaFluor 488 fluorophore engineered to the residues located in the R-helix of the C-tail of EcClC, Bell and

coworkers demonstrated that the ion transporting process involves conformation change in the C-tail (Bell *et al.* 2006). Although the bacterial CLC contains almost no C-tail region when compared with eukaryotic CLC, the tyrosine residue located mid-way along the last membrane-resident helix, R, has a coordination effect on the S_{int} site Cl^- binding, indicating that the extended C-tail domain of eukaryotic CLC might have a pore modification effect (Bell *et al.* 2006).

1.5.6 Important sequence in the C-tail

The C-tail has been identified as playing various roles in channel function. Whether the whole C-tail, part of C-tail or certain stretches of sequence located in the C-tail are important for function has been investigated using C-tail truncation, internal deletion and functional complementation studies. Based on the truncation experiments performed on ClC-0, ClC-1 and ClC-5, when the sequences after CBS1 were deleted, although the remaining channel contained most of the sequences for forming the ion-permeation pore according to the bacterial CLC X-ray structure (Dutzler *et al.* 2002), the channel is unable to function. However, channel function can be restored by co-expressing the deleted parts in *Xenopus* oocytes (Schmidt-Rose & Jentsch 1997a; Maduke, Williams & Miller 1998; Estévez *et al.* 2004; Mo *et al.* 2004). Function of truncated channel can be rescued but the splitting point is critical for their functional reconstitution. Restoration of function did not occur when the split was made before CBS1 (Schmidt-Rose & Jentsch 1997a). However, on the other hand, when the co-expression of $N_{1\text{-}720}$ (split between CBS1 and CBS2) and $C_{598\text{-}988}$ (split before CBS1) of ClC-1 is performed in *Xenopus* oocytes, function restoration occurs even though there is an overlapping region (Schmidt-Rose & Jentsch 1997a). Thus, not only the position of split is important for the functional restoration of split channels but also intact sequence for forming correct structural domains is critical for channel function.

According to the above experiments, these chloride channels are obviously unable to function properly without a C-tail region. In fact, among the mammalian CLC, there are various lengths of C-tail. The longest one occurs in ClC-1. In order to narrow down the important sequence for channel function, serial truncation experiments have been performed in full-length rat and human ClC-1. These experiments suggested that channel function can be observed without the last 100 amino acids but when more than 125 amino acids were deleted in rat ClC-1 or 110 amino acids deleted in human ClC-1, channel function was abolished (Hryciw *et al.* 1998; Wu, W *et al.* 2006). In contrast, in split channel experiments ($N_{1\text{-}720}$ + $C_{721\text{-}x}$), human ClC-1 functioned without the last 118 amino acids that contained most of distal sequence after CBS2 ($C_{721\text{-}870}$) but no chloride current was measured when the deletion extended to the amino acids inside CBS2 (130 amino acids deleted equivalent to $C_{721\text{-}858}$) (Estévez *et al.* 2004). Internal deletion of the hydrophobic stretch, D13 (T845-L863 of rClC-1 equivalent to T839-L857 of hClC-1), located inside CBS2 of rat ClC-1 has little consequence on channel function (Hryciw *et al.* 1998). Even the whole of CBS2 (C820-E871) of human ClC-1 can be deleted without abolishing channel function, but channel function was destroyed when sequence inside CBS2 in the split ClC-1 channel was perturbed (Estévez *et al.* 2004). Most of the interlinker sequence (C666-E800 of hClC-1) between CBS1 and CBS2 can be deleted without significant effect on channel function but function was destroyed if the deletion occurred prior to CBS2, Q807-P813 (QEQLSQP), in the interlinker region of hClC-1 (Estévez *et al.* 2004). Channel current cannot be detected without CBS1 sequence (Estévez *et al.* 2004; Wu, W *et al.* 2006) but is able to be detected when either CBS1 or CBS2 was replaced with corresponding CBS from ClC-0, ClC-K1, ClC-5, or ClC-7 and even when CBS1 was substituted with the CBS1 of IMPDH demonstrating the high conservation of CBS domains in CBS-containing proteins. Two CBS1 domains arranged in the C-tail is able to generate functional channels in contrast to an arrangement of two CBS2 domains

(Estévez *et al.* 2004). Although this result demonstrated CBS domains are highly conserved and interchangeable with various CBS-containing proteins and ClC-1 can probably function with a single CBS domain, surprisingly Wu and colleagues identified a 26 amino acid sequence located immediately after the CBS2 domain that was sufficient for functional restoration in split channel experiments (Wu, W *et al.* 2006). These results seem to contradict the importance of the sequence prior to CBS2 proposed by Estévez and colleagues but is in agreement with the disruption of post CBS sequence by deletion of 130 amino acids at the C-tail (Estévez *et al.* 2004). On the other hand, in a study of the *S. cerevisiae* chloride channel (ScClC) that has been classified as within the same subgroup as ClC-5, relocation of CBS2 to the N-terminus of ScClC does not abolish function (Schwappach *et al.* 1998). Thus the function of CBS2 was suggested not to be position dependent (Schwappach *et al.* 1998). Function cannot be rescued by transplanting the corresponding C-tail region of ClC-2 onto ScClC (Schwappach *et al.* 1998). Interestingly, the function of this ScClC/ClC-2 chimera can be restored by transplanting the CBS2 from ScClC to the N-terminus (Schwappach *et al.* 1998). Taken together, these results indicate that channel function is able to be obtained with a shortened C-tail. However, whether CBS2 is necessary and whether the post or pre-sequence of CBS2 are key sequences for channel function still remains to be unravelled.

1.6 PROJECT AIMS

In my project, I have focused on investigating the function and structure of the C-tail of ClC-1. Split channel strategies were used in these studies. In order to eliminate the inconsistent results produced by *Xenopus* oocytes due to seasonal change or unhealthy oocyte production (Goldin 2006) and the difficulty of extrapolating the results from *Xenopus* oocytes to mammalian expression systems, my first aim was to establish the split channel system in mammalian cells. Two mammalian vectors were used to carry the

constructs for the N-terminal membrane-resident region and the C-tail region separately. The vector containing the C-tail region insert was simultaneously able to co-express green fluorescent protein (GFP) under the control of internal ribosomal entry site (IRES). GFP expression was correlated with the transfection efficiency and the expression level of both N- and C-terminal domains (Marshall *et al.* 1995; Trouet *et al.* 1997). The success of the system was tested by the co-expression of a previously well-established split channel model, $N_{1\text{-}720}$ + $C_{721\text{-}988}$, and the measured chloride currents were compared with those of the full-length wild-type construct.

Aim 1: To establish functional ClC-1 channel complementation in a mammalian expression system by co-transfecting plasmid DNA from two mammalian vectors.

Once established, the split channel system could be used to achieve the second and the third aims. In order to study the essential C-tail region of ClC-1, one of my colleagues had used a split channel strategy expressing the ClC-1 truncation mutant, $N_{1\text{-}720}$, in *Xenopus* oocytes and found that a peptide, $C_{863\text{-}988}$, which had 142 amino acids deleted at the N-terminus of $C_{721\text{-}988}$, was, nevertheless, able to restore the $N_{1\text{-}720}$ channel function (Wu, W *et al.* 2006). Further deletion of the C-terminal end by 100 amino acids generated a 26 amino acid peptide, $C_{863\text{-}888}$ (Figure 1.15), that was still able to restore function, but with reduced chloride currents. These results implied that the essential amino acids were located within $C_{863\text{-}888}$ for functional restoration. Since it was not known whether this was the minimal supplementary peptide, I decided to attempt further tests in which $C_{863\text{-}888}$ was progressively shortened by deletion of 3' and 5' amino acids. These functional restoration experiments in the mammalian split channel system were to test for the robustness of the result obtained in *Xenopus* oocytes and also to refine the important amino acid sequence.

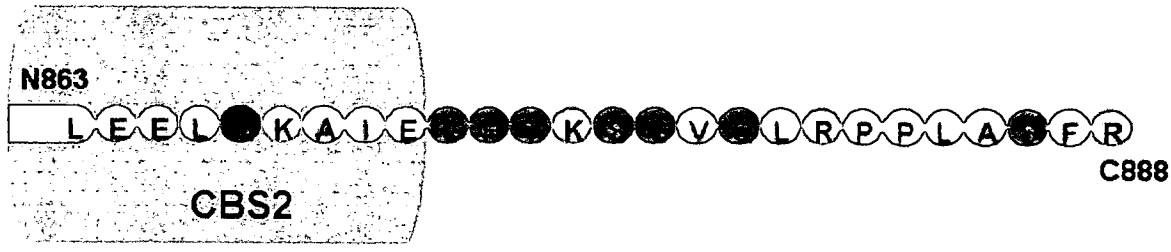

Figure 1.15 Cartoon picture of the previously-defined 26 amino acid peptide

The sequence of the 26 amino acid peptide covered the amino acid residues from 863 to 888. The first nine amino acids located at the N-terminus of the peptide are the distal region of CBS2.

Aim 2: To attempt to repeat the short peptide supplementary reconstitution experiment in the mammalian expression system and to extend the study, if possible, by examining supplementation using even shorter peptides.

The second reason for using the split channel system was to attempt to restore the function of naturally-occurring C-tail truncated mutants by co-expressing a minimal peptide sequence. Channel function could not be detected without the C-tail region. By studying the performance of the split channels, generally channel function was able to be rescued when the cut occurred in the inter-linker region of CBS1 and CBS2. The typical successful model is $N_{1\text{-}720}$ + $C_{721\text{-}988}$ of hClC-1 with similar complementary constructs prepared in ClC-0 (Maduke, Williams & Miller 1998) and ClC-5 (Mo *et al.* 2004), showing that function could also be restored in those channels by reconstitution. In these studies, three naturally-occurring nonsense mutations have been selected. Two of them are truncated in the middle (E717X) and almost at the end (Q807X) of the inter-linker sequence and the third one is truncated after CBS2 (G872X). E717X and Q807X are associated with the recessive myotonic phenotype but G872X is associated with both the recessive and the dominant phenotypes (Colding-Jørgensen 2005). $C_{721\text{-}988}$ was co-expressed with these three

truncated mutants to investigate the extent of functional restoration.

Aim 3: To attempt to restore function to various naturally-occurring C-tail-truncated mutants of hClC-1 by co-expressing the well-known, and well-expressed, C-tail fragment, $C_{721\text{-}988}$.

Recently, thirteen novel missense mutations were screened from myotonia congenita patients. These have been provided to our laboratory from various sources for characterisation in advance of publication of the clinical details. In order to know more about how the mutations affect the channel function and lead to myotonia, I decided to use site-directed mutagenesis to create the corresponding mutations in WT hClC-1. Among these mutants, three are located in the C-tail region: R691S, E724A and V851M. Two, R691 and E724, are located in the inter-linker sequence between CBS1 and CBS2 and V851 is located in the beta 2 domain of CBS2. The R691 and E724 residues are not at all conserved while V851 is, perhaps, totally conserved in the CLC family. This makes mutations of these C-tail residues particularly interesting with respect to why all of them (conserved and unconserved) should be associated with clinical myotonia. Secondly, it would also be of interest to know how a specific dysfunction in each of these channel mutants might give rise to myotonia.

Aim 4: To characterize newly found missense mutations located in the C-tail region of hClC-1 via heterologous expression.

When I began my project in mid 2002, there was no crystal or other structural information relating to the cytoplasmic C-tail of eukaryotic CLC proteins, largely because such tails are

not present in most prokaryotic CLCs. I, therefore, decided to attempt to produce C-tail peptides by bacterial expression for structural analysis. Two C-tails, $C_{575\text{-}988}$ and $C_{721\text{-}988}$, were selected for expression. $C_{575\text{-}988}$ covers the whole C-tail sequence while $C_{721\text{-}988}$ covers only half of C-tail sequence containing a single CBS domain. Similar regions have been tested previously for protein expression in our laboratory using both bacterial and baculovirus expression systems and Maduke and colleagues using bacterial system (Maduke, Williams & Miller 1998). In each case, the expressed proteins were contained within inclusion bodies which hampered further structural analysis. My strategy, therefore, was to improve protein solubility by expressing thioredoxin-fused C-tail peptides (LaVallie *et al.* 2000). To facilitate protein purification by metal-chelating chromatography, it was my intention to engineer recombinant proteins tagged with six histidine residues.

Aim 5: To express mg quantities of C-tail peptides using a bacterial expression system and to establish methods of purification.

CHAPTER TWO: GENERAL MATERIALS AND METHODS

2.1 INTRODUCTION

In this chapter, the common methods for construction of the chloride channel mutants for patch-clamping and protein expression will be described.

2.2 CHEMICALS AND WATER

All chemicals were Analytical grade or Molecular Biology grade and purchased from established suppliers. Where a supplier is referred to in the text, the name is indicated in the first instance. Addresses of suppliers of reagents and equipment are documented in Appendix B. Ultrapure water obtained from the Milli-Q (MQ) water purification system (Millipore) with resistivity level of 18.2 Megaohms (MΩ).cm at 25°C and total organic carbon (TOC) level below 10 ppb was used for solution preparation.

2.3 CULTIVATION OF BACTERIA

Propagation of bacteria cloned with desired DNA is an important tool for preparation of plasmid DNA for further cloning, polymerase chain reaction (PCR), construction of mutants and protein expression. In this section the general method of preparation of reagents and media for cultivation of bacteria and introduction of the bacterial strains that I used in my project will be described.

2.3.1 Growth media

Media and reagents used for cultivation of bacteria were sterilized by autoclaving at 121°C under a pressure of 15 pound per square inch (psi) for 15 min or filtering though a 0.22 μm springe-filter if the chemicals were heat sensitive.

2.3.1.1 Luria-Bertani (LB) broth

One litre (L) of LB broth was prepared by mixing 25 g of Luria Broth Base (Oxoid) with MQ water and sterilized by autoclaving. It consists of 1% (w/v) pancreatic digest of casein, 0.5% (w/v) yeast extract, 170 mM NaCl. LB broth was used for cultivation of bacteria harbouring recombinant plasmids for plasmid preparation and protein expression. A final concentration of 100 μg/ml of ampicillin was added to the sterilized LB broth before use, if necessary.

2.3.1.2 LB agar

LB agar is used for single bacterial colony growing and isolation. It consists of LB broth ingredients and 1.5% (w/v) Bacto agar. Appropriate antibiotic is added to the LB agar cooled to 50°C after autoclaving if necessary. LB-agar plates were prepared by pouring approximately 20 ml of LB agar per petri dish of 80 mm diameter.

2.3.1 3 Ampicillin preparation

Ampicillin (Sigma) is the only antibiotic used in the present experiments. Working stock solution of ampicillin was prepared with sterilized MQ water to a final concentration of 50 mg/ml. This solution was sterilized by filtering though a 0.22 μm syringe-filter and kept at –20°C until used. The working concentration of ampicillin in LB broth or LB agar was 100 μg/ml.

2.3.2 Bacterial strains

2.3.2.1 XL1-Blue *E.coli* strain

XL1-Blue subcloning-grade competent cells were purchased from Stratagene. These are ready made competent cells and are used for general plasmid propagation. Their genotype is endA1 (endonuclease deficient), recA (recombination deficient) and hsdR$^-$ (hsdR

mutation); the hsdR mutation prevents the cleavage of cloned DNA by EcoK (hsdR) endonuclease system, the recA mutation helps ensure insert stability and the endA1 mutation greatly improves the quality of plasmid miniprep DNA.

2.3.2.2 BL21(DE3) *E.coli* strain

BL21(DE3) *E.coli* strain was purchased from Novagen. It was used for T7 promoter-driven protein expression vector, e.g. Thx/pET32a (Section 2.10). The chromosome of BL21(DE3) already has the bacteriophage T7 gene 1 inserted into it. Bacteriophage T7 RNA polymerase is the product of this gene. The gene is expressed under the control of isopropy-1-thio-β-D-galactopyranoside (IPTG) inducible lacUV5 promoter. Expressed bacteriophage T7 polymerase binds to the bacteriophage T7 promoter of the Thx/pET32a vector for protein expression of target gene downstream of the promoter. The BL21(DE3) strain is deficient in lon protease and lacks the ompT outer membrane protease that can degrade protein during purification. Cells were made competent by the method mentioned in Section 2.4.1.

2.3.3 Storage of strains

Permanent stocks of hosts with or without recombinant DNA are best kept as glycerol stocks. Single colonies were inoculated into 50 ml LB broth containing 100 μg/ml of ampicillin if necessary in a 250 ml flask. Culture was grown at 37°C with vigorous shaking until the absorbance at 600 nm reached 0.6-0.8. One ml of glycerol stock was prepared by mixing 900 μl of culture and 100 μl 80% (v/v) glycerol and kept at -80°C.

2.4 INTRODUCTION OF PLASMID DNA INTO COMPETENT CELLS

2.4.1 Preparation of competent cells

A single colony was picked from a LB agar plate streaked with a bacterial strain that was

incubated 12-16 hr at 37°C. This single colony was then used to inoculate a 5 ml LB broth and grown at 37°C overnight with vigorous shaking. One ml of overnight culture was transferred to 100 ml of fresh LB broth on the next day and incubated at 37°C with vigorous shaking. Cells were kept on ice for 20 min after the optical density of cells had reached 0.5 (by measuring the absorbance 600 nm). Cells were transferred to two 50 ml chilled centrifuge tubes and centrifuged for 10 min at 5,000 x g at 4°C. Supernatants were discarded and 5 ml of chilled 0.1 M $MgCl_2$ solution was added to each tube to suspend the cell pellets. Suspended cells were kept on ice for 10 min. Centrifugation was performed at 5,000 x g for 10 min at 4°C. Supernatants were discarded. Cell pellets were suspended by adding 1 ml per tube of chilled 0.1 M $CaCl_2$. Cells were kept on ice for 2 hr after which glycerol was added to a final concentration 10 % (v/v). The cells were dispensed as 50 µl aliquots in microcentrifuge tubes and frozen immediately by placing the tubes in liquid nitrogen. Frozen cells were stored at -80°C until use.

2.4.1 Transformation of plasmid DNA to competent cells

Plasmid DNA (0.1-50 ng) or ligation reaction up to 5 µl was transferred to 50 µl thawed competent cells on ice. The mixture was incubated on ice for 20 min. Heat shock was performed by placing tubes in a 42°C water bath for 45 s. Tubes were placed on ice for 2 min, LB broth was added to a final volume of 1 ml and these were incubated at 37°C for 30 min with shaking at 250 rpm. Cells were harvested by centrifugation at 18,000 x g for 30 s. Supernatants were removed, the pellet was suspended in 200 µl of LB broth and evenly spread on a LB plate with 100 µg/ml of ampicillin added if necessary. The plate was incubated at 37°C for 12-16 hr.

2.5 Extraction and purification of DNA plasmids

There are three methods for DNA purification. Two of the methods, alkaline lysis with

SDS and QIAGEN® Plasmid Midi Kit, are for DNA extraction from bacterial cells depending on the DNA purity required. Alkaline lysis with SDS was used for general DNA plasmid preparation but the QIAGEN® Plasmid Midi Kit was used instead where high purity DNA is needed for transfection in human embryonic kidney (HEK) cells (Section 2.17). The third method was used to purify DNA fragments on agarose gel. Generally, after restriction enzyme digestion, digested DNA fragments have been fractionated on a 1% (w/v) agarose gel and desired DNA bands were extracted and purified by QIAquick® Gel Extraction Kit.

2.5.1 Alkaline lysis with SDS

A single bacterial colony from a freshly streaked LB plate with 100 μg/ml ampicillin was picked and inoculated in 3 ml LB broth containing 100 μg/ml ampicillin in a 10 ml centrifuge tube. The culture was incubated overnight at 37°C with vigorous shaking. Half of the culture (1.5 ml) was transferred to a microcentrifuge tube and was centrifuged at 18,000 x g for 30 s. Supernatant was discarded and the bacterial pellets were suspended in 150 μl chilled resuspension buffer (50 mM Tris-HCl at pH8.0, 10 mM EDTA, 100 μg/ml RNase A). Cells were lysed by adding 200 μl freshly prepared lysis buffer (200 mM NaOH, 1% (w/v) SDS). The contents were mixed by inverting the tube five times. After placing the tube on ice, 150 μl of chilled neutralisation buffer (3M potassium acetate at pH5.5) was added. Contents were mixed by inverting the tube five times, incubated on ice for 5 min and centrifuged at 18,000 x g for 5 min. Supernatants were transferred to a fresh tube with 200 μl of chloroform. Contents were mixed thoroughly and centrifuged at 18,000 x g for 5 min. The upper aqueous layer was transferred to a fresh tube with 2 volumes of chilled 100% ethanol, kept at -20°C for an hour and centrifuged at 18,000 x g for 30 min. Supernatants were discarded, pellets were washed with 200 μl 70% (v/v) ethanol, tubes were centrifuged for 5 min at 18,000 x g and supernatants were again discarded. Pellets

were air dried and dissolved in 20 µl of sterilized MQ water.

2.5.2 QIAGEN® plasmid midi kit

Up to 100 µg of plasmid can be purified from 25 ml culture by using the QIAGEN® Plasmid Midi Kit. Procedure is followed according to the QIAGEN® plasmid purification handbook. A single bacterial colony from a freshly streaked LB plate with 100 µg/ml ampicillin was picked and inoculated in 5 ml LB broth containing 100 µg ampicillin as a starter culture. The inoculated broth was grown at 37°C for 8 hr with vigorous shaking. A new 25 ml LB broth containing 100 µg ampicillin was seeded with 50 µl of starter culture. This new seeded culture was grown at 37°C for 16 hr with vigorous shaking. Bacterial cells were harvested from the 16 hr culture by centrifugation at 6,000 x g for 15 min at 4°C. Supernatant was discarded and pellets were suspended in 4 ml of Buffer P1 (50 mM Tris-HCl at pH8.0, 10 mM EDTA, 100 µg/ml RNase A). Bacterial cells were lysed by adding 4 ml of Buffer P2 (200 mM NaOH, 1% (w/v) SDS). The contents were mixed gently by inverting five times and incubated at room temperature for 5 min. Mixture solution was neutralized by adding 4 ml of chilled buffer P3 (3 M potassium acetate at pH5.5). The solution was mixed by inverting and incubated on ice for 15 min. Cells were centrifuged twice at 20,000 x g for 30 min at 4°C. Supernatant was loaded to a Buffer QBT (50 mM MOPS at pH7.0, 750 mM NaCl, 15% (v/v) isopropanol, 0.15% (v/v) Triton X-100) equilibrated resin that contained in QIAGEN-tip 100. Resin was washed twice with 10 ml of Buffer QC (50 mM MOPS at pH7.0, 1 M NaCl, 15% isopropanol). DNA was eluted with 5 ml of Buffer QF (50 mM Tris-HCl at pH8.5, 1.25 M NaCl, 15% (v/v) isopropanol). Eluted DNA was precipitated by adding 3.5 ml isopropanol and the mixture was then centrifuged at 15,000 x g for 30 min at 4°C. Supernatants were discarded. DNA pellets were washed with 2 ml of 70% (v/v) ethanol and centrifuged at 15,000 x g for 10 min. Supernatants were discarded. The pellet was air-dried for 10 min and DNA was

dissolved in 50 µl of sterilized MQ water.

2.5.3 QIAquick® gel extraction kit

Digested DNA fragments fractionated by agarose gel electrophoresis (Section 2.6.1) were purified by QIAquick® Gel Extraction Kit (Qiagen). A fragment of the desired size on the agarose gel was excised by a clean and sharp scalpel and transferred to a weighed microcentrifuge tube. Weight of the excised agarose gel was determined. Kit provided Buffer QG with pH indicator (300 µl) was added to gel of mass 100 mg. Gel mixture was incubated at 50°C for 10 min until the gel slice had completely dissolved. Dissolved gel solution was transferred to a QIAquick® spin column in the 2 ml collection tube provided. DNA was bound on the silica-gel membrane of the spin column. Excess solution was removed by centrifugation for 1 min at 18,000 x g. Flow-through in the collection tube was discarded. The column was washed by adding 750 µl of kit provided Buffer PE and the solution was centrifuged for 1 min at 18,000 x g. Flow-through was discarded. In order to ensure all the washing solution was removed, one more centrifugation at 18,000 x g for 1 min was performed. A new microcentrifuge tube for collecting eluted DNA was attached to the QIAquick® column. Sterilized MQ water (20 µl) was applied to the QIAquick® column for DNA elution and the tube with column was centrifuged at 18,000 x g for 1 min. Eluted DNA in the new microcentrifuge tube was stored at -20°C until use.

2.6 DNA ANALYSIS

2.6.1 DNA agarose gel electrophoresis

2.6.1.1 DNA gel preparation

Agarose gel 1% (w/v) was used to separate DNA fragment sizes from 0.5 kb to 10 kb. Gel was prepared by mixing 100 ml TAE (40 mM Tris-HCl at pH7.6, 20 mM acetic acid, 1 mM EDTA) electrophoresis buffer with 1 g of agarose. The slurry was heated in a

microwave oven until the agarose melted.

2.6.1.2 Gel casting and electrophoresis

The agarose solution was cooled to 60°C and poured into the gel tray (Bio-Rad) with the comb in place. After the gel was completely solidified and the comb was removed, the gel was placed in the electrophoresis tank (Bio-Rad). Enough TAE buffer was added into the electrophoresis tank to a depth of about 1 mm above the agarose gel. Samples were mixed with gel-loading buffer IV (0.25% (w/v) bromophenol blue and 40% (w/v) sucrose in water) (Sambrook & Russell 2001). The sample mixtures were loaded into the well of the submerged gel. DNA marker (Section 2.6.2) was loaded into one of the slots of the gel. A constant voltage of 100 V was applied. When the bromophenol blue had migrated almost to the end of the gel, electrophoresis was stopped.

2.6.1.3 DNA agarose gel staining and visualisation

Gel was placed into the appropriated volume of 0.5 μg/ml ethidium bromide (EtBr) stain that can cover the gel entirely for 5-15mins. Gel was destained with MQ water in a volume the same as the EtBr stain solution for 5 to 10 mins and then rinsed briefly with MQ water to remove any residual staining solution. Destained gel was placed on an ultraviolet (UV) transilluminator (UltraLum) for nucleic acid visualisation and analysis. DNA-EtBr complexes are able to be illuminated with UV light of 254, 302, or 366 nm. Sensitivity decreases with illumination at higher wavelengths. For result recording and photographing, 254 nm UV light was used. If the gel was to be used for DNA extraction, 302 nm or higher wavelength was used for reduction of DNA nicking. The visualised images were captured with a CCD video camera module (Sony) and saved as tif files and re-produced using iPhoto Plus V3.1 software (Ulead).

2.6.2 Estimation of the molecular Size of DNA fragments

Two DNA ladders were used to estimate the molecular size of DNA fragments. The 1 kb DNA ladder (BioLabs) has 10 DNA bands ranging from 0.5 to 10 kb. The 2-Log DNA ladder (BioLabs) has 19 DNA bands ranging from 0.1 to 10 kb. The 1 kb DNA ladder was used at 0.5 μg per well or the 2-Log DNA ladder was used at 1 μg per well and loaded parallel with the sample in the DNA gel electrophoresis for estimating the size of DNA fragments in the sample.

2.6.3 Determination of DNA concentration

The concentration of DNA was determined using GeneQuant II (Amersham). The absorbance of the DNA sample was measured at wavelengths 260 nm and 280 nm. A sample absorbance of one at 260 nm corresponded to 50 μg/ml of double strand DNA (dsDNA). Ratio of absorbance readings at wavelength 260 nm to 280 nm was an indicator of DNA purity. Ideally this ratio is 1.8 (Sambrook & Russell 2001).

2.7 DNA CLONING

2.7.1 Restriction enzyme digestion

At least ten units of appropriate restriction enzymes (BioLabs and, Promega) were used for digestion of 1 μg of DNA with company's supplied restriction enzyme buffers. If necessary, bovine serum albumin (BSA) was added to the reaction mixture according to the manufacturer's guideline. Total volume of the reaction mixture was made up to 20 μl with sterilized MQ water and incubated at 37°C for 3 hr.

2.7.2 DNA ligation

T4 DNA ligase (BioLabs) was used to catalyse the formation of a phosphodiester bond between juxtaposed 5' phosphate and 3' hydroxyl termini in dsDNA. Cohesive end ligation

reactions set up by mixing T4 DNA ligase buffer (50 mM Tris-HCl at pH7.5, 10 mM $MgCl_2$, 10 mM DDT, 1 mM ATP, 25 μg/ml BSA) and 400 units of T4 DNA ligase with the DNAs to be ligated in a concentration of 0.1 to 1 μM. Sterilized MQ water was added to make the final volume of the ligation mixture up to 20 μl and was incubated at room temperature for 10 min.

2.8 DNA SEQUENCING

It is important to verify the DNA sequence of the mutant constructs to confirm introduction of the desired mutations and that no unwanted mutations occur during PCR. The Sequencing Centre of the Institute of Medical and Veterinary Science (IMVS) provides analysis and running of cleaned up sequencing reactions performed by the client using a 3700 ABI Prism™ capillary DNA sequencer (Applied Biosystems). The system accepts DNA sequencing reactions performed by the method of ABI Prism BigDye Terminator Cycle Sequencing Ready Reaction version 3.1 (Section 2.8.1, Applied Biosystems) and recommended purification of sequencing products by isopropanol precipitation (Section 2.8.2). SouthPath & Flinders Sequencing Facility (FUSA) provided a similar service as IMVS and included performing cycle sequencing reactions using BigDye Terminator v3.1 chemistry and analysis of the products using an Applied Biosystems 3100 Genetic Analyser. Recommended amounts of dsDNA were 2.5 μg in 10 μl and of primer were 6.4 pmoles in 2 μl for successful analysis in the FUSA.

2.8.1 DNA sequencing reactions

DNA sequencing reactions were performed with ABI Prism BigDye Terminator Cycle Sequencing Ready reaction version 3.1 kit (Applied Biosystems). Reaction mixtures consisted of 150-300 ng of dsDNA template, 3.2 pmoles of sequencing primer and 4-8 μl of the ABI Prism BigDye Terminator Ready reaction mix. In the Ready reaction mix, the

dye terminator, deoxynucleoside triphosphates (dATP, dCTP, dITP, dUTP), AmpliTaq DNA polymerase, $MgCl_2$, and buffer (Tris-HCl at pH9.0) were already premixed. Sterilized MQ water was added to make up to a final volume of 20 µl. Light mineral oil (40 µl) was added to overlay the reaction mixture. Reaction was performed in the DNA Thermal Cycler 480 (Applied Biosystems) with twenty-five cylces of denaturation at 96°C for 30 s, annealing at 50°C for 15 s and elongation at 60°C for 4 min. Once the cycles were finished, the reaction was held at 16°C until performing product purification (Section 2.8.2).

2.8.2 Purification of extension products

Amplified products after the sequencing reaction were subjected to isopropanol precipitation for purification. Oil overlay was removed carefully. Eighty µl of 75% (v/v) isopropanol was added. Contents were mixed by inverting a few times. Extension products were precipitated by leaving the mixture at room temperature for 15 min. Contents were centrifuged at 12,000 x g for 20 min and supernatants discarded. DNA pellets were washed with 150 µl of 70% (v/v) isopropanol. Contents were centrifuged at 12,000 x g for 15 min, supernatants removed and DNA pellet dried at 65°C for 5 min before sending to the sequencing centre at the IMVS.

2.9 MUTANT DNA CONSTRUCTIONS

Site-Directed Mutagenesis (Section 2.9.2) was used to introduce several nucleotide mutations in the desired template DNA. This method allows site-specific mutations to be created directly in the full-length dsDNA template and eliminates the need for subcloning into specialized vectors. An overview of the Site-directed mutagenesis method is shown in Figure 2.1. It utilises a pair of oligonucleotides primed on a denatured dsDNA template during thermocycling and DNA synthesis in a linear fashion by a high-fidelity DNA polymerase (*Pfu* or *Pwo*). Staggered nicks were generated in the mutated plasmids. In

order to reduce the background colonies that came from non-mutated wild-type DNA template in the site-directed mutagenesis, the amplified products were treated with the restriction enzyme *Dpn* I, which specifically cleaves fully methylated $G^{me6}ATC$ sequence, to remove the bacterially generated DNA used as template in the site-directed mutagenesis but not the DNA synthesized during the process. Mutants made by the site-directed mutagensis method were for transfection in the HEK cells (Section 3.2.4). Chloride conductance of mutants was measured using the patch-clamp technique (Section 3.2.5.1).

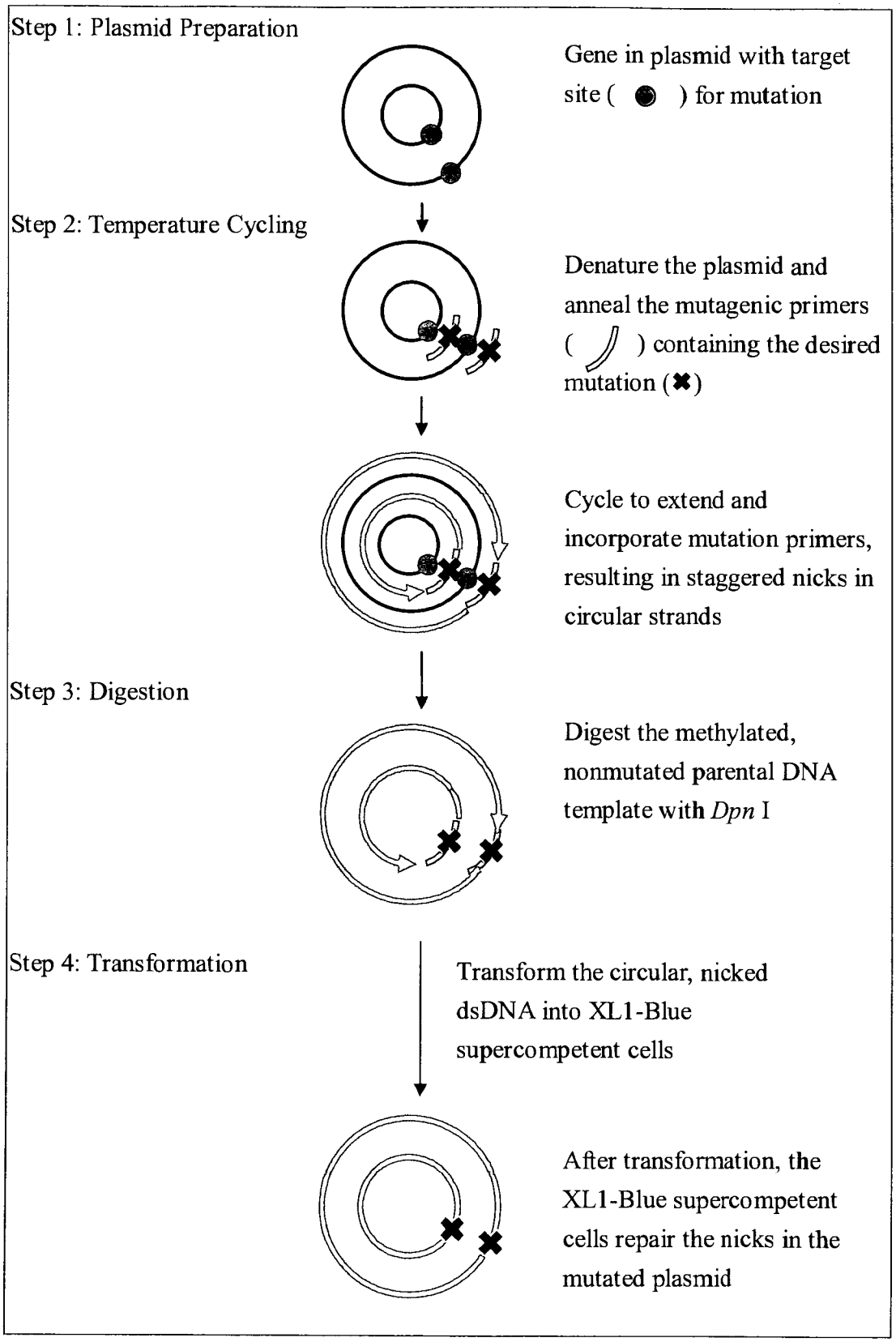

Figure 2.1 Overview of the site-directed mutagenesis method

2.9.1 Primer synthesis and preparation

All primers were synthesized by Sigma-Genosys with standard purification. The synthesized primer pellets were suspended in sterilized MQ water to a final concentration of 10 µg/µl as a stock solution and stored at –20°C until used. Working primer solution in a concentration of 100 ng/µl was prepared from stock solution by diluting ten fold with sterilized MQ water and stored at –20°C.

2.9.2 Site-directed mutagenesis

2.9.2.1 Primer design

Desired mutations were set in the middle of each of a pair of the mutagenic oligonucleotide primers with 10 to 15 bases of correct sequence on both sides of the mutation site. These pairs of primers anneal to the same sequence of opposite strands of DNA template. The length of primer was approximately 25 to 45 bp, with a minimum 40% GC content and terminated in a G or C residue. Melting temperature (T_m) of the primers was 78°C or greater and was calculated by the following formula mentioned from the instruction manual.

$T_m = 81.5 + 0.41(\%GC\ content) - 675/\ number\ of\ base\ pair\ of\ primer - \%\ mismatch$

2.9.2.2 Site-directed mutagenesis reaction mixture set up

Either *Pwo* DNA polymerase (Roche) or *Pfu* DNA polymerase (Promega) was used for amplification of the desired mutant DNA in the site-directed mutagenesis. Two master mixes were set up individually in two sterilized 0.65 ml microcentrifuge tubes on ice. Each final volume was 25 µl made up by sterilized MQ water. The master mix One contained 200 µM each of dATP, dCTP, dGTP and dTTP (Promega), 125 ng each of forward and reverse mutagenic primers and 50-100 ng dsDNA template. The master mix Two contained

5 µl 10X *Pwo* PCR buffer (100 mM Tris-HCl at pH8.85 at 20°C, 250 mM KCl, 50 mM $(NH_4)_2SO_4$, 20 mM $MgSO_4$) and 2.5 unit of Pwo DNA polymerase or 5 µl 10X Pfu PCR buffer (200 mM Tris-HCl at pH8.8 at 25°C, 100 mM KCl, 100 mM $(NH_4)_2SO_4$, 20 mM $MgSO_4$, 1 mg/ml nuclease-free BSA, 1% (v/v) Triton X-100) and 1.25 units of *Pfu* DNA polymerase. The Mg^{2+} concentration can be optimised to increase the amplified products in the reaction mixture performed using *Pwo* DNA polymerase. Optimum concentration was determined by replacing normal 10X *Pwo* PCR buffer with 10X *Pwo* PCR buffer without $MgSO_4$ and adding various volumes of the 25 mM $MgSO_4$ stock solution provided in the kit to ascertain maximal amplification.

2.9.2.3 Thermocycling conditions for site-directed mutagenesis

An Eppendorf Mastercycler Personal (Eppendorf) was used for performing thermocycling amplification. Each site-directed mutagenesis procedure comprised one cycle of denaturation at 95°C for 30 s followed by twenty cycles of denaturation at 95°C for 30 s, annealing at 55°C for 30 s and elongation at 68°C for 2 min per one kb of DNA template length. Reactions were stopped at 16°C and the amplified products were kept at 4°C until analysed by DNA agarose gel electrophosis (Section 2.6.1).

2.9.2.4 Digesting the amplified products by *Dpn* I restriction enzyme

The *Dpn* I restriction enzyme is specific for methylated and hemimethylated DNA. DNA isolated from almost all *E.coli* strains is dam methylated. Thus, original template DNA without mutation is susceptible to *Dpn* I digestion. Ten units of *Dpn* I were used per tube of site-directed mutagenesis amplified products and incubated at 37°C for 1 hr. About one tenth of *Dpn* I digested products were transferred into XL1-Blue subcloning-grade competent cells for transformation. Mutants colonies were selected by restriction enzyme digestion and correct sequences of mutants were confirmed by DNA sequencing (Section

2.8).

2.10 PROTEIN CONCENTRATION DETERMINATION

2.10.1 Bicinchoninic acid (BCA) method

The BCA™ Protein Assay Kit (Pierce) is a detergent-compatible method. In an alkaline system, protein forms a colour-complex with bicinchoninic acid. BCA working reagent was prepared by mixing 50 parts BCA Reagent A with 1 part of BCA Reagent B. Samples (25 µl) were mixed with 200 µl of BCA™ working reagent in 96-well plate. Plates were incubated at 37°C for 30 min and the absorbance at 562 nm was measured using a Mutiskan Ascent microplate reader (Thermo). Protein concentration was again determined from a calibration curve using BSA as a protein standard.

2.11 PROTEIN ANALYSIS

2.11.1 Polyacrylamide gel electrophoresis (PAGE)

SDS-PAGE is a denaturing and reducing gel electrophoresis (Laemmli 1970). Protein samples were separated by electrophoresis after being treated with heat in the presence of a reducing agent, DTT, and a denaturing agent, SDS. DTT reduces any disulfide bridges present that are holding together the protein tertiary structure. SDS is an anionic detergent which binds strongly and denatures the secondary and non–disulfide–linked tertiary structures. As a result, the protein was unravelled into its constituent peptide chain after the treatment. Bound SDS contributes negative charge to the denatured protein in a proportion to its mass. The approximate mass of separated protein bands can be estimated with reference to protein markers of known molecular size under the same conditions. Gels were prepared as a 4% stacking gel (pH6.8) (for concentrating the protein samples into stacked bands before they enter the separating gel) layered on the top of a 12% acrylamide separating gel (pH8.8). Protein samples were diluted 1:5 with sample buffer (0.225M

Tris-HCl at pH6.8; 50% (v/v) glycerol; 5% (w/v) SDS; 0.05% (w/v) bromophenol blue and 0.25 M DTT). After heating the sample mixture at 100°C for 5 min, 20 μl of the mixture was applied to the sample slot. Electrophoresis was carried out at a constant voltage of 200 V for about 45 min. Gels were stained for 1 hr with Coomassie Brilliant Blue R-150 (Bio-Rad) dissolved in a solution of 40% (v/v) methanol and 10% (v/v) acetic acid. Finally, the gels were destained in 40% (v/v) methanol and 10% (v/v) acetic acid.

2.11.2 Western blot

Protein samples were separated by SDS-PAGE (Section 2.11.1) with prestained protein marker (Invitrogen, Bio-Rad). After electrophoresis, 12% SDS-PAGE gels were immersed in ice-cold transfer buffer (25mM Tris-HCl at pH8.3, 192 mM glycine, 20% (v/v) methanol and 0.1% (w/v) SDS) for 5 min, assembled with a 0.45 micron nitrocellulose membrane (Bio-Rad) in a sandwich of two layers of filter paper and fiber pads and submerged in transfer buffer in a Mini Trans-Blot Cell (Bio-Rad). Proteins were electrotransferred at a constant voltage 100 V for 1 hr using a Bio-Ice Cooling Unit to absorb the heat generated during rapid electrophoretic transfers.

2.11.2.1 Target protein recognized by anti-C-tail antibody

Transblotted membranes were washed with Phosphate buffered saline (PBS; 10 mM phosphate buffer at pH7.4, 2.7 mM KCl, 137 mM NaCl) for 5 min and non-specific binding was blocked with blocking buffer of 5% (w/v) skim milk power (Diploma) in PBS for 1 hr at room temperature. Primary antibody, (anti-C-tail) raised against the final 15 amino acids of rat ClC-1 (Gurnett *et al.* 1995), was diluted 500 times with blocking buffer. Membranes were incubated with the primary antibody at 4°C overnight and washed three times with PBS-T (PBS with 0.05% (v/v) Tween-20) for 10 min. The second antibody was goat anti-rabbit IgG (H+L) horseradish peroxidase conjugate (Bio-Rad). Membranes were

incubated with 1:500 diluted second antibody for 1 hr at room temperature and then washed twice with PBS-T and once with PBS.

2.11.3 Signal development of antibody recognized protein band on Western blot

2.11.3.1 Chromogenic detection

Liquid 3,3'-diaminobenzidine tetrahydochloride (DAB) -plus Substrate Kit (Zymed) was used to detect the horseradish peroxidase conjugated antibody. Working substrate solution was prepared by mixing 10 drops each of the kit-provided Solutions one, two and three with MQ water to a the final volume of 10 ml. Working substrate solution was poured onto the nylon transfer membrane and incubated at room temperature until the brown coloured band reached the desired intensity, after which the chromogenic reaction was stopped by rinsing the membrane with MQ water. Membranes were air dried and stored.

2.11.3.2 Enhanced chemiluminescence (ECL) detection

For ECL, the whole process had to be performed in a darkroom. Freshly prepared 5 ml solution A (0.1 M Tris-HCl at pH8.0, 0.4 mM p-coumaric acid, 2.5 mM Luminol) and 5 ml solution B (0.1 M Tris-HCl at pH8.0, 0.018% (v/v) H_2O_2) were poured on the nylon transfer membrane for 1 min with agitation. The liquid was discarded. The membrane was placed in between two stacks of plastic wraps and covered with the Curix ultra UV-C medical X-ray film (AGFA). This whole setting was put inside an exposure cassette for 5 to 60 s. Film was passed through the CP1000 automatic film processor (AGFA) for development. Exposure time was adjusted dependent on the luminescence intensity of the membrane signal.

2.12 Maintenance of human embryonic kidney (HEK) cells

Either HEK293 or HEK293T cells were used in experiments for the expression of

wild-type ClC-1 and its mutants for the patch-clamp analysis of chloride current. Throughout the text of this thesis, the term "HEK" will cover either HEK293 or HEK293T cells.

2.12.1 General condition for cultivation of HEK cells

HEK cells were cultured in T-25 cm^2 flasks and the cells were split when they reached 70-80% confluency. The procedure for subculturing the HEK cells in Section 2.16.3. Cells were maintained in a 37°C incubator (Sanyo) containing a humidified atmosphere of 5% CO_2 in air. Cells were cultured in Dulbecco's Modified Eagle Medium (D-MEM, Gibco) supplemented with 0.1 mM MEM Non-Essential Amino Acids (Gibco), 4 mM L-Glutamine (Sigma) and 10% (v/v) fetal bovine serum (FBS, Sigma). Throughout the text of this thesis, D-MEM+ is corresponding to D-MEM with all three supplements.

2.12.2 Revival of frozen HEK cells

When required a frozen vial of HEK cells was thawed rapidly by briefly immersing the vial in a 37°C water bath. The outside surface of the vial was wiped with 70% (v/v) ethanol immediately upon thawing and then the entire contents were transferred to a T-25 cm^2 flask containing 4 ml of pre-warmed D-MEM+ and incubated at 37°C, 5% CO_2, in a humidified incubator. Cells were examined under an inverted microscope the next day. Successfully revived cells showed a flat morphology and adhered well to the bottom of the flask. Cells were passaged upon reaching 70-80 % confluency within 2 to 4 days (Section 2.12.3).

2.12.3 Passaging the HEK cells

Cells were split when they reached 70-80 % confluency. The medium was removed and the cells were washed with D-MEM. Cells were trypsinized by adding 1 ml of trypsin- EDTA

solution (0.25% w/v trypsin and 0.02% w/v EDTA, Sigma) and incubated at room temperature for about 3 min until the cells had detached. Trypsinization was stopped by adding 5 ml D-MEM+. Cells were counted (Section 2.12.5) and an aliquot of 2 to 5 x 10^4 viable cells/cm^2 was seeded into 4 ml of pre-warmed D-MEM+ in T-25cm^2 flask.

2.12.4 Freezing cells

Mid log phase cells in a T-25 cm^2 flask were treated with 1 ml of trypsin-EDTA solution until the cells were detached from the floor of the flask. Cells were counted (Section 2.12.5) and centrifuged at 125 x g for 10 min. Supernatant was aspirated. A desirable density of cells for the preparation of frozen stock is at least 1-2 x 10^6 cells/ml in freezing medium (typically, 10% D-MEM, 80% FBS and 10% DMSO). Cells were dispensed as 1 ml aliquots into sterile cryovials. Cells in cryovials were frozen slowly at –20°C for 1-2 hr and then transferred to –80°C overnight. Finally, the cells were stored in liquid nitrogen until revival (Section 2.12.2).

2.12.5 Viable cell counts using trypan blue

Trypan blue stains dead cells (which have damaged membranes) but not the viable cells. One part of 0.4% (w/v) trypan blue in PBS was mixed with 5 parts of cell suspension and allowed to stand for 5 min at room temperature. A small aliquot (approximate 10 μl) of the mixture was transferred to a KOVA® Glasstic® slide 10 Grid chamber (Hycor). Both stained and unstained cells were observed under an inverted microscope. Unstained cells within the lines of the nine small 0.33 mm grid squares were counted and the number of cells per ml was determined by the following equation described from the company's instruction manual.

Number of cells per ml = Number of cells averaged in nine square grids x 90 x 10^3

CHAPTER THREE: ESTABLISHING A MAMMALIAN EXPRESSION SYSTEM FOR FUNCTIONAL COMPLEMENTATION EXPERIMENTS IN ClC-1

3.1 INTRODUCTION

Functional complementation experiments in proteins have been performed either with fragments produced by limited proteolysis (Galakatos & Walsh 1987; Schonberger *et al.* 1996), by chemical cleavage (Li & Bewley 1976), or by site-directed mutagenesis (Pecorari *et al.* 1996) to study the correct folding of the cleaved fragment and the essential region for functional activity. Similarly, analyses of CLC proteins have used functional complementation strategies for determining the essential and individual globular structures of their C-tails (Schmidt-Rose & Jentsch 1997a; Maduke, Williams & Miller 1998; Estévez *et al.* 2004; Hebeisen *et al.* 2004; Mo *et al.* 2004; Wu *et al.* 2006). *Xenopus* oocytes have been commonly used for functional characterisation of plasma membrane proteins (Sigel & Minier 2005) and also have been used for detection of the resultant pharmacological properties of different subunit combinations of transmitter-gated ion channels, eg, from the *Torpedo* nicotinic acetylcholine receptor (Mishina *et al.* 1984) and the pentameric $GABA_A$ receptor (Sigel *et al.* 1990). Co-expression of complementary domains of various ion channels have then been rationally performed in the *Xenopus* oocyte expression system to test for functional recombination (Schmidt-Rose & Jentsch 1997a; Estévez *et al.* 2004; Mo *et al.* 2004; Csanady *et al.* 2005; Wu *et al.* 2006).

When I began this project (in mid 2002), mammalian expression systems for full-length CLC had been well established. Mutations had been introduced into the full-length CLC and expressed in cultured mammalian cells for electrophysiological analysis. There had been no reports, however, of co-transfection of two complementary CLC cDNAs,

co-expression of the respective protein products nor of their functional recombination in mammalian cells. Owing to the difficulties of interpretation of expression experiments in *Xenopus* oocytes systems compared with channel function in native muscle cells, the problem of importing new *Xenopus* into Australia and the expenses associated with housing them in our facility due to strict quarantine regulations, I chose to utilize cultured mammalian cells for all of my functional complementation work. In order to do this, I decided to use the original mammalian vector, pCIneo (which had accommodated the full-length hClC-1 for mutagenesis analysis), to clone the N-terminal membrane-resident region of hClC-1. In conjunction with this, an IRES bicistonic expression vector, pMSCV-IRES-GFP (pMIG), which has an internal ribosome entry site (IRES), would permit the translation of two open reading frames from one messenger RNA. In this case, one reading frame would encode the modified C-tail peptide and the other a GFP protein for assessing the expression efficiency in the HEK cells.

Aim: To establish functional hClC-1 channel complementation in a mammalian expression system by co-transfecting plasmid DNA from two mammalian vectors.

According to functional complementation experiments previously performed on CLC, when the channel was split within the sequence between CBS1 and CBS2, co-expression of the two resultant non-functional individual fragments was able to rescue channel function, comparable with that of wild-type full-length CLC (Schmidt-Rose & Jentsch 1997a; Maduke, Williams & Miller 1998; Estévez *et al.* 2004; Hebeisen *et al.* 2004; Mo *et al.* 2004; Wu *et al.* 2006). Representative complementary fragments for hClC-1 are $N_{1\text{-}720}$ + $C_{721\text{-}988}$ and these had been used by us as the positive control for split channel recombination in the *Xenopus* oocyte system (Wu *et al.* 2006). They would also be used

here to provide evidence for the functional reconstitution in the mammalian system (see later).

3.2 EXPERIMENTAL PROCEDURES

3.2.1 Modification of the multi-cloning site of the pMIG

The original pMIG vector (a gift from Peter Diamond, Hanson Institute, Adelaide, Australia) contains *Eco*RI, *Hpa*I and *Xho*I sites in the multi-cloning site. In order to establish a new multi-cloning site including a *Bam*HI site before the *Eco*RI site for the later cloning step, the site-directed mutagenesis approach (Section 2.9.2) provided a simple solution. To modify the multi-cloning site of pMIG a pair of appropriate primers (BEpMIG_forward, CTA GGC GCC GGG ATC CGA ATT CCT CGA GGA TCA ATT CC and BEpMIG_reverse, GGA ATT GAT CCT CGA GGA ATT CGG ATC CCG GCG CCT AG) were prepared. After that the original *Eco*RI and *Hpa*I sites were substituted by a *Bam*HI (pink letters in the BEpMIG_forward primer) and *Eco*RI site (blue letters in the BEpMIG_forward primer), respectively. A plasmid map of the modified vector, designated as BEpMIG, is shown in Figure 3.1.

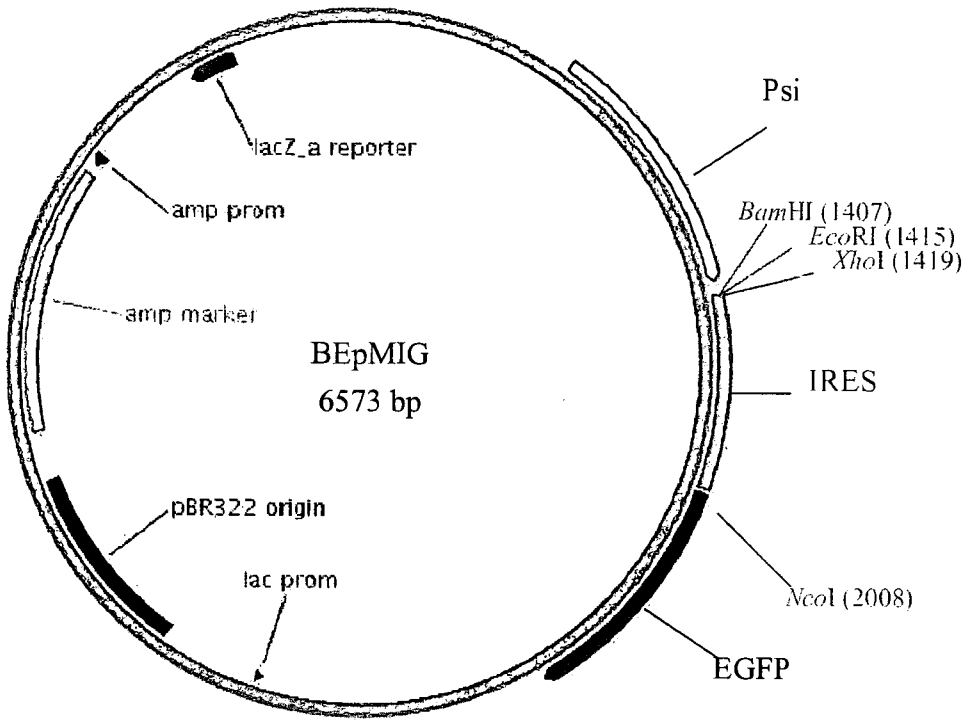

Figure 3.1 Plasmid map of BEpMIG

The multiple cloning site was re-organized to *Bam*HI, *Eco*RI and *Xho*I sites. The IRES permits the translation of two open reading frames, one encodes the recombinant protein of interest and the other a reporter gene, such as enhanced green fluorescent protein (EGFP), from one mRNA.

3.2.2 Introduction of a *Bam*HI site at the N-terminus of the $C_{721-988}$ peptides in pTLN

A pair of BamhG721 primers (Sense: 5'-GGC AGA TCG CGA GGA TCC ATG GAG GGC AAG AGC GAG C-3' and antisense: 3'-GCT CGC TCT TGC CCT CCA TGG ATC CTC GCG ATC TGC C-5') were used to introduce *Bam*HI sites (underlined) into the $C_{721-988}$/pTLN constructs using site-directed mutagenesis (Section 2.9.2)

3.2.3 *Bam*HI restriction enzyme digestion

In order to distinguish the mutated clone from the non-mutated one, the constructs were digested by *Bam*HI restriction enzyme. After digestion mutated constructs separated by 1% agarose electrophoresis showed as linear DNA rather than undigested circular DNA.

Verified clones were inserted into the BEpMIG vector.

3.2.4 Cloning of the $C_{721-988}$ peptide into BEpMIG

Plasmids containing the *Bam*HI-modified $C_{721-988}$ peptide as well as the BEpMIG vector were digested with *Bam*HI and *Eco*RI restriction enzymes. Linearised $C_{721-988}$ peptide were ligated into linearised BEpMIG vector. Schematic diagrams of the cloning steps are shown in Figure 3.2. Resultant $C_{721-988}$/BEpMIG colonies underwent restriction enzyme selection by *Nco*I. Two fragments were generated when the $C_{721-988}$ was successfully cloned into the BEpMIG vector. After selection of correct DNA constructs, these were sequenced at the IMVS Sequencing Centre to confirm the correct sequence of the insert in the BEpMIG vector. Sequencing results are shown in Appendix C.

Step 1: Digestion of BEpMIG and $C_{721-988}$ fragment in pTLN ($C_{721-988}$/pTLN) with *Bam*HI and *Eco*RI restriction enzymes

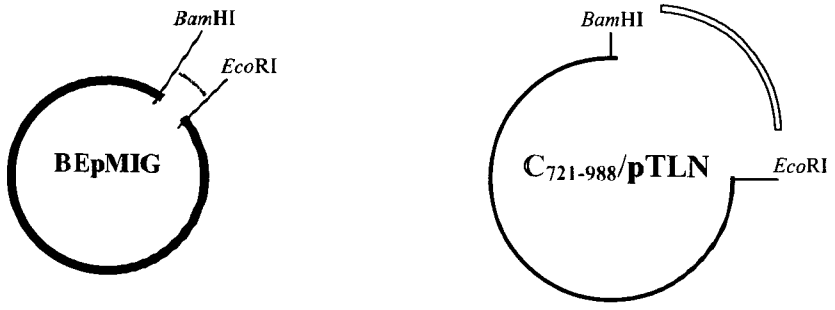

Step 2: The digested fragment (hClC/C_X) was ligated with the linearised BEpMIG vector

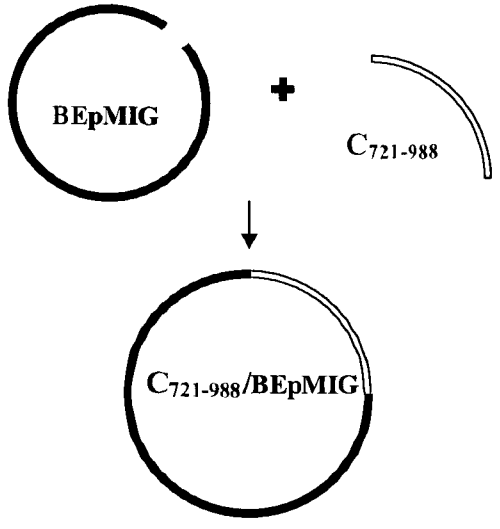

Figure 3.2 Schematic diagrams of the cloning steps of $C_{721-988}$ fragment into BEpMIG vector

3.2.5 Co-transfection of N_{1-720} and $C_{721-988}$ constructs in HEK cells

Five different DNA transfection reactions listed in Table 3.1 were set up as pilot studies to ensure that functional complementation experiments in my mammalian expression system could elicit a chloride current the same as full-length hClC-1 expression.

Table 3.1 List of DNAs used in six sets of DNA transfection reactions

Transfection reaction	DNA used for transfection
1	Negative control (No DNA)
2	BEpMIG
3	N_{1-720}/pCIneo + BEpMIG
4	$C_{721-988}$/BEpMIG
5	N_{1-720}/pCIneo + $C_{721-988}$/BEpMIG

Reaction one is the negative control for the assessment of background current characteristics in the HEK cells. Measured patch-clamp currents from transfections two to four were compared with it to confirm the empty BEpMIG expression vector and that the N-terminal and C-terminal constructs expressed alone (with empty BEpMIG) show no current distinguishable from control. Reaction five was the positive control for split channel reconstitution which was achieved by co-expression of typical functional complementary N- and C-terminal constructs (Schmidt-Rose & Jentsch 1997a).

In each transfection reaction, about 1 μg of total DNA was diluted with D-MEM to a final volume 21 μl. Plus™ reagent (4 μl, Invitrogen) was added to pre-complex the DNA. Reaction mixtures were incubated for 15 mins at room temperature. Lipofectamine™ stock reagent (Invitrogen) was diluted by adding 1 μl to 174 μl of D-MEM and set aside. The diluted lipofectamine was added immediately to the pre-complexed DNA-Plus when the first 15 min incubation ended, proceeding directly into another 15 min incubation. HEK cells were harvested by trypsinization (Section 2.12.3), counted (Section 2.12.5) and diluted to 2 x 10^5 cells/ml. Diluted cells (200 μl) were transferred to DNA-Plus-lipofectamine reagent mixture. Aliquots of the cells/DNA mixture (100 μl) were transferred onto the top of acid treated glass slides (5 mm x 10 mm) which were placed

inside the wells of 12-well plate. Plates were incubated at 37°C under 5% CO_2 for 4 hr. Reactions were stopped by rinsing cells once with D-MEM after which 1 ml of D-MEM+ was added to the well and incubated at 37°C under 5% CO_2 for 24 hr.

3.2.6 Electrophysiological study

3.2.6.1 Patch-clamping

Patch-clamp experiments were conducted on an anti-vibration table (Newport) at room temperature in the whole-cell configuration, as we have described previously (Rychkov *et al.* 1996). Cells were continuously superfused with filtered bath solution containing 140 mM NaCl, 4 mM KCl, 2 mM $CaCl_2$, 1 mM $MgCl_2$, 5 mM HEPES adjusted to pH7.4 with NaOH and observed under an inverted phase-contrast microscope with normal and fluorescence light source. Patch pipettes were pulled from borosilicate glass and coated with Sylgard (Dow Corning) using a Flaming/Brown micropipette puller model P-97 (Sutter) with four pulling steps and the tip of the pipette was fire polished. Typical resistance of a pulled pipette was 1-2 MΩ when filled with the pipette solution and immersed in bath solution. Standard pipette solution contained 75 mM Cs-glutamate, 40 mM CsCl, 10 mM EGTA and 10 mM HEPES adjusted to pH7.2 with KOH. Series resistance did not exceed 4 MΩ and was 80% compensated. An Axopatch 200B microelectrode amplifier (Axon Instruments) measured currents that were filtered at 5 kHz.

3.2.6.2 Voltage steps protocols

Three protocols named as activation, tail-1 and tail-2 were used to analyse the WT hClC-1 and mutant chloride currents.

The activation protocol was used to examine the characteristic currents, which were observed as, rapid deactivation upon hyperpolarisation and an inward rectification at

negative potentials. With this protocol, the channels were activated by stepping to +40 mV for 80 ms from -30 mV holding potential and deactivating currents were then induced by stepping from -140 mV to +80 mV for 80 ms with 20 mV increments.

The tail-1 and tail-2 protocols were used to determine the apparent open probability of overall gating (P_o^o) and common gating (P_o^c), respectively, as described below in Section 3.2.6.3. Although a real open probability can be determined when it is possible to observe and analyse single channel current traces, where the observations are on whole-cells (e.g. because single channel conductance is too small), the ensemble currents are merely reflections of the apparent open probability of all channels under the existing conditions.

In my tail-1 protocol, voltages were stepped from -140 mV to +60 mV from a holding potential of -30 mV for 160 ms and these conditioning pulses were followed by a test pulse to -100 mV for 40 ms.

My tail-2 protocol was similar except for a short additional conditioning pulse to +180 mV for a duration 0.4 ms before the -100 mV test pulse step. This short additional conditioning step was to ensure activation of all the protopore gating so that the current in response to the test pulse would be modulated only by common gating (Accardi & Pusch 2000).

Apparent open probabilities of protopore gating (P_o^p) were then determined by dividing the individual values for P_o^o by the respective values for P_o^c at each voltage. Voltage steps applied in the activation, tail-1 and tail-2 protocols are shown in Figure 3.3-3.5. For all protocols the holding potential was -30 mV, that is, approximately the normal resting potential of HEK cells.

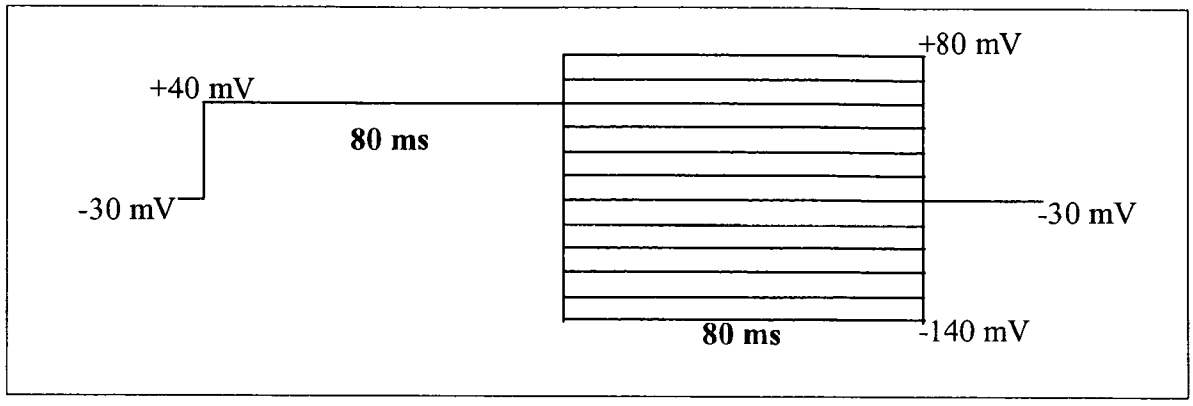

Figure 3.3 Voltage steps of activation protocol

Test pulses of 80 ms duration, ranging from -140 mV to +80mV in 20 mV increments were each preceded by a 80 ms prepulse to +40 mV.

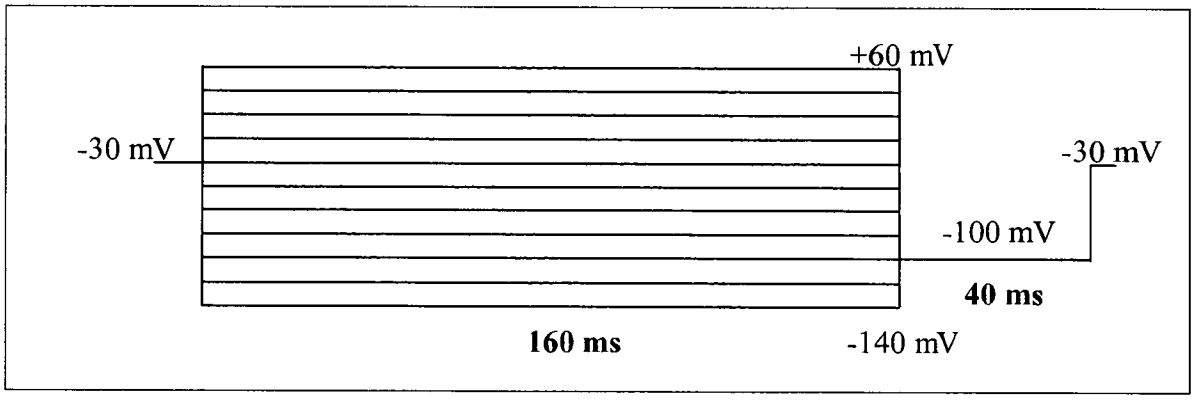

Figure 3.4 Voltage steps of tail-1 protocol

Conditioning pulse of 160 ms duration ranging from +60 mV to -140 mV in -20 mV decrements were each followed by a 40 ms test pulse to -100 mV.

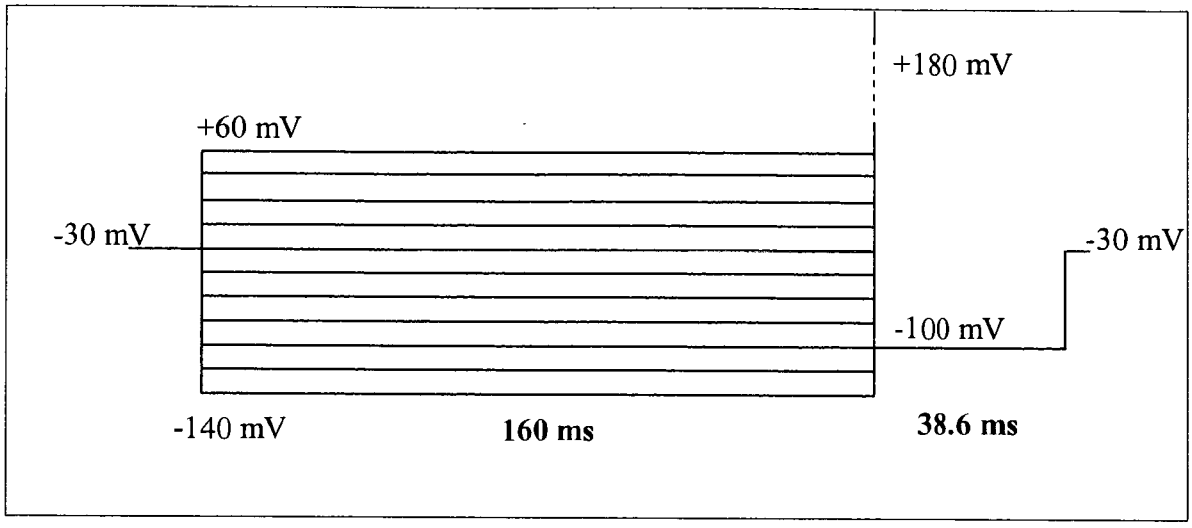

Figure 3.5 Voltage steps of tail-2 Protocol

As for the tail-1 protocol except for an additional conditioning step to +180 mV for 0.4 ms between the 160 ms conditioning and 38.6 ms test pulse to ensure all the protopore gates are opened by that +180 mV pulse.

3.2.6.3 Data analysis

Data was collected using a Digidata 1322A digitizer (Axon Instruments). The tail currents resulting from the tail-1 and tail-2 protocols were fitted by a double exponential equation (Eq 3.1) to estimate the peak tail current, I_{max}, by extrapolating the curve back to the beginning of the pulse (Aromataris *et al.* 2001; Bennetts *et al.* 2001) using pCLAMP v9 software (Axon Instruments). Examples of current traces of WT hClC-1 in response to tail-1 and tail-2 protocols are shown in Figure 3.6 and Figure 3.7, respectively.

$$I = A_1\exp(t/\tau_1)+A_2\exp(t/\tau_2)+C \qquad \textbf{(Eq. 3.1)}$$

Where A_1 and A_2 represent the amplitude of the fast and slow exponential components of current deactivation, τ_1 and τ_2 are their constants, t is time, C represents the amplitude of the steady-state component and $I_{max}=I_{(t=0)}$.

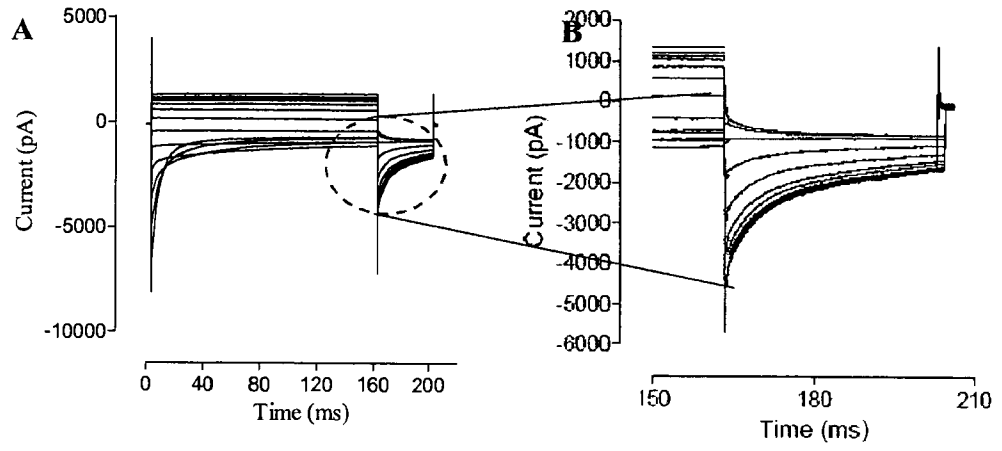

Figure 3.6 Example of current traces from hClC-1 in response to the tail-1 protocol

(A) The first 160 ms is the conditioning pulse period with voltage steps from +60 mV to -140 mV. The circled region is the -100 mV test pulse region for 40 ms. The current traces from the test pulse region were fitted with double exponential equation (Eq. 3.1) to obtain the peak tail current. **(B)** The enlarged region of the circled area from **(A)** shows red dots that indicate the approximate values of the peak tail current obtained by extrapolation of the fitted curves (in blue).

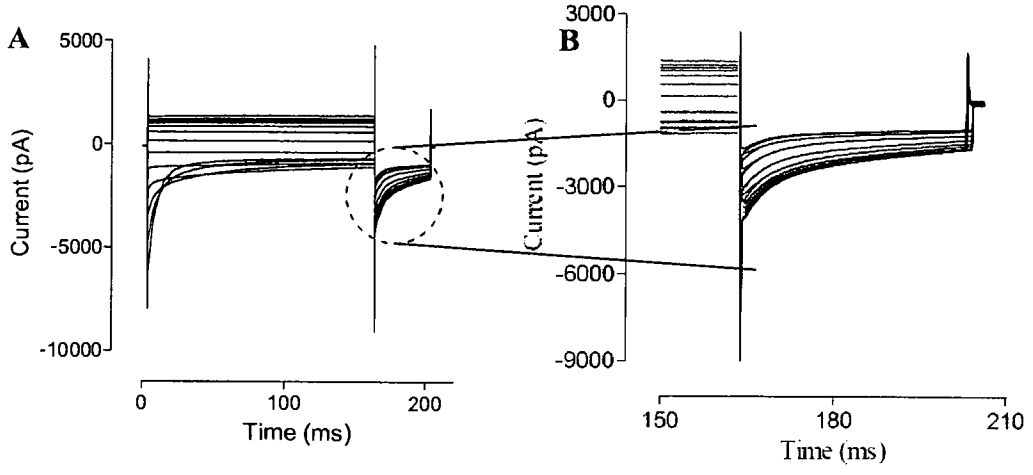

Figure 3.7 Example of current traces of hClC-1 response to the tail-2 protocol

(A) The circled region is the -100 mV test pulse region for 40 ms after a short +180mV conditioning pulse to ensure all the protopore gates are opened. The current traces from the test pulse region were fitted with double exponential equation (Eq. 3.1) to obtain the peak tail current. **(B)** The enlarged region of the circled area from **(A)** shows red dots that indicate the approximate values of the peak tail current obtained by extrapolation of the fitted curves (in blue).

Peak tail currents obtained in this way for each conditioning or test voltage were normalized and fitted with a Boltzmann distribution equation (Eq. 3.2). Typical results, expressed as P_o^o, P_o^c and P_o^p are shown in Figure 3.10, 3.11 and 3.12, respectively. A Boltzmann function is normally used to fit data where charge distributions are involved, for example, in relation to the voltage dependence of voltage gated cation channels in which the gating depends on a defined charged voltage sensor. Its derivation is based on the hypothesis that the energy of the charged voltage sensor is given by the charge (q) multiplied by the electric field (E) in which it is found (qE). The exponential of qE/kT then represents the rate at which the sensor passes some energy barrier while the open probabilities of gating depend on these rates and the electric field is proportional to the voltage (V). In the case of CLC chloride channels, there is no defined voltage sensor and voltage-dependent gating is associated with permeation of the singly charged chloride ion along with some consequent conformational change. Perhaps because a chloride ion opens the protopore to many chloride ions by, itself, passing some energy barrier, the Boltzmann function fits the apparent open probability data for CLC channels and has been used for this purpose by all authors in the field.

$$P_o(V) = P_{min} + (1-P_{min})/(1+\exp((V_{½}-V)/k)) \qquad \textbf{(Eq. 3.2)}$$

Where P_{min} is minimum P_o at a very hyperpolarised potential, V is the membrane potential, $V_{½}$ is the potential at which $P_o=(1+P_{min})/2$ (half-maximal activation) and k is the slope factor. The maximum P_o is presumed to be 1 (Rychkov *et al.* 1996; Bennetts *et al.* 2001). All these analyses were done using GraphPad Prism software. At least three different cell measurements were used for analysis and results are given as means ± S.E.M.

3.3 RESULTS

3.3.1 Electrophysiological measurements on positive and negative controls

Currents in HEK cells transfected with either BEpMIG, N_{1-720}/pCIneo + BEpMIG or $C_{721-988}$/BEpMIG, alone, measured by patch-clamping were indistinguishable from "no DNA" transfected HEK cells. Their current traces in response to the activation protocol are shown in Figure 3.8. These were small, generally linear and with no kinetic features in any way similar to those of WT hClC-1 chloride currents.

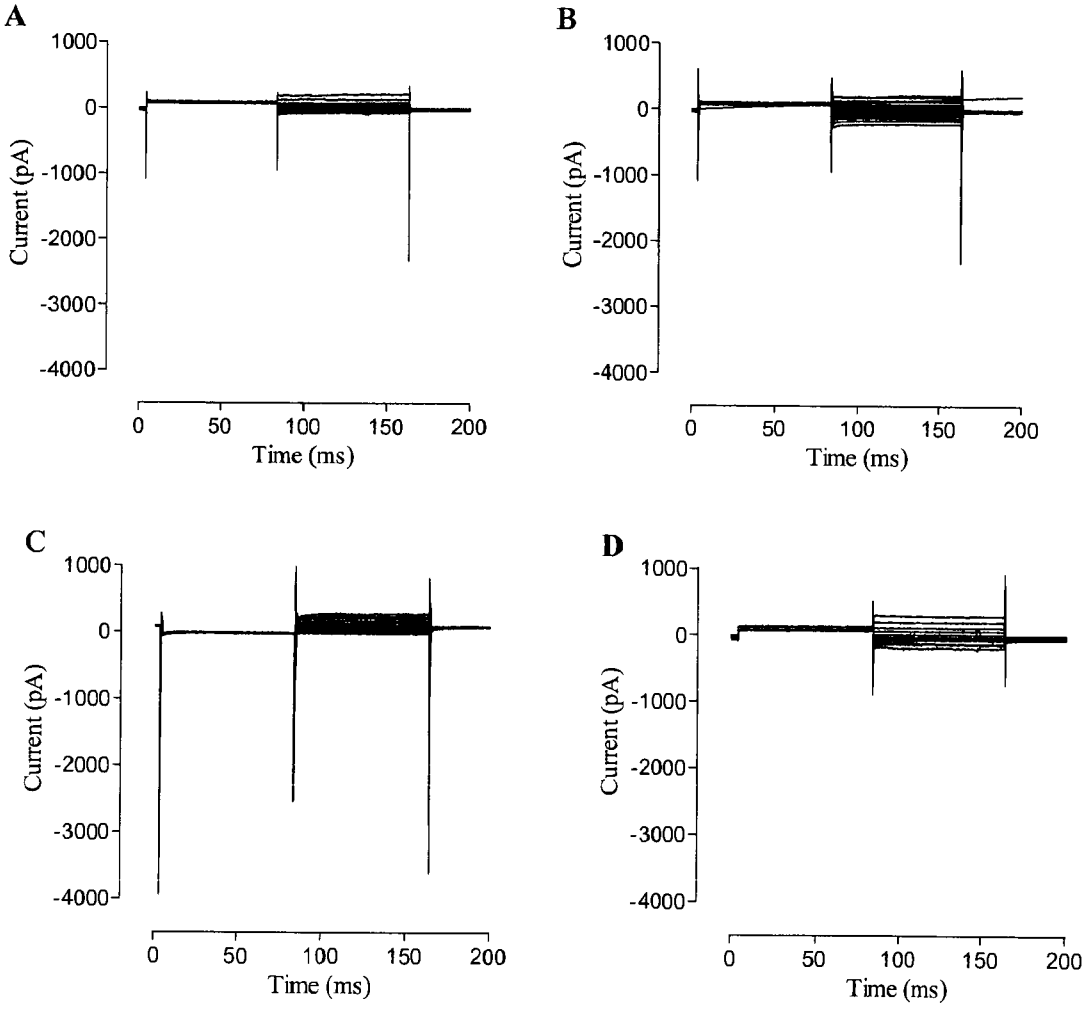

Figure 3.8 Current traces measured from "no DNA" transfected HEK cell (A), BEpMIG transfected HEK cell (B), N_{1-720}/pCIneo+BEpMIG transfected HEK cell (C) and $C_{721-988}$/BEpMIG transfected HEK cell

Currents were all small and had none of the characteristics of WT hClC-1 chloride currents (see below, Figure 3.9. Current traces were obtained from the activation protocol: 80 ms test pulses ranging from -140 mV to +80 mV in 20 mV increments each preceded by a 80 ms conditioning pulse to +40 mV.

By contrast, HEK cells co-transfected with $N_{1\text{-}720}$/pCIneo and $C_{721\text{-}988}$/BEpMIG showed typical ClC-1 chloride currents in response to the activation protocol (Figure 3.9). Currents are inwardly rectifying and display a rapid, partial deactivation upon hyperpolarisation. Using the tail-1 protocol, P_o^o (Figure 3.10) was determined and the $V_{½}$ is –66.5 mV ± 1.5. The P_o^c (Figure 3.11) and the P_o^p (Figure 3.12) were determined by using the tail-2 protocol and by dividing the individual values for P_o^o by the respective values for P_o^c at each voltage, respectively. Table 3.2 is a summary of the Boltzmann parameters (including $V_{½}$, k and P_{min}) of $N_{1\text{-}720}$/pCIneo + $C_{721\text{-}988}$/BEpMIG compared with full-length hClC-1/pCIneo result which was obtained by my colleague, Dr. Jennie Cederholm and was corrected for junction potentials

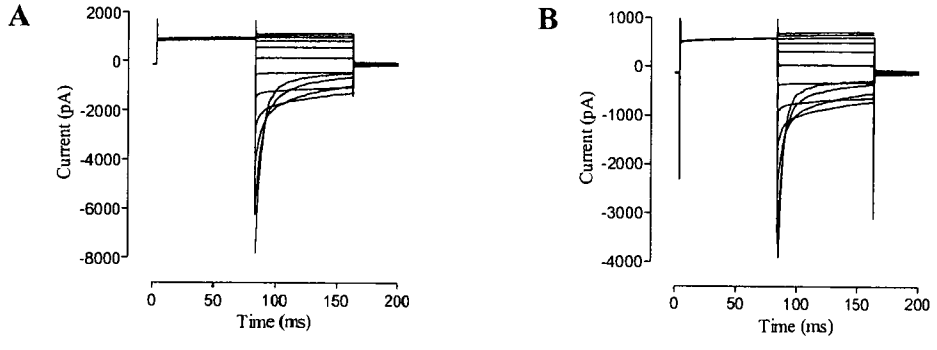

Figure 3.9 Current traces in a whole cell patch of full-length hClC-1/pCIneo (A) and $N_{1\text{-}720}$/pCIneo + $C_{721\text{-}988}$/BEpMIG (B) co-transfected HEK cell evoked by the activation protocol

Channels reconstituted from the co-expressed complimentary fragments have characteristics that are indistinguishable from those of full-length WT hClC-1 channels.

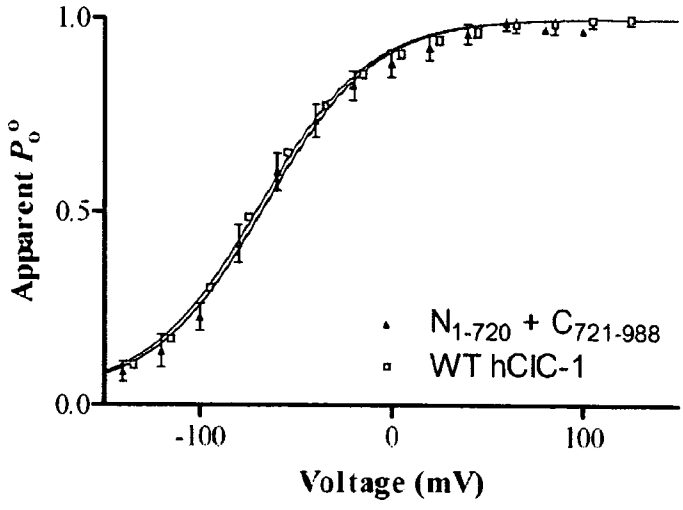

Figure 3.10 Overall apparent open probability (P_o^o) of full-length WT hClC-1 and split channel construct (N_{1-720} + $C_{721-988}$)

Overall apparent overall open probabilities of split channel construct (N_{1-720} + $C_{721-988}$, green), indistinguishable from those of WT (brown), were derived from instantaneous currents obtained by extrapolating tail currents of patch-clamped HEK cells in the tail-1 protocol and the data were fitted by a Boltzmann distribution equation (Eq. 3.2). Results are given as means ± S.E.M. (n=8 for full-length WT hClC-1 and n=3 for the split channel, N_{1-720} + $C_{721-988}$). Boltzmann parameters ($V_{½}$, k and P_{min}) are shown in Table 3.2.

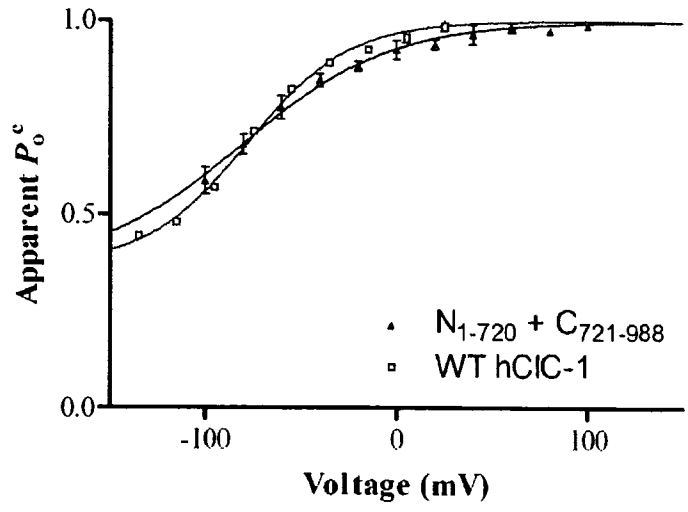

Figure 3.11 Apparent open probability for common gate (P_o^c) of full-length WT hClC-1 and split channel construct (N_{1-720} + $C_{721-988}$)

Very similar apparent open probabilities of common gating, for full-length WT hClC-1 (brown) and split channel construct (N_{1-720} + $C_{721-988}$, green) are shown. They were derived from instantaneous currents obtained by extrapolating tail currents of patch-clamped HEK cells in the tail-2 protocol and the data were fitted with a Boltzmann distribution equation (Eq. 3.2). Results are given as means ± S.E.M. (n=8 for full-length WT hClC-1 and n=3 for split channel for N_{1-720} + $C_{721-988}$). Boltzmann parameters ($V_{½}$, k and P_{min}) are shown in Table 3.2.

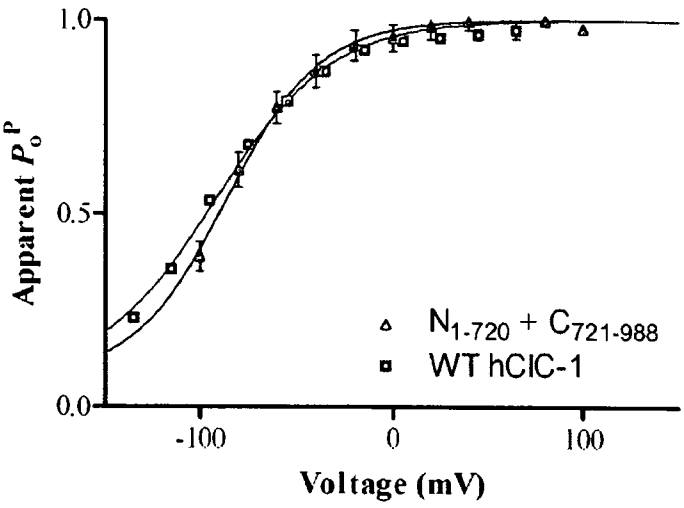

Figure 3.12 Apparent open probability for the protopore gate (P_o^P) of full-length WT hClC-1 and split channel construct N_{1-720} + $C_{721-988}$

Apparent open probabilities of protopore gating, for full-length WT hClC-1 (brown) and split channel construct (N_{1-720} + $C_{721-988}$, green), were derived by dividing the individual values for P_o^o by the respective values for P_o^c at each voltage and the data were fitted with a Boltzmann distribution equation (Eq. 3.2). Again they are practically indistinguishable. Results are given as means ± S.E.M. (n=8 for full-length WT hClC-1 and n=3 for split channel for N_{1-720} + $C_{721-988}$). Boltzmann parameters ($V_{½}$, k and P_{min}) are shown in Table 3.2.

Table 3.2 Summary of the Boltzmann parameters of overall, common and protopore gating of full-length WT hClC-1 and split channel construct (N_{1-720} + $C_{721-988}$)

(*fixed for curve fitting)

	hClC-1 (n=8)			N_{1-720} + $C_{721-988}$ (n=3)		
GATING	$V_{½}$ (mV)	k	P_{min}	$V_{½}$ (mV)	k	P_{min}
Overall	-69.3±1.0	28.8±1.0	0.03*	-66.5±1.5	28.7±1.4	0.03*
Common	-77.9±4.0	26.5±2.2	0.37	-80.8±15	39.0±4.6	0.36*
Protopore	-91.6±6.5	30.1±3.0	0.08*	-85.9±8.8	24.1±2.9	0.08*

3.4 DISCUSSION

3.4.1 Establishing a mammalian expression system for split ClC-1 channel experiments

I have demonstrated the success of my mammalian split channel expression system by co-expression of N_{1-720}/pCIneo with $C_{721-988}$/BEpMIG. Chloride channel properties measured from the co-expression are indistinguishable from those of full-length WT hClC-1 channel previously expressed in the mammalian cells. Previously, most of the split channel experiments using CLC proteins have been done in the *Xenopus* oocyte expression system (Schmidt-Rose & Jentsch 1997a; Maduke, Williams & Miller 1998; Estévez *et al.* 2004; Mo *et al.* 2004; Wu *et al.* 2006), whereas, in fact, mammalian cells should provide the most appropriate biological environment for the expression of human genes. Discrepancies have been ascribed to the differences of expression systems, capped mRNA injection in the *Xenopus* oocyte system compared with DNA transfection in the mammalian cell system. Comparing some previous split channel results obtained from other groups using *Xenopus* oocytes or mammalian cells for ClC-1 expression, anomalous results have been seen (Estévez *et al.* 2004; Hebeisen *et al.* 2004). Estévez and colleagues, using *Xenopus* oocytes for expression of ClC-1, showed that deletion of CBS2 is tolerated but not deletion of CBS1 (Estévez *et al.* 2004), whereas, Hebeisen and colleagues presented the opposite result using mammalian tsA201 cells for expression (Hebeisen *et al.* 2004). We do not know what the significant difference between these two systems, but it has been reported that certain channel results have been able to be obtained from one system but not the other (Goldin 2006). This might be due to some endogenous channel signal (Ackerman, Wickman & Clapham 1994; Kowdley *et al.* 1994; Buyse *et al.* 1997; Reyes *et al.* 2004) or endogenous mRNA interaction (Sigel 1990). Sigel has mentioned that *Xenopus* oocytes contain a large pool of untranslated endogenous mRNA which might be

triggered to translate during the process of introducing exogenous mRNA, the protein products, in turn, interacting with each other and forming a functional channel (Sigel 1990).

In our laboratory, full-length, mutated and truncated hClC-1 cDNAs have, over a number of years, been expressed in human embryonic kidney (HEK) cells, for functional characterisation. Two mammalian expression vectors have been used for co-transfection in HEK cells. One is pCIneo for inserting hClC-1 cDNA while the other is pEGFP for expressing enhanced green fluorescent protein (EGFP). Visualisation of these green fluorescent protein (GFP) expressing cells indicated that they were transfected and also that they were probably expressing hClC-1 protein simultaneously. This allowed ready identification of the co-transfected cells for functional characterisation.

In order to establish my split channel system in mammalian cells, the two-vector procedure was maintained. To accommodate hClC-1 cDNA with its C-tail truncated, pCIneo was again used. But instead of using pEGFP for expression of GFP, BEpMIG vector, which is a bicistronic mammalian expression vector, was used. The notable feature of BEpMIG is that it contains an internal ribosome entry site (IRES) from encephalomyocarditis virus (ECMV). This IRES element permits the translation of two open reading frames from one mRNA. The first gene, C-terminal cDNA, inserted downstream of the promoter was translated in a cap-dependent way and the second gene, GFP cDNA, located after IRES was translated in a cap-independent manner. Studies have identified that the second gene expression level is lower than that of the first gene (Trouet *et al.* 1997; Mizuguchi *et al.* 2000). It is for this reason that the C-terminal peptide was inserted in the first gene position, to ensure that it was expressed. Thus, the BEpMIG vector served two purposes here. Firstly,

it is acting as a reporter gene expression vector, identifying the transfected cells (Marshall *et al.* 1995). Secondly, the intensity of the GFP signal should be correlated with the expression level of the C-terminal fragment (Trouet *et al.* 1997).

CHAPTER FOUR: IMPAIRED CHLORIDE CHANNEL FUNCTION, ASSOCIATED WITH MYOTONIA, RESTORED BY CO-EXPRESSION OF THE $C_{721-988}$ FRAGMENT WITH DISEASE-CAUSING NONSENSE MUTANTS OF HUMAN ClC-1 IN MAMMALIAN CELLS

4.1 INTRODUCTION

In the human skeletal muscle voltage-gated chloride channel (hClC-1), more than 20 nonsense mutations have been identified that are associated with myotonic muscle disease (Colding-Jorgensen 2005). As might be expected since they are likely to give rise to truncated, non-functional ClC-1 protein, most of the nonsense mutations cause the recessive myotonic phenotype. There is one nonsense mutant, R894X, close to the C-terminus of ClC-1, that is reported to be involved in both dominant and recessive phenotypes. Using site-directed mutagenesis, heterologous expression and electrophysiological studies, the behaviour of this C-terminal truncated mutant has been revealed in previous studies. It conducts mutant chloride currents with alteration of voltage dependence. The pure recessive phenotype nonsense mutants that have been reported have at least 117 or more amino acids deleted from the C-terminus. Electrophysiological studies have shown that the functions of most of these mutants were abolished (Estévez *et al.* 2004; Hebeisen *et al.* 2004; Wu *et al.* 2006).

Interestingly, certain site-directed non-functional C-terminal truncated CLC mutants were able to have their activity restored by co-expression of the complementary missing fragment *in vitro* (Schmidt-Rose & Jentsch 1997a; Maduke, Williams & Miller 1998). Thus, applying appropriate functional complementation might be able to alleviate conditions caused by similar nonsense mutations. This has been demonstrated for certain

Dent's disease nonsense mutations in ClC-5 that have been co-expressed in *Xenopus* oocytes with the complementary missing C-terminal peptide to restore channel function to that of wild type (Mo *et al.* 2004). We propose that a similar functional complementation strategy could be applied to hClC-1 for functional restoration of naturally occurring nonsense mutations.

To test this hypothesis, three different nonsense mutations found in myotonia congenita patients were selected to determine if the channel function could be restored to that of full-length wild-type hClC-1 by co-expression with a single C-tail fragment, Gly721 to Leu 988, in the established mammalian expression system described in Chapter III. Mutant hClC-1 cDNAs were generated by introducing an E717X stop codon between CBS1 and CBS2 (Plassart-Schiess *et al.* 1998), a Q807X stop codon generated nine amino acids before CBS2 (Chen *et al.* 2001) and an G872X stop codon generated at the end of CBS2 which mimicked fs872X (de Diego *et al.* 1999). Constructs were expressed in the human embryonic kidney cell (HEK293) expression system. Patch-clamping was used to analyse the chloride current of the mutants and co-transfected channels

Aim: To attempt to restore function to various naturally-occurring C-terminal-truncated mutants of hClC-1 by co-expressing the well-known, and well-expressed, C-terminal fragment, $C_{721\text{-}988}$.

4.2 EXPERIMENTAL PROCEDURES

4.2.1 Construction of DNAs mimicking naturally-occurring C-terminal truncated mutants

4.2.1.1 Primers designed for mutant construction

Three disease-associated C-terminal truncated mutants of hClC-1 were selected, E717X, Q807X and fs872X (represented by G872X). The first two mutations cause the recessive phenotype and the latter one causes the dominant phenotype. Three pairs of primers were designed for constructing the corresponding mutants. The primer sequences are shown in Table 4.1. They are named h717X, h807X and h872X. Site-directed mutagenesis (Section 2.9.2) was used to introduce two consecutive stop codons (TGATAG) in a full-length hClC-1.

Table 4.1 Primer sequences for constructing naturally-occurring C-terminal truncated mutants

The sequences in red colour are two consecutive stop codons. The underlined nucleotides encode the final amino acid of the mutant being constructed.

h717X	D716
forward	5'GGATGAGGATGAGGACTGATAGCTCTCTGGCAAGAGCG
reverse	3'CGCTCTTGCCAGAGAGCTATCAGTCCTCATCCTCATCC
h807X	E806
forward	5'GATTGAGGCCTGGGAGTGATAGCAGCTGAGCCAGCCTG
reverse	3'CAGGCTGGCTCAGCTGCTATCACTCCCAGGCCTCAATC
h872X	E871
forward	5'CAGAAGGCCATTGAGTGATAGACCAAGTCTGGGGTG
reverse	3'CACCCCAGACTTGGTCTATCACTCAATGGCCTTCTG

4.2.1.2 Molecular method for construction of mutants

A full-length hClC-1 in a pGEM-4Z vector (Promega) was used as DNA template in the site-directed mutagenesis for construction of mutants. Construction methods were as described in Section 2.9. The sequences of constructed mutants were verified by DNA sequencing with Sp6-F promoter sequencing primer, ATT TAG GTG ACA CTA TAG AA, at the FUSA Sequencing Facility (Section 2.8).

4.2.1.3 Cloning of mutants into the pCIneo

Three sequences, confirmed as pGEM-4Z mutant constructs ($N_{1\text{-}716}$/, $N_{1\text{-}806}$/ and $N_{1\text{-}871}$/pGEM-4Z) and pCIneo vector were digested by *Nhe*I and *EcoR*I. Digested fragments were separated by agarose electrophoresis (Section 2.6.1). Corresponding vector and mutated gene fragments were purified by QIAquick Gel extraction Kit (Section 2.5.3) and ligated together (Section 2.7.2). Schematic diagrams of the cloning steps are shown in Figure 4.1.

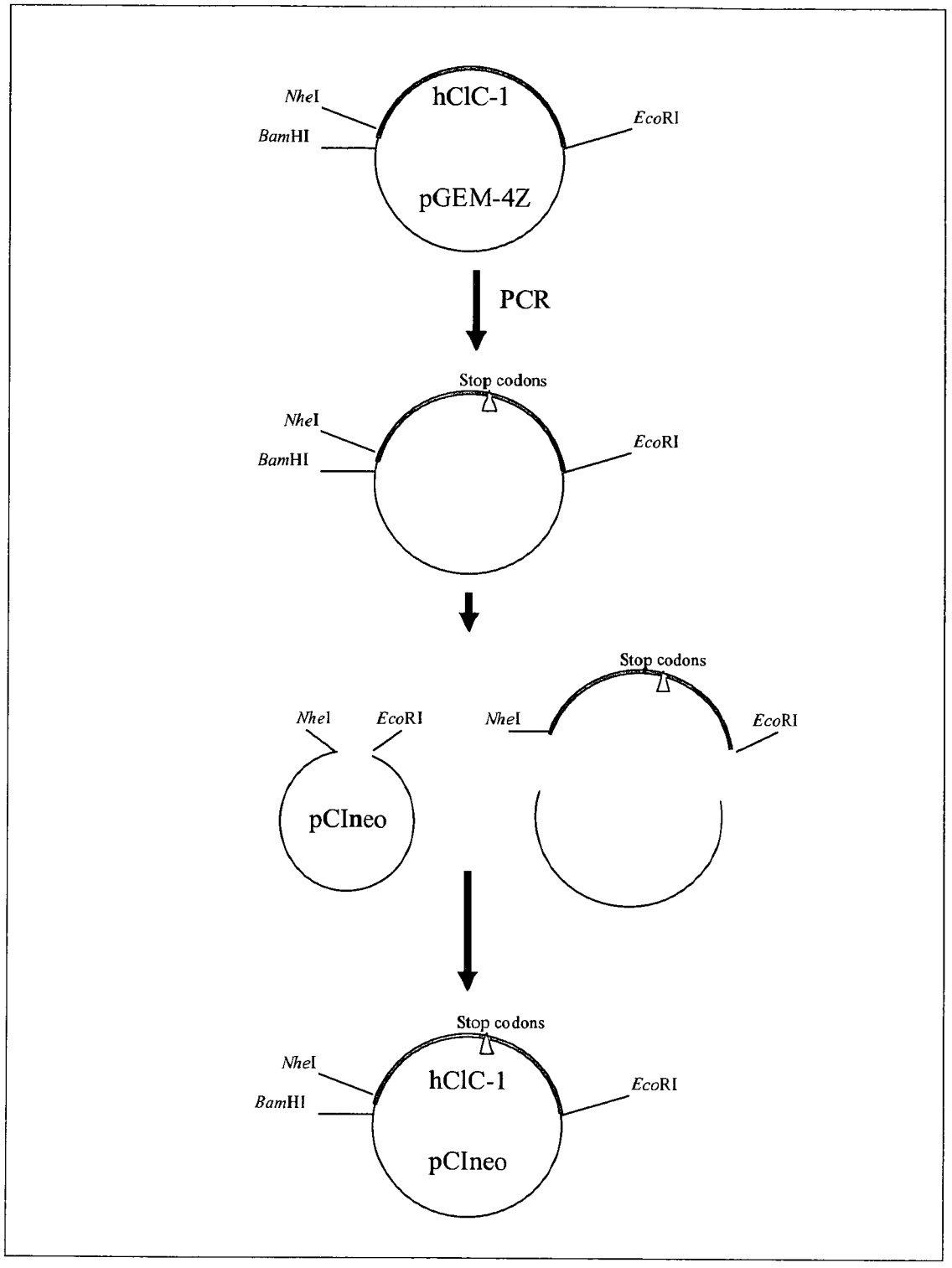

Figure 4.1 Schematic diagrams showing steps involved in sub-cloning the mutant constructs from pGEM-4Z into pCIneo vector

4.2.2 Co-transfection of with C-terminal truncated mutants with the $C_{721-988}$ construct

Six different DNA co-transfection experiments, as listed in Table 4.2, were set up. Each construct was employed at a DNA concentration of 0.5 μg.

Table 4.2 List of DNAs used in six sets of DNA co-transfection experiments

Transfection reaction	DNA used for transfection
1	N_{1-716}/pCIneo + BEpMIG
2	N_{1-806}/pCIneo + BEpMIG
3	N_{1-871}/pCIneo + BEpMIG
4	N_{1-716}/pCIneo + $C_{721-988}$/BEpMIG
5	N_{1-806}/pCIneo + $C_{721-988}$/BEpMIG
6	N_{1-871}/pCIneo + $C_{721-988}$/BEpMIG

4.2.3 Electrophysiology

Transfected HEK cells were incubated for 24 hour before electrophysiological study and two protocols, tail-1 and tail-2, were used for analysis of channel open probability (Section 3.2.6.2). At least three sets of recordings were used for analysis and results are given as means ± S.E.M.

4.3 RESULTS

4.3.1. Electrophysiological study of C-terminal truncated mutants

Currents elicited from HEK cells transfected with C-terminal truncated mutants N_{1-716} and N_{1-806} could not be distinguished from those of untransfected cells (Figure 4.2). Unexpectedly, however, chloride currents, albeit with altered inward rectification and gating properties (Figure 4.3), were found in the HEK cells expressing N_{1-871} mutants.

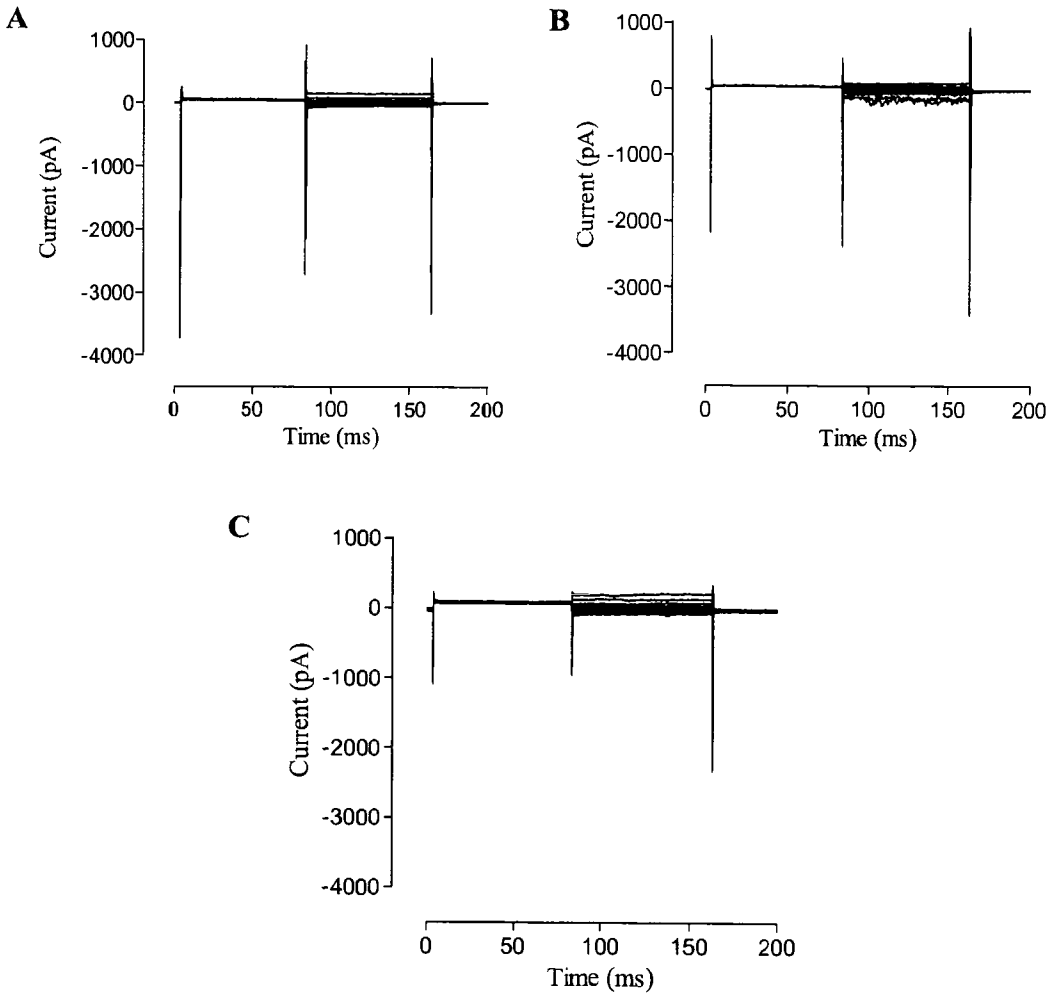

Figure 4.2 The current traces of the $N_{1\text{-}716}$, $N_{1\text{-}806}$ and no DNA transfected HEK cells in response to the standard activation protocol

HEK cells transfected with $N_{1\text{-}716}$ construct **(A)**, $N_{1\text{-}806}$ construct **(B)** and no DNA **(C)** showed none of the characteristic hClC-1 currents normally observed when stimulated by the usual activation protocol composed of 80 ms test pulses ranging from -140 mV to +80 mV in 20 mV increments each preceded by a 80 ms conditioning pulse to +40 mV.

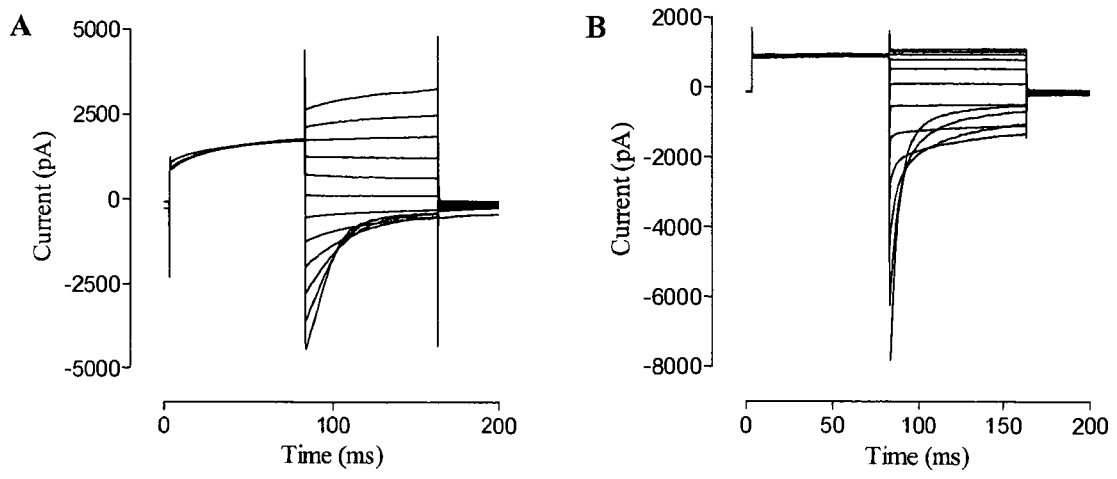

Figure 4.3 The current traces of the $N_{1\text{-}871}$ construct and WT split channel $N_{1\text{-}720}$ + $C_{721\text{-}988}$ co-transfected HEK cells in response to the standard activation protocol

HEK cells transfected with $N_{1\text{-}871}$ construct **(A)** have large currents, with kinetics and other characteristics similar to, but distinct from those of WT split channel co-transfection **(B)**.

4.3.2. Electrophysiological study of co-transfection of C-terminal truncated mutants with $C_{721\text{-}988}$

Co-transfection of the $C_{721\text{-}988}$ fragment with each of the C-terminal truncated mutants, allowed generation of characteristic chloride currents in response to activation with tail-1 and tail-2 protocols. Results were interpreted and reported as open probability of the overall gates (P_o^o) (Figure 4.4), common gate (P_o^c) (Figure 4.5) and protopore gate (P_o^p) (Figure 4.6). Half-maximum activation potentials ($V_{½}$) were determined and the results are shown in Table 4.3. In general, the channel properties of $N_{1\text{-}716}$ and $N_{1\text{-}806}$ co-expressed with $C_{721\text{-}988}$ come close to those of the control $N_{1\text{-}720}$ + $C_{721\text{-}988}$, with $V_{½}$ being about 77-86% as negative as controls. In contrast to $N_{1\text{-}716}$ and $N_{1\text{-}806}$, $N_{1\text{-}871}$ was able to conduct chloride current when expressed alone. In accord with the dramatic right shift of its open probability curve ($V_{½}$ value of overall, common and protopore gating are all shifted to the right by 91.6mV, 101.7mV and 59.7mV, respectively, Table 4.3), this C-tail truncated

channel must tend to be closed in the normal physiological voltage range. Co-transfection with $C_{721\text{-}988}$ has only a slight effect on its channel properties, $V_{½}$ of overall gate, common and protopore gate were shifted back to the left by 21.7mV, 15.1mV and 14.6mV, respectively, (Table 4.3) but this is probably not a substantial improvement compared with the dramatic restoration of function of *N*716 and *N*806.

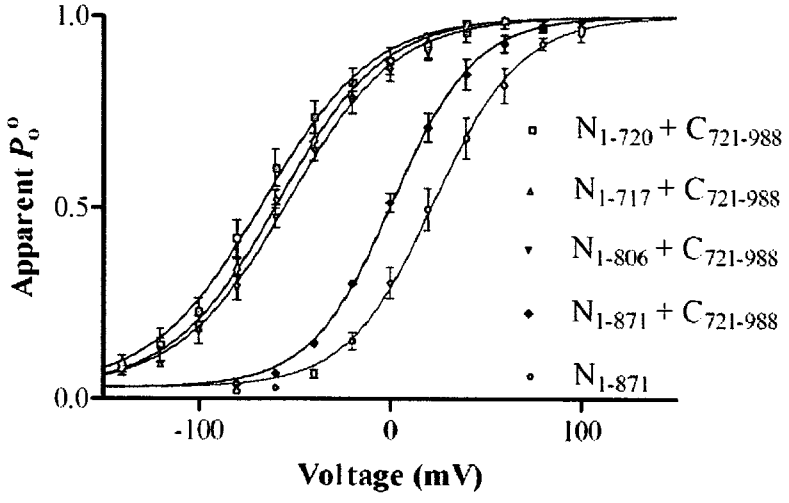

Figure 4.4 Overall apparent open probability (P_o^o) of split and C-terminal truncated channels

Overall apparent open probabilities, for split and C-terminal truncated channels, were derived from instantaneous currents obtained by extrapolating tail currents of patch-clamped HEK cells in the tail-1 protocol (160 ms conditioning pulse ranging from +60 mV to -140 mV in -20 mV decrements each followed by a 40 ms test pulse to -100 mV). Co-expression of the $C_{721\text{-}988}$ fragment with either $N_{1\text{-}716}$ (red) or $N_{1\text{-}806}$ (purple) restores the C-terminal truncated channel function close to the WT split channel (green). On the other hand, the co-expression of $N_{1\text{-}871}$ with $C_{721\text{-}988}$ (dark blue) makes little substantial improvement (n=3) compared with $N_{1\text{-}871}$ expressed alone. Boltzmann parameters ($V_{½}$, k and P_{min}) are shown in Table 4.3.

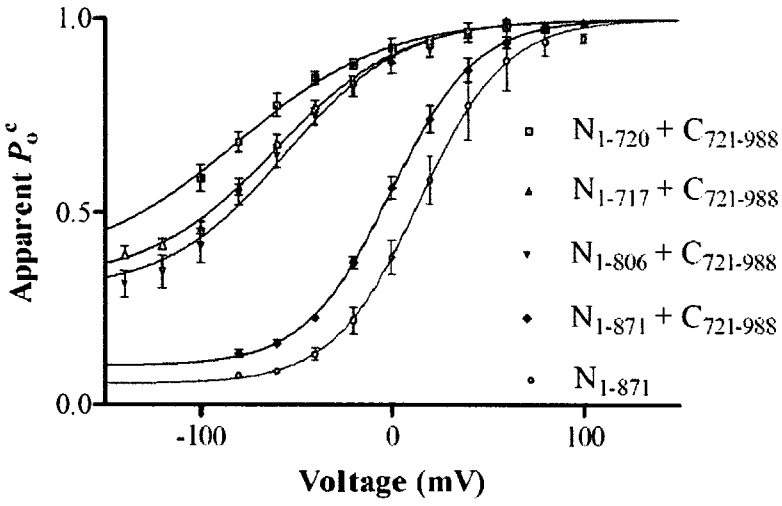

Figure 4.5 Apparent open probability for common gate (P_o^c) of split and C-terminal truncated channels

Apparent open probabilities of common gating, for split and C-terminal truncated channels, were derived from instantaneous currents obtained by extrapolating tail currents of patch-clamped HEK cells in the tail-2 protocol (as for the tail-1 protocol except for an additional conditioning pulse at 180 mV for 0.4 ms between the 160 ms conditioning pulse and 38.6 ms test pulse to ensure all the protopore gates are opened). Co-expression of the $C_{721-988}$ fragment with either N_{1-716} (red) or N_{1-806} (purple) restores the C-terminal truncated channel function close to the WT split channel (green). On the other hand, the co-expression of N_{1-871} with $C_{721-988}$ (dark blue) makes no substantial improvement (n=3) compared with N_{1-871} expressed alone. Boltzmann parameters ($V_{½}$, k and P_{min}) are shown in Table 4.3.

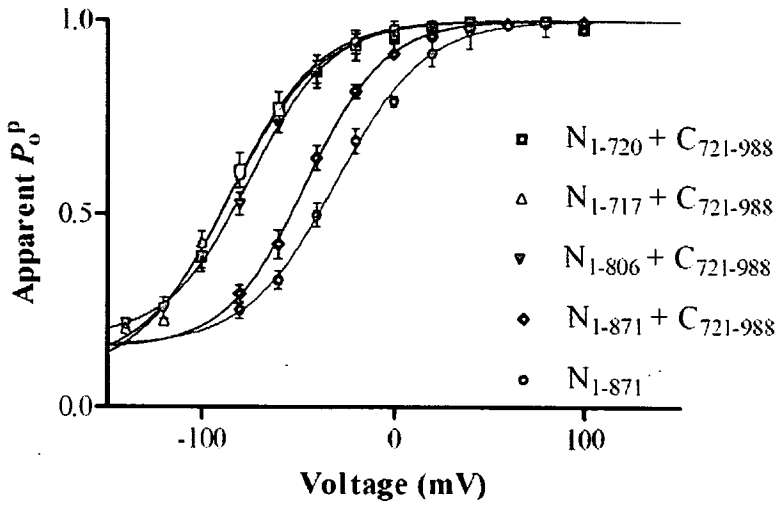

Figure 4.6 Apparent open probability for protopore gate (P_o^p) of split and C-terminal truncated channels

Apparent open probabilities of protopore gating, for split and C-terminal truncated channels, were derived by dividing the values for overall open probability by the values for the open probability of the common gate at each voltage, as described in Section 3.2.6.2. Co-expression of the $C_{721-988}$ fragment with either N_{1-716}(red) or N_{1-806} (purple) restores the C-terminal truncated channel function close to the WT split channel (green). While co-expression of N_{1-871} with $C_{721-988}$ (dark blue) makes some improvement (n=3), it is not on the same scale as the complete restoration of function of N_{1-716} and N_{1-806}. Boltzmann parameters ($V_{½}$, k and P_{min}) are shown in Table 4.3.

Table 4.3 Summary of the Boltzmann parameters of overall (A), common (B) and protopore (C) gating for the split and C-terminal truncated channels

A. Overall gating (*fixed for curve fitting)

Constructs	$V_{½}$ (mV)	k	P_{min}	n
$N_{1-720} + C_{721-988}$	-66.5±1.5	28.7±1.4	0.03*	3
$N_{1-716} + C_{721-988}$	-58.5±1.7	27.6±1.2	0.03*	3
$N_{1-806} + C_{721-988}$	-53.8±2.6	28.3±1.9	0.03±0.03	3
$N_{1-871} + C_{721-988}$	1.3±1.6	21.7±1.2	0.03*	3
N_{1-871}	23.1±2.3	22.9±1.9	0.03*	3

B. Common gating

Constructs	$V_{½}$ (mV)	k	P_{min}	n
$N_{1-720} + C_{721-988}$	-80.8±15	39.0±4.6	0.36*	3
$N_{1-716} + C_{721-988}$	-60.6±3.6	33.0±2.2	0.33±0.02	3
$N_{1-806} + C_{721-988}$	-55.6±2.0	30.8±1.8	0.30*	3
$N_{1-871} + C_{721-988}$	-0.6±0.5	22.6±0.4	0.10±0.01	3
N_{1-871}	14.5±1.0	22.8±0.8	0.06±0.01	3

C. Protopore gating

Constructs	$V_{½}$ (mV)	k	P_{min}	n
$N_{1-720} + C_{721-988}$	-85.9±8.8	24.1±2.9	0.08*	3
$N_{1-716} + C_{721-988}$	-84.6±2.7	22.8±1.8	0.11±0.04	3
$N_{1-806} + C_{721-988}$	-74.9±1.7	21.3±1.2	0.18±0.02	3
$N_{1-871} + C_{721-988}$	-45.8±1.8	20.5±1.0	0.15±0.03	3
N_{1-871}	-30.3±2.9	23.2±1.7	0.16±0.04	3

4.4 DISCUSSION

4.4.1 Electrophysiological studies of nonsense mutants

The aim of this work was to use the ClC-1 $C_{721-988}$ fragment containing CBS2 to investigate its functional restoration efficiency in regard to three naturally-occurring C-terminal truncation mutants in which CBS2 was either deleted or retained. The three mutants were E717X (N_{1-716}), Q807X (N_{1-806}) and fs872X (N_{1-871}). Of these, the last one retained CBS2 but the sequence was truncated immediately afterwards, while the other two were truncated from different sites within the interlinker sequence between CBS1 and CBS2. Mutants without CBS2 did not show chloride currents when they were expressed alone which is in agreement with the truncation experiments performed in most members of the CLC family (Schmidt-Rose & Jentsch 1997a; Maduke, Williams & Miller 1998; Mo *et al.* 2004). However, N_{1-871}, which contained CBS2, showed mutant currents in which the voltage dependence was shifted to more positive potentials compared to wild-type. At present, N_{1-871} is the shortest continuous length of hClC-1 channel sequence that retains chloride currents when expressed in the mammalian expression system (a construct, E864X, however, has been associated with currents when expressed in *Xenopus* oocytes (Macías et al. 2007). Our results is in agreement with the truncation split channel (N_{1-720} + $C_{721-870}$) co-expression experiment performed by Estévez and coworkers in *Xenopus* oocytes (Estévez *et al.* 2004). Thus, basic channel function can be obtained without (at least) the last 117/118 amino acids, although $V_{½}$ of gating was shifted to considerably more positive values (Table 4.3), indicating that the numbers of channels open were reduced in the physiological voltage range. A very similar positive shift of ~50 mV in $V_{½}$ for P_o^o was found for E871X (equivalent to N_{1-870}) expressed in *Xenopus* oocytes (Macías et al. 2007).

The major structural difference between mutants N_{1-806} and N_{1-871} was in whether the CBS2

region was absent or present, respectively. Mutant N_{1-806} did not show any chloride current. Despite some observations that internal deletion of sequence such as D13 inside CBS2 (Hryciw *et al.* 1998) and even the whole CBS2 sequence (Estévez *et al.* 2004) are without significant effect on channel properties, here, the results once again seemed to demonstrate the requirement of CBS2 for channel function. Collectively, the sequences around CBS2 might act as both guiding sequence for structural interaction and for modulating the conformational structure of the ClC channel. An important role for part of the CBS2 sequence has been proposed by Wu and colleagues (Wu *et al.* 2006). They demonstrated that channel function remained in the co-expression experiment of $C_{863-888}$ with N_{1-720} in *Xenopus* oocytes. In other studies, the distal sequences after CBS2 have been shown to exert a structural modification effect on the outer pore vestibule (Hebeisen & Fahlke 2005). A study conducted by Estévez and coworkers (Estévez *et al.* 2004), however, showed that CBS2 was not essential in a continuous internal deletion mutant but its absence did destroy the channel function if the deletion occurred in a split channel configuration. N-terminal and C-terminal sequences are still covalently attached in the internal CBS2 deleted mutants, whereas, in a split channel, the separation points are no longer connected covalently. The latter, without connection between putative guiding sequences pre and/or post CBS2, might not allow an appropriate conformation and so a functional channel might not be able to form. In our case, distal sequences after CBS2 were totally truncated in the mutant N_{1-871}. The modification effect on the outer pore vestibule, observed by Hebeisen and Fahlke 2005, is presumably reduced in this mutant and the gating properties are changed. In addition, several site directed mutations (H838A, H835R, A862E/K and E865A/K) located inside CBS2 have been identified as affecting common gating properties (Estévez *et al.* 2004). Since CBS2 is still intact in N_{1-871} and the few identified important amino acids have not been eliminated by the truncation, so the basic chloride current is retained.

4.4.2 Functional restoration of nonsense mutants by co-expressing with $C_{721-988}$

In the co-expression experiment, chloride currents were restored to similar to WT hClC-1 by supplement of $C_{721-988}$ to the mutants N_{1-716} and N_{1-806} but there was no substantial improvement in channel function of mutant N_{1-871}. We can presume that CBS2 is necessary for interaction with the structure formed from the N-terminal membrane-resident domain. The shortest N-terminal domain used here was N_{1-716}, thus the sequences interacting with CBS2 should be between 1 and 716. According to the topological structure of CLC (Figure 1.3), the possible interacting region should be located intracellularly. Helices A and R along with helix loops D-E, F-G, H-I and J-K would be potential candidates. However, solid evidence has not been able to be demonstrated in the present study. Presumably, once CBS2 has interacted with the relevant region of mutants N_{1-716} and N_{1-806}, correct configuration of the pore and gates is formed and chloride ions are conducted as usual. By contrast, mutant N_{1-871} already contains CBS2 in its structure and appropriate interaction can occur between this inherent CBS2 and the assumed relevant part of the membrane-resident domain. But in the absence of the distal carboxyl tail sequence, some pore vestibule modification occurs (Hebeisen & Fahlke 2005), therefore an inadequate pore structure is obtained and conduction of chloride ions can be distinguished from wild-type hClC-1. It is likely that further supplement of $C_{721-988}$ containing CBS2 and the whole missing carboxyl terminal region beyond N_{1-871} is unable to displace the inherent CBS2 efficiently to restore the channel function to wild type rather than merely moving $V_{½}$ to a slightly less positive value. The result might further imply that part of CBS2 acts as a guiding sequence to the interaction region. This interaction could then enable complete permeation pore formation while further appropriate modification of the pore structure might require the distal sequence downstream from CBS2.

4.4.3 Therapeutic potential

Gene therapy has been proposed, and tested *in vitro* and *in vivo* in animal models, for treating various human diseases, from some such as cystic fibrosis (Ziady & Davis 2006), myotonia (Falk *et al.* 2001; Foster, Foster & Dickson 2006) and erectile dysfunction (Schiff & Melman 2006), which are ion channel-related, to others, such as Duchenne muscular dystrophy (Foster, Foster & Dickson 2006), which are not. Most of them have adopted whole gene delivery as the way to rescue the diseases. This has, however, always encountered problems that include, exceeding the carrying capacity of viral vectors, ineffective cell transfection or insufficient gene expression (Foster, Foster & Dickson 2006). Alternative strategies have, therefore, been developed such as oligonucleotide-mediated gene therapy, various RNA interventions and short fragment homologous recombination to reduce the size of the genetic material that must be delivered. Among these, a method using a trans-splicing ribozyme to repair chloride channel (ClC-1) function has been proposed, however, the repair efficiency for this method was very low (Rogers *et al.* 2002). Interestingly, a morpholino antisense oligonucleotide-induced exon 7a skipping has been used to reverse the production of a truncated ClC-1, caused by a splicing defect, to the normal full-length form (Wheeler *et al.* 2007). Choride channels of the CLC family have a distinctive ability allowing them to be functionally reconstituted from complementary split components. Here, I have performed the test of co-expressing non-complementary sequences for possible functional restoration of nonsense mutants. My results show that by using a construct such as $C_{721\text{-}988}$, to treat C-terminal truncations that occur after CBS1 (but not after CBS2) we might have some chance of rescuing the channel function of certain nonsense mutants associated with recessive generalized myotonia. The symptoms of the recessive disorder are usually worse than those of the dominant (Colding-Jørgensen 2005), being characterised by later onset with moderate to severe myotonia. As well, there is generalized muscular hypertrophy, paradoxically accompanied

by transient and even permanent weakness, atrophy of forearm and neck muscles and myopathic electromyographic and histological changes (Colding-Jørgensen 2005). So far, in the mammalian expression system, I have found that functional restoration of naturally occurring hClC-1 nonsense mutations is only successful on co-expression with the relatively large $C_{721-988}$ C-terminal fragment. Our ability to use much smaller fragments to complement large hClC-1 C-terminal truncations in *Xenopus* oocytes (Wu *et al.* 2006), however, suggests that technical refinements may allow this to be achieved also in mammalian cells. Delivering a small part of the C-terminal sequence is likely to be easier than full complementation or delivery of the whole gene while remaining successful in repairing channel function in the case of various CLC nonsense mutations.

CHAPTER FIVE: ATTEMPTED FUNCTIONAL RESTORATION OF A C-TERMINAL TRUNCATED MUTANT BY SUPPLEMENTATION WITH SHORT C-TAIL FRAGMENTS

5.1 INTRODUCTION

In a previous PhD project conducted in our laboratory, Dr. Weiping Wu had used the split channel approach in the *Xenopus* oocytes to study the essential amino acid sequence in the C-tail for functional restoration of C-tail truncated mutants. An initially successful supplementary C-tail peptide ($C_{721-988}$) had been gradually shortened (Wu *et al.* 2006) until deletion of 142 amino acids at the N-terminus of $C_{721-988}$ allowed functional restoration in N_{1-720} + $C_{863-988}$. Further deletion of 100 amino acids at the C-terminus of $C_{863-988}$ generated a peptide, $C_{863-888}$, retaining only 26 amino acids. Surprisingly, even it was able to restore channel function when co-expressed with the non-functional N-terminal membrane-resident region (N_{1-720}) (Wu *et al.* 2006). This result implied that the $C_{863-888}$ peptide contained essential amino acids that were required to co-operate with the N-terminal domain to restore channel function.

Although 26 amino acids constitute a really short peptide for functional restoration of ClC-1, there is no hint to say that it is the shortest peptide for this purpose. In an extension of this experiment, I used the split channel system that I have developed in HEK cells (Chapter III) to assess the effect of $C_{863-888}$ and of further deletions of both 5' or 3' amino acids from this peptide sequence on functional restoration of $C_{721-988}$. Five new peptides (Figure 5.1) were thus designed beginning from $C_{863-888}$.

Aim: To attempt to repeat the short peptide supplementary reconstitution experiment in the mammalian expression system and to extend the study, if possible, by examining supplementation using even shorter peptides.

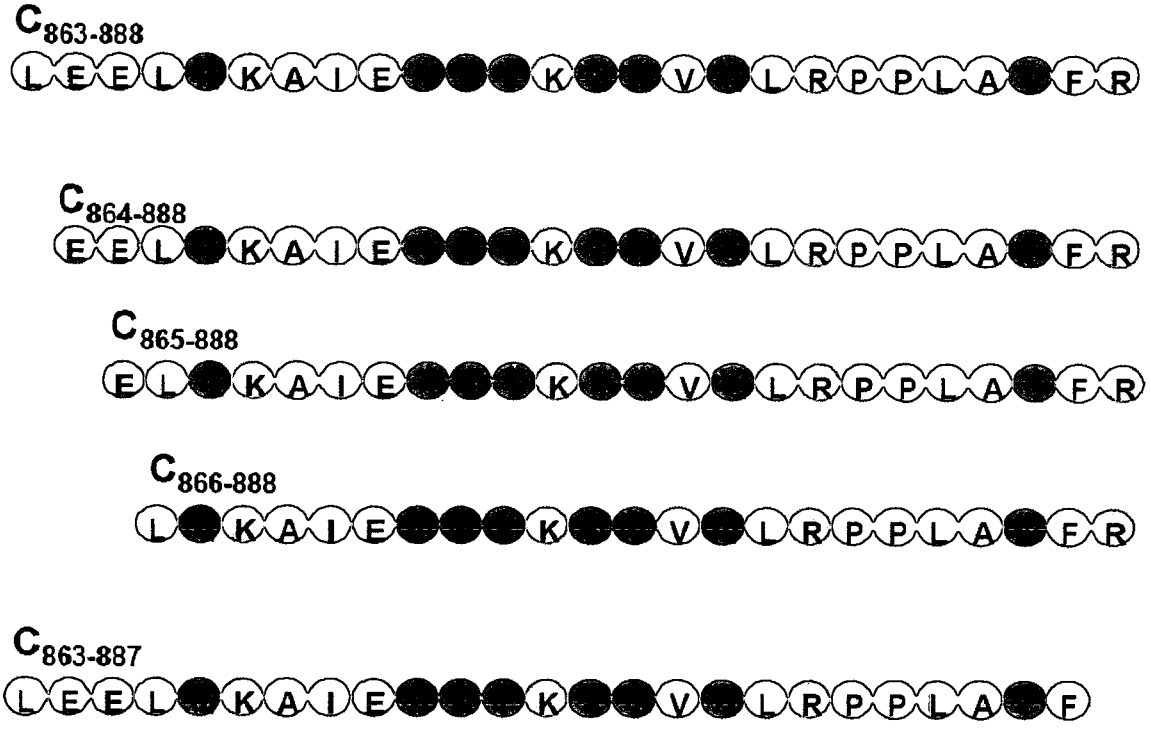

Figure 5.1 Cartoon picture of the 26 amino acid peptide and the five proposed shorter peptides

At the top, $C_{863\text{-}888}$, is the original peptide that had the ability to rescue chloride channel function when co-expressed with $N_{1\text{-}720}$ in *Xenopus* oocytes. Peptides $C_{864\text{-}888}$, $C_{865\text{-}888}$ and $C_{866\text{-}888}$ were to be constructed with one, two and three amino acids deleted from the N-terminus of $C_{863\text{-}888}$, respectively. Peptides $C_{863\text{-}887}$ and $C_{863\text{-}886}$ have one and two amino acids deleted from the C-terminus compared to peptide $C_{863\text{-}888}$.

5.2 EXPERIMENTAL PROCEDURES

At the beginning of my PhD in 2002, I had generated all the shortened peptide cDNA constructs (shown as peptide sequences in Figure 5.1) in the pTLN vector using site-directed mutagenesis and intended to perform the further study in *Xenopus* oocytes. However, difficulties associated with continuing to use the *Xenopus* system in our laboratory and my wish to first test the robustness of the $C_{863\text{-}888}$ in the functional restoration of $N_{1\text{-}720}$ led me to try the split channel experiments in HEK cells. Already prepared constructs had to be re-cloned into the BEpMIG vector. Here, I will focus on the methodology necessary to re-clone the peptide cDNA constructs from the pTLN vector into BEpMIG mammalian vector. The methodology for construction of $C_{863\text{-}888}$ can be found in the thesis in Dr. Weiping Wu (2002) and a similar method, which I used for constructing the shortened peptide cDNAs, is described in Appendix D.

5.2.1 Introduction of a *Bam*HI site at the N-terminus of the C-terminal peptides in pTLN

A restriction enzyme site, *Bam*HI, was created at the N-terminus of each C-terminal peptide in pTLN using site-directed mutagenesis. I used BamhL863 primers to introduce *Bam*HI sites into my $C_{863\text{-}998}$, $C_{863\text{-}888}$, $C_{863\text{-}887}$, $C_{863\text{-}886}$ and $C_{863\text{-}885}$ constructs in pTLN vectors. Again, BamhE864, BamhE865 and BamhL866 primers were used to introduce *Bam*HI sites into $C_{864\text{-}888}$, $C_{865\text{-}888}$ and $C_{866\text{-}888}$ in pTLN vectors. Primer sequences are shown in Table 5.1.

Table 5.1 Primers for appending *Bam*HI sites onto the C-terminal peptide constructs inserted in pTLN vectors

The sequence of the *Bam*HI site (GGATCC) has been underlined and followed by the start codon (ATG) in red and a Glycine (GAG) residue in green. The nucleotides shown in bold correspond to the amino acid residue number (in blue) indicated on the primer.

	BamhL863
forward	5′ GGCAGATCGCGAGGATCCATGGAG**CTG**GAGGAG
reverse	3′ CTCCTCCAGCTCCATGGATCCTCGCGATCTGCC
	BamhE864 E864
forward	5′ GGCAGATCGCGAGGATCCATGGAG**GAG**GAGC
reverse	3′ GCTCCTCCTCCATGGATCCTCGCGATCTGCC
	BamhE865 E865
forward	5′ GGCAGATCGCGAGGATCCATGGAG**GAG**CTACAG
reverse	3′ CTGTAGCTCCTCCATGGATCCTCGCGATCTGCC
	BamhL866 L866
forward	5′ GGCAGATCGCGAGGATCCATGGAG**CTA**CAGAAG
reverse	3′ CTCCTGTAGCTCCATGGATCCTCGCGATCTGCC

5.2.2 *Bam*HI restriction enzyme digestion

In order to distinguish the mutated clone from the non-mutated one, the constructs were digested by *Bam*HI restriction enzyme (Section 2.7.1). After digestion mutated constructs separated by 1% agarose electrophoresis (Section 2.6.1) showed as linear DNA rather than undigested circular DNA. Verified clones were inserted into the BEpMIG vector.

5.2.3 Cloning of C-terminal peptides into BEpMIG

Plasmids containing the *Bam*HI-modified C-terminal peptide constructs as well as the BEpMIG vector were digested with *Bam*HI and *Eco*RI restriction enzymes. Linearised C-terminal peptide constructs were ligated individually into linearised BEpMIG vector.

Resultant colonies underwent restriction enzyme selection by *Nco*I. Two fragments were generated when the peptides were successfully cloned into the BEpMIG vector. After selection of correct DNA constructs, these were sequenced at the IMVS Sequencing Centre to confirm the correct sequence of the insert in the BEpMIG vector. Sequencing results are shown in Appendix C.

5.2.4 DNA transfection in HEK cells

Each C-terminal peptide, $C_{863\text{-}988}$, $C_{863\text{-}888}$, $C_{863\text{-}887}$, $C_{863\text{-}886}$, $C_{864\text{-}888}$, $C_{865\text{-}888}$ and $C_{866\text{-}888}$, was transfected alone into HEK cells to confirm that the measured currents were indistinguishable from the negative control. Co-transfection experiments were performed afterwards for each C-terminal peptide and the N-terminal membrane-resident construct, $N_{1\text{-}720}$. About 1 μg of total DNAs were transfected into HEK cells using Lipofectamine™ -Plus™ reagent (Section 3.2.5). Activation, tail-1 and tail-2 protocols (Section 3.2.6.2) were used in patch-clamp experiments (Section 3.2.6.1) to obtain the raw current trace, tail-current for the determination of overall gating and tail-current for the determination of common gating, respectively, to compare the results obtained from functional complementary channel $N_{1\text{-}720} + C_{721\text{-}988}$ as shown in Chapter III. Detailed information about each of protocols and their uses in determining channel open probabilities have been mentioned in the methods section 3.2.6 of Chapter III.

5.2.5 Detection of protein expression level of $C_{721\text{-}988}$ and $C_{863\text{-}988}$ by Western blotting

Two peptides ($C_{721\text{-}988}$/BEpMIG and $C_{863\text{-}988}$/BEpMIG) were transfected individually into HEK cells using the procedure explained in Section 3.2.5. After 24 hours incubation, cells were subjected to extraction using 8 M urea solution. Extracted proteins were separated by SDS-PAGE (section 2.11.1) and this was followed by immunoblotting with primary antibody (anti-C-tail antibody, which was raised against the final 15 amino acids of human

ClC-1 (Gurnett *et al.* 1995) (Section 2.11.2)). The second antibody was goat anti-rabbit IgG (H+L) horseradish peroxidase conjugate (Bio-Rad) used against the primary antibody. Protein recognised by primary and secondary antibodies was visualised using the method of enhanced chemiluminescence (ECL) (Section 2.11.3.2).

5.3 RESULTS

5.3.1 Electrophysiological measurements of N_{1-720} co-expressed separately with each of the C-terminal peptide constructs

Seven constructs ($C_{863-988}$, $C_{863-888}$, $C_{863-887}$, $C_{863-886}$, $C_{864-888}$, $C_{865-888}$ and $C_{866-888}$) were individually transfected into HEK cells. Signals measured were indistinguishable from HEK cells with no transfected DNA indicating that ClC-1 current could not be elicited following individual transfection. Co-transfection of each peptide construct with the N-terminal construct (N_{1-720}) was then performed and the currents observed were, unexpectedly, still indistinguishable from the negative control. The current traces for each peptide co-transfection in response to the activation protocol are shown in Figure 5.2.

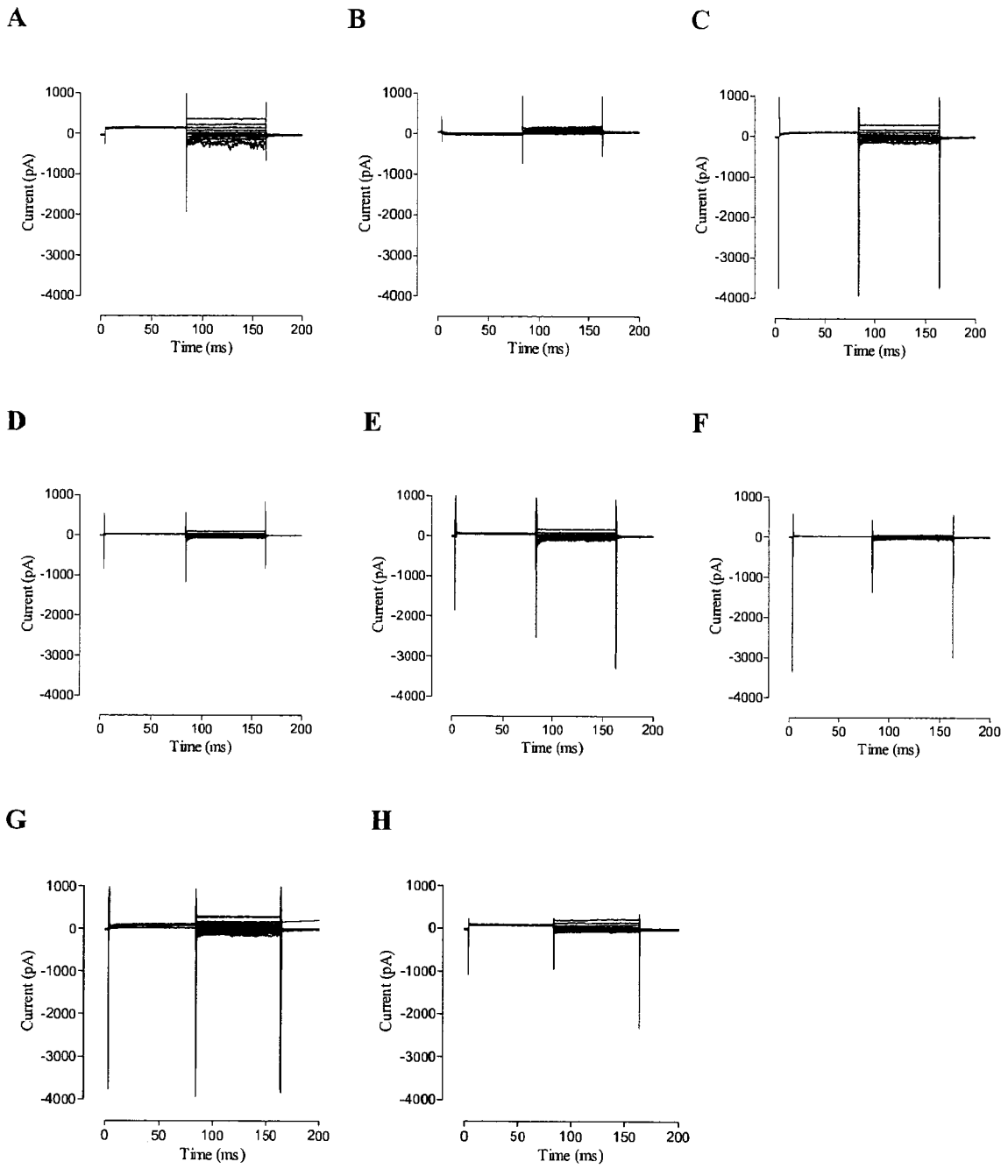

Figure 5.2 Current traces of N_{1-720} co-transfected with the short peptides in HEK cells in response to the activation protocol

Current traces of N_{1-720} co-transfected with $C_{863-988}$ (A); $C_{863-888}$ (B); $C_{863-887}$(C); $C_{863-886}$(D); $C_{864-888}$(E); $C_{865-888}$(F) and $C_{866-888}$ (G) are indisdinguishable from the negative control (H).

5.3.2 Protein expression of the C-terminal peptides ($C_{721-988}$ and $C_{863-988}$) in HEK cells

One of the concerns about the failure of functional restoration observed from the C-terminal peptides with N_{1-720} is the possibility of defective protein synthesis. To test for a synthesis defect, $C_{863-988}$ was used as a representative for all C-terminal short peptides, since it, also, seemed incapable of restoring chloride current when apparently expressed with N_{1-720}. By immunoblot analysis (Figure 5.3) of the protein expression level of $C_{721-988}$ and $C_{863-988}$ using anti-C-tail antibody (Gurnett *et al.* 1995), both of the constructs were expressed in comparable quantities. The observed molecular size of $C_{721-988}$ is around 27 kDa which is in reasonable agreement with its predicted mass from sequence calculation of ~27 kDa; however, the observed size of $C_{863-988}$, at ~8 kDa was slightly lower than the sequence calculation value of ~13 kDa.

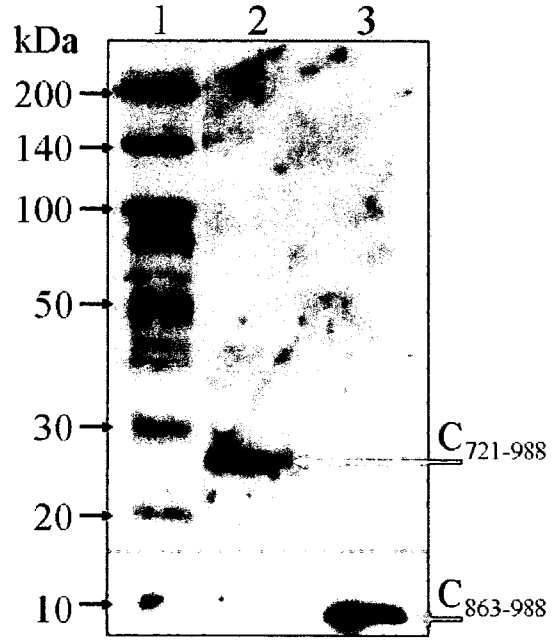

Figure 5.3 Western blot of $C_{721-988}$ and $C_{863-988}$ expressed protein in HEK cells

Protein samples with biotinylated protein marker (lane 1) were separated using 7.5% SDS-PAGE. Molecular sizes of protein marker were labeled at the left hand side. Lane 2 is the $C_{721-988}$ expressed protein and lane 3 is $C_{863-988}$ expressed protein. The detected fragments were recognized by anti C-tail antibody which was directed against the final 15 amino acids of hClC-1.

5.4 DISCUSSION

5.4.1 Attempted functional supplementation of N_{1-720} with short C-terminal peptides

These studies have continued some of the investigations from one of my previous colleagues, Dr. Wu (Wu *et al.* 2006), who made truncation modifications on the $C_{721-988}$ peptide and co-expressed these modified peptides with N_{1-720} in *Xenopus* oocytes. I had attempted to repeat and further investigate her results in my newly developed split channel expression system in HEK cells (as described in Chapter III), however, for reasons that I was unable to define precisely, I was unable to reproduce her findings. According to Dr Wu results, importantly, when $C_{863-988}$ was co-expressed with N_{1-720}, wild-type current could be elicited. If 100 amino acids of $C_{863-988}$ were then truncated from its C-terminus leaving a 26 amino acid peptide, $C_{863-888}$, and this was co-expressed with N_{1-720}, chloride currents were obtained that were small but, again, qualitatively similar to wild-type ClC-1. Based on Dr Wu's results, most of the N-terminal and C-terminal sequences of $C_{721-988}$ are dispensable leaving the 26 amino acids located around the distal end of CBS2 to rescue channel function. In order to continue on from her investigation and narrow down the important amino acids of the $C_{721-988}$ tail, co-expressions with N_{1-720} were performed in the mammalian system using peptides that were successful in the functional rescue of channel function in *Xenopus* oocytes ($C_{863-988}$, $C_{863-888}$) along with each of five progressively modified peptides ($C_{863-887}$, $C_{863-886}$, $C_{864-888}$, $C_{865-888}$ and $C_{866-888}$). This was intended to perform a robust test of the functional importance of the sequence of these peptides in the most appropriate biological milieu. Positive results would provide strong confirmation of the importance of this short peptide domain for channel functions. Unfortunately, none of the peptides were able to rescue the channel function. Immunoblotting of expressed protein (Figure 5.3) provides some evidence that one of the unexpectedly non functional peptides, $C_{863-988}$, was expressed in comparable amounts to $C_{721-988}$. Failure of protein synthesis is, therefore, not likely to be the reason for the absence of functional rescue. However, it was

noticeable that the apparent molecular weight of the peptide (at the resolution of the SDS-PAGE gel) was less than the predicted 13 kDa. Peptide purification would be necessary for mass spectrometry to provide an absolute confirmation of the protein size. Some protein breakdown could conceivably affect the ability of the peptide to interact with the N-terminal region. The most likely region of disruption is that immediately after aa863, since the C-terminal of $C_{863\text{-}998}$ appears to be intact (because it is detected by the antibody that recognises the final 15 amino acids at the C-terminus (Gurnett *et al.* 1995) and the minimal functional C-tail truncated mutant, $N_{1\text{-}870}$ (as mentioned in Chapter IV, Figure 4.3), had also supported the view that the important sequence should be located on the N-terminal end of $C_{863\text{-}988}$. Unfortunately, this includes the $\alpha 2$ region of CBS2, the integrity of which seems to be essential to CLC channel function (Maduke, Williams & Miller 1998; Estévez *et al.* 2004).

CHAPTER SIX: CHARACTERIZATION OF THREE NOVEL MYOTONIA-ASSOCIATED MISSENSE MUTATIONS IN THE C-TAIL REGION OF HUMAN CLC-1 VIA HETEROLOGOUS EXPRESSION

6.1 INTRODUCTION

Mutations in the human skeletal muscle voltage-gated chloride channel cause dominant (Thomsen's disease) and recessive (Becker's disease) myotonia congenita. Mutations that cause recessive myotonia usually lead to a strong reduction or total loss of chloride channel function while mutations that cause dominant myotonia usually affect the common gating properties and shift the voltage dependence of activation to positive voltages (Pusch *et al.* 1995; Saviane, Conti & Pusch 1999). More than 80 mutations have been published throughout the *CLCN1* gene and over 67% are missense mutations (Colding-Jørgensen 2005). Recently, my research group obtained a list of thirteen unpublished novel missense mutations found from myotonia congenita patients. These were provided to Professor Bretag by collaborators, in each case, a diagnosis of myotonia congenita having been made by a neurologist according to the usual criteria. As is appropriate at this stage, we do not have access to clinical notes or any other data on individual patients. In order to know more about how these mutations affect the channel function and lead to myotonia, I have used site-directed mutagenesis to create each of the corresponding mutations in WT hClC-1. Among the mutants, there are three mutations found located in the C-tail region. They are R691S, E724A and V851M. The R691 and E724 are located in the inter-linker sequence between CBS1 and CBS2 and V851 is located in the middle of CBS2 (Figure 6.1). R691 and E724 are not conserved residues but V851 is a highly conserved residue among CLC family (Figure 6.2). Because of their location with respect to my project on C-tail structure and function, these three mutants were chosen as the first to be

characterized. I studied channel kinetics and open probability of these mutant channels in the physiological potential range using the patch-clamp.

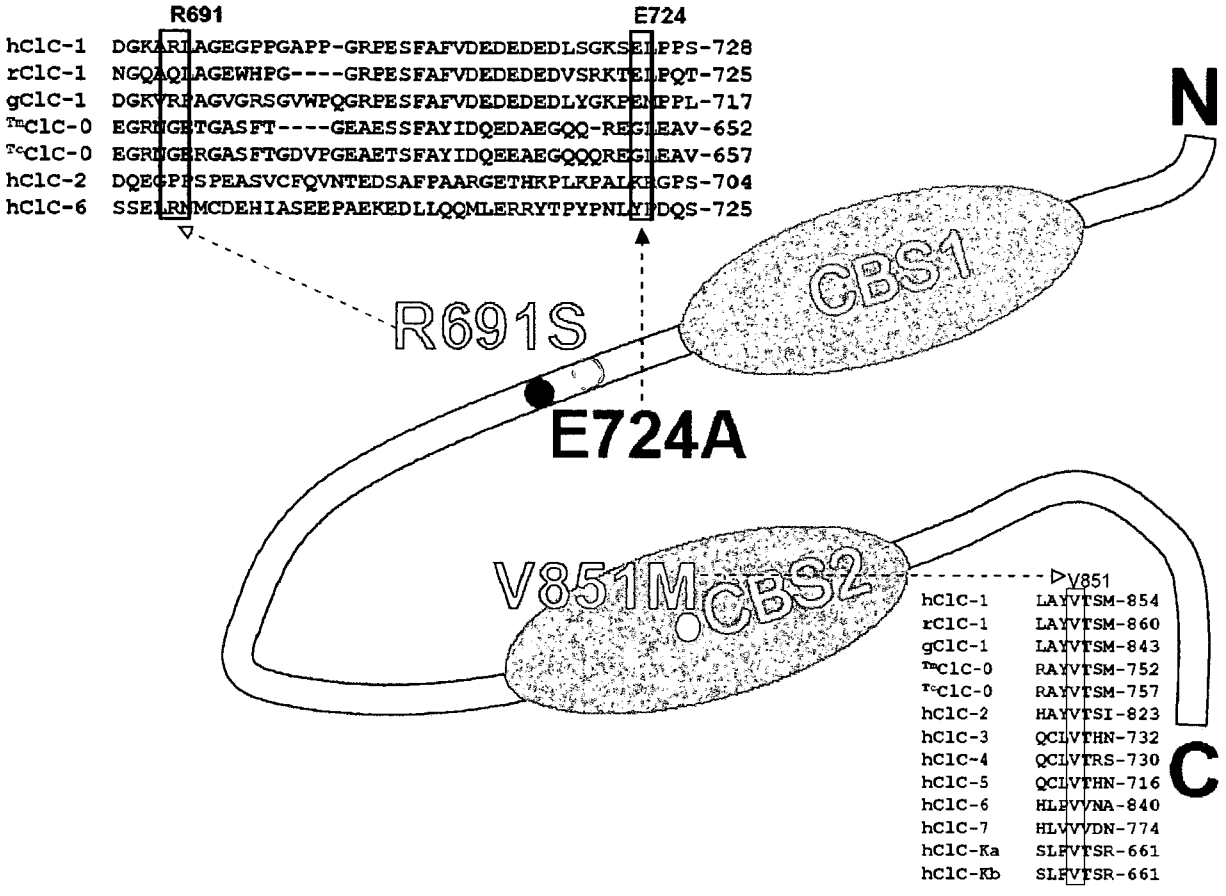

Figure 6.1 Approximate locations of the thirteen novel mutations on C-tail of human ClC-1

R691 (pink dot) and E724 (blue dot) are located close to the N-terminal end of the inter-linker sequence between CBS1 and CBS2. V851 (red dot) is located in the middle of CBS2. R691 and E724 residues are not conserved among CLC family while V851 is a highly conserved residue among CLC family, as shown in the respective sequences.

Aim: To characterize newly found missense mutations located in the C-tail region of hClC-1 via heterologous expression.

6.2 EXPERIMENTAL PROCEDURES

6.2.1 Create missense mutations on human ClC-1

Thirteen missense mutants were constructed by site-directed mutagenesis (Section 2.9.2). A pair of primers, sense and antisense, were designed per mutant. Their primer sequences are shown in Table 6.1. A full-length WT hClC-1 in a pGEM-4Z vector (Promega) was used as DNA template in the site-directed mutagenesis. The sequences of constructed mutants were verified by DNA sequencing with P7F sequencing primer, 5'-CCT GAC CTT GGC TGG AAC CAG CTC AGC-3', at the FUSA Sequencing Facility (Section 2.8). The sequencing results are shown in Appendix E.

Table 6.1 Primer sequences for constructing thirteen missense mutants of hClC-1

Mutant	Primer Name	Primer Sequence (5' to 3')
V851M	V851M_sense	5'-TCCACCTCGCTTACATGACCAGCATGGGG-3'
	V851M_antisense	5'-CCCCATGCTGGTCATGTAAGCGAGGTGGA-3'
E724A	E724A_sense	5'-CTCTGGCAAGAGCGCGCTTCCTCCTTCCC-3'
	E724A_antisense	5'-GGGAAGGAGGAAGCGCGCTCTTGCCAGAG-3'
R691S	R691S_sense	5'-GACGGGAAGGCGAGCCTGGCTGGGGAG-3'
	R691S_antisense	5'-CTCCCCAGCCAGGCTCGCCTTCCCGTC-3'
G551D	G551D_sense	5'-ATTTGCTTCGAATTAACGGATCAGATTGCTCACATCCTG-3'
	G551D_antisense	5'-CAGGATGTGAGCAATCTGATCCGTTAATTCGAAGCAAAT-3'
T550R	T550R_sense	5'-AGCTGTGATTTGCTTCGAATTAAGGGGTCAGATTGC-3'
	T550R_antisense	5'-GCAATCTGACCCCTTAATTCGAAGCAAATCACAGCT-3'
P480S	P480S_sense	5'-GCCACCACTATGCCCATAAGCTGCGGAGGC-3'
	P480S_antisense	5'-GCCTCCGCAGCTTATGGGCATAGTGGTGGC-3'

Table 6.1 (Con't)

Mutant	Primer Name	Primer Sequence (5' to 3')
W433R	W433R_sense	5'-CAGTACTTTGTTTGACAACAATACAAGGGTGAAACACGC-3'
	W433R_antisense	5'-GCGTGTTTCACCCTTGTATTGTTGTCAAACAAAGTACTG-3'
M373L	M373L_sense	5'-GCATCGCCAAGTCTTGCTCGGTGTCCG-3'
	M373L_antisense	5'-CGGACACCGAGCAAGACTTGGCGATGC-3'
A298T	A298T_sense	5'-TCACCTCCACCTACTTTACTGTTCGGAACTACTG-3'
	A298T_antisense	5'-CAGTAGTTCCGAACAGTAAAGTAGGTGGAGGTGA-3'
F297S	F297S_sense	5'-GAGGTCACCTCCACCTACAGTGCTGTTCGGAACTACTG-3'
	F297S_antisense	5'-CAGTAGTTCCGAACAGCACTGTAGGTGGAGGTGACCTC-3'
K215R	K215R_sense	5'-AAAGCCTTTGTGGCCAGGGTTGTCGCCCTG-3'
	K215R_antisense	5'-CAGGGCGACAACCCTGGCCACAAAGGCTTT-3'
S189C	S189C_sense	5'-CCCAGGCTGTTGGCTGTGGAATCCCC-3'
	S189C_antisense	5'-GGGGATTCCACAGCCAACAGCCTGGG-3'
R47W	R47W_sense	5'-CCAGCACAGGCTCTGGAAGGATGCAGG-3'
	R47W_antisense	5'-CCTGCATCCTTCCAGAGCCTGTGCTGG-3'

6.2.2 Cloning of C-tail missense mutants into the pCIneo

Three sequences, confirmed as pGEM-4Z mutant constructs (R691S/, E724A/ and V851M/pGEM-4Z) and pCIneo vector were digested by *Nhe*I and *Eco*RI. Digested fragments were separated by agarose electrophoresis (Section 2.6.1). Corresponding vector and mutated gene fragments were purified by QIAquick Gel extraction Kit (Section 2.5.3) and ligated together (Section 2.7.2).

6.2.3 Transfection of C-tail missense mutants' DNA in HEK cells

About 0.5 to 1 μg of mutant DNA and 50 ng pEGFP plasmid DNA were used in

co-transfection reaction in HEK cells. D-MEM (Dulbecco's Modified Eagle Medium) was added to DNA mixtures to a final volume 200μl followed by 1μl of Plus™ reagent (Invitrogen) and incubated for 5 min at room temp. Then, 3 μl of Lipofectamin LTX™ (Invitrogen) was added to the DNA/D-MEM/Plus mixture and incubated for 30 min at room temp after which 200μl of 2.5 x 10^4 HEK Cells were included in the transfection mixture. Aliquots of the cells/DNA mixture (80 μl) were transferred onto the top of acid treated glass covers (5 mm x 10 mm) which were placed inside the wells of 24-well plate. These were then incubated at 37°C under 5% CO_2 for 5 hr after which 1 ml of D-MEM+ (D-MEM supplemented with 0.1 mM MEM Non-Essential Amino Acids, 4 mM L-Glutamine and 10% (v/v) fetal bovine serum)was added to the well and incubated at 37°C under 5% CO_2 for 24 hr.

6.2.4 Electrophysiology

Transfected HEK cells were incubated for 24 hr before electrophysiological study (Section 3.2.5) and two protocols, tail-1 and tail-2, (Section 3.2.6.2) were used for analysis of channel open probability. At least three sets of recordings were used for analysis and results are given as means ± S.E.M.

6.3 Results

6.3.1. Electrophysiological studies of missense mutants

Current traces in response to the activation protocol were used to compare the basic characteristic of the missense mutants with WT hClC-1. Typical current patterns for WT hClC-1 show rapid deactivation upon hyperpolarisation and an inward rectification at negative potentials (Figure 6.2A). Those C-tail missense mutants, R691S, E724A and V851M, showed very similar current traces to those of WT (Figure 6.2).

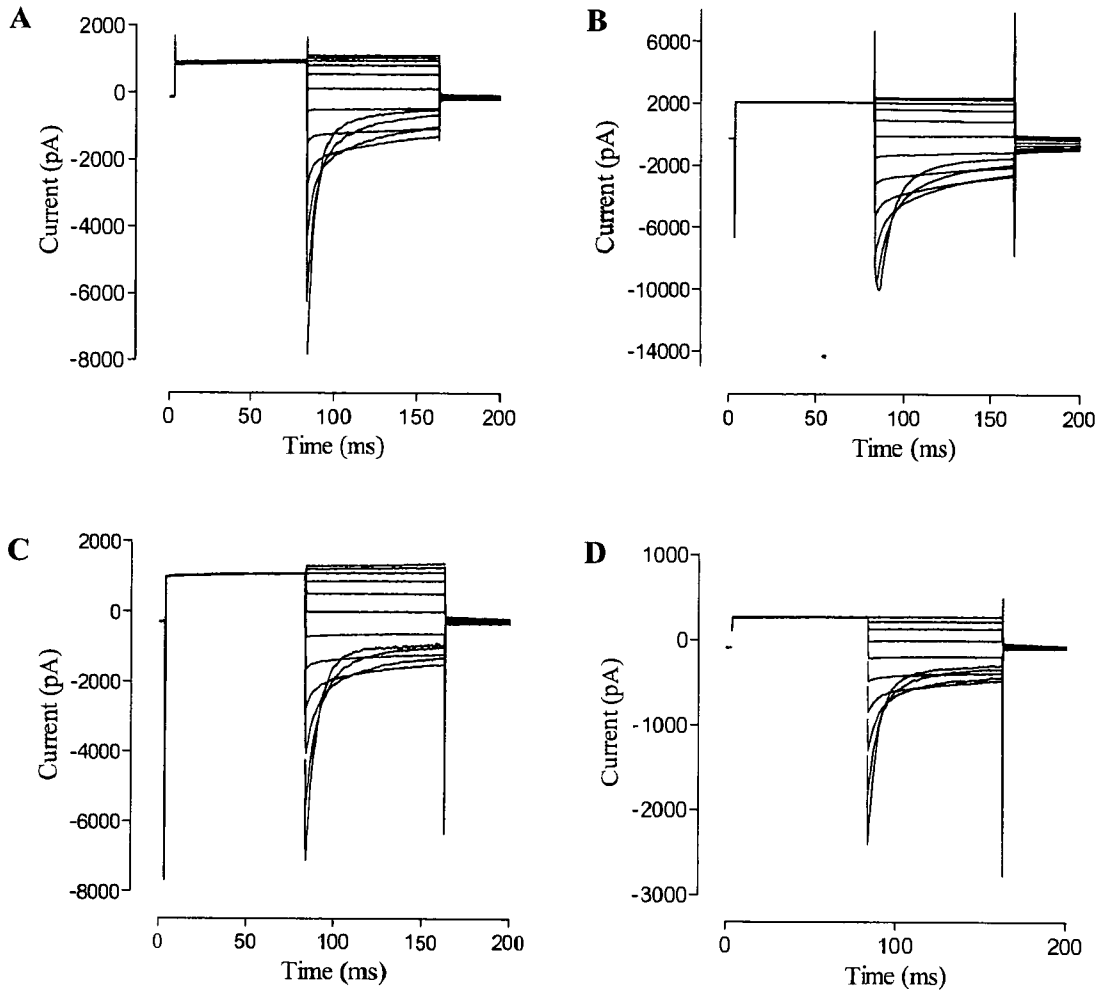

Figure 6.2 Current traces of WT hClC-1 and C-tail missense mutants

The current traces were recorded from R691S **(B)**, E724A **(C)** and V851M **(D)** in response to the activation protocol (80 ms test pulses ranging from -140 mV to +80 mV in 20 mV increments each preceded by a 80 ms conditioning pulse to +40 mV) are practically the same as WT hClC-1 **(A)**.

Further studies, using the tail-1 and tail-2 protocols (Section 3.2.6.2) to determine the voltage dependence of channel gating, have been performed. Results of apparent open probability of overall gating (P_o^o), common gating (P_o^c) and protopore gating (P_o^p) are shown in Figure 6.3, Figure 6.4 and Figure 6.5, respectively. The summary of Boltzmann parameters is shown in Table 6.2.

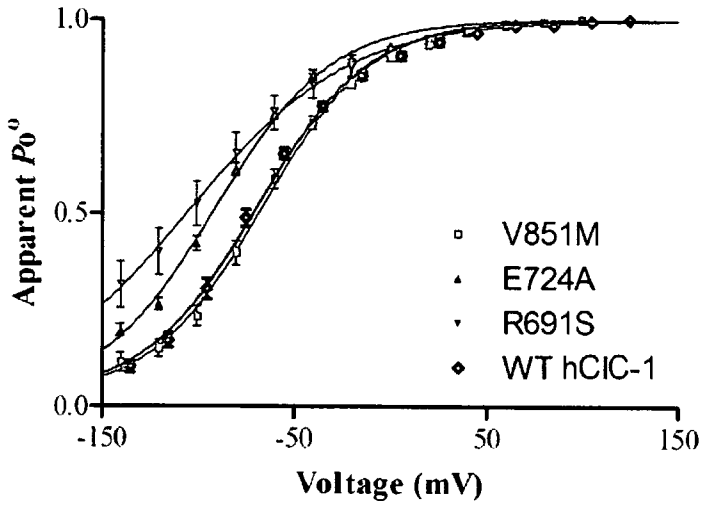

Figure 6.3 Overall apparent open probability for channel (P_o^o) of WT hClC-1 and C-tail missense mutants

The curves of overall apparent open probabilities for channel for WT hClC-1 (black) and V851M (red) look very similar to each other while R691S (purple) and E724A (blue) appear to be slightly shifted to the left. The results are given as means ± S.E.M. (n=8 for WT hClC-1, n=3 for R691S, n=4 for E724A and n=5 for V851M). Boltzmann parameters ($V_{½}$, k and P_{min}) are shown in Table 6.2.

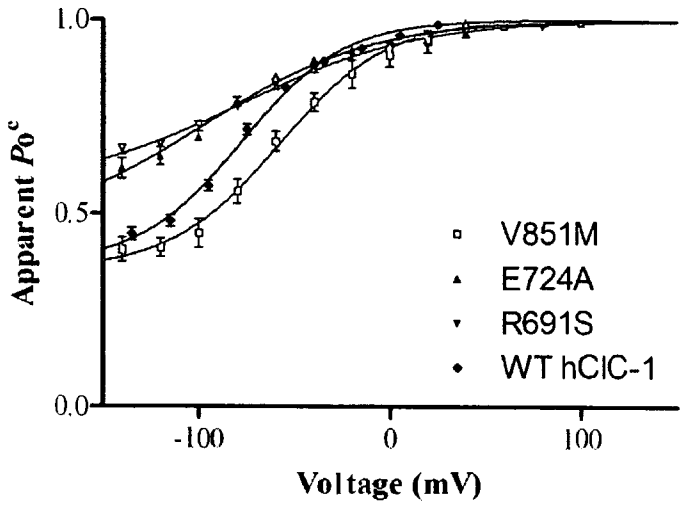

Figure 6.4 Apparent open probability for common gate (P_o^c) of split and C-tail truncated channels

The curves of apparent open probabilities for the common gate for V851M (red) are shifted to the right while R691S (purple) and E724A (blue) are slightly shifted to the left compared to the WT hClC-1 (black). The results are given as means ± S.E.M. (n=8 for WT hClC-1, n=3 for R691S, n=4 for E724A and n=5 for V851M). Boltzmann parameters ($V_{½}$, k and P_{min}) are shown in Table 6.2.

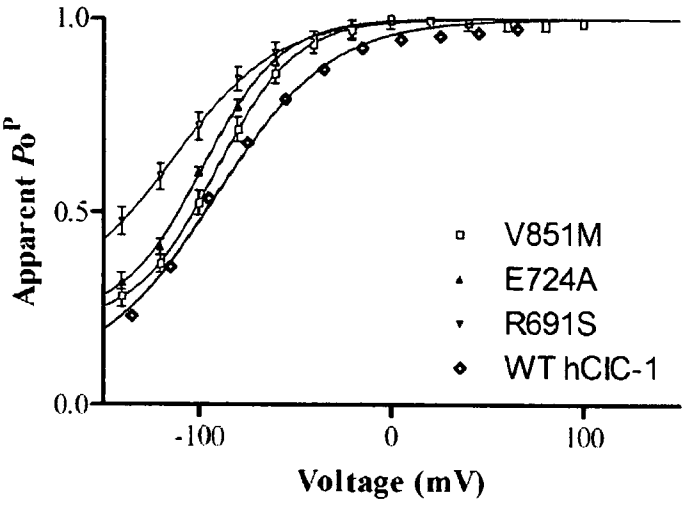

Figure 6.5 Apparent open probability for protopore gate (P_o^P) of WT hClC-1 and C-tail missense mutants

The curves of apparent open probabilities for protopore gate for both E724A (blue) and V851M (red) are shifted to the right while R691S (purple) is perhaps shifted to the left at potentials more negative than -100mV. The results are given as means ± S.E.M. (n=8 for WT hClC-1, n=3 for R691S, n=4 for E724A and n=5 for V851M). Boltzmann parameters ($V_{½}$, k and P_{min}) are shown in Table 6.2.

Table 6.2 Summary of the Boltzmann parameters of overall (A), common (B) and protopore (C) gating for the WT hClC-1 and C-tail missense mutants

A. Overall gating (*fixed for curve fitting)

Constructs	$V_{½}$ (mV)	k	P_{min}	*n*
WT hClC-1	-69.3±1.0	28.8±1.0	0.03*	8
R691S	-102.9±0.9	40.9±0.9	0.03*	3
E724A	-90.2±0.9	29.7±0.8	0.03*	4
V851M	-66.5±1.1	28.3±1.0	0.03*	5

B. Common gating

Constructs	$V_{½}$ (mV)	k	P_{min}	*n*
WT hClC-1	-77.9±3.7	26.5±2.2	0.4±0.03	8
R691S	-77.8±7.6	45.6±3.3	0.6±0.03	3
E724A	-97.1±11	43.5±4.3	0.5±0.06	4
V851M	-58.3±4.9	28.3±3.3	0.4±0.03	5

C. Protopore gating

Constructs	$V_{½}$ (mV)	k	P_{min}	*n*
WT hClC-1	-91.6±6.5	30.1±3.0	0.08*	8
R691S	-113.3±10	28.8±4.1	0.3±0.12	3
E724A	-98.1±1.9	20.5±1.1	0.2±0.02	4
V851M	-91.4±3.2	20.9±2.0	0.2±0.04	5

6.4 Discussion

In the present study, I have constructed thirteen novel myotonia mutations in a mammalian expression vector. All of them are missense mutations and three of them (R691S, E724A and V851M) are located in the C-tail region. Since my project is studying the function and structure of the C-tail, I believed these three myotonia-associated mutations would give me further information about how these channel mutations could cause myotonia. The R691 and E724 residues are not conserved among CLC family members. They are located on the inter-linker sequence between CBS1 and CBS2 and this inter-linker sequence has shown high sequence variation in the CLC family. This region is mainly providing flexibility for assembly of the structure formed by CBS1 and CBS 2. The V851 residue is a highly conserved residue throughout all eukaryotic CLC proteins including yeast and is located on the β2 segment of the CBS2 domain. Based on this background information, I would predict that the R691 and E724 mutations should not cause serious functional changes in the ClC-1 channel but, probably, V851M would have significant consequences, possibly showing a big shift of voltage dependence of activation to a more positive value which is characteristic of the mutated ClC-1 channel in myotonic disease. However, in electrophysiological studies on the three mutant channels expressed in HEK cells, the current traces in response to the activation protocol have shown characteristics similar to WT hClC-1 (Figure 6.2). They maintained the typical pattern of a rapid deactivation upon hyperpolarisation and an inward rectification at negative potentials. Using the tail-1 protocol to determine the overall open probability of gating (P_o^o), I found that the $V_{½}$ of V851M only shifted to a more positive value by 3mV (Table 6.2). However, the open probability curve of overall gating of the R691S and E724A are rather shifted to the left than the right indicating that the mutant channels are more likely to be open in the physiological potential range which does not seem to be a chloride channel behaviour that could be associated with myotonia disease. The $V_{½}$ values for overall gating of R691S and

E724A are shifted to the left by 32.0 mV and 18.2 mV (Table 6.2), respectively. The $V_{½}$ values of common gating and protopore gating of R691S are also shifted to the left (rather than right, as usually seen for myotonic mutants) and $P_o^c{}_{min}$ is 50% greater than in WT. Thus, the results that I have observed do not seem to be able to predict the clinical consequences caused by R691S. E724A has very similar properties to R691S. The $V_{½}$ value of P_o^o, P_o^c and P_o^p are all shifted to a more negative value which cannot be described as causing a myotonic effect. Since I do not have access to the clinical records of the people who have these mutations, it is hard to compare and understand how and why these mutations should cause myotonia (especially the R691S mutation). For V851M, $V_{½}$ values are all mildly shifted to positive values. It might cause myotonia but should not cause severe symptoms even though this residue is highly conserved. Thus V851 might have other functional effects on ClC-1 rather than alteration of channel gating. Also, I believe that the cause of the myotonia in the person with E724 might not be able to be observed, since the $V_{½}$ of overall gating is more or less showing that this mutant channel can have sufficient channels open in the physiological range even though the $V_{½}$ of fast gating is slightly shifted to right. This residue might have some effect on the fast gating structure but not enough to alter the normal channel function significantly.

CHAPTER SEVEN: PROTEIN EXPRESSION OF CARBOXYL-TAIL FRAGMENTS

7.1 INTRODUCTION

A dimeric structure for the CLC family of channels/transporters has been solidly confirmed by the X-ray structure of bacterial CLC (Mindell *et al.* 2001; Dutzler *et al.* 2002). The structure revealed that each subunit is composed of 18 α-helices and has a single ion-permeation pore. Two and three ions were recognized inside the conduction pore in the closed and open state, respectively (Dutzler, Campbell & MacKinnon 2003). The side chain of a highly conserved glutamate residue (E148 of EcClC) among CLC family has been observed blocking the extracellular vestibule of the conduction pore in a closed state mutant (Dutzler *et al.* 2002; Dutzler, Campbell & MacKinnon 2003). Blocking can be eliminated by protonation (Dutzler, Campbell & MacKinnon 2003). A mechanism of fast gating was proposed through regulation of the glutamate side chain movement (Dutzler, Campbell & MacKinnon 2003). Bacterial CLC has a short extended C-tail (Dutzler *et al.* 2002). The final (R) helix, which penetrates part-way through the membrane, connects the membrane-resident region and the C-tail. A conserved tyrosine residue (Y445 of EcClC) located in the R-helix was found to contribute a stabilizing effect on an ion in the pore (Dutzler *et al.* 2002; Dutzler, Campbell & MacKinnon 2003). Using site-directed fluorescence studies on EcClC, Bell and coworkers proposed that the gating process, not only involves single glutamate side chain movement, but also involves conformational changes of the R-helix in relation to its environment (Bell *et al.* 2006).

Compared with bacterial CLC, eukaryotic CLC has an extensive long C-tail containing two cystathionine-β-synthase (CBS) motifs (Bateman 1997). These motifs have been found in

various unrelated proteins and a role in binding adenosyl-nucleotide has been proposed (Scott *et al.* 2004). Several CLC members (ClC-1, ClC-2, ClC-4 and ClC-5) have been found to have ATP binding capability (Scott *et al.* 2004; Bennetts *et al.* 2005; Wellhauser *et al.* 2006), modifying gating properties and establishing full functional activity in the presence of ATP. Recently a role of sensing ionic strength has been suggested in studies of the osmoregulatory ABC transporter, OpuA (Biemans-Oldehinkel, Mahmood & Poolman 2006). Mutations in the C-tail of CLC proteins has contributed significant abnormal gating behaviour or even abolished function in the C-tail truncated mutants (Fong, Rehfeldt & Jentsch 1998; Mo *et al.* 2004; Colding-Jorgensen 2005). A variety of functional roles has been proposed for the C-tail of CLC proteins such as trafficking (Schwappach *et al.* 1998; Carr, Simmons & Sayer 2003; Estévez *et al.* 2004; Mo *et al.* 2004), cellular energy sensing (Scott *et al.* 2004), interaction with regulatory proteins (Schwake, Friedrich & Jentsch 2001; Ogura *et al.* 2002; Hryciw *et al.* 2003; Hryciw *et al.* 2004), influencing functional properties, particularly of common gating (Fong, Rehfeldt & Jentsch 1998; Estévez *et al.* 2004; Wu *et al.* 2006), and conformational modification (Hebeisen & Fahlke 2005; Bell *et al.* 2006).

Experiments involving the co-injection of N- and C-terminal mRNA of ClC-0 or ClC-1 in *Xenopus* oocytes have demonstrated that the structure of the C-tail after CBS1 can be folded individually and then restores the function of the complementary N-terminal constructs (Schmidt-Rose & Jentsch 1997a; Maduke, Williams & Miller 1998). Functional restoration has also been observed when the corresponding distal, ClC-0, C-tail peptide, having been expressed in, and purified from, bacterial cells, is injected into *Xenopus* oocytes expressing the complementary N-terminal domain (Maduke, Williams & Miller 1998). Consequently, the distal C-tail was thought to behave as an individual unit and should be a good candidate for structural analysis.

In the present studies, a major aim was, therefore, to establish a protein expression and purification method for ClC-1 C-tail proteins. Expression of two tail proteins from the region of the amino acids 575 (whole tail, $C_{575\text{-}988}$) and 721 to the C-terminus (distal tail, $C_{721\text{-}988}$) was attempted.

Aim: To express mg quantities of C-tail peptides using a bacterial expression system and to establish methods of purification.

7.2 EXPERIMENTAL PROCEDURES

7.2.1 Construction of $C_{575-988}$/BEpMIG for electrophysiological studies

7.2.1.1 Construction of $C_{575-988}$ in BEpMIG

A pair of primers called BamhP575 (forward sequence, G GCC AAC ATG GTG GCC GGA TCC ATG GAG CCC TCT CTC TAT GAC AGC and reverse sequence GCT GTC ATA GAG AGA GGG CTC CAT GGA TCC GGC CAC CAT GTT GGC C) to introduce a *Bam*HI site (underlined), start codon (green) and the glycine (red) in the hClC-1 before the amino acid residue 575 (Proline in blue) were used for making mutants using site-directed mutagenesis (Section 2.9.2). Plasmid DNA of hClC-1/BEpMIG was used as DNA template in the site-directed mutagenesis. Constructed mutants were digested by *Bam*HI restriction enzyme, two fragments were generated and the fragment containing upstream sequence of newly introduced *Bam*HI site was discarded. The remained fragment was ligated (Section 2.7.2) and sequence of the mutant was verified by DNA sequencing through FUSA sequencing Facility (Section 2.8).

7.2.1.2 Mutant constructs transfected to HEK cells for electrophysiological studies

Two transfection reactions were set up. They are single DNA, $C_{575-988}$/BEpMIG, transfection and double DNAs, N_{1-720}/pCIneo + $C_{575-988}$/BEpMIG, co-transfection to HEK cells. Transfected cells were incubated at 37°C under 5% CO_2 for 24 hr before performing patch-clamping (Section 3.2.6).

7.2.2 Construction of C-tail fragments for protein expression

C-tail cDNAs were generated with a pair of primers that flanked the specific 5' and 3'

regions of hClC-1 cDNA in pTLN vector (hClC-1/pTLN) by PCR method.

7.2.2.1 Primers design for construction of C-tail fragments

The upstream primers for construction C-tail fragments $C_{721\text{-}988}$ and $C_{575\text{-}988}$ were named 3ChG721 and 3ChP575, respectively. Both of the upstream primers contained *Nco*I restriction site for subcloning to expression vector, 3C protease cleavage sequences (LFQGP) and the first eighteen nucleotides sequence of the $C_{721\text{-}988}$ or the first nineteen nucleotides sequence of $C_{575\text{-}988}$. One common downstream primer hClC-1pTLNEco was combined with either one upstream primer in PCR for construction of the corresponding C-tail fragment. Downstream primer sequence was complementary to the reverse sequences of pTLN constructs and contained an *Eco*RI site. Primer sequences are shown in Table 7.1.

Table 7.1 Primers for construction of C-tail fragments

Sequences in blue and red colour are *Nco*I and *Eco*RI restriction sites, respectively. Sequences in red framed box are 3C protease cleavage sequences. Sequences in green colour are corresponding part of the N-terminus coding sequence of the C-tail fragments. The yellow colour highlighted nucleotides represents the first amino acid residue of the corresponding C-tail fragments of hClC-1.

Primers	Primer Sequences
	*Nco*I 3C protease site 575
3ChP575	TTTTTTGCCATGGCTCTGGAAGTTCTGTTCCAGGGGCCCTCTCTATGACAGCATC
	*Nco*I 3C protease site 721
3ChP721	TTTTTTGCCATGGCTCTGGAAGTTCTGTTCCAGGGGCCCGGCAAGAGCGAGCTTCCTCC
	*Eco*RI
hClC-1pTLNEco	GATCCCCCGGGCTGCAGAATTC

7.2.2.2 PCR conditions for construction of C-tail fragments

Pwo DNA polymerase was used in the PCR for construction of the C-tail fragments. According to the manufacture's manual (Roche Applied Science), a standard reaction mixture (50 μl) with 600 nM each of upstream and downstream primer, 50 ng DNA template (hClC-1/pTLN), 200 μM each of dNTP and 1 x *Pwo* PCR buffer with 20 mM $MgSO_4$ was prepared in a thin wall PCR tube. The tube was placed into the Mastercycler™ Personal (*Eppendorf*). Initial denaturation was performed for 5 min at 94°C, followed by thirty-five cycles of denaturation at 95°C for 1 min, annealing at 50°C for 30s and elongation at 72°C for 45s for the $C_{721\text{-}988}$ construct (~800 bp) and 2 min for the $C_{575\text{-}988}$ construct (~1.2 kbp). Final extension was carried out at 72°C for 7 min. The reaction was stopped at 16°C and the amplified product kept at 4°C until analysed by 1% agarose gel electrophoresis (Section 2.6.1).

7.2.2.3 Cloning of C-tail fragments into the protein expression vector

Bacterial expression vector, Thx/pET32a (Novogen), was used in the protein expression. Expressed proteins were fused with thioredoxin and His-tag to facilitate protein solubility and purification. Both of the amplified $C_{721\text{-}988}$ and $C_{575\text{-}988}$ cDNA fragments and circular Thx/pET32a vector plasmids were digested (Section 2.7.1) with *Nco*I and *Eco*RI restriction enzyme. A dominant DNA fragment, (~5.9 kbp of Thx/pET32a, ~800 bp of $C_{721\text{-}988}$ and ~1.2 kbp of $C_{575\text{-}988}$) observed in each reaction in 1% agarose gel electrophoresis were purified by QIAquick Gel Extraction Kit (Section 2.5.3). $C_{721\text{-}988}$ and $C_{575\text{-}988}$ were cloned into Thx/pET32a individually by T4 ligase (Section 2.7.2). Ligated products were transformed (Section 2.4.2) to XL1-Blue bacterial strain. (Section 2.3.2.1)

7.2.2.4 Verification of the resultant DNA with insert and correct DNA sequence

Initially, double restriction enzymes (*Nco*I and *Eco*RI) digestion was used to get general confirmation that the C-tail fragments were cloned into the vectors. Two fragments were generated from the clone with insert. The clones confirmed to contain the insert in the vectors were selected for DNA sequencing reactions (Section 2.8). Results were analysed by Sequencing Centre of IMVS. Three sequencing primers, pET32a_fw, pET32a_rv and T7 pro_fw were used to verify the insert sequence of Thx/pET32a. Primer sequences are shown in Table 7.2.

Table 7.2 Primer sequences of pET32a_fw, pET32a_rv and T7 pro_fw

Name of primer	Sequence
pET32a_fw	CGA ACG CCA GCA CAT GGA CA
pET32a_rv	TTA GCA GCC GGA TCT CAG TG
T7 pro_fw	TAA TAC GAC TCA CTA TA

7.2.3 Protein expression

7.2.3.1 Procedure for protein expression

Either Thx-$C_{721\text{-}988}$/pET32a or Thx-$C_{575\text{-}988}$/pET32a were transformed into BL21(DE3) and grown on LB agar plates with supplementary 100 μg/ml ampicillin. A single colony was picked and inoculated into 50 ml of LB broth containing ampicillin at 100 μg/ml and incubated at 37°C with vigorous shaking until the optical density of the culture reached 0.6 at 600 nm. Half of the culture was then transferred to a new tube. A final concentration of 1mM Isopropyl β-D-1-thiogalactopyranoside (IPTG) was added to one of the cultures. This culture was labelled as "induced sample". The culture without IPTG added was labelled as

"non-induced sample". Both cultures were continually grown for 3 hr at 37°C. Cell pellets were harvested by centrifugation at 5,000 x g for 5 min at 4°C and stored at –80°C.

7.2.3.2 Detection of target protein expression using 1 ml cell culture

Cell pellets harvested from 1 ml IPTG-induced and non-induced cell cultures were suspended in 20 µl of SDS-PAGE sample buffer and subjected to SDS-PAGE analysis (Section 2.11.1) followed by Western blotting (Section 2.11.2). Targeted C-tail protein would be recognized by anti-C-tail antibody directed against the last 15 amino acids of mammalian ClC-1 (Gurnett *et al.* 1995).

7.2.4 Protein extraction

7.2.4.1 Extraction of protein from IPTG- induced cell pellets using the Native method for Thx-$C_{721-988}$ and Thx-$C_{575-988}$ protein

Cell pellets harvested from either Thx-$C_{721-988}$/pET32a or Thx-$C_{575-988}$/pET32a expression were suspended in lysis buffer (20 mM Tris-HCl at pH8.0, 1% (v/v) Triton X-100) containing 1 mM phenylmethylsulfonylfluoride (PMSF, Sigma) and a tablet of complete mini EDTA-free protease inhibitor cocktail (Roche) per 50 ml buffer. Lysozyme (Sigma) at a concentration of 1 mg/ml was added to the cell suspension and incubated at room temperature for 15 min. After separating the soluble fraction from the insoluble debris by centrifugation, the soluble fraction was utilised for protein purification.

7.2.4.2 Extraction of protein from IPTG- induced cell pellets using the denaturing method for Thx-$C_{575-988}$ protein

Cell pellets harvested from Thx-$C_{575-988}$/pET32a expression were found to be insoluble in the lysis buffer without denaturant, thus, the samples had to suspended in the lysis buffer containing 6M Urea (20 mM Tris-HCl at pH8.0, 1% (v/v) Triton X-100 containing 6M Urea). Proteins were stirred for 30 min at room temperature. After separating the soluble fraction from the insoluble debris by centrifugation, the soluble fraction was stored in -80°C.

7.2.5 Protein purification of Thx-$C_{721-988}$

Extracted proteins (10 mg) of Thx-$C_{721-988}$/pET32a expression were mixed with 1 ml Ni-NTA resin (Qiagen), which had been pre-equilibrated with 20 mM Tris-HCl at pH8.0, 300 mM NaCl, 20 mM imidazole and 1% (v/v) Triton-X100 (buffer A), in a column. Column contents were then washed with 5 volumes of buffer A containing 150 mM imidazole. Protein was eluted with 20 mM Tris-HCl at pH7.0 300 mM NaCl, 500 mM imidazole and 1% (v/v) Triton-X100. Eluted proteins were collected in fractions by Pharmacia Frac 100 fraction collector (Amersham) and their concentrations were determined by the BCA method (Section 2.10.1). Purity of protein from each fraction was assessed by SDS-PAGE (Section 2.11.1).

7.2.6 Cleavage of Thx-tag from purified Thx-$C_{721-988}$ protein by proteases

The purified Thx-$C_{721-988}$ protein (50 μg) was subjected to His-3C protease (1 unit, Novogen) digestion in the digestion buffer (1.5mM Tris-HCl, pH7.0) containing 1mM EDTA and DTT at 4°C for overnight.

7.2.7 Separation of Thx-tag and protease from $C_{721-988}$ fragment by Ni-NTA chromatography

Digested protein was transferred to SpectraPor® dialysis tubing (Sigma) with 12 kDa molecular weight cut off (MWCO) for buffer exchange. The ratio of sample to dialysis buffer (20 mM Tris-Cl, pH 7.2, 10% (v/v) glycerol, 20 mM β-mercaptoethanol) volume was 1:1000. Dialysis was performed at 4°C with constant stirring for 5 hours and the process was repeated once with renewed buffer. Buffer exchanged sample was mixed with buffer (20 mM Tris-Cl, pH7.2, 10% (v/v) glycerol, 20 mM β-mercaptoethanol) equilibrated overnight with Ni-NTA resin at 4°C. Sample/Ni-NTA mixture was then loaded onto a column and stepwise concentrations (20, 30, 40, 50 and 500mM) of imidazole-containing buffers were used to elute the proteins from the column.

7.2.8 Molecular weight determination of purified Thx-$C_{721-988}$ and $C_{721-988}$ using mass spectrometry

Purified protein (either Thx-$C_{721-988}$ or $C_{721-988}$) was concentrated to 1 mg per ml by NANOSEP™ microconcentrators (Pall) with 3 kDa MWCO membrane. Molecular weight determination was performed on a PE/Sciex API-100 electrospray-ionization mass spectrometer (Applied Biosystems). Protein samples (20 μl) were injected into a 1 x 10 mm reverse phase column for desalting and separation by a linear gradient of acetonitrile from 20% to 70% (v/v). The primary mass spectrum was transformed to give a true-mass profile using BioMultiView program.

7.3 RESULTS

7.3.1 Electrophysiology recording of $C_{575-988}$ plus N_{1-720} co-transfected HEK cells

Mutant construct, $C_{575-988}$/BEpMIG was successfully generated using the site-directed mutagenesis approach and the DNA sequence (Appendix C) was verified. A functional complementation experiment using co-expression with N_{1-720} was then performed. Current trace of $C_{575-988}$ + N_{1-720} (Figure 7.1A) recorded from activation protocol (40mV conditioning-pulse for 80ms from -30mV holding potential and tested by stepping from -140mV to 80mV for 80ms with 20mV increments, Section 3.2.6.2) shows the pattern typical of WT hClC-1 (Figure 7.1B) with inward rectifying current response and rapid deactivation at hyperpolarisation voltage and partial channel open during resting potential (Steinmeyer, Ortland & Jentsch 1991; Pusch, Steinmeyer & Jentsch 1994). Wild-type hClC-1 results obtained earlier by Dr. Jennie Cederholm are used for comparison with my current work.

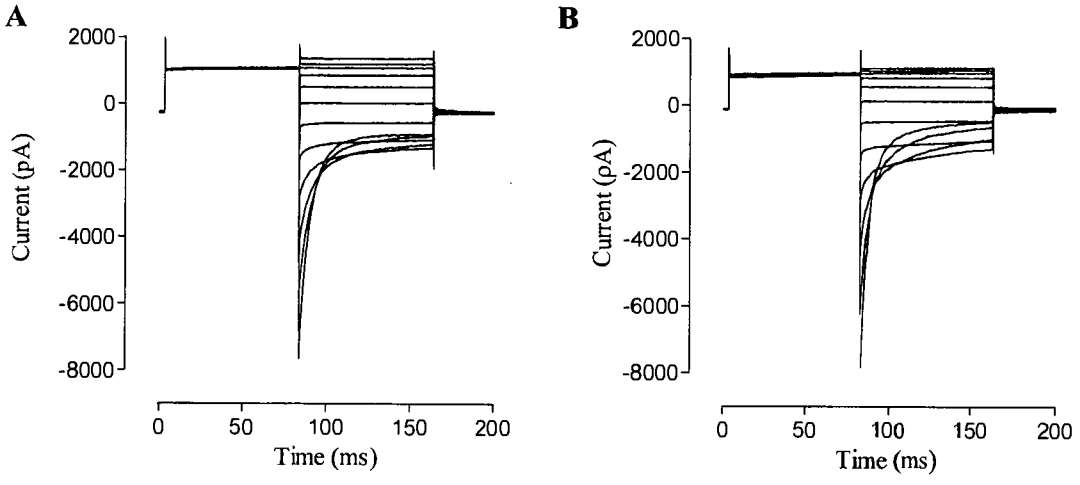

Figure 7.1 Current traces of normal appearance in a whole cell patch from a N_{1-720}/pCIneo + $C_{575-988}$/BEpMIG (A) and hClC-1/pCIneo(B) co-transfected HEK cell evoked by the standard activation protocol

The current traces from the whole cell patch of N_{1-720}/pCIneo + $C_{575-988}$/BEpMIG (**A**) in response to the activation protocol showed a typical WT hClC-1 pattern (**B**) with an inwardly rectifying current

response and a rapid deactivation at hyperpolarisating voltages and partial channel opening at resting potential. The activation protocol consists of a 40mV conditioning step for 80ms from -30mV holding potential followed by steps from -140mV to 80mV for 80ms with 20mV increments (Section 3.2.6.2).

7.3.2 Construction of $C_{575-988}$ and $C_{721-988}$ cDNA for cloning into Thx/pET32a

Peptide expression constructs for $C_{575-988}$ (1351 bp) and $C_{721-988}$ (913 bp) resulted in cDNAs of the expected size on 1% TAE agarose gels (Figure 7.2). These included the extra sequence of restriction enzyme sites, 3C protease cleavage site, the downstream sequence after the stop codon of the hClC-1 gene up to the *Eco*RI site and poly T tail of the forward primer which added 106 bp to the C-tail fragment reading sequence. Generally, both of the N-terminal primers for construction of the $C_{575-988}$ and $C_{721-988}$ have similar GC content and so the same annealing temperature, 50°C, can be applied in both of the PCRs. Although there were some DNA smears observed from the PCR product of the $C_{575-988}$ cDNA, the main fragment could be purified by gel extraction (Section 2.5.3). Different extension times, 45 s for the $C_{721-988}$ and 2 min for the $C_{575-988}$ cDNA, were required, depending on the size of final products.

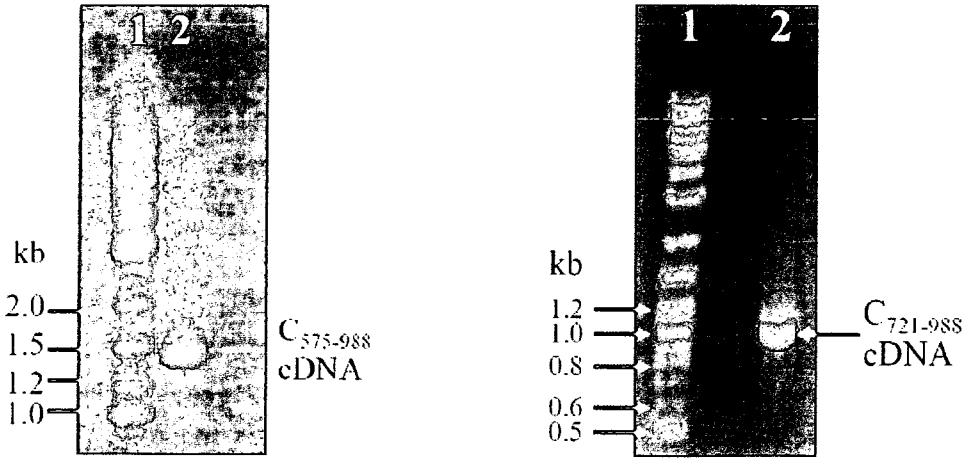

Figure 7.2 $C_{575-988}$ cDNA (A) and $C_{721-988}$ cDNA (B) visualized by ethidium bromide staining on a 1.0% TAE agarose gel

Lanes 1 of (A) and (B) are DNA Ladders. Lane 2 of (A) is $C_{575-988}$ cDNA and of (B) is $C_{721-988}$ cDNA constructed through PCR. The $C_{575-988}$ cDNA is located slightly lower than the 1.5 kbp fragment of the DNA ladder and the $C_{721-988}$ cDNA is located around the 1 kbp fragment of the DNA ladder. The sizes of the both cDNA fragments are in agreement with their predicted size of 1.3 kbp and 0.9 kbp, respectively.

7.3.3 Insert clones were verified by DNA sequencing

Following the methods outlined in Section 7.2.2.3, $C_{575-988}$ and $C_{721-988}$ were cloned into Thx/pET32a successfully. Sequencing results (Appendix F) of Thx-$C_{575-988}$/pET32a and Thx-$C_{721-988}$/pET32 showed that no inadvertent mutations were introduced.

7.3.4 Detection of protein expression

7.3.4.1 Thx-$C_{721-988}$/pET32a expression

Both induced and non-induced samples from the Thx-$C_{721-988}$/pET32a expression were analysed on SDS-PAGE (Figure 7.3). There is an obvious expressed protein band around 60 kDa (which is larger than the predicted molecular weight of 47 kDa) in the induced cell sample compared with the non-induced sample. This highly expressed protein band was recognized by anti-C-tail antibody (Gurnett *et al.* 1995) in western blotting (Figure 7.4) but no similar protein band was detected in the non-induced sample. These results support the conclusion that the desired protein has been successfully expressed. Its accurate molecular weight has been determined to be 46.94 kDa using Mass spectrometry, as described in Section 7.3.6.

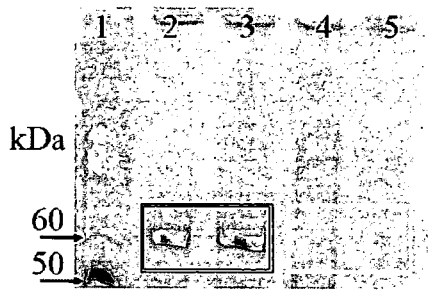

Figure 7.3 SDS-PAGE analysis of Thx-$C_{721-988}$/pET32a protein expression

Lane 1 is protein marker with the molecular weight indicated on the left hand side. Lane 2 and 3 are protein extracts of induced sample. Lane 4 and 5 are protein extracts of non-induced sample. The bands enclosed in a red square are highly expressed bands when compared with non-induced sample at the same position enclosed in a yellow square.

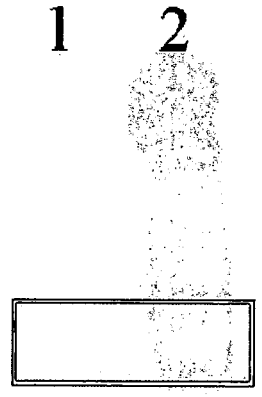

Figure 7.4 Western Blots result of Thx-$C_{721-988}$/pET32a expressed protein

Lane 1 is non-induced sample and lane 2 is induced sample corresponding to the samples of SDS-PAGE shown in Figure 7.3.

7.3.4.2 Thx-$C_{575-988}$/pET32a expression

Another C-tail fragment, $C_{575-988}$, was highly expressed using the Thx/pET32a vector. Expressed proteins were analysed by SDS-PAGE (Figure 7.5A) and the highly expressed protein band located at 100 kDa was recognized by anti-C-tail antibody (Figure 7.5B). However, this Thx-$C_{575-988}$ protein was mainly allocated in insoluble fraction (Figure 7.6).

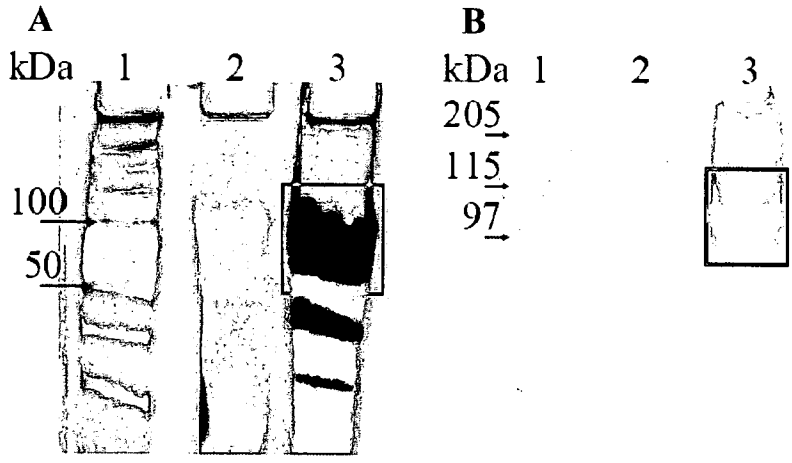

Figure 7.5 SDS-PAGE (A) and Western blot (B) analysis of Thx-$C_{575-988}$/pET32a expressed protein

Lane 1 is protein marker with the molecular weight indicated on the left hand side. Lane 2 is non-induced sample. Lane 3 is induced sample. The transblotted membrane (**B**) demonstrated that the Thx-$C_{575-988}$ protein band in red square was recognized by anti-C-tail antibody shown in brown colour.

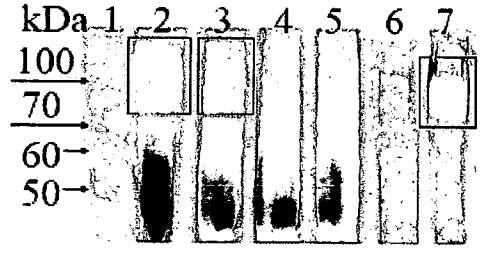

Figure 7.6 SDS-PAGE analysis of the solubility of Thx-$C_{575-988}$/pET32a expressed protein

Lane 1 is a Protein marker with the molecular weight indicated on the left hand side. Lane 2 and 4 are insoluble extract and soluble fraction after lysozyme treatment. Lane 3 and 5 are insoluble extract and soluble fraction after both lysozyme treatment and sonication. Lane 6 is insoluble debris undissolved in 8 M urea. Lane 7 is insoluble extract after both lysozyme treatment and sonication dissolved in 8 M urea. Red rectangle enclosed the Thx-$C_{575-988}$ protein was found mainly in insoluble fraction (lane 2 & 3) and dissolved fraction (lane 7) in 8 M urea.

7.3.5 Protein purification of $C_{721-988}$ peptide

As the expressed $C_{575-988}$ was found mostly in the insoluble fraction, protein purification was initially performed on the $C_{721-988}$ peptide. Protein expressed from 10 ml culture of $C_{721-988}$/pET32a was loaded onto a 1 ml Ni-NTA packed column, washed with 150 mM imidazole-containing buffer and eluted by 500 mM imidazole-containing buffer. A small amount of target protein can be found in the eluate using 150 mM imidazole, however, it was mainly (0.2 mg) eluted by 500 mM imidazole-containing buffer and with a faint contaminant band around 53 kDa (Figure 7.7).

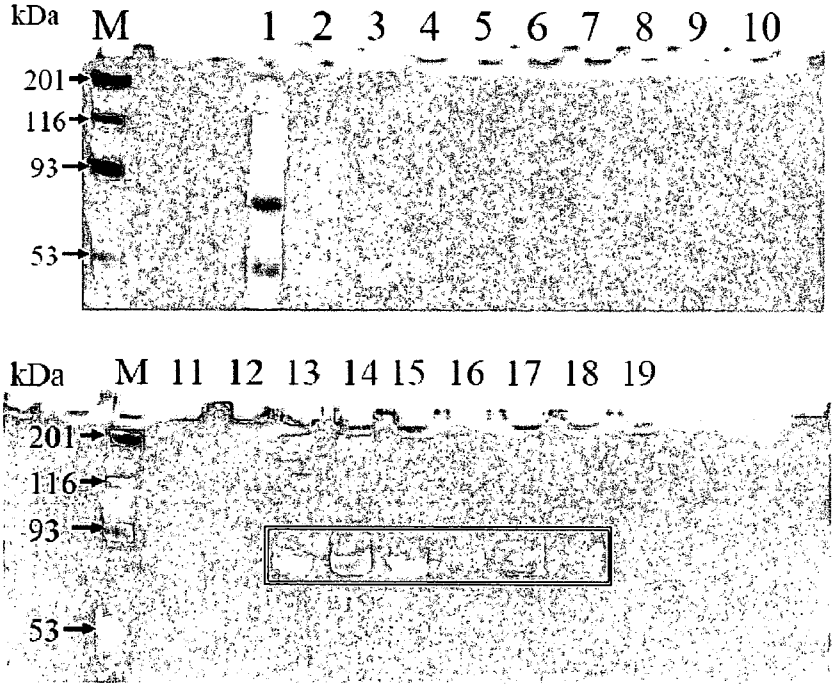

Figure 7.7 Thx-$C_{721-988}$ protein was partially purified by adding a 150 mM imidazole washing step and the samples were analysed by SDS-PAGE

Lane M is protein marker with the molecular weight indicated on the left hand side. Lane 1 is crude sample. Lanes 2 to 6 are the samples collected from washing through using 20 mM imidazole-containing buffer. Lanes 7 to 11 are the samples collected from washing through using 150 mM imidazole-containing buffer. Lanes 12 to 19 are the sample fractions collected from elution using 500 mM imidazole-containing buffer. The Thx-$C_{721-988}$ proteins are indicated in the red rectangle.

7.3.6. Molecular weight determination of Thx-$C_{721-988}$

According to the amino acid sequence of Thx-$C_{721-988}$, its molecular weight is predicted to be approximately 47 kDa but observed to be much larger at about 60 kDa on 12 % SDS-PAGE (Figure 7.3). Thus, a more precise protein molecular weight determination method was adopted. Purified Thx-$C_{721-988}$ was subjected to molecular weight determination by mass spectrometry (Section 7.2.8). A single peak with molecular weight of 46.94 kDa is shown on the mass spectrum (Figure 7.8).

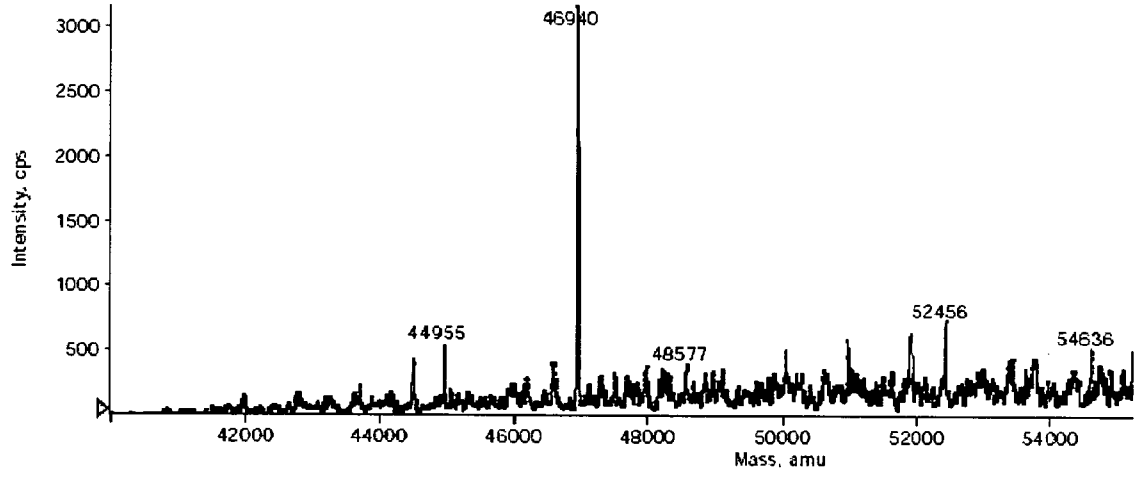

Figure 7.8 Mass spectrum of Thx-$C_{721-988}$

Single peak observed from the mass spectrum represented the Thx-$C_{721-988}$ with molecular weight 46.94 kDa

7.3.7 Purification of His-3C digested Thx-$C_{721-988}$ protein

A complete digestion of Thx-$C_{721-988}$ by His-3C was prepared (Figure 7.9). The digested mixture of Thx and $C_{721-988}$ protein were loaded onto a Ni-NTA column for a second step of purification to separate the Thx, His-3C and $C_{721-988}$ proteins. The fractions collected from the purification steps were analysed by SDS-PAGE (Figure 7.10) which showed that $C_{721-988}$ had been successfully separated from Thx-tag and His-3C with $C_{721-988}$ found in the wash through and the Thx-tag able to be eluted using 500mM imidazole buffer.

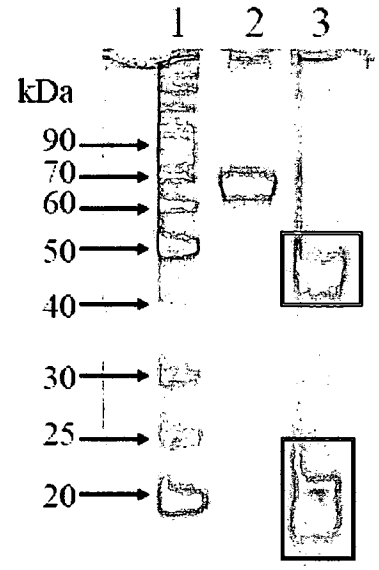

Figure 7.9 SDS-PAGE analysis of Thx-$C_{721-988}$ proteins digested by His-3C

Lane 1 is protein marker with the molecular weight indicated on the left hand side. Lane 2 is undigested Thx-$C_{721-988}$. Lane 3 is digested fragments contained $C_{721-988}$ in the red square and Thx-tag in the green rectangle.

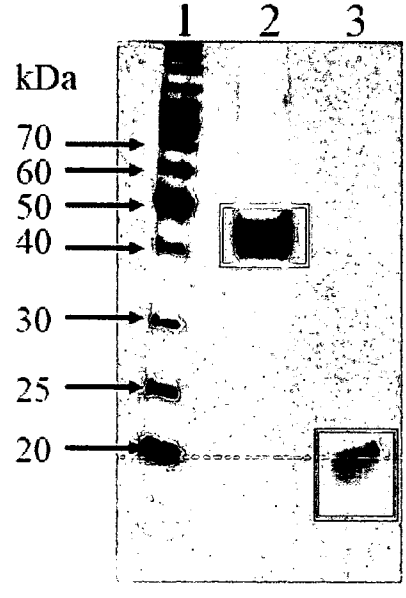

Figure 7.10 SDS-PAGE analysis of $C_{721-988}$ purification by Ni-NTA

Lane 1 is protein marker with the molecular weight indicated on the left hand side. Lane 2 is wash through and $C_{721-988}$ is enclosed in a red rectangle. Lane 3 is eluate using 500 mM imidazole buffer and the Thx-tag is shown in a green rectangle.

7.3.8. Molecular weight determination of purified $C_{721-988}$

Here again, I used mass spectrometry to determine the molecular weight of $C_{721-988}$ rather than relying on comparison with molecular weight markers on the SDS-PAGE. According to its amino acid sequence the $C_{721-988}$ protein should be approximately 29 kDa. However, two peaks with molecular weights of 29.01 kDa and 26.98 kDa were observed in the mass spectrum (Figure 7.11). The former molecular weight which matched with the molecular weight determined from amino acid sequence calculation probably represented the intact $C_{721-988}$ fragment but the latter weight may represent a modified fragment of $C_{721-988}$ with part of its C-terminus cleaved off. Using the peptide sequence calculation software (Paw), subtraction of a peptide, QGPSLRSTDEEDEDELIL, located at the extreme C-terminus after a leucine residue (Appendix A) leaves a C-terminus truncated protein with molecular weight 27 kDa. Thus, I propose that the smaller sized protein peak represents a cleaved C-terminus product due to proteolysis. Coincidently, spontaneous proteolysis at the C-terminus of the purified C-tail protein of ClC-0 had also been observed by Meyer and Dutzler (Meyer & Dutzler 2006).

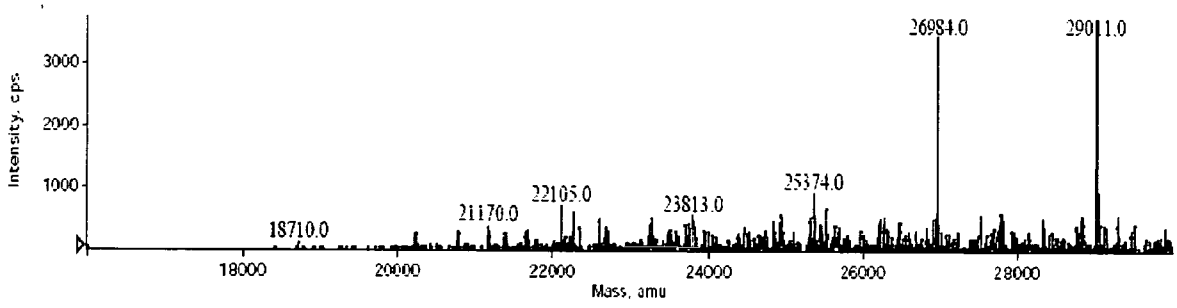

Figure 7.11 Mass spectrum of $C_{721-988}$

Two dominant peaks were observed in $C_{721-988}$ analysis, possibly representing the whole peptide (29.01 kDa) and the peptide with part of its C-terminus cleaved off (26.98 kDa).

7.4 DISCUSSION

7.4.1 Protein expression

Up to now, there has been no publication that has mentioned using purified human ClC-1 C-tail proteins for further studies. In my project, I have established human C-tail protein expression and preliminary purification. Both of the Thx-$C_{721-988}$ and Thx-$C_{575-988}$ have been successfully expressed in high yield with low background protein contaminants (Figure 7.3 and Figure 7.5). Thx-$C_{721-988}$ was found to be totally soluble in my defined native buffer, whereas, Thx-$C_{575-988}$ was partly soluble and mainly found in the insoluble fraction. These results demonstrated that thioredoxin fusion protein enhanced the yield of both of the C-tail proteins following expression and improved the solubility of expressed $C_{721-988}$ but only had a mild effect on the solubility of expressed $C_{575-988}$. Previously, one of our colleagues used pQE30 bacterial expression system for rat ClC-1 C-tail, $C_{573-994}$, protein expression (Simpson 2002). Although the target protein was expressed and recognized by anti-C-tail antibody, the yield was relatively small, and had high amounts of contaminating proteins present. In addition, the expressed protein tended to form inclusion bodies. This situation has also been reported by Maduke and colleagues (Maduke, Williams & Miller 1998). During their ClC-0 C-tail expression using a bacterial system, C-tail fragments generated by splitting in the interlinker sequence of CBS1 and CBS2 (Q644 of ClC-0 equivalent to L719 of hClC-1 and Y677 of ClC-0 equivalent to F768 of hClC-1) showed expression but formed mainly inclusion bodies. In the present studies, protein expression yield and solubility have been improved by using Thx/pET32a vector. Target protein was expressed as thioredoxin fusion protein. Thioredoxin fusion is aimed at enhancing the solubility of the target protein and the protein expression yield (LaVallie *et al.* 2000). Based on protein quantification before and after purification, the amounts of

total protein expressed and of partially-purified target protein have been estimated. About 0.2 mg of total protein per ml of bacterial culture were produced from my expression system and about 26% of protein was identified as Thx-C-tail protein. Theoretically, 200ml of expressed culture would then be able to produce more than 10 mg of Thx-C-tail protein which should be enough for various types of structural analysis such as NMR or X-ray crystallography. However, dramatic losses of protein were observed when separating the C-tail protein from the thioredoxin fusion protein. Improvements in the protein purification system in the later steps were necessary to reduce the amount of protein lost.

7.4.2 C-tail region selected for protein expression

I first demonstrated that two terminal fragments, $C_{721\text{-}988}$ and $C_{575\text{-}988}$, of the hClC-1 C-tail were able to be constructed and expressed as individual units, capable of functional reconstitution when co-expressed with membrane-resident fragment hClC-1 $N_{1\text{-}720}$. They were successfully used for my protein expression and purification project. Previous studies (Schmidt-Rose & Jentsch 1997a; Maduke, Williams & Miller 1998) have provided strong evidence that the distal C-tail (containing CBS2) is individual, globular and water soluble with strong structural integrity. Therefore, this structure has become one of the C-tail protein expression candidates in the present studies. Using a functional reconstitution strategy, individual C-tail units capable of complementing N-terminal constructs were found in ClC-0 and ClC-1 (Schmidt-Rose & Jentsch 1997a; Maduke, Williams & Miller 1998). Following this work, the hClC-1 C-tail structure, $C_{721\text{-}988}$, complementary to the N-terminal sequence, $N_{1\text{-}720}$, has commonly been used as the positive control for split channel experiments (Estévez *et al.* 2004; Hebeisen *et al.* 2004; Wu *et al.* 2006). Similarly, $C_{652\text{-}805}$ from ClC-0, equivalent to $C_{728\text{-}988}$ of hClC-1, has been expressed in a bacterial system (Maduke, Williams & Miller 1998). The partially purified and refolded protein was

injected into oocytes expressing N-terminal region and demonstrated the functional restoration ability of bacterially expressed C-tail (Maduke, Williams & Miller 1998).

Besides using $C_{721-988}$ for protein expression, $C_{575-988}$ was prepared for protein expression. Individual functional structure of $C_{575-988}$ was initially confirmed by split channel co-expression with N_{1-720} in HEK cell experiments (Result section 7.3.1). Although $C_{721-988}$ is a suitable individual folding unit for structural analysis, it has only about half of the sequence of the whole cytoplasmic C-tail of hClC-1 and contains only a single CBS domain. The disadvantage of using $C_{721-988}$ for C-tail structure analysis is that this sequence would not be able to represent the structure of the whole C-tail. Thus, the other construct, $C_{575-988}$, that covered the whole C-tail region and the R-helix was included for expression in the present studies. Since there was no functional restoration when a split was made in the region between the residues 597 and 598 (Schmidt-Rose & Jentsch 1997a), there was no pre-existing evidence that $C_{575-988}$ was an individual folding unit. Split channel experiments were thus performed to assess the capability for functional restoration during co-expression with the N-terminal region. The mammalian split channel expression system established in Chapter III was used in this experiment. According to one of the results obtained by Schmidt-Rose and Jentsch, $C_{579-988}$ was able to achieve functional rescue of N_{1-720} (Schmidt-Rose & Jentsch 1997a) in *Xenopus* oocytes. There was though no evidence that N_{1-574} could be expressed successfully. Thus, rather than using N_{1-574} + $C_{575-988}$ functional complementation was performed in the N_{1-721} + $C_{575-988}$ configuration. Wild-type ClC-1 chloride conductance was obtained (Figure 7.1) in this case in HEK cells. Hence, $C_{575-988}$ is able to fold independently to rescue channel function and is a suitable candidate for protein expression and structural analysis. In addition, there is a conserved residue (Tyrosine) in the R-helix that has been proposed to contribute effects on ion coordination in the conduction pore (Dutzler *et al.* 2002; Dutzler, Campbell & MacKinnon 2003).

Including the R-helix region inside the $C_{575\text{-}988}$ structure might give an idea of how the connection is formed between the ion conduction pore and the C-tail.

CHAPTER EIGHT: GENERAL DISCUSSION AND FURTHER DIRECTIONS

8.1 GENERAL DISCUSSION

The first X-ray structure of the CLC channel/transporter was derived from bacteria (Dutzler *et al.* 2002). It provided a picture of how the ion conduction pore is formed by the N-region membrane-resident domain of the protein and confirmed that CLC has a double-barreled structure. However, bacterial CLCs only have a very short cytoplasmic C-tail (~17 amino acids) which was unable to provide information about the extensive C-tail structure present in eukaryotic CLCs (ranging from 161 to 318 amino acids). Importantly, the C-tail structure of eukaryotic CLCs is required for function (Schmidt-Rose & Jentsch 1997a). If parts of that sequence were deleted, CLCs were unable to conduct chloride ions. However, when co-expressing complementary missing tail portions with specific site-directed C-tail truncated mutants in *Xenopus* oocytes, channel function could be restored (Schmidt-Rose & Jentsch 1997a).

8.1.1 Split hClC-1 expression in HEK cells

However, at the time I began my PhD project, the split channel experiments on CLC channels had all been performed in *Xenopus* oocytes (Schmidt-Rose & Jentsch 1997a; Maduke, Williams & Miller 1998; Estévez *et al.* 2004; Mo *et al.* 2004; Wu *et al.* 2006). Expression of CLC channels in mammalian cells had been used but only to study the functional consequence of point mutations and terminal truncations on continuous CLC sequence (Fahlke *et al.* 1996; Fahlke, Beck & George 1997a; Fahlke, Durr & George 1997b; Fahlke *et al.* 1997c; Wagner *et al.* 1998) . There were no accounts of split CLC channel experiments in cultured mammalian cells published at that time. I believed that it

would be useful to establish a CLC split channel system using mammalian cells to provide results more comparable with conditions in native muscle and to reduce the discrepancies that seemed to arise from using different expression systems (Estévez *et al.* 2004; Hebeisen *et al.* 2004; Goldin 2006). My success in the establishment of the split hClC-1 channel in mammalian cells has been demonstrated here by co-expression of N_{1-720} and $C_{721-988}$ hClC-1 which produced similar channel properties to full-length WT hClC-1. In the middle of my project, coincidently, Hebeisen and Fahlke published some results from split hClC-1 split channel experiments in mammalian tsA201cells (Hebeisen *et al.* 2004). The simultaneous success of their study has supported the need for, and usefulness of, setting up the split channel expression system in mammalian cells.

8.1.2 Functional reconstitution of naturally-occurring nonsense mutants using supplement of C-tail peptide

There are dominant and recessive phenotypes of myotonia congenita. Most of the recessive phenotypes arise from the nonsense mutations in hClC-1 and these patients show more severe symptoms than patients with dominant phenotypes. Here, I have presented and demonstrated how co-expression of C-tail peptide, $C_{721-988}$, with some naturally-occurring C-tail truncated mutants is able to restore function to the otherwise non-functional truncated channels, E717X and Q807X. These findings provide proof of concept for a possible therapy method for the recessive phenotype patients whose disease is caused by certain nonsense mutations. Nowadays, various therapy methods have been suggested for different human genetic diseases, like myotonia congenita. Whole gene delivery may be one of the ways but these methods have been typically been found to be less efficient than required (Duan 2006). Short peptide delivery methods such as oligonucleotide-mediated gene therapy (Rando 2002) and short fragment homologous recombination (Goncz *et al.*

2002; Kapsa *et al.* 2002) have been suggested to improve the efficiency. In this regard, CLC proteins have a distinctive advantage in their ability allowing them to be functionally reconstituted from split components. Thus, supplementation of a short C-tail peptide might be able to be developed for gene therapy in this case. In addition, the shortest functional continuous hClC-1 has been found in this study, demonstrating that the essential sequences for channel function are located within the amino acid residues from 1 to 870.

8.1.3 Attempted functional restoration of C-tail truncated mutant by supplementation with short C-tail fragment

This study was an extension of the investigation conducted by a previous PhD student in our laboratory, Dr. Weiping Wu. She found that a 26 amino acid peptide, $C_{863\text{-}888}$, was able to restore the function of the C-tail truncated channel, $N_{1\text{-}720}$. I believed that this short peptide would be more appropriate and effective in gene delivery for therapy purpose. Further studies on the possibility of using this $C_{863\text{-}888}$ fragment for functional restoration of $N_{1\text{-}720}$ were conducted in my newly set up split channel expression using HEK cells. Six more peptides with one or more amino acids truncated at the either ends were constructed to test for the essential and minimum amino acids for functional restoration. Unexpectedly, all the results of $N_{1\text{-}720}$ supplementation with the C-tail peptides have shown no functional restoration, not even the supplementation with the untruncated $C_{863\text{-}888}$ peptide. Furthermore, I have used immunoblotting to detect the protein expression levels for $C_{721\text{-}988}$ and $C_{863\text{-}988}$ to investigate if the protein expression level might affect the efficiency of functional restoration in this case. Both of the peptides have produced a similar quantity of protein when compared using the detection intensity, however, the molecular weight of $C_{863\text{-}988}$ seems to be reduced slightly. The antibody used here for immunoblotting was to detect the final 15 amino acids (Gurnett *et al.* 1995) at the C-terminus of hClC-1, thus there

is a possibility the N-terminus of $C_{863-988}$ was cleaved during proteolysis in the HEK cell expression system. The N-terminus of $C_{863-888}$ would be an important sequence compared with the C-terminus. According to the previous result and the structure of the CBS domain, the N-terminus sequence of $C_{863-988}$ involves the α2 region of CBS2. Also, based on my results for N_{1-870} obtained in Chapter IV, it is obvious that truncation of the C-terminal sequence after amino acid residue 870 does not totally abolish chloride channel function. Although my results here cannot reproduce the results discovered in *Xenopus* oocytes, it has not been uncommon to observe contradictory results with different expression systems (Estévez *et al.* 2004; Hebeisen *et al.* 2004). In this case, proteolysis in the HEK cell mammalian system would be one of the main possibilities leading to my failure to reproduce similar results to those found using *Xenopus* oocytes and it needs to be further investigated.

8.1.4 Characterization of three novel myotonia-associated missense mutations in the C-tail region of human ClC-1 via heterologous expression

Recently, thirteen novel mutations have been screened from myotonic patients and the predicted amino acid mutations have been reported to our group for characterisation. I have constructed the corresponding mutations in the hClC-1 gene to study their functional consequences using the HEK cell expression system. Three of the mutations (R691S, E724A and V851M) are located in the C-tail region. Here, I have prioritized study the functional effect of these particular mutations because I believed that they might give further information on the functional effect of myotonia-associated mutations on C-tail. To my surprise, except for the highly conserved residue V851M which shifted apparent open probability to a more positive value, the other two mutants, R691S and E724A are more and less similar to WT hClC-1. They have maintained a sufficient channel opening in the

physiological potential range with no implication that these mutations would cause myotonia. Since the amino acids mutations were predicted from the nucleotide alteration obtained from the screening of hClC-1 gene sequence, the effect of these nucleotide mutations might be anticipated incorrectly. In a 1994 study, a nucleotide alteration (G979A) was found in exon 8 of hClC-1 (Lorenz *et al.* 1994) from which the author had predicted two possible effects. One might lead to the substitution of an isoleucine for a valine at the amino acid residue position 327 (V327I) but the other would be a splice defect. After a functional consequence study of V327I hClC-1 mutant in *Xenopus* oocytes, the results showed there was no significant channel property difference from WT hClC-1. As the mutation was associated with recessive myotonia, the author concluded that the splice defect would be the cause of the myotonia for this nucleotide alteration. Thus, I would suggest that the two amino acid substitutions with WT properties that I have studied here, may not be showing the real effect of the nucleotide alteration that causes the myotonia in these cases. Further investigation of the effects of these nucleotide substitutions are clearly necessary.

8.1.5 Protein expression of C-tail peptide

At the time I began my attempt at expression and purification of the C-tail protein, there was no existing information about the C-tail structure. Most of the groups studying eukaryotic CLCs appear to have attempted to produce C-tail proteins for structural analysis but the expressed proteins were insoluble (Maduke, Williams & Miller 1998) and impeded the way towards structural analysis. Here, I have used thioredoxin fused expression vector to facilitate soluble C-tail protein production in a bacterial system. A his-tag has been interposed between the thioredoxin and C-tail structure to enable subsequent protein purification by metal affinity chromatography. In this way, the $C_{721\text{-}988}$ tail peptide was

successfully expressed in a soluble form and purified to a homogeneity assessed by SDS-PAGE analysis with coomassic blue staining. In 2005, the first X-ray crystallography of C-tail structure for ClC-0 (Meyer & Dutzler 2006) has been published and the group has used a bacterial expression system for the ClC-0 C-tail protein production and a his-tag to facilitate the protein purification. I believe that the protein expression and purification strategies that I have used here have been in the right direction. Coincidently, the phenomenon of the C-terminus cleavage on the expressed C-tail has been found in both ClC-0 (Meyer & Dutzler 2006) and in my current work using $C_{721\text{-}988}$.

To sum up, I have established a useful HEK cell expression system for split channel experiments in ClC-1 in our laboratory and, in doing so, have confirmed similar work that was undertaken at the same time in another laboratory (Hebeisen *et al.* 2004). This method should be able to be used to produce results comparable to those found in native mammalian muscle and might prove superior to the *Xenopus* oocyte system in this regard. Using the HEK cell expression system, I have, for the first time, demonstrated that supplementation of a C-tail peptide was able to restore the function of certain naturally-occurring, myotonia-associated, nonsense mutants of ClC-1. This result provides an alternative method, potentially more effective than whole gene approaches (Duan 2006), for gene therapy of the recessive myotonic disorder. Also, here, I have shown the shortest functional continuous length of C-terminal truncated hClC-1 peptide, $N_{1\text{-}870}$. This observation is of considerable significance as it confirms that the final amino acids of CBS2 are essential in terminally-truncated (as opposed to internally deleted) hClC-1 (Hryciw *et al.* 1998; Hebeisen *et al.* 2004). A similar terminal truncation of ClC-0 produces a strange, hyperpolarisation-activated channel (Maduke, Williams & Miller 1998). Although I have been unable to repeat the functional restoration power of the 26 amino acid peptide, $C_{863\text{-}888}$, discovered by Dr. Weiping Wu (Wu *et al.* 2006), in the newly

established HEK cell system, my work strongly supports the view that essential amino acids of the C-tail are located in the N-terminal region of $C_{863-988}$ and probably within the region $C_{863-888}$. This constitutes the first supportive evidence for the importance of the α2 region of CBS2 in hClC-1. Absence of pronounced functional consequences of the two newly described myotonia-associated mutations when mimicked in HEK cells hints that these mutations might not be due simply to amino acid substitution in the gene. Instead, the malfunction in patients might be due to interference with transcription, with gene splicing, or for other extra-exonic reasons. Although I am not the first to note this kind of discrepancy between the presence of clinical myotonia, detectable hClC-1 variations and functional expression in heterologous systems (Lorenz *et al.* 1994), my results again serve to underline the requirement for additional research, beyond the usual sub-exonic regions, in these enigmatic cases.

8.2 FURTHER DIRECTIONS

8.2.1 Using animal model to strengthen the functional restoration hypothesis

In order to further explore the idea of functional restoration of nonsense mutations using a C-tail peptide (gene or peptide therapy) in myotonic patients, we should move from the cell model to the animal. A mouse model would probably be the best choice to start, for example, dystrophin-deficient mdx mice and transgenic mice with different dystrophin and dystrophin-associated protein mutations have been used in the studies of Duchenne muscular dystrophy (Straub *et al.* 1997). Although, the shortened peptides, $C_{863-988}$ and smaller, did not produce consistent results in cell models, it is still worthwhile to synthesize these peptides and to test them in an animal model. Also, it would be appropriate to find out the minimal sequence of C-tail peptide that is required for functional restoration. Using a shorter peptide construct for gene delivery should be much

easier. If the 26 amino acids peptide, $C_{863-888}$, show functional restoration in an animal model, protein/peptide therapy might also be another direction for disease treatment. The symptoms of certain recessive myotonic disease patients might be able to be treated by protein/peptide delivery though parenteral or oral routes of administration in the future (Kumar, Soppimath & Nachaegari 2006).

8.2.2 Using fluorescence resonance energy transfer and site-directed mutagenesis to test for the CBS2 interaction hypothesis

In my results shown in Chapter IV, the mutant, N_{1-871}, with CBS2 but lacking the distal sequence produced mutant currents. The supplemented $C_{721-988}$ peptide with both CBS2 and distal sequence was unable to restore the current back to wild-type. I suggested that CBS2 might be the major domain for attaching the downstream structure to the upstream structure and guiding the distal sequence into place to configure the channel conduction pore in normal functional conformation (Hebeisen & Fahlke 2005). However, as N_{1-871} already has CBS2 to interact, the same CBS2 structure supplied by $C_{721-988}$ might not be able to displace the original CBS2 domain as there may be no advantage in energy gain for this structural rearrangement. In order to test this hypothesis, particularly as to whether CBS2 is the core structure for interaction, mutations should be created in the CBS2 domain of N_{1-871} so as to weaken a possible interaction. According to the recent X-ray structure of the C-tail domain from ClC-0 (Meyer & Dutzler 2006), the possible region to weaken this interaction might be the amino acids at the interface between the CBS1 and CBS2 domains. Supplementing the $C_{721-988}$ peptide to this mutated N_{1-871} to investigate whether the function can be improved back to wild-type would be possible to demonstrate my hypothesis. In addition, using fluorescence resonance energy transfer (FRET) methods by attaching a reporter probe in the sequence of CBS1 of N_{1-871} and a quencher probe in the

sequence of CBS2 of $C_{721-988}$ would further demonstrate the interaction. These results would be very important in solving some of the mysteries of whether CBS2 is necessary for channel function or not and in determining its role in the guiding the distal structure into place with N-terminal membrane-resident domains.

8.2.3 Using peptide melting point analysis to determine the protein stability

Recalling the results shown in Chapter V, the shortened C-tail peptides, $C_{863-988}$ and smaller, which have restored the function of the N_{1-720} truncated channel in the *Xenopus* oocyte expression system, did not give similar results in HEK cells. It would be interesting to determine the possible factors that caused this discrepancy and would be helpful to expand our knowledge of the usage of these two systems for channel expression and functional characterization. In accordance with the Western blot analysis (Figure 5.3), the molecular weight of $C_{863-988}$ is smaller than the predicted value. Protein degradation might be a reason. Mass spectroscopy could be used to find the accurate molecular weight of the purified $C_{863-988}$ peptide to determine whether the peptide was degraded or not. Also, protein degradation might imply that the $C_{863-988}$ is synthesized in HEK cells with reduced stability and that it triggers the inherent protective proteolytic system to degenerate the exogenous peptide. Proteolytic processes has have been counted as a regulatory mechanism to eliminate abnormal and mutated proteins (Goldberg & Dice 1974). In order to know whether these peptides show different stability when they are produced in different expression systems, peptide melting point can be used as stability indicator. Dynamic light scattering and circular dichroism techniques can be used to determine the peptide melting point during the thermal denaturating process. Collectively, these results would be helpful in solving the puzzles about the contradictory results that have occurred in ion channel expression and also would be a test assay in the future for researchers to decide which

expression systems should be appropriate for certain channel studies.

8.2.4 Allosteric effect on C-tail structure by nucleotides

Previously, some mutations that occur in the proposed ATP-binding pocket have been shown to cause a change in common gating (Bennetts *et al.* 2005). Thus, understanding the mechanism of ATP induced conformational changes might be helpful in revealing the common gating transition mechanism and how the C-tail structure regulates the opening and closing of ion conduction pores. In order to refine the conformational change mechanism, FRET measurement could be used. N-methylanthraniloyl (mant) derivative of ATP fluorophore has a similar structure to TNP-ATP, both of them being ribose-modified ATP analogues (Jameson & Eccleston 1997) but they have different excitation and emission wavelengths. One of the advantages of using mant-ATP to continue the study would be that the absorption wavelength (364 nm) of mant-ATP is close to the maximum emission wavelength (350 nm) of tryptophan. $C_{721\text{-}988}$ has two intrinsic tryptophan residues. If the ATP-binding site is close enough to the tryptophan residues, excitation of the protein/mant-ATP complex at 290 nm (excitation wavelength for tryptophan), would allow us to observe a fluorescence emission at 448nm by mant-ATP rather than the 350 nm emission of tryptophan (Moore & Lohman 1994). The change of energy level of the fluorescence emission during the conformational change process would indicate how the structural rearrangement is related to the tryptophans. In addition, specific mutants with a single tryptophan would be useful to determine precisely the conformational change with respect to that mutated residue position without the confusion of a fluorescence signal from two tryptophans. Furthermore, in regard to the studies performed by Bennetts and colleagues (Bennetts *et al.* 2005), ADP and AMP had similar effects to ATP. Thus, further extension of these allosteric studies using mant-ADP and mant-AMP would be worthwhile

to investigate the extent of the effect on C-tail structure of different nucleotides.

8.2.5 Scale up the protein expression and purification steps for further investigation of the structure of C-tails

Finally, the protein expression system has now been established in our laboratory for C-tail peptide production. The process can be scaled up to produce large quantities of C-tail peptide for further structural analysis. Furthermore, production of important C-tail fragments and its site-directed mutants in large amount (10mg/ml) with high purity can be used for NMR and X-ray crystallography to determine the 3D-structure.

BIBLIOGRAPHY

Accardi, A, Ferrera, L & Pusch, M 2001, 'Drastic reduction of the slow gate of human muscle chloride channel (ClC-1) by mutation C277S', *J Physiol,* vol. 534, no. Pt 3, Aug 1, pp. 745-52.

Accardi, A, Kolmakova-Partensky, L, Williams, C & Miller, C 2004, 'Ionic currents mediated by a prokaryotic homologue of CLC Cl- channels', *J Gen Physiol,* vol. 123, no. 2, Feb, pp. 109-19.

Accardi, A & Miller, C 2004, 'Secondary active transport mediated by a prokaryotic homologue of ClC Cl- channels', *Nature,* vol. 427, no. 6977, Feb 26, pp. 803-7.

Accardi, A & Pusch, M 2000, 'Fast and slow gating relaxations in the muscle chloride channel CLC-1', *J Gen Physiol,* vol. 116, no. 3, Sep, pp. 433-44.

Accardi, A, Walden, M, Nguitragool, W, Jayaram, H, Williams, C & Miller, C 2005, 'Separate ion pathways in a Cl-/H+ exchanger', *J Gen Physiol,* vol. 126, no. 6, Dec, pp. 563-70.

Ackerman, MJ, Wickman, KD & Clapham, DE 1994, 'Hypotonicity activates a native chloride current in Xenopus oocytes', *J Gen Physiol,* vol. 103, no. 2, Feb, pp. 153-79.

Ahmed, N, Ramjeesingh, M, Wong, S, Varga, A, Garami, E & Bear, CE 2000, 'Chloride channel activity of ClC-2 is modified by the actin cytoskeleton', *Biochem J,* vol. 352 Pt 3, Dec 15, pp. 789-94.

Arakawa, T, Philo, JS & Kita, Y 2001, 'Kinetic and thermodynamic analysis of thermal unfolding of recombinant erythropoietin', *Biosci Biotechnol Biochem,* vol. 65, no. 6, Jun, pp. 1321-7.

Aromataris, EC, Rychkov, GY, Bennetts, B, Hughes, BP, Bretag, AH & Roberts, ML 2001, 'Fast and slow gating of CLC-1: differential effects of 2-(4-chlorophenoxy) propionic acid and dominant negative mutations', *Mol Pharmacol,* vol. 60, no. 1, Jul, pp. 200-8.

Arreola, J, Begenisich, T, Nehrke, K, Nguyen, HV, Park, K, Richardson, L, Yang, B, Schutte, BC, Lamb, FS & Melvin, JE 2002, 'Secretion and cell volume regulation by salivary acinar cells from mice lacking expression of the Clcn3 Cl- channel gene', *J Physiol,* vol. 545, no. Pt 1, Nov 15, pp. 207-16.

Ashcroft, FM & Kakei, M 1989, 'ATP-sensitive K+ channels in rat pancreatic beta-cells: modulation by ATP and Mg2+ ions', *J Physiol,* vol. 416, Sep, pp. 349-67.

Bateman, A 1997, 'The structure of a domain common to archaebacteria and the homocystinuria disease protein', *Trends Biochem Sci,* vol. 22, no. 1, Jan, pp. 12-3.

Beck, CL, Fahlke, C & George, AL, Jr. 1996, 'Molecular basis for decreased muscle chloride conductance in the myotonic goat', *Proc Natl Acad Sci U S A,* vol. 93, no. 20, Oct 1, pp. 11248-52.

Bell, SP, Curran, PK, Choi, S & Mindell, JA 2006, 'Site-Directed Fluorescence Studies of a Prokaryotic ClC Antiporter', *Biochemistry,* vol. 45, no. 22, Jun 6, pp. 6773-82.

Bennetts, B, Roberts, ML, Bretag, AH & Rychkov, GY 2001, 'Temperature dependence of human muscle ClC-1 chloride channel', *J Physiol,* vol. 535, no. Pt 1, Aug 15, pp. 83-93.

Bennetts, B, Rychkov, GY, Ng, HL, Morton, CJ, Stapleton, D, Parker, MW & Cromer, BA 2005, 'Cytoplasmic ATP-sensing domains regulate gating of skeletal muscle ClC-1 chloride channels', *J Biol Chem,* vol. 280, no. 37, Sep 16, pp. 32452-8.

Biemans-Oldehinkel, E, Mahmood, NA & Poolman, B 2006, 'A sensor for intracellular ionic strength', *Proc Natl Acad Sci U S A,* vol. 103, no. 28, Jul 11, pp. 10624-9.

Birkenhager, R, Otto, E, Schurmann, MJ, Vollmer, M, Ruf, EM, Maier-Lutz, I, Beekmann, F, Fekete, A, Omran, H, Feldmann, D, Milford, DV, Jeck, N, Konrad, M, Landau, D, Knoers, NV, Antignac, C, Sudbrak, R, Kispert, A & Hildebrandt, F 2001, 'Mutation of BSND causes Bartter syndrome with sensorineural deafness and kidney failure', *Nat Genet,* vol. 29, no. 3, Nov, pp. 310-4.

Bornhorst, JA & Falke, JJ 2000, 'Purification of proteins using polyhistidine affinity tags', *Methods Enzymol,* vol. 326, pp. 245-54.

Bosl, MR, Stein, V, Hubner, C, Zdebik, AA, Jordt, SE, Mukhopadhyay, AK, Davidoff, MS, Holstein, AF & Jentsch, TJ 2001, 'Male germ cells and photoreceptors, both dependent on close cell-cell interactions, degenerate upon ClC-2 Cl(-) channel disruption', *Embo J,* vol. 20, no. 6, Mar 15, pp. 1289-99.

Bradford, MM 1976, 'A rapid and sensitive method for the quantitation of microgram quantities of protein utilizing the principle of protein-dye binding', *Anal Biochem,* vol. 72, May 7, pp. 248-54.

Brandt, S & Jentsch, TJ 1995, 'ClC-6 and ClC-7 are two novel broadly expressed members of the CLC chloride channel family', *FEBS Lett,* vol. 377, no. 1, Dec 11, pp. 15-20.

Bretag, AH 1987, 'Muscle chloride channels', *Physiol Rev,* vol. 67, no. 2, Apr, pp. 618-724.

Brugnoni, R, Galantini, S, Confalonieri, P, Balestrini, MR, Cornelio, F & Mantegazza, R 1999, 'Identification of three novel mutations in the major human skeletal muscle chloride channel gene (CLCN1), causing myotonia congenita', *Hum Mutat,* vol. 14, no. 5, Nov, p. 447.

Bush, GL, Tassin, AM, Friden, H & Meyer, DI 1991, 'Secretion in yeast. Purification and in vitro translocation of chemical amounts of prepro-alpha-factor', *J Biol Chem,* vol. 266, no. 21, Jul 25, pp. 13811-4.

Buyse, G, Trouet, D, Voets, T, Missiaen, L, Droogmans, G, Nilius, B & Eggermont, J 1998, 'Evidence for the intracellular location of chloride channel (ClC)-type proteins: co-localization of ClC-6a and ClC-6c with the sarco/endoplasmic-reticulum Ca2+ pump SERCA2b', *Biochem J,* vol. 330 (Pt 2), Mar 1, pp. 1015-21.

Buyse, G, Voets, T, Tytgat, J, De Greef, C, Droogmans, G, Nilius, B & Eggermont, J 1997, 'Expression of human pICln and ClC-6 in Xenopus oocytes induces an identical endogenous chloride conductance', *J Biol Chem,* vol. 272, no. 6, Feb 7, pp. 3615-21.

Bykova, EA, Zhang, XD, Chen, TY & Zheng, J 2006, 'Large movement in the C terminus of CLC-0 chloride channel during slow gating', *Nat Struct Mol Biol,* vol. 13, no. 12, Dec, pp. 1115-9.

Campos-Xavier, AB, Casanova, JL, Doumaz, Y, Feingold, J, Munnich, A & Cormier-Daire, V 2005, 'Intrafamilial phenotypic variability of osteopetrosis due to chloride channel 7 (CLCN7) mutations', *Am J Med Genet A,* vol. 133, no. 2, Mar 1, pp. 216-8.

Carr, G, Simmons, N & Sayer, J 2003, 'A role for CBS domain 2 in trafficking of chloride channel CLC-5', *Biochem Biophys Res Commun,* vol. 310, no. 2, Oct 17, pp. 600-5.

Chalhoub, N, Benachenhou, N, Rajapurohitam, V, Pata, M, Ferron, M, Frattini, A, Villa, A & Vacher, J 2003, 'Grey-lethal mutation induces severe malignant autosomal recessive osteopetrosis in mouse and human', *Nat Med,* vol. 9, no. 4, Apr, pp. 399-406.

Chance, B 1970, 'Fluorescent probe environment and the structural and charge changes in energy coupling of mitochondrial membranes', *Proc Natl Acad Sci U S A,* vol. 67, no. 2, Oct, pp. 560-71.

Chen, L, Lang, D, Joncourt, F, Gallati, S & Burgunder, J-M 2001, 'www.medecine.unige.ch/ssn/abstracts2001/pharmacol.htm.'

Chen, MF & Chen, TY 2001, 'Different fast-gate regulation by external Cl(-) and H(+) of the muscle-type ClC chloride channels', *J Gen Physiol,* vol. 118, no. 1, Jul, pp. 23-32.

Chen, TY 1998, 'Extracellular zinc ion inhibits ClC-0 chloride channels by facilitating slow gating', *J Gen Physiol,* vol. 112, no. 6, Dec, pp. 715-26.

Chen, TY 2005, 'Structure and function of clc channels', *Annu Rev Physiol,* vol. 67, pp. 809-39.

Chen, TY & Miller, C 1996, 'Nonequilibrium gating and voltage dependence of the ClC-0 Cl- channel', *J Gen Physiol,* vol. 108, no. 4, Oct, pp. 237-50.

Cleiren, E, Benichou, O, Van Hul, E, Gram, J, Bollerslev, J, Singer, FR, Beaverson, K, Aledo, A, Whyte, MP, Yoneyama, T, deVernejoul, MC & Van Hul, W 2001, 'Albers-Schonberg disease (autosomal dominant osteopetrosis, type II) results from mutations in the ClCN7 chloride channel gene', *Hum Mol Genet,* vol. 10, no. 25, Dec 1, pp. 2861-7.

Colding-Jørgensen, E 2005, 'Phenotypic variability in myotonia congenita', *Muscle Nerve,* vol. 32, no. 1, Jul, pp. 19-34.

Csanady, L, Chan, KW, Nairn, AC & Gadsby, DC 2005, 'Functional roles of nonconserved structural segments in CFTR's NH2-terminal nucleotide binding domain', *J Gen Physiol,* vol. 125, no. 1, Jan, pp. 43-55.

De Angeli, A, Monachello, D, Ephritikhine, G, Frachisse, JM, Thomine, S, Gambale, F & Barbier-Brygoo, H 2006, 'The nitrate/proton antiporter AtCLCa mediates nitrate accumulation in plant vacuoles', *Nature,* Jul 26.

de Diego, C, Gamez, J, Plassart-Schiess, E, Lasa, A, Del Rio, E, Cervera, C, Baiget, M, Gallano, P & Fontaine, B 1999, 'Novel mutations in the muscle chloride channel CLCN1 gene causing myotonia congenita in Spanish families', *J Neurol,* vol. 246, no. 9, Sep, pp. 825-9.

Denton, J, Nehrke, K, Yin, X, Beld, AM & Strange, K 2006, 'Altered gating and regulation of a carboxy-terminal ClC channel mutant expressed in the Caenorhabditis elegans oocyte', *Am J Physiol Cell Physiol,* vol. 290, no. 4, Apr, pp. C1109-18.

Devuyst, O, Christie, PT, Courtoy, PJ, Beauwens, R & Thakker, RV 1999, 'Intra-renal and subcellular distribution of the human chloride channel, CLC-5, reveals a pathophysiological basis for Dent's disease', *Hum Mol Genet,* vol. 8, no. 2, Feb, pp. 247-57.

Dhani, SU & Bear, CE 2006, 'Role of intramolecular and intermolecular interactions in ClC channel and transporter function', *Pflugers Arch,* vol. 451, no. 6, Mar, pp. 708-15.

Dhani, SU, Mohammad-Panah, R, Ahmed, N, Ackerley, C, Ramjeesingh, M & Bear, CE 2003, 'Evidence for a functional interaction between the ClC-2 chloride channel and the retrograde motor dynein complex', *J Biol Chem,* vol. 278, no. 18, May 2, pp. 16262-70.

Dickerson, LW, Bonthius, DJ, Schutte, BC, Yang, B, Barna, TJ, Bailey, MC, Nehrke, K, Williamson, RA & Lamb, FS 2002, 'Altered GABAergic function accompanies hippocampal degeneration in mice lacking ClC-3 voltage-gated chloride channels', *Brain Res,* vol. 958, no. 2, Dec 27, pp. 227-50.

Duan, D 2006, 'Challenges and opportunities in dystrophin-deficient cardiomyopathy gene therapy', *Hum Mol Genet,* vol. 15 Spec No 2, Oct 15, pp. R253-61.

Duan, D, Winter, C, Cowley, S, Hume, JR & Horowitz, B 1997, 'Molecular identification of a volume-regulated chloride channel', *Nature,* vol. 390, no. 6658, Nov 27, pp. 417-21.

Duan, D, Ye, L, Britton, F, Horowitz, B & Hume, JR 2000, 'A novel anionic inward rectifier in native cardiac myocytes', *Circ Res,* vol. 86, no. 4, Mar 3, pp. E63-71.

Dubendorff, JW & Studier, FW 1991, 'Controlling basal expression in an inducible T7 expression system by blocking the target T7 promoter with lac repressor', *J Mol Biol,* vol. 219, no. 1, May 5, pp. 45-59.

Duffield, M, Rychkov, G, Bretag, A & Roberts, M 2003, 'Involvement of helices at the dimer interface in ClC-1 common gating', *J Gen Physiol,* vol. 121, no. 2, Feb, pp. 149-61.

Duffield, MD, Rychkov, GY, Bretag, A & Roberts, ML 2005, 'zinc inhibits human ClC-1 muscle chloride channel by interacting with its common gating mechanism', *J Physiol,* vol. 568, no. 1, pp. 5-12.

Dutzler, R, Campbell, EB, Cadene, M, Chait, BT & MacKinnon, R 2002, 'X-ray structure of a ClC chloride channel at 3.0 A reveals the molecular basis of anion selectivity', *Nature,* vol. 415, no. 6869, Jan 17, pp. 287-94.

Dutzler, R, Campbell, EB & MacKinnon, R 2003, 'Gating the selectivity filter in ClC chloride channels', *Science,* vol. 300, no. 5616, Apr 4, pp. 108-12.

Ebner, KV 1983, 'Fluorescent probe study with 1-anilino-8-naphthalene sulfonate on acetylglutamate activation, ATP binding and conformational changes of the rat liver carbamoyl-phosphate synthetase', *Biochim Biophys Acta,* vol. 746, no. 1-2, Jul 28, pp. 87-96.

Eggermont, J, Buyse, G, Voets, T, Tytgat, J, De Smedt, H, Droogmans, G & Nilius, B 1997, 'Alternative splicing of ClC-6 (a member of the CIC chloride-channel family) transcripts generates three truncated isoforms one of which, ClC-6c, is kidney-specific', *Biochem J,* vol. 325 (Pt 1), Jul 1, pp. 269-76.

Embark, HM, Bohmer, C, Palmada, M, Rajamanickam, J, Wyatt, AW, Wallisch, S, Capasso, G, Waldegger, P, Seyberth, HW, Waldegger, S & Lang, F 2004, 'Regulation of CLC-Ka/barttin by the ubiquitin ligase Nedd4-2 and the serum- and glucocorticoid-dependent kinases', *Kidney Int,* vol. 66, no. 5, Nov, pp. 1918-25.

Estévez, R, Boettger, T, Stein, V, Birkenhager, R, Otto, E, Hildebrandt, F & Jentsch, TJ 2001, 'Barttin is a Cl- channel beta-subunit crucial for renal Cl- reabsorption and inner ear K+ secretion', *Nature,* vol. 414, no. 6863, Nov 29, pp. 558-61.

Estévez, R & Jentsch, TJ 2002, 'CLC chloride channels: correlating structure with function', *Curr Opin Struct Biol,* vol. 12, no. 4, Aug, pp. 531-9.

Estévez, R, Pusch, M, Ferrer-Costa, C, Orozco, M & Jentsch, TJ 2004, 'Functional and structural conservation of CBS domains from CLC chloride channels', *J Physiol,* vol. 557, no. Pt 2, Jun 1, pp. 363-78.

Fahlke, C 2001, 'Ion permeation and selectivity in ClC-type chloride channels', *Am J Physiol Renal Physiol,* vol. 280, no. 5, May, pp. F748-57.

Fahlke, C, Beck, CL & George, AL, Jr. 1997a, 'A mutation in autosomal dominant myotonia congenita affects pore properties of the muscle chloride channel', *Proc Natl Acad Sci U S A,* vol. 94, pp. 2729-2734.

Fahlke, C, Desai, RR, Gillani, N & George, AL, Jr. 2001, 'Residues lining the inner pore vestibule of human muscle chloride channels', *J Biol Chem,* vol. 276, no. 3, Jan 19, pp. 1759-65.

Fahlke, C, Durr, C & George, AL, Jr. 1997b, 'Mechanism of Ion Permeation in Skeletal Muscle Chloride Channels', *J Gen Physiol,* vol. 110, pp. 551-564.

Fahlke, C, Rosenbohm, A, Mitrovic, N, George, AL, Jr. & Rudel, R 1996, 'Mechanism of voltage-dependent gating in skeletal muscle chloride channels', *Biophys J,* vol. 71, no. 2, Aug, pp. 695-706.

Fahlke, C, Yu, HT, Beck, CL, Rhodes, TH & George, AL, Jr. 1997c, 'Pore-forming segments in voltage-gated chloride channels', *Nature,* vol. 390, no. 6659, Dec 4, pp. 529-32.

Falk, T, Kilani, RK, Yool, AJ & Sherman, SJ 2001, 'Viral vector-mediated expression of K+ channels regulates electrical excitability in skeletal muscle', *Gene Ther,* vol. 8, no. 18, Sep, pp. 1372-9.

Faraldo-Gomez, JD & Roux, B 2004, 'Electrostatics of ion stabilization in a ClC chloride channel homologue from Escherichia coli', *J Mol Biol,* vol. 339, no. 4, Jun 11, pp. 981-1000.

Farrant, M & Cull-Candy, S 1993, 'GABA receptors, granule cells and genes', *Nature,* vol. 361, no. 6410, Jan 28, pp. 302-3.

Flores, CA, Niemeyer, MI, Sepulveda, FV & Cid, LP 2006, 'Two splice variants derived from a Drosophila melanogaster candidate ClC gene generate ClC-2-type Cl- channels', *Mol Membr Biol,* vol. 23, no. 2, Mar-Apr, pp. 149-56.

Fong, P, Rehfeldt, A & Jentsch, TJ 1998, 'Determinants of slow gating in ClC-0, the voltage-gated chloride channel of Torpedo marmorata', *Am J Physiol,* vol. 274, no. 4 Pt 1, Apr, pp. C966-73.

Foster, K, Foster, H & Dickson, JG 2006, 'Gene therapy progress and prospects: Duchenne muscular dystrophy', *Gene Ther,* vol. 13, no. 24, Dec, pp. 1677-85.

Friedrich, T, Breiderhoff, T & Jentsch, TJ 1999, 'Mutational analysis demonstrates that ClC-4 and ClC-5 directly mediate plasma membrane currents', *J Biol Chem,* vol. 274, no. 2, Jan 8, pp. 896-902.

Furukawa, T, Ogura, T, Katayama, Y & Hiraoka, M 1998, 'Characteristics of rabbit ClC-2 current expressed in Xenopus oocytes and its contribution to volume regulation', *Am J Physiol,* vol. 274, no. 2 Pt 1, Feb, pp. C500-12.

Furukawa, T, Ogura, T, Zheng, YJ, Tsuchiya, H, Nakaya, H, Katayama, Y & Inagaki, N 2002, 'Phosphorylation and functional regulation of ClC-2 chloride channels expressed in Xenopus oocytes by M cyclin-dependent protein kinase', *J Physiol,* vol. 540, no. Pt 3, May 1, pp. 883-93.

Galakatos, NG & Walsh, CT 1987, 'Specific proteolysis of native alanine racemases from Salmonella typhimurium: identification of the cleavage site and characterization of the clipped two-domain proteins', *Biochemistry,* vol. 26, no. 25, Dec 15, pp. 8475-80.

Gandhi, R, Elble, RC, Gruber, AD, Schreur, KD, Ji, HL, Fuller, CM & Pauli, BU 1998, 'Molecular and functional characterization of a calcium-sensitive chloride channel from mouse lung', *J Biol Chem,* vol. 273, no. 48, Nov 27, pp. 32096-101.

Geelen, D, Lurin, C, Bouchez, D, Frachisse, JM, Lelievre, F, Courtial, B, Barbier-Brygoo, H & Maurel, C 2000, 'Disruption of putative anion channel gene AtCLC-a in Arabidopsis suggests a role in the regulation of nitrate content', *Plant J,* vol. 21, no. 3, Feb, pp. 259-67.

Goldberg, A & Dice, J 1974, 'Intracellular protein degradation in mammalian and bacterial cells', *Annu Rev Biochem,* vol. 43, pp. 835-869.

Goldin, A 2006, 'Expression of Ion Channels in Xenopus Oocytes', in *Expression and Analysis of Recombinant Ion Channels*, eds. J Jeffrey & J Derek, WILEY-VCH Verlag GmbH & Co., pp. 1-25.

Goncz, KK, Prokopishyn, NL, Chow, BL, Davis, BR & Gruenert, DC 2002, 'Application of SFHR to gene therapy of monogenic disorders', *Gene Ther,* vol. 9, no. 11, Jun, pp. 691-4.

Gottesman, S, Roche, E, Zhou, Y & Sauer, RT 1998, 'The ClpXP and ClpAP proteases degrade proteins with carboxy-terminal peptide tails added by the SsrA-tagging system', *Genes Dev,* vol. 12, no. 9, May 1, pp. 1338-47.

Gouaux, E & Mackinnon, R 2005, 'Principles of selective ion transport in channels and pumps', *Science,* vol. 310, no. 5753, Dec 2, pp. 1461-5.

Greene, JR, Brown, NH, DiDomenico, BJ, Kaplan, J & Eide, DJ 1993, 'The GEF1 gene of Saccharomyces cerevisiae encodes an integral membrane protein; mutations in which have effects on respiration and iron-limited growth', *Mol Gen Genet,* vol. 241, no. 5-6, Dec, pp. 542-53.

Grunder, S, Thiemann, A, Pusch, M & Jentsch, TJ 1992, 'Regions involved in the opening of CIC-2 chloride channel by voltage and cell volume', *Nature,* vol. 360, no. 6406, Dec 24-31, pp. 759-62.

Gunther, W, Luchow, A, Cluzeaud, F, Vandewalle, A & Jentsch, TJ 1998, 'ClC-5, the chloride channel mutated in Dent's disease, colocalizes with the proton pump in endocytotically active kidney cells', *Proc Natl Acad Sci U S A,* vol. 95, no. 14, Jul 7, pp. 8075-80.

Gunther, W, Piwon, N & Jentsch, TJ 2003, 'The ClC-5 chloride channel knock-out mouse - an animal model for Dent's disease', *Pflugers Arch,* vol. 445, no. 4, Jan, pp. 456-62.

Gurnett, CA, Kahl, SD, Anderson, RD & Campbell, KP 1995, 'Absence of the skeletal muscle sarcolemma chloride channel ClC-1 in myotonic mice', *J Biol Chem,* vol. 270, no. 16, Apr 21, pp. 9035-8.

Hanke, W & Miller, C 1983, 'Single chloride channels from Torpedo electroplax. Activation by protons', *J Gen Physiol,* vol. 82, no. 1, Jul, pp. 25-45.

Haug, K, Warnstedt, M, Alekov, AK, Sander, T, Ramirez, A, Poser, B, Maljevic, S, Hebeisen, S, Kubisch, C, Rebstock, J, Horvath, S, Hallmann, K, Dullinger, JS, Rau, B, Haverkamp, F, Beyenburg, S, Schulz, H, Janz, D, Giese, B, Muller-Newen, G, Propping, P, Elger, CE, Fahlke, C, Lerche, H & Heils, A 2003, 'Mutations in CLCN2 encoding a voltage-gated chloride channel are associated with idiopathic generalized epilepsies', *Nat Genet,* vol. 33, no. 4, Apr, pp. 527-32.

Hebeisen, S, Biela, A, Giese, B, Muller-Newen, G, Hidalgo, P & Fahlke, C 2004, 'The role of the carboxyl terminus in ClC chloride channel function', *J Biol Chem,* vol. 279, no. 13, Mar 26, pp. 13140-7.

Hebeisen, S & Fahlke, C 2005, 'Carboxy-terminal truncations modify the outer pore vestibule of muscle chloride channels', *Biophys J,* vol. 89, no. 3, Sep, pp. 1710-20.

Hechenberger, M, Schwappach, B, Fischer, WN, Frommer, WB, Jentsch, TJ & Steinmeyer, K 1996, 'A family of putative chloride channels from Arabidopsis and functional complementation of a yeast strain with a CLC gene disruption', *J Biol Chem,* vol. 271, no. 52, Dec 27, pp. 33632-8.

Henegariu, O, Heerema, NA, Dlouhy, SR, Vance, GH & Vogt, PH 1997, 'Multiplex PCR: critical parameters and step-by-step protocol', *Biotechniques,* vol. 23, no. 3, Sep, pp. 504-11.

Hennecke, M, Kwissa, M, Metzger, K, Oumard, A, Kroger, A, Schirmbeck, R, Reimann, J & Hauser, H 2001, 'Composition and arrangement of genes define the strength of IRES-driven translation in bicistronic mRNAs', *Nucleic Acids Res,* vol. 29, no. 16, Aug 15, pp. 3327-34.

Hinzpeter, A, Lipecka, J, Brouillard, F, Baudoin-Legros, M, Dadlez, M, Edelman, A & Fritsch, J 2006, 'Association between Hsp90 and the ClC-2 chloride channel upregulates channel function', *Am J Physiol Cell Physiol,* vol. 290, no. 1, Jan, pp. C45-56.

Hiratsuka, T 2003, 'Fluorescent and colored trinitrophenylated analogs of ATP and GTP', *Eur J Biochem,* vol. 270, no. 17, Sep, pp. 3479-85.

Hryciw, DH, Ekberg, J, Lee, A, Lensink, IL, Kumar, S, Guggino, WB, Cook, DI, Pollock, CA & Poronnik, P 2004, 'Nedd4-2 functionally interacts with ClC-5: involvement in constitutive albumin endocytosis in proximal tubule cells', *J Biol Chem,* vol. 279, no. 53, Dec 31, pp. 54996-5007.

Hryciw, DH, Rychkov, GY, Hughes, BP & Bretag, AH 1998, 'Relevance of the D13 region to the function of the skeletal muscle chloride channel, ClC-1', *J Biol Chem,* vol. 273, no. 8, Feb 20, pp. 4304-7.

Hryciw, DH, Wang, Y, Devuyst, O, Pollock, CA, Poronnik, P & Guggino, WB 2003, 'Cofilin interacts with ClC-5 and regulates albumin uptake in proximal tubule cell lines', *J Biol Chem,* vol. 278, no. 41, Oct 10, pp. 40169-76.

Hubner, CA & Jentsch, TJ 2002, 'Ion channel diseases', *Hum Mol Genet,* vol. 11, no. 20, Oct 1, pp. 2435-45.

Ignoul, S & Eggermont, J 2005, 'CBS domains: structure, function, and pathology in human proteins', *Am J Physiol Cell Physiol,* vol. 289, no. 6, Dec, pp. C1369-78.

Iyer, R, Iverson, TM, Accardi, A & Miller, C 2002, 'A biological role for prokaryotic ClC chloride channels', *Nature,* vol. 419, no. 6908, Oct 17, pp. 715-8.

Jameson, DM & Eccleston, JF 1997, 'Fluorescent nucleotide analogs: synthesis and applications', *Methods Enzymol,* vol. 278, pp. 363-90.

Janosik, M, Kery, V, Gaustadnes, M, Maclean, KN & Kraus, JP 2001, 'Regulation of human cystathionine beta-synthase by S-adenosyl-L-methionine: evidence for two catalytically active conformations involving an autoinhibitory domain in the C-terminal region', *Biochemistry,* vol. 40, no. 35, Sep 4, pp. 10625-33.

Jentsch, TJ, Gunther, W, Pusch, M & Schwappach, B 1995, 'Properties of voltage-gated chloride channels of the ClC gene family', *J Physiol,* vol. 482, Jan, pp. 19S-25S.

Jentsch, TJ, Stein, V, Weinreich, F & Zdebik, AA 2002, 'Molecular structure and physiological function of chloride channels', *Physiol Rev,* vol. 82, no. 2, Apr, pp. 503-68.

Jentsch, TJ, Steinmeyer, K & Schwarz, G 1990, 'Primary structure of Torpedo marmorata chloride channel isolated by expression cloning in Xenopus oocytes', *Nature,* vol. 348, no. 6301, Dec 6, pp. 510-4.

Jhee, KH, McPhie, P & Miles, EW 2000, 'Domain architecture of the heme-independent yeast cystathionine beta-synthase provides insights into mechanisms of catalysis and regulation', *Biochemistry,* vol. 39, no. 34, Aug 29, pp. 10548-56.

Jordt, SE & Jentsch, TJ 1997, 'Molecular dissection of gating in the ClC-2 chloride channel', *Embo J,* vol. 16, no. 7, Apr 1, pp. 1582-92.

Kamoun, PP 1988, 'Denaturation of globular proteins by urea: breakdown of hydrogen or hydrophobic bonds?' *Trends Biochem Sci,* vol. 13, no. 11, Nov, pp. 424-5.

Kapsa, RM, Quigley, AF, Vadolas, J, Steeper, K, Ioannou, PA, Byrne, E & Kornberg, AJ 2002, 'Targeted gene correction in the mdx mouse using short DNA fragments: towards application with bone marrow-derived cells for autologous remodeling of dystrophic muscle', *Gene Ther,* vol. 9, no. 11, Jun, pp. 695-9.

Kasper, D, Planells-Cases, R, Fuhrmann, JC, Scheel, O, Zeitz, O, Ruether, K, Schmitt, A, Poet, M, Steinfeld, R, Schweizer, M, Kornak, U & Jentsch, TJ 2005, 'Loss of the chloride channel ClC-7 leads to lysosomal storage disease and neurodegeneration', *Embo J,* vol. 24, no. 5, Mar 9, pp. 1079-91.

Kass, RS 2005, 'The channelopathies: novel insights into molecular and genetic mechanisms of human disease', *J Clin Invest,* vol. 115, no. 8, Aug, pp. 1986-9.

Kawasaki, M, Uchida, S, Monkawa, T, Miyawaki, A, Mikoshiba, K, Marumo, F & Sasaki, S 1994, 'Cloning and expression of a protein kinase C-regulated chloride channel abundantly expressed in rat brain neuronal cells', *Neuron,* vol. 12, no. 3, Mar, pp. 597-604.

Keiler, KC, Waller, PR & Sauer, RT 1996, 'Role of a peptide tagging system in degradation of proteins synthesized from damaged messenger RNA', *Science,* vol. 271, no. 5251, Feb 16, pp. 990-3.

Kemp, BE 2004, 'Bateman domains and adenosine derivatives form a binding contract', *J Clin Invest,* vol. 113, no. 2, Jan, pp. 182-4.

Kennan, A, Aherne, A, Palfi, A, Humphries, M, McKee, A, Stitt, A, Simpson, DA, Demtroder, K, Orntoft, T, Ayuso, C, Kenna, PF, Farrar, GJ & Humphries, P 2002, 'Identification of an IMPDH1 mutation in autosomal dominant retinitis pigmentosa (RP10) revealed following comparative microarray analysis of transcripts derived from retinas of wild-type and Rho(-/-) mice', *Hum Mol Genet,* vol. 11, no. 5, Mar 1, pp. 547-57.

Kery, V, Poneleit, L & Kraus, JP 1998, 'Trypsin cleavage of human cystathionine beta-synthase into an evolutionarily conserved active core: structural and functional consequences', *Arch Biochem Biophys,* vol. 355, no. 2, Jul 15, pp. 222-32.

Kidd, JF, Ramjeesingh, M, Stratford, F, Huan, LJ & Bear, CE 2004, 'A heteromeric complex of the two nucleotide binding domains of cystic fibrosis transmembrane conductance regulator (CFTR) mediates ATPase activity', *J Biol Chem,* vol. 279, no. 40, Oct 1, pp. 41664-9.

Kieferle, S, Fong, P, Bens, M, Vandewalle, A & Jentsch, TJ 1994, 'Two highly homologous members of the ClC chloride channel family in both rat and human kidney', *Proc Natl Acad Sci U S A,* vol. 91, no. 15, Jul 19, pp. 6943-7.

Ko, YH & Pedersen, PL 1995, 'The first nucleotide binding fold of the cystic fibrosis transmembrane conductance regulator can function as an active ATPase', *J Biol Chem,* vol. 270, no. 38, Sep 22, pp. 22093-6.

Koch, MC, Steinmeyer, K, Lorenz, C, Ricker, K, Wolf, F, Otto, M, Zoll, B, Lehmann-Horn, F, Grzeschik, KH & Jentsch, TJ 1992, 'The skeletal muscle chloride channel in dominant and recessive human myotonia', *Science,* vol. 257, no. 5071, Aug 7, pp. 797-800.

Konrad, M, Vollmer, M, Lemmink, HH, van den Heuvel, LP, Jeck, N, Vargas-Poussou, R, Lakings, A, Ruf, R, Deschenes, G, Antignac, C, Guay-Woodford, L, Knoers, NV, Seyberth, HW, Feldmann, D & Hildebrandt, F 2000, 'Mutations in the chloride channel gene CLCNKB as a cause of classic Bartter syndrome', *J Am Soc Nephrol,* vol. 11, no. 8, Aug, pp. 1449-59.

Kornak, U, Kasper, D, Bosl, MR, Kaiser, E, Schweizer, M, Schulz, A, Friedrich, W, Delling, G & Jentsch, TJ 2001, 'Loss of the ClC-7 chloride channel leads to osteopetrosis in mice and man', *Cell,* vol. 104, no. 2, Jan 26, pp. 205-15.

Kowdley, GC, Ackerman, SJ, John, JE, 3rd, Jones, LR & Moorman, JR 1994, 'Hyperpolarization-activated chloride currents in Xenopus oocytes', *J Gen Physiol,* vol. 103, no. 2, Feb, pp. 217-30.

Koyasu, S, Nishida, E, Kadowaki, T, Matsuzaki, F, Iida, K, Harada, F, Kasuga, M, Sakai, H & Yahara, I 1986, 'Two mammalian heat shock proteins, HSP90 and HSP100, are actin-binding proteins', *Proc Natl Acad Sci U S A,* vol. 83, no. 21, Nov, pp. 8054-8.

Kuchenbecker, M, Schu, B, Kurz, L & Rudel, R 2001, 'Topology of the human skeletal muscle chloride channel hClC-1 probed with hydrophilic epitope insertion', *Pflugers Arch,* vol. 443, no. 2, Nov, pp. 280-8.

Kumar, TR, Soppimath, K & Nachaegari, SK 2006, 'Novel delivery technologies for protein and peptide therapeutics', *Curr Pharm Biotechnol,* vol. 7, no. 4, Aug, pp. 261-76.

Laachouch, JE, Desmet, L, Geuskens, V, Grimaud, R & Toussaint, A 1996, 'Bacteriophage Mu repressor as a target for the Escherichia coli ATP-dependent Clp Protease', *Embo J,* vol. 15, no. 2, Jan 15, pp. 437-44.

Laemmli, UK 1970, 'Cleavage of structural proteins during the assembly of the head of bacteriophage T4', *Nature,* vol. 227, no. 5259, Aug 15, pp. 680-5.

Lange, PF, Wartosch, L, Jentsch, TJ & Fuhrmann, JC 2006, 'ClC-7 requires Ostm1 as a beta-subunit to support bone resorption and lysosomal function', *Nature,* vol. 440, no. 7081, Mar 9, pp. 220-3.

LaVallie, ER, Lu, Z, Diblasio-Smith, EA, Collins-Racie, LA & McCoy, JM 2000, 'Thioredoxin as a Fusion Partner for Production of Soluble Recombinant Proteins in Escherichia coli', *Methods in Enzymology,* vol. 326, pp. 322-340.

Lee, ME & van der Vegt, NF 2006, 'Does urea denature hydrophobic interactions?' *J Am Chem Soc,* vol. 128, no. 15, Apr 19, pp. 4948-9.

Lehnherr, H & Yarmolinsky, MB 1995, 'Addiction protein Phd of plasmid prophage P1 is a substrate of the ClpXP serine protease of Escherichia coli', *Proc Natl Acad Sci U S A,* vol. 92, no. 8, Apr 11, pp. 3274-7.

Levchenko, I, Smith, CK, Walsh, NP, Sauer, RT & Baker, TA 1997, 'PDZ-like domains mediate binding specificity in the Clp/Hsp100 family of chaperones and protease regulatory subunits', *Cell,* vol. 91, no. 7, Dec 26, pp. 939-47.

Li, CH & Bewley, TA 1976, 'Human pituitary growth hormone: restoration of full biological activity by noncovalent interaction of two fragments of the hormone', *Proc Natl Acad Sci U S A,* vol. 73, no. 5, May, pp. 1476-9.

Li, SJ, Kawazaki, M, Ogasahara, K & Nakagawa, A 2006, 'The Intracellular Region of ClC-3 Chloride Channel Is in a Partially Folded State and a Monomer', *J Biochem (Tokyo),* vol. 139, no. 5, May, pp. 813-20.

Li, X, Shimada, K, Showalter, LA & Weinman, SA 2000, 'Biophysical properties of ClC-3 differentiate it from swelling-activated chloride channels in Chinese hamster ovary-K1 cells', *J Biol Chem,* vol. 275, no. 46, Nov 17, pp. 35994-8.

Li, X, Wang, T, Zhao, Z & Weinman, SA 2002, 'The ClC-3 chloride channel promotes acidification of lysosomes in CHO-K1 and Huh-7 cells', *Am J Physiol Cell Physiol,* vol. 282, no. 6, Jun, pp. C1483-91.

Lin, YW, Lin, CW & Chen, TY 1999, 'Elimination of the slow gating of ClC-0 chloride channel by a point mutation', *J Gen Physiol,* vol. 114, no. 1, Jul, pp. 1-12.

Lloyd, SE, Gunther, W, Pearce, SH, Thomson, A, Bianchi, ML, Bosio, M, Craig, IW, Fisher, SE, Scheinman, SJ, Wrong, O, Jentsch, TJ & Thakker, RV 1997a, 'Characterisation of renal chloride channel, CLCN5, mutations in hypercalciuric nephrolithiasis (kidney stones) disorders', *Hum Mol Genet,* vol. 6, no. 8, Aug, pp. 1233-9.

Lloyd, SE, Pearce, SH, Gunther, W, Kawaguchi, H, Igarashi, T, Jentsch, TJ & Thakker, RV 1997b, 'Idiopathic low molecular weight proteinuria associated with hypercalciuric nephrocalcinosis in Japanese children is due to mutations of the renal chloride channel (CLCN5)', *J Clin Invest,* vol. 99, no. 5, Mar 1, pp. 967-74.

Lorenz, C, Meyer-Kleine, C, Steinmeyer, K, Koch, MC & Jentsch, TJ 1994, 'Genomic organization of the human muscle chloride channel CIC-1 and analysis of novel mutations leading to Becker-type myotonia', *Hum Mol Genet,* vol. 3, no. 6, Jun, pp. 941-6.

Ludewig, U, Pusch, M & Jentsch, TJ 1996, 'Two physically distinct pores in the dimeric ClC-0 chloride channel', *Nature,* vol. 383, no. 6598, Sep 26, pp. 340-3.

Lurin, C, Geelen, D, Barbier-Brygoo, H, Guern, J & Maurel, C 1996, 'Cloning and functional expression of a plant voltage-dependent chloride channel', *Plant Cell,* vol. 8, no. 4, Apr, pp. 701-11.

MacGregor, GG, Dong, K, Vanoye, CG, Tang, L, Giebisch, G & Hebert, SC 2002, 'Nucleotides and phospholipids compete for binding to the C terminus of KATP channels', *Proc Natl Acad Sci U S A,* vol. 99, no. 5, Mar 5, pp. 2726-31.

Macías, MJ, Teijido, O, Zifarelli, G, Martin, P, Ramirez-Espain, X, Zorzano, A, Palacin, M, Pusch, M & Estévez, R 2007, 'Myotonia-related mutations in the distal C-terminus of ClC-1 and ClC-0 chloride channels affect the structure of a poly-proline helix', *Biochem J,* vol. 403, no. 1, Apr 1, pp. 79-87.

Maduke, M, Pheasant, DJ & Miller, C 1999, 'High-level expression, functional reconstitution, and quaternary structure of a prokaryotic ClC-type chloride channel', *J Gen Physiol,* vol. 114, no. 5, Nov, pp. 713-22.

Maduke, M, Williams, C & Miller, C 1998, 'Formation of CLC-0 chloride channels from separated transmembrane and cytoplasmic domains', *Biochemistry,* vol. 37, no. 5, Feb 3, pp. 1315-21.

Markovic, S & Dutzler, R 2007, 'The structure of the cytoplasmic domain of the chloride channel ClC-Ka reveals a conserved interaction interface', *Structure,* vol. 15, no. 6, Jun, pp. 715-25.

Marshall, J, Molloy, R, Moss, GW, Howe, JR & Hughes, TE 1995, 'The jellyfish green fluorescent protein: a new tool for studying ion channel expression and function', *Neuron,* vol. 14, no. 2, Feb, pp. 211-5.

Matsumura, Y, Uchida, S, Kondo, Y, Miyazaki, H, Ko, SB, Hayama, A, Morimoto, T, Liu, W, Arisawa, M, Sasaki, S & Marumo, F 1999, 'Overt nephrogenic diabetes insipidus in mice lacking the CLC-K1 chloride channel', *Nat Genet,* vol. 21, no. 1, Jan, pp. 95-8.

Meier, M, Janosik, M, Kery, V, Kraus, JP & Burkhard, P 2001, 'Structure of human cystathionine beta-synthase: a unique pyridoxal 5'-phosphate-dependent heme protein', *Embo J,* vol. 20, no. 15, Aug 1, pp. 3910-6.

Meyer, S & Dutzler, R 2006, 'Crystal Structure of the Cytoplasmic Domain of the Chloride Channel ClC-0', *Structure,* vol. 14, no. 2, Feb, pp. 299-307.

Meyer, S, Savaresi, S, Forster, IC & Dutzler, R 2007, 'Nucleotide recognition by the cytoplasmic domain of the human chloride transporter ClC-5', *Nat Struct Mol Biol,* vol. 14, no. 1, Jan, pp. 60-7.

Middleton, RE, Pheasant, DJ & Miller, C 1996, 'Homodimeric architecture of a ClC-type chloride ion channel', *Nature,* vol. 383, no. 6598, Sep 26, pp. 337-40.

Middleton, RE, Pheasant, DJ & Miller, C 1994, 'Purification, reconstitution, and subunit composition of a voltage-gated chloride channel from Torpedo electroplax', *Biochemistry,* vol. 33, no. 45, Nov 15, pp. 13189-98.

Milan, D, Jeon, JT, Looft, C, Amarger, V, Robic, A, Thelander, M, Rogel-Gaillard, C, Paul, S, Iannuccelli, N, Rask, L, Ronne, H, Lundstrom, K, Reinsch, N, Gellin, J, Kalm, E, Roy, PL, Chardon, P & Andersson, L 2000, 'A mutation in PRKAG3 associated with excess glycogen content in pig skeletal muscle', *Science,* vol. 288, no. 5469, May 19, pp. 1248-51.

Miller, C 2006, 'ClC chloride channels viewed through a transporter lens', *Nature,* vol. 440, no. 7083, Mar 23, pp. 484-9.

Miller, MD, Schwarzenbacher, R, von Delft, F, Abdubek, P, Ambing, E, Biorac, T, Brinen, LS, Canaves, JM, Cambell, J, Chiu, HJ, Dai, X, Deacon, AM, DiDonato, M, Elsliger, MA, Eshagi, S, Floyd, R, Godzik, A, Grittini, C, Grzechnik, SK, Hampton, E, Jaroszewski, L, Karlak, C, Klock, HE, Koesema, E, Kovarik, JS, Kreusch, A, Kuhn, P, Lesley, SA, Levin, I, McMullan, D, McPhillips, TM, Morse, A, Moy, K, Ouyang, J, Page, R, Quijano, K, Robb, A, Spraggon, G, Stevens, RC, van den Bedem, H, Velasquez, J, Vincent, J, Wang, X, West, B, Wolf, G, Xu, Q, Hodgson, KO, Wooley, J & Wilson, IA 2004, 'Crystal structure of a tandem cystathionine-beta-synthase (CBS) domain protein (TM0935) from Thermotoga maritima at 1.87 A resolution', *Proteins,* vol. 57, no. 1, Oct 1, pp. 213-7.

Mindell, JA, Maduke, M, Miller, C & Grigorieff, N 2001, 'Projection structure of a ClC-type chloride channel at 6.5 A resolution', *Nature,* vol. 409, no. 6817, Jan 11, pp. 219-23.

Mishina, M, Kurosaki, T, Tobimatsu, T, Morimoto, Y, Noda, M, Yamamoto, T, Terao, M, Lindstrom, J, Takahashi, T, Kuno, M & et al. 1984, 'Expression of functional acetylcholine receptor from cloned cDNAs', *Nature,* vol. 307, no. 5952, Feb 16-22, pp. 604-8.

Mizuguchi, H, Xu, Z, Ishii-Watabe, A, Uchida, E & Hayakawa, T 2000, 'IRES-dependent second gene expression is significantly lower than cap-dependent first gene expression in a bicistronic vector', *Mol Ther,* vol. 1, no. 4, Apr, pp. 376-82.

Mo, L, Xiong, W, Qian, T, Sun, H & Wills, NK 2004, 'Coexpression of complementary fragments of ClC-5 and restoration of chloride channel function in a Dent's disease mutation', *Am J Physiol Cell Phyiol,* vol. 286, pp. C79-C86.

Moczydlowski, EG & Fortes, PA 1981, 'Characterization of 2',3'-O-(2,4,6-trinitrocyclohexadienylidine)adenosine 5'-triphosphate as a fluorescent probe of the ATP site of sodium and potassium transport adenosine triphosphatase. Determination of nucleotide binding stoichiometry and ion-induced changes in affinity for ATP', *J Biol Chem,* vol. 256, no. 5, Mar 10, pp. 2346-56.

Monaghan, AS, Mintenig, GM & Sepulveda, FV 1997, 'Outwardly rectifying Cl- channel in guinea pig small intestinal villus enterocytes: effect of inhibitors', *Am J Physiol,* vol. 273, no. 5 Pt 1, Nov, pp. G1141-52.

Mondal, S & Venkataraman, V 2005, 'In situ monitoring of polymerase extension rate and adaptive feedback control of PCR by using fluorescence measurements', *J Biochem Biophys Methods,* vol. 65, no. 2-3, Dec 31, pp. 97-105.

Moore, KJ & Lohman, TM 1994, 'Kinetic mechanism of adenine nucleotide binding to and hydrolysis by the Escherichia coli Rep monomer. 1. Use of fluorescent nucleotide analogues', *Biochemistry,* vol. 33, no. 48, Dec 6, pp. 14550-64.

Nakamura, A, Fukuda, A, Sakai, S & Tanaka, Y 2006, 'Molecular cloning, functional expression and subcellular localization of two putative vacuolar voltage-gated chloride channels in rice (Oryza sativa L.)', *Plant Cell Physiol,* vol. 47, no. 1, Jan, pp. 32-42.

Nilius, B, Eggermont, J, Voets, T & Droogmans, G 1996, 'Volume-activated Cl- channels', *Gen Pharmacol,* vol. 27, no. 7, Oct, pp. 1131-40.

Ogura, T, Furukawa, T, Toyozaki, T, Yamada, K, Zheng, YJ, Katayama, Y, Nakaya, H & Inagaki, N 2002, 'ClC-3B, a novel ClC-3 splicing variant that interacts with EBP50 and facilitates expression of CFTR-regulated ORCC', *Faseb J,* vol. 16, no. 8, Jun, pp. 863-5.

Oswald, C, Jenewein, S, Smits, SH, Holland, IB & Schmitt, L 2008, 'Water-mediated protein-fluorophore interractions modulate the affinity of an ABC-ATPase/TNP-ADP complex', *J Struct Biol.,* vol. 162, no. 1, 2008 Apr, pp. 85-93.

Palmada, M, Dieter, M, Boehmer, C, Waldegger, S & Lang, F 2004, 'Serum and glucocorticoid inducible kinases functionally regulate ClC-2 channels', *Biochem Biophys Res Commun,* vol. 321, no. 4, Sep 3, pp. 1001-6.

Parsell, DA, Silber, KR & Sauer, RT 1990, 'Carboxy-terminal determinants of intracellular protein degradation', *Genes Dev,* vol. 4, no. 2, Feb, pp. 277-86.

Pecorari, F, Guilbert, C, Minard, P, Desmadril, M & Yon, JM 1996, 'Folding and functional complementation of engineered fragments from yeast phosphoglycerate kinase', *Biochemistry,* vol. 35, no. 11, Mar 19, pp. 3465-76.

Pedersen, TH, de Paoli, F & Nielsen, OB 2005, 'Increased excitability of acidified skeletal muscle: role of chloride conductance', *J Gen Physiol,* vol. 125, no. 2, Feb, pp. 237-46.

Picollo, A & Pusch, M 2005, 'Chloride/proton antiporter activity of mammalian CLC proteins ClC-4 and ClC-5', *Nature,* vol. 436, no. 7049, Jul 21, pp. 420-3.

Pitson, SM, Moretti, PA, Zebol, JR, Zareie, R, Derian, CK, Darrow, AL, Qi, J, D'Andrea, RJ, Bagley, CJ, Vadas, MA & Wattenberg, BW 2002, 'The nucleotide-binding site of human sphingosine kinase 1', *J Biol Chem,* vol. 277, no. 51, Dec 20, pp. 49545-53.

Piwon, N, Gunther, W, Schwake, M, Bosl, MR & Jentsch, TJ 2000, 'ClC-5 Cl- -channel disruption impairs endocytosis in a mouse model for Dent's disease', *Nature,* vol. 408, no. 6810, Nov 16, pp. 369-73.

Plassart-Schiess, E, Gervais, A, Eymard, B, Lagueny, A, Pouget, J, Warter, JM, Fardeau, M, Jentsch, TJ & Fontaine, B 1998, 'Novel muscle chloride channel (CLCN1) mutations in myotonia congenita with various modes of inheritance including incomplete dominance and penetrance', *Neurology,* vol. 50, no. 4, Apr, pp. 1176-9.

Porath, J, Carlsson, J, Olsson, I & Belfrage, G 1975, 'Metal chelate affinity chromatography, a new approach to protein fractionation', *Nature,* vol. 258, no. 5536, Dec 18, pp. 598-9.

Pornillos, O & Chang, G 2006, 'Inverted repeat domains in membrane proteins', *FEBS Lett,* vol. 580, no. 2, Jan 23, pp. 358-62.

Purdy, MD & Wiener, MC 2000, 'Expression, purification, and initial structural characterization of YadQ, a bacterial homolog of mammalian ClC chloride channel proteins', *FEBS Lett,* vol. 466, no. 1, Jan 21, pp. 26-8.

Pusch, M, Jordt, SE, Stein, V & Jentsch, TJ 1999, 'Chloride dependence of hyperpolarization-activated chloride channel gates', *J Physiol,* vol. 515 (Pt 2), Mar 1, pp. 341-53.

Pusch, M, Ludewig, U & Jentsch, TJ 1997, 'Temperature dependence of fast and slow gating relaxations of ClC-0 chloride channels', *J Gen Physiol,* vol. 109, no. 1, Jan, pp. 105-16.

Pusch, M, Ludewig, U, Rehfeldt, A & Jentsch, TJ 1995a, 'Gating of the voltage-dependent chloride channel CIC-0 by the permeant anion', *Nature,* vol. 373, no. 6514, Feb 9, pp. 527-31.

Pusch, M, Steinmeyer, K & Jentsch, TJ 1994, 'Low single channel conductance of the major skeletal muscle chloride channel, ClC-1', *Biophys J,* vol. 66, no. 1, Jan, pp. 149-52.

Pusch, M, Steinmeyer, K, Koch, MC & Jentsch, TJ 1995b, 'Mutations in dominant human myotonia congenita drastically alter the voltage dependence of the CIC-1 chloride channel', *Neuron,* vol. 15, no. 6, Dec, pp. 1455-63.

Ramjeesingh, M, Li, C, She, YM & Bear, CE 2006, 'Evaluation of the membrane-spanning domain of ClC-2', *Biochem J,* vol. 396, no. 3, Jun 15, pp. 449-60.

Rando, TA 2002, 'Oligonucleotide-mediated gene therapy for muscular dystrophies', *Neuromuscul Disord,* vol. 12 Suppl 1, Oct, pp. S55-60.

Reyes, JP, Hernandez-Carballo, CY, Perez-Cornejo, P, Meza, U, Espinosa-Tanguma, R & Arreola, J 2004, 'Novel outwardly rectifying anion conductance in Xenopus oocytes', *Pflugers Arch,* vol. 449, no. 3, Dec, pp. 271-7.

Rogers, CS, Vanoye, CG, Sullenger, BA & George, AL, Jr. 2002, 'Functional repair of a mutant chloride channel using a trans-splicing ribozyme', *J Clin Invest,* vol. 110, no. 12, Dec, pp. 1783-9.

Rosenberg, I 2005, 'Getting Started with Protein Purification', in *Protein analysis and purification: benchtop techniques*, 2nd ed. edn, Boston, Mass., p. 121.

Rychkov, GY, Astill, DS, Bennetts, B, Hughes, BP, Bretag, AH & Roberts, ML 1997, 'pH-dependent interactions of Cd2+ and a carboxylate blocker with the rat ClC-1 chloride channel and its R304E mutant in the Sf-9 insect cell line', *J Physiol,* vol. 501 (Pt 2), Jun 1, pp. 355-62.

Rychkov, GY, Pusch, M, Astill, DS, Roberts, ML, Jentsch, TJ & Bretag, AH 1996, 'Concentration and pH dependence of skeletal muscle chloride channel ClC-1', *J Physiol,* vol. 497 (Pt 2), Dec 1, pp. 423-35.

Rychkov, GY, Pusch, M, Roberts, ML & Bretag, AH 2001, 'Interaction of hydrophobic anions with the rat skeletal muscle chloride channel ClC-1: effects on permeation and gating', *J Physiol,* vol. 530, no. Pt 3, Feb 1, pp. 379-93.

Sakamoto, H, Kawasaki, M, Uchida, S, Sasaki, S & Marumo, F 1996, 'Identification of a new outwardly rectifying Cl- channel that belongs to a subfamily of the ClC Cl- channels', *J Biol Chem,* vol. 271, no. 17, Apr 26, pp. 10210-6.

Sambrook, J & Russell, D 2001, *Molecular cloning: a laboratory manual,* 3 edn, Cold Spring Harbor Laboratory Press, New York.

Saviane, C, Conti, F & Pusch, M 1999, 'The muscle chloride channel ClC-1 has a double-barreled appearance that is differentially affected in dominant and recessive myotonia', *J Gen Physiol,* vol. 113, no. 3, Mar, pp. 457-68.

Scheel, O, Zdebik, AA, Lourdel, S & Jentsch, TJ 2005, 'Voltage-dependent electrogenic chloride/proton exchange by endosomal CLC proteins', *Nature,* vol. 436, no. 7049, Jul 21, pp. 424-7.

Schiff, JD & Melman, A 2006, 'Ion channel gene therapy for smooth muscle disorders: relaxing smooth muscles to treat erectile dysfunction', *Assay Drug Dev Technol,* vol. 4, no. 1, Feb, pp. 89-95.

Schirmer, EC, Glover, JR, Singer, MA & Lindquist, S 1996, 'HSP100/Clp proteins: a common mechanism explains diverse functions', *Trends Biochem Sci,* vol. 21, no. 8, Aug, pp. 289-96.

Schmidt-Rose, T & Jentsch, TJ 1997a, 'Reconstitution of functional voltage-gated chloride channels from complementary fragments of CLC-1', *J Biol Chem,* vol. 272, no. 33, Aug 15, pp. 20515-21.

Schmidt-Rose, T & Jentsch, TJ 1997b, 'Transmembrane topology of a CLC chloride channel', *Proc Natl Acad Sci U S A,* vol. 94, no. 14, Jul 8, pp. 7633-8.

Schmitt, J, Hess, H & H.G., S 1993, 'Affinity purification of histidine-tagged proteins', *Molecular Biology Reports,* vol. 18, pp. 223-230.

Scholl, U, Hebeisen, S, Janssen, AG, Muller-Newen, G, Alekov, A & Fahlke, C 2006, 'Barttin modulates trafficking and function of ClC-K channels', *Proc Natl Acad Sci U S A,* vol. 103, no. 30, Jul 25, pp. 11411-6.

Schonberger, O, Knox, C, Bibi, E & Pines, O 1996, 'Split invertase polypeptides form functional complexes in the yeast periplasm in vivo', *Proc Natl Acad Sci U S A,* vol. 93, no. 18, Sep 3, pp. 9612-7.

Schriever, AM, Friedrich, T, Pusch, M & Jentsch, TJ 1999, 'CLC chloride channels in Caenorhabditis elegans', *J Biol Chem,* vol. 274, no. 48, Nov 26, pp. 34238-44.

Schwake, M, Friedrich, T & Jentsch, TJ 2001, 'An internalization signal in ClC-5, an endosomal Cl-channel mutated in dent's disease', *J Biol Chem,* vol. 276, no. 15, Apr 13, pp. 12049-54.

Schwappach, B, Stobrawa, S, Hechenberger, M, Steinmeyer, K & Jentsch, TJ 1998, 'Golgi localization and functionally important domains in the NH2 and COOH terminus of the yeast CLC putative chloride channel Gef1p', *J Biol Chem,* vol. 273, no. 24, Jun 12, pp. 15110-8.

Schwiebert, EM, Cid-Soto, LP, Stafford, D, Carter, M, Blaisdell, CJ, Zeitlin, PL, Guggino, WB & Cutting, GR 1998, 'Analysis of ClC-2 channels as an alternative pathway for chloride conduction in cystic fibrosis airway cells', *Proc Natl Acad Sci U S A,* vol. 95, no. 7, Mar 31, pp. 3879-84.

Scott, JW, Hawley, SA, Green, KA, Anis, M, Stewart, G, Scullion, GA, Norman, DG & Hardie, DG 2004, 'CBS domains form energy-sensing modules whose binding of adenosine ligands is disrupted by disease mutations', *J Clin Invest,* vol. 113, no. 2, Jan, pp. 274-84.

Semisotnov, GV, Rodionova, NA, Razgulyaev, OI, Uversky, VN, Gripas, AF & Gilmanshin, RI 1991, 'Study of the "molten globule" intermediate state in protein folding by a hydrophobic fluorescent probe', *Biopolymers,* vol. 31, no. 1, Jan, pp. 119-28.

Shan, X, Dunbrack, RL, Jr., Christopher, SA & Kruger, WD 2001, 'Mutations in the regulatory domain of cystathionine beta synthase can functionally suppress patient-derived mutations in cis', *Hum Mol Genet,* vol. 10, no. 6, Mar 15, pp. 635-43.

Sigel, E 1990, 'Use of Xenopus oocytes for the functional expression of plasma membrane proteins', *J Membr Biol,* vol. 117, no. 3, Sep, pp. 201-21.

Sigel, E, Baur, R, Trube, G, Mohler, H & Malherbe, P 1990, 'The effect of subunit composition of rat brain GABAA receptors on channel function', *Neuron,* vol. 5, no. 5, Nov, pp. 703-11.

Sigel, E & Minier, F 2005, 'The Xenopus oocyte: system for the study of functional expression and modulation of proteins', *Mol Nutr Food Res,* vol. 49, no. 3, Mar, pp. 228-34.

Simon, DB, Bindra, RS, Mansfield, TA, Nelson-Williams, C, Mendonca, E, Stone, R, Schurman, S, Nayir, A, Alpay, H, Bakkaloglu, A, Rodriguez-Soriano, J, Morales, JM, Sanjad, SA, Taylor, CM, Pilz, D, Brem, A, Trachtman, H, Griswold, W, Richard, GA, John, E & Lifton, RP 1997, 'Mutations in the chloride channel gene, CLCNKB, cause Bartter's syndrome type III', *Nat Genet,* vol. 17, no. 2, Oct, pp. 171-8.

Simpson, B 2002, 'Mutagenic and purification studies of the carboxyl tail of ClC-1, the skeletal muscle chloride channel [Thesis]', Health Sciences, Univeristy of South Australia.

Sintchak, MD, Fleming, MA, Futer, O, Raybuck, SA, Chambers, SP, Caron, PR, Murcko, MA & Wilson, KP 1996, 'Structure and mechanism of inosine monophosphate dehydrogenase in complex with the immunosuppressant mycophenolic acid', *Cell,* vol. 85, no. 6, Jun 14, pp. 921-30.

Steinmeyer, K, Ortland, C & Jentsch, TJ 1991, 'Primary structure and functional expression of a developmentally regulated skeletal muscle chloride channel', *Nature,* vol. 354, no. 6351, Nov 28, pp. 301-4.

Steinmeyer, K, Schwappach, B, Bens, M, Vandewalle, A & Jentsch, TJ 1995, 'Cloning and functional expression of rat CLC-5, a chloride channel related to kidney disease', *J Biol Chem,* vol. 270, no. 52, Dec 29, pp. 31172-7.

Stewart, RC, VanBruggen, R, Ellefson, DD & Wolfe, AJ 1998, 'TNP-ATP and TNP-ADP as probes of the nucleotide binding site of CheA, the histidine protein kinase in the

chemotaxis signal transduction pathway of Escherichia coli', *Biochemistry,* vol. 37, no. 35, Sep 1, pp. 12269-79.

Stobrawa, SM, Breiderhoff, T, Takamori, S, Engel, D, Schweizer, M, Zdebik, AA, Bosl, MR, Ruether, K, Jahn, H, Draguhn, A, Jahn, R & Jentsch, TJ 2001, 'Disruption of ClC-3, a chloride channel expressed on synaptic vesicles, leads to a loss of the hippocampus', *Neuron,* vol. 29, no. 1, Jan, pp. 185-96.

Straub, V, Rafael, JA, Chamberlain, JS & Campbell, KP 1997, 'Animal models for muscular dystrophy show different patterns of sarcolemmal disruption', *J Cell Biol,* vol. 139, no. 2, Oct 20, pp. 375-85.

Stryer, L 1968, 'Fluorescence spectroscopy of proteins', *Science,* vol. 162, no. 853, Nov 1, pp. 526-33.

Studier, FW 1991, 'Use of bacteriophage T7 lysozyme to improve an inducible T7 expression system', *J Mol Biol,* vol. 219, no. 1, May 5, pp. 37-44.

Sun, TX, Das, BK & Liang, JJN 1997, 'Conformational and Functional Differences between Recombinant Human Lens aA- and aB-Crystallin', *J Biol Chem,* vol. 272, no. 10, pp. 6220-6225.

Thiemann, A, Grunder, S, Pusch, M & Jentsch, TJ 1992, 'A chloride channel widely expressed in epithelial and non-epithelial cells', *Nature,* vol. 356, no. 6364, Mar 5, pp. 57-60.

Thomas, P & Smart, TG 2005, 'HEK293 cell line: a vehicle for the expression of recombinant proteins', *J Pharmacol Toxicol Methods,* vol. 51, no. 3, May-Jun, pp. 187-200.

Trouet, D, Nilius, B, Voets, T, Droogmans, G & Eggermont, J 1997, 'Use of a bicistronic GFP-expression vector to characterise ion channels after transfection in mammalian cells', *Pflugers Arch,* vol. 434, no. 5, Sep, pp. 632-8.

Uchida, S, Sasaki, S, Furukawa, T, Hiraoka, M, Imai, T, Hirata, Y & Marumo, F 1993, 'Molecular cloning of a chloride channel that is regulated by dehydration and expressed predominantly in kidney medulla', *J Biol Chem,* vol. 268, no. 6, Feb 25, pp. 3821-4.

Vanoye, CG & George, AL, Jr. 2002, 'Functional characterization of recombinant human ClC-4 chloride channels in cultured mammalian cells', *J Physiol,* vol. 539, no. Pt 2, Mar 1, pp. 373-83.

Vanoye, CG, MacGregor, GG, Dong, K, Tang, L, Buschmann, AS, Hall, AE, Lu, M, Giebisch, G & Hebert, SC 2002, 'The carboxyl termini of K(ATP) channels bind nucleotides', *J Biol Chem,* vol. 277, no. 26, Jun 28, pp. 23260-70.

Venglarik, CJ, Singh, AK, Wang, R & Bridges, RJ 1993, 'Trinitrophenyl-ATP blocks colonic Cl- channels in planar phospholipid bilayers. Evidence for two nucleotide binding sites', *J Gen Physiol,* vol. 101, no. 4, Apr, pp. 545-69.

Wagner, S, Deymeer, F, Kurz, LL, Benz, S, Schleithoff, L, Lehmann-Horn, F, Serdaroglu, P, Ozdemir, C & Rudel, R 1998, 'The dominant chloride channel mutant G200R causing fluctuating myotonia: clinical findings, electrophysiology, and channel pathology', *Muscle Nerve,* vol. 21, no. 9, Sep, pp. 1122-8.

Waldegger, S, Jeck, N, Barth, P, Peters, M, Vitzthum, H, Wolf, K, Kurtz, A, Konrad, M & Seyberth, HW 2002, 'Barttin increases surface expression and changes current properties of ClC-K channels', *Pflugers Arch,* vol. 444, no. 3, Jun, pp. 411-8.

Walker, PA, Leong, LE, Ng, PW, Tan, SH, Waller, S, Murphy, D & Porter, AG 1994, 'Efficient and rapid affinity purification of proteins using recombinant fusion proteases', *Biotechnology (N Y),* vol. 12, no. 6, Jun, pp. 601-5.

Wang, SS, Devuyst, O, Courtoy, PJ, Wang, XT, Wang, H, Wang, Y, Thakker, RV, Guggino, S & Guggino, WB 2000, 'Mice lacking renal chloride channel, CLC-5, are a model for Dent's disease, a nephrolithiasis disorder associated with defective receptor-mediated endocytosis', *Hum Mol Genet,* vol. 9, no. 20, Dec 12, pp. 2937-45.

Wang, ZY & Portis, AR, Jr. 1991, 'A fluorometric study with 1-anilinonaphthalene-8-sulfonic acid (ANS) of the interactions of ATP and ADP with rubisco activase', *Biochim Biophys Acta,* vol. 1079, no. 3, Sep 20, pp. 263-7.

Weinreich, F & Jentsch, TJ 2001, 'Pores formed by single subunits in mixed dimers of different CLC chloride channels', *J Biol Chem,* vol. 276, no. 4, Jan 26, pp. 2347-53.

Wellhauser, L, Kuo, HH, Stratford, FL, Ramjeesingh, M, Huan, LJ, Luong, W, Li, C, Deber, CM & Bear, CE 2006, 'Nucleotides bind to the C-terminus of ClC-5', *Biochem J,* vol. 398, no. 2, Sep 1, pp. 289-94.

Wheeler, TM, Lueck, JD, Swanson, MS, Dirksen, RT & Thornton, CA 2007, 'Correction of ClC-1 splicing eliminates chloride channelopathy and myotonia in mouse models of myotonic dystrophy', *J Clin Invest,* vol. 117, no. 12, Dec, pp. 3952-7.

Wrong, OM, Norden, AG & Feest, TG 1994, 'Dent's disease; a familial proximal renal tubular syndrome with low-molecular-weight proteinuria, hypercalciuria, nephrocalcinosis, metabolic bone disease, progressive renal failure and a marked male predominance', *Qjm,* vol. 87, no. 8, Aug, pp. 473-93.

Wu, F, Roche, P, Christie, PT, Loh, NY, Reed, AA, Esnouf, RM & Thakker, RV 2003, 'Modeling study of human renal chloride channel (hCLC-5) mutations suggests a structural-functional relationship', *Kidney Int,* vol. 63, no. 4, Apr, pp. 1426-32.

Wu, W, Rychkov, GY, Hughes, BP & Bretag, AH 2006, 'Functional complementation of truncated human skeletal-muscle chloride channel (hClC-1) using carboxyl tail fragments', *Biochem J,* vol. 395, no. 1, Apr 1, pp. 89-97.

Yamamoto-Mizuma, S, Wang, GX, Liu, LL, Schegg, K, Hatton, WJ, Duan, D, Horowitz, TL, Lamb, FS & Hume, JR 2004, 'Altered properties of volume-sensitive osmolyte and anion channels (VSOACs) and membrane protein expression in cardiac and smooth muscle myocytes from Clcn3-/- mice', *J Physiol,* vol. 557, no. Pt 2, Jun 1, pp. 439-56.

Yao, H & Hersh, LB 2006, 'Characterization of the binding of the fluorescent ATP analog TNP-ATP to insulysin', *Arch Biochem Biophys,* vol. 451, no. 2, Jul 15, pp. 175-81.

Yehezkel, G, Hadad, N, Zaid, H, Sivan, S & Shoshan-Barmatz, V 2006, 'Nucleotide-binding sites in the voltage-dependent anion channel: characterization and localization', *J Biol Chem,* vol. 281, no. 9, Mar 3, pp. 5938-46.

Yoshikawa, M, Uchida, S, Ezaki, J, Rai, T, Hayama, A, Kobayashi, K, Kida, Y, Noda, M, Koike, M, Uchiyama, Y, Marumo, F, Kominami, E & Sasaki, S 2002, 'CLC-3 deficiency leads to phenotypes similar to human neuronal ceroid lipofuscinosis', *Genes Cells,* vol. 7, no. 6, Jun, pp. 597-605.

Zhang, R, Evans, G, Rotella, FJ, Westbrook, EM, Beno, D, Huberman, E, Joachimiak, A & Collart, FR 1999, 'Characteristics and crystal structure of bacterial inosine-5'-monophosphate dehydrogenase', *Biochemistry,* vol. 38, no. 15, Apr 13, pp. 4691-700.

Zhang, XD, Tseng, PY & Chen, TY 2008, 'ATP inhibition of CLC-1 is controlled by oxidation and reduction', *J Gen Physiol,* vol. 132, no. 4, Oct, pp. 421-8.

Zhou, X, Cahoon, M, Rosa, P & Hedstrom, L 1997, 'Expression, purification, and characterization of inosine 5'-monophosphate dehydrogenase from Borrelia burgdorferi', *J Biol Chem,* vol. 272, no. 35, Aug 29, pp. 21977-81.

Ziady, AG & Davis, PB 2006, 'Current prospects for gene therapy of cystic fibrosis', *Curr Opin Pharmacol,* vol. 6, no. 5, Oct, pp. 515-21.

Zifarelli, G & Pusch, M 2008, 'The muscle chloride channel ClC-1 is not directly regulated by intracellular ATP', *J Gen Physiol,* vol. 131, no. 2, Feb, pp. 109-16.

Zuniga, L, Niemeyer, MI, Varela, D, Catalan, M, Cid, LP & Sepulveda, FV 2004, 'The voltage-dependent ClC-2 chloride channel has a dual gating mechanism', *J Physiol,* vol. 555, no. Pt 3, Mar 16, pp. 671-82.

APPENDIX A: Multiple sequence alignment of CLC

```
hClC-1          MEQSRSQQRGGEQSWWGSDPQYQYMPFEHCTSYGLPSENGGLQHRLRKDAGPRHNVHPTQ 60
rClC-1          MERSQSQQHGGEQSWWGTAPQYQYMPFEHCTSYGLPSENGGLQHRPRKDLGPRHNAHPTQ 60
gClC-1          ----------GEPSWWGS-AQYQYMPFEHCTSYGLPSEDGGLQRRLRRTQAP-CQRHPTQ 48
TmClC-0         ------------------------MSHEKNEASGYP------------------------ 12
TcClC-0         ------------------------MSHEKNEASGNP------------------------ 12
hClC-2          ----------MAAAAAEEGMEPPALQHEQTLMYGRYTQDLG----------AFAKEEAAR 40
hClC-3          ------MTNGGSINSSTHLLDLLDEPIPGVGTYDDFHTIDWVRE---------------- 38
hClC-4          ------MVNAGAMSGSGNLMDFLDEPFPDVGTYEDFHTIDWLRE---------------- 38
hClC-5          --------------------MDFLEEPIPGVGTYDDFNTIDWVRE---------------- 25
hClC-6          -----MAGCRGSLCCCCR-----WCCCCGERETRTPEELTILG----------------- 33
hClC-7          -----MANVSKKVSWSGRDRDDEEAAPLLRRTARPGGGTPLLNGAGPGAARQSPRSALFR 55
hClC-Ka         ----------------------------MEELVGLR------------------------ 8
hClC-Kb         ----------------------------MEEFVGLR------------------------ 8
EcClC           ------------------------------------------------------------
StClC           ------------------------------------------------------------
                :                                                :
Topology        
```

```
hClC-1          IYGHHKEQFSDREQD--------------IGMPKKTGSSSTVDSKDEDHYSKCQDCIHRL 106
rClC-1          IYGHHKEQYSYQAQD--------------RGIPKKTDSSSTVDSLDEDHYSKCQDCVHRL 106
gClC-1          IYGHHKGQFSGKEQD--------------NEMPKTMGSSASVDSKDEDHYSKCQDCMHRL 94
TmClC-0         ------EAQSWKSQE--------------AMLGARTEVS---------RWRAVKNCLYRH 43
TcClC-0         ------EAQSWKAQE--------------AMLGVKTEVS---------RWRAVKNCLYRH 43
hClC-2          IRLGGPEPWKGPPSS--------------RAAPELLEYGRS-------RCARCRVCSVRC 79
hClC-3          --KCKDRERHRRINS--------------KKKESAWEMTKSLYDAWSGWLVVTLTGLASG 82
hClC-4          --KSRDTDRHRKITS--------------KSKESIWEFIKSLLDAWSGWVVMLLIGLLAG 82
hClC-5          --KSRDRDRHREITN--------------KSKESTWALIHSVSDAFSGWLLMLLIGLLSG 69
hClC-6          ----ETQEEEDEILP--------------------RKDYESLDYDRCINDPYLEVLETMD 69
hClC-7          VGHMSSVELDDELLDPDMDPPHPFPKEIPHNEKLLSLKYESLDYDNSENQLFLEEERRIN 115
hClC-Ka         ------EGFSGDP----------------VTLQELWGPCP--------HIRRAIQGGLEW 38
hClC-Kb         ------EGSSGNP----------------VTLQELWGPCP--------LIRRGIRGGLEW 38
EcClC           ----MKTDTPSLETP-------------------------------QAARLRRRQLIRQ 24
StClC           ----MKTDTSTFLAQ-------------------------------QIVRLRRRDQIRR 24
                :                                                :
Topology        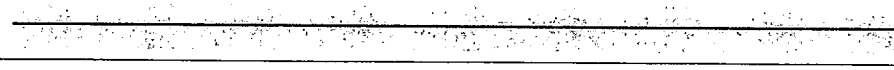
```

Boundary between cytoplasmic N-terminal region and transmembrane region

```
hClC-1          GQVVRRKLGEDWIFLVLLGLLMALVSWSMDYVSAKSLQAYKWS----------------Y 150
rClC-1          GRVLRRKLGEDWIFLVLLGLLMALVSWCMDYVSAKSLQAYKWT----------------Y 150
gClC-1          GLVVRRKLGEDWIFLVLLGLLMALVSWCMDYVSAKTLQAYKWS----------------Y 138
TmClC-0         ---LVKVLGEDWIFLLLLGALMALVSWAMDFIGSRGLRFYKYL----------------F 84
TcClC-0         ---LVKVLGEDWIFLLLLGALMALVSWAMDFIGSRGLRFYKYL----------------F 84
hClC-2          HKFLVSRVGEDWIFLVLLGLLMALVSWVMDYAIAACLQAQQWM----------------S 123
hClC-3          ALAGLIDIAADWMTDLKEGICLSALWYNHEQCCWGSNETTFEERDKCPQWKTWAELIIGQ 142
hClC-4          TLAGVIDLAVDWMTDLKEGVCLSAFWYSHEQCCWTSNETTFEDRDKCPLWQKWSELLVNQ 142
hClC-5          SLAGLIDISAHWMTDLKEGICTGGFWFNHEHCCWNSEHVTFEERDKCPEWNSWSQLIIST 129
hClC-6          NKKGRRYEAVKWMVVFAIGVCTGLVGLFVDFFVRLFTQLKFGVVQTS----------VEE 119
hClC-7          HTAFRTVEIKRWVICALIGILTGLVACFIDIVVENLAGLKYRVIKGN----------IDK 165
hClC-Ka         LKQKVFRLGEDWYFLMTLGVLMALVSYAMNFAIGCVVRAHQWL----------------Y 82
hClC-Kb         LKQKLFRLGEDWYFLMTLGVLMALVSCAMDLAVESVVPAHQWL----------------Y 82
EcClC           LLERDKTPLAILFMAAVVGTLVGLAAVAFDKGVAWLQNQFMGA----------------L 68
StClC           LMQRDKTPLAILFMAAVVGTLTGLVGVAFEKAVSWVQNMRIGA----------------L 68
                                    *   .   :
Topology        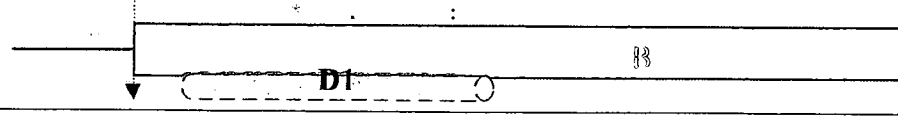
                                                    D1
```

```
hClC-1      AQMQPSLPLQFLVWVTFPLVLILFSALFCHLISPQAVGSGIPEMKTILRGVVLKEYLTMK 210
rClC-1      AQMQPSLPLQYLAWVTFPLILILFSALFCQLISPQAVGSGIPEMKTILRGVVLKEYLTLK 210
gClC-1      YQMQPSLPLQFLVWVGFPLTLILFSALFCQLISPQAVGSGIPEMKTILRGVVLKEYLTLK 198
TmClC-0     ALVEGNIGLQYLVWVCYPLALILFSSLFCQIVSPQAVGSGIPELKTIIRGAVLHEYLTLR 144
TcClC-0     AMVEGNLGLQYLVWVCYPLILILFSSLFCQIVSPQAVGSGIPELKTIIRGAVLHEYLTLR 144
hClC-2      RGLNTSILLQYLAWVTYPVVLITFSAGFTQILAPQAVGSGIPEMKTILRGVVLKEYLTLK 183
hClC-3      AEGPGSYIMNYIMYIFWALSFAFLAVSLVKVFAPYACGSGIPEIKTILSGFIIRGYLGKW 202
hClC-4      SEGASAYILNYLMYILWALLFAFLAVSLVRVFAPYACGSGIPEIKTILSGFIIRGYLGKW 202
hClC-5      DEGAFAYIVNYFMYVLWALLFAFLAVSLVKVFAPYACGSGIPEIKTILSGFIIRGYLGKW 189
hClC-6      CSQKGCLALSLLELLGFNLTFVFLASLLV-LIEPVAAGSGIPEVKCYLNGVKVPGIVRLR 178
hClC-7      FTEKGGLSFSLLLWATLNAAFVLVGSVIVAFIEPVAAGSGIPQIKCFLNGVKIPHVVRLK 225
hClC-Ka     REIGDSHLLRYLSWTVYPVALVSFSSGFSQSITPSSGGSGIPELKTMLAGVILEDYLDIK 142
hClC-Kb     REIGDSHLLRYLSWTVYPVALVSFSSGFSQSITPSSGGSGIPEVKTMLAGVVLEDYLDIK 142
EcClC       VHTADNYPLLLTVAFLCSAVLAMFGYFLVRKYAPEAGGSGIPEIEGALE--DQRPVRWWR 126
StClC       VQVADHAFLLWPLAFILSALLAMVGYFLVRKFAPEAGGSGIPEIEGALE--ELRPVRWWR 126
                      .          :  ..  :      * : *****:::   :
Topology
```



E148 of EcClC suggested to be involved in the fast gating mechanism and is highly conversed among ClCs except Ka and Kb

```
hClC-1      AFVAKVVALTAGLGSG--IPVGKEGPFVHIASICAAVLS------KFMSVFCGVYEQPYY 262
rClC-1      AFVAKVVALTAGLGSG--IPVGKEGPFVHIASICAAVLS------KFMSMFSGVYEQPYY 262
gClC-1      AFVAKVVALTAGLGSG--IPVGKEGPFVHIASICAAILS------KFMSVFCGVYEQPYY 250
TmClC-0     TFVAKTVGLTVALSAG--FPLGKEGPFVHIASICATLLN------QLLCFISGRREEPYY 196
TcClC-0     TFVAKTVGLTVALSAG--FPLGKEGPFVHIASICATLLN------QLLCFISGRREEPYY 196
hClC-2      TFIAKVIGLTCALGSG--MPLGKEGPFVHIASMCAALLS------KFLSLFGGIYENESR 235
hClC-3      TLMIKTITLVLAVASG--LSLGKEGPLVHVACCCGN----------IFSYLFPKYSTNEA 250
hClC-4      TLLIKTVTLVLVVSSG--LSLGKEGPLVHVACCCGN----------FFSSLFSKYSKNEG 250
hClC-5      TLVIKTITLVLAVSSG--LSLGKEGPLVHVACCCGN----------ILCHCFNKYRKNEA 237
hClC-6      TLLCKVLGVLFSVAGG--LFVGKEGPMIHSGSVVGAGLPQFQSISLRKIQFNFPYFRSDR 236
hClC-7      TLVIKVSGVILSVVGG--LAVGKEGPMIHSGSVIAAGISQGRSTSLKRDFKIFEYFRRDT 283
hClC-Ka     NFGAKVVGLSCTLATGSTLFLGKVGPFVHLSVMIAAYLG------RVRTTTIGEPENKSK 196
hClC-Kb     NFGAKVVGLSCTLACGSTLFLGKVGPFVHLSVMMAAYLG------RVRTTTIGEPENKSK 196
EcClC       VLPVKFFGGLGTLGGG--MGLGPEGPTVQIGGNISR----------MVLDIFRLKGDE 172
StClC       VLPVKFIGGMGTLGAG--MVLGPEGPTVQIGGNLGR----------MVLDVFRMRSAE 172
              :  *       :  *  : :*: ** :: .   .  :
Topology
```

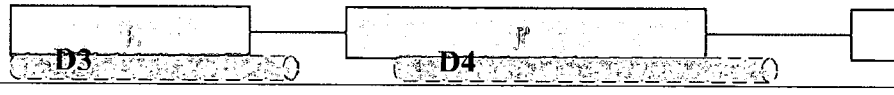

E203 of EcClC suggested to be involved in proton transport and this residue is highly conserved among ClC-3 to 7

```
hClC-1      Y-SDILTVGCAVGVGCCFGTPLGGVLFSIEVT--STYFAVRNYWRGFFAATFSAFVFRVL 319
rClC-1      Y-TDILTVGCAVGVGCCFGTPLGGVLFSIEVT--STYFAVRNYWRGFFAATFSAFVFRVL 319
gClC-1      Y-TDMLTVGCAVGVGCCFGTPLGGVLFSIEVT--STYFAVRNYWRGFFAATFSAFVFRVL 307
TmClC-0     LRADILTVGCALGISCCFGTPLAGVLFSIEVT--CSHFGVRSYWRGFLGGAFSAFIFRVL 254
TcClC-0     LRADILTVGCALGISCCFGTPLAGVLFSIEVT--CSHFGVRSYWRGFLGGAFSAFIFRVL 254
hClC-2      N-TEMLAAACAVGVGCCFAAPIGGVLFSIEVT--STFFAVRNYWRGFFAATFSAFIFRVL 292
hClC-3      KKREVLSAASAAGVSVAFGAPIGGVLFSLEEV--SYYFPLKTLWRSFFAALVAAFVLRSI 308
hClC-4      KRREVLSAAAAAGVSVAFGAPIGGVLFSLEEV--SYYFPLKTLWRSFFAALVAAFTLRSI 308
hClC-5      KRREVLSAAAAAGVSVAFGAPIGGVLFSLEEV--SYYFPLKTLWRSFFAALVAAFTLRSI 295
hClC-6      DKRDFVSAGAAAGVAAAFGAPIGGTLFSLEEG--SSFWNQGLTWKVLFCSMSATFTLNFF 294
hClC-7      EKRDFVSAGAAAGVSAAFGAPVGGVLFSLEEG--ASFWNQFLTWRIFFASMISTFTLNFV 341
hClC-Ka     Q-NEMLVAAAAVGVATVFAAPFSGVLFSIEVM--SSHFSVRDYWRGFFAATCGAFIFRLL 253
hClC-Kb     Q-NEMLVAAAAVGVATVFGAPFSGVLFSIEVM--SSHFSVWDYWRGFFAATCGAFMFRLL 253
EcClC       ARHTLLATGAAAGLAAAFNAPLAGILFIIEEMRPQFRYTLISIKAVFIGVIMSTIMYRIF 232
StClC       ARHTLLATGAAAGLSAAFNAPLAGILFIIEEMRPQFRYNLISIKAVFTGVIMSSIVFRIF 232
                 .: ...* *:.  * :*..: ** :*       :       :     .::   . .
Topology
```

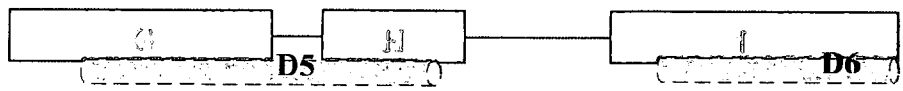

```
hClC-1      AVWNKDA-----VTITALFRTNFR------MDFPFDLKELPAFAAIGICCGLLGAVFVYL 368
rClC-1      AVWNKDA-----VTITALFRTNFR------MDFPFDLKELPAFAVIGICCGFLGAVFVYL 368
gClC-1      AVWNKDA-----VTITALFRTNFR------MDFPFDLQELPAFAIIGICCGFLGAVFVYL 356
TmClC-0     SVWVKDT-----VTLTALFKTNFR------GDIPFDLQEMPAFAIIGIASGFFGALFVYL 303
TcClC-0     SVWVKDT-----VTLTALFKTNFR------GDIPFDLQELPAFAIIGIASGFFGALFVYL 303
hClC-2      AVWNRDE-----ETITALFKTRFR------LDFPFDLQELPAFAVIGIASGFGGALFVYL 341
hClC-3      NP---FG-----NSRLVLFYVEYH--------TPWYLFELFPFILLGVFGGLWGAFFIRA 352
hClC-4      NP---FG-----NSRLVLFYVEYH--------TPWYMAELFPFILLGVFGGLWGTLFIRC 352
hClC-5      NP---FG-----NSRLVLFYVEFH--------TPWHLFELVPFILLGIFGGLWGALFIRT 339
hClC-6      RSGIQFGSWGSFQLPGLLNFGEFKCSDSDKKCHLWTAMDLGFFVVMGVIGGLLGATFNCL 354
hClC-7      LS-IYHGNMWDLSSPGLINFGRF---DSEK--MAYTIHEIPVFIAMGVVGGVLGAVFNAL 395
hClC-Ka     AVFNSEQ-----ETITSLYKTSFR------VDVPFDLPEIFFFVALGGICGVLSCAYLFC 302
hClC-Kb     AVFNSEQ-----ETITSLYKTSFR------VDVPFDLPEIFFFVVLGGLCGILGSAYLFC 302
EcClC       NH-----------EVALIDVGKLS---------DAPLNTLWLYLILGIIFGIFGPIFNKW 272
StClC       NG-----------EAPIIEVGKLS---------DAPVNTLWLYLILGIIFGCVGPVFNSL 272

Topology
```




```
hClC-1      HRQVMLGVRKHKALSQFLAKHRLLYPGIVTFVIASFTFPPGMGQFMAGELMPREAISTLF 428
rClC-1      HRQVMLGVRKHKALSQFLAKHRLLYPGIVTFVIASLTFPPGMGQFMAGELMPREAISTLF 428
gClC-1      HRQVMLGVRKHKVLSQFLAKHRLLYPGIVTFVIASFTFPPGIGQFMAGELMPREAISTLF 416
TmClC-0     NRQIIVFMRKKNFVTKILKKQRLIYPAVVTFVLATLRFPPGVGQFFGAGLMPRETINSLF 363
TcClC-0     NRQIIVFMRKKNFVTKILKKQRLIYPAVVTFVLATLRFPPGVGQFFGAGLMPRETINSLF 363
hClC-2      NRKIVQVMRKQKTINRFLMRKRLLFPALVTLLISTLTFPPGFGQFMAGQLSQKETLVTLF 401
hClC-3      N--IAWCRRRKSTKFG---KYPVLEVIIVAAITAVIAFPNPYTRLNTSELIKELFTDCGP 407
hClC-4      N--IAWCRRRKTTRLG---KYPVLEVIVVTAITAIIAYPNPYTRQSTSELISELFNDCGA 407
hClC-5      N--IAWCRKRKTTQLG---KYPVIEVLVVTAITAILAFPNEYTRMSTSELISELFNDCGL 394
hClC-6      N--KRLAKYRMRNVHPKPKLVRVLESLLVSLVTTVVVFVASMVLGECRQMSSSSQIGNDS 412
hClC-7      N--YWLTMFRIRYIHR--PCLQVIEAVLVAAVTATVAFVLIYSSRDCQPLQG----GSMS 447
hClC-Ka     QRTFLSFIKTNRYSSKLLATSKPVYSALATLLLASITYPPGVGHFLASRLSMKQHLDSLF 362
hClC-Kb     QRIFFGFIRNNRFSSKLLATSKPVYSALATLVLASITYPPSAGRFLASRLSMKQHLDSLF 362
EcClC       VLGMQDLLHR---VHGGNITKWVLMGGAIGGLCGLLGFVAPATSGGGFNLIPIATAGNFS 329
StClC       VLRTQDMFQR---FHGGEIKKWVLMGGAIGGLCGILGLIEPAAAGGGFNLIPIAAAGNFS 329

Topology
```




```
hClC-1      DNNTWV----------------------KHAGDPESLGQSAVWIHPRVNVVIIIFLFFVM 466
rClC-1      DNNTWV----------------------KHIGDPKSLGQSAVWIHPQVNVVIIILLFFVM 466
gClC-1      DNNTWV----------------------KHMGDPESLGRSAVWIHPKASVVLVLLLFFIM 454
TmClC-0     DNYTWT----------------------KTI-DPRGLGNSAQWFIPHLNIFIVMALYFVM 400
TcClC-0     DNYTWT----------------------KTI-DPRGLGNSAQWFIPHLNIFIVMALYFVM 400
hClC-2      DNRTWVRQ--------------------GLVEELEPPSTSQAWNPPRANVFLTLVIFILM 441
hClC-3      LESSS-----------LCDYRNDMNASKIVDDIPDRPAGIGVYSA-----IWQLCLALIF 451
hClC-4      LESSQ-----------LCDYINDPNMTRPVDDIPDRPAGVGVYTA-----MWQLALALIF 451
hClC-5      LDSSK-----------LCDYENRFNTSK-GGELPDRPAGVGVYSA-----MWQLALTLIL 437
hClC-6      FQLQVTEDVNSSIKTFFCPNDTYNDMATLFFNPQESAILQLFHQD-GTFSPVTLALFFVL 471
hClC-7      YPLQL-----------FCADGEYNSMAAAFFNTPEKSVVSLFHDPPGSYNPLTLGLFTLV 496
hClC-Ka     DNHSWALMT-------------QNSSPPWPEELDPQHLWWEWYHPRFTIFGTLAFFLVM 408
hClC-Kb     DNHSWALMT-------------QNSSPPWPEELDPQHLWWEWYHPRFTIFGTLAFFLVM 408
EcClC       ------------------------------------------------MGMLVFIFVA 339
StClC       ------------------------------------------------VGLLLFIFIT 339

Topology
```

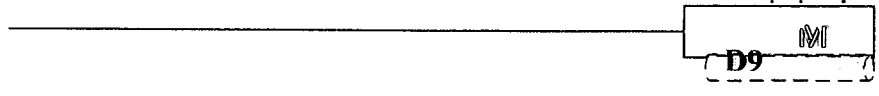

```
hClC-1      KFWMSIVATTMPIPCGGFMPVFVLGAAFGRLVGEIMAMLFP-------DGILFDDIIYKI 519
rClC-1      KFWMSIVATTMPIPCGGFMPVFVLGAAFGRLVGEIMAMLFP-------EGILFDDIIYKI 519
gClC-1      KFWMSIVATTMPIPCGGFMPVFVLGAAFGRLVGEIMAMLFP-------DGILFDNIIYKI 507
TmClC-0     HFWMAALAVTMPVPCGAFVPVFNLGAVLGRFVGELMALLFP-------DGLVSNGNLYHI 453
TcClC-0     HFWMAALAVTMPVPCGAFVPVFNLGAVLGRFVGELMALLFP-------DGLVSNGNLYHI 453
hClC-2      KFWMSALATTIPVPCGAFMPVFVIGAAFGRLVGESMAAWFP-------DGIHTDSSTYRI 494
hClC-3      KIIMTVFTFGIKVPSGLFIPSMAIGAIAGRIVGIAVEQLAYYHHDWFIFKEWCEVGADCI 511
hClC-4      KIVVTIFTFGMKIPSGLFIPSMAVGAIAGRMVGIGVEQLAYHHHDWIIFRNWCRPGADCV 511
hClC-5      KIVITIFTFGMKIPSGLFIPSMAVGAIAGRLLGVGMEQLAYYHQEWTVFNSWCSQGADCI 497
hClC-6      YFLLACWTYGISVPSGLFVPSLLCGAAFGRLVAN-------------VLKSYIGLGHIYS 518
hClC-7      YFFLACWTYGLTV-AGVFIPSLLIGAAWGRLFG--------------ISLSYLTGAAIWA 542
hClC-Ka     KFWMLILATTIPMPAGYFMPIFILGAAIGRLLGEALAVAFP-------EGIVTGGVTNPI 461
hClC-Kb     KFWMLILATTIPMPAGYFMPIFVYGAAIGRLFGETLSFIFP-------EGIVAGGITNPI 461
EcClC       RVITTLLCFSSGAPGGIFAPMLALGTVLGTAFGMVAVELFP---------------QYHL 384
StClC       RVVTTLLCFSSGAPGGIFAPMLALGTLLGTAFGMAAAVLFP---------------QYHL 384
                .          .  * * * :  *:  .  ..
Topology
```

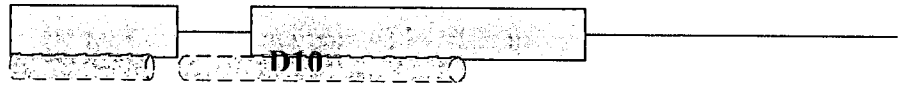


```
hClC-1      LPGGYAVIGAAALTG-AVSHTVSTAVICFELTGQIAHILPMMVAVILANMVAQSLQ-PSL 577
rClC-1      LPGGYAVIGAAALTG-AVSHTVSTAVICFELTGQIAHILPMMVAVILANMVAQSLQ-PSL 577
gClC-1      LPGGYAVIGAAALTG-AVSHTVSTAVICFELTGQIAHILPMMVAVILANMVAQSLH-SSL 565
TmClC-0     LPGEYAVIGAAAMTG-AVTHAVSTAVICFELTGQISHVLPMMVAVILANMVAQGLQ-PSL 511
TcClC-0     LPGEYAVIGAAAMTG-AVTHAVSTAVICFELTGQISHVLPMMVAVILANMVAQGLQ-PSL 511
hClC-2      VPGGYAVVGAAALAG-AVTHTVSTAVIVFELTGQIAHILPVMIAVILANAVAQSLQ-PSL 552
hClC-3      TPGLYAMVGAAACLGGVTRMTVSLVVIVFELTGGLEYIVPLMAAVMTSKWVGDAFGREGI 571
hClC-4      TPGLYAMVGAAACLGGVTRMTVSLVVIMFELTGGLEYIVPLMAAAVTSKWVADAFGKEGI 571
hClC-5      TPGLYAMVGAAACLGGVTRMTVSLVVIMFELTGGLEYIVPLMAAAMTSKWVADALGREGI 557
hClC-6      --GTFALIGAAAFLGGVVRMTISLTVILIESTNEITYGLPIMVTLMVAKWTGDFFN-KGI 575
hClC-7      DPGKYALMGAAAQLGGIVRMTLSLTVIMMEATSNVTYGFPIMLVLMTAKIVGDVFI-EGL 601
hClC-Ka     MPGGYALAGAAAFSG-AVTHTISTALLAFELTGQIVHALPVLMAVLAANAIAQSCQ-PSF 519
hClC-Kb     MPGGYALAGAAAFSG-AVTHTISTALLAFEVTGQIVHALPVLMAVLAANAIAQSCQ-PSF 519
EcClC       EAGTFAIAGMGALLAASIRAPLTGIILVLEMTDNYQLILPMIITGLGATLLAQFTGGKPL 444
StClC       EAGTFAIAGMGALMAASVRAPLTGIVLVLEMTDNYQLILPMIITCLGATLLAQFLGGKPL 444
              * :*: * .*  .     .:: :: :* *.    .*:: . : :.  .:      :
Topology
```

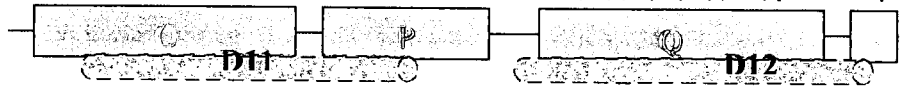

Boundary between cytoplasmic C-terminal region and transmembrane region

```
hClC-1      YDSIIQVKKLPYLPDLG-----WNQLSKYTIFVEDIMVRDVKFVSASYTYGELRTLLQTT 632
rClC-1      YDSIIQVKKLPYLPDLG-----WNQLSKFTIFVEDIMVRDVKFVSASCTYGELRNLLQTT 632
gClC-1      YDSIIQVKKLPYLPDLG-----WNQLSKFTIFVEDIMVRDVKFVSASCTYEELRNLLQTT 620
TmClC-0     YDSIIQIKKLPYLPELS-----WSSANKYNIQVGDIMVRDVTSIASTSTYGDLLHVLRQT 566
TcClC-0     YDSIIQIKKLPYLPELS-----WSSANKYNIQVGDIMVRDVTSIASTSTYGDLLHVLRQT 566
hClC-2      YDSIIEIKKLPYLPELG-----WGRHQQYRVRVEDIMVRDVPHVALSCTFRDLRLALHRT 607
hClC-3      YEAHIELNGYPFLDAKEEFEFTHTTLAADVMRPRRNDPPLAVLTQDNMTVDDIENMINET 631
hClC-4      YEAHIHLNGYPFLDVKD--EFTHRTLATDVMRPRRGEPPLSVLTQDSMTVEDVETLIKET 629
hClC-5      YDAHIELNGYPFLEAKE--EFAHKTLAMDVMKPRRNDPLLTVLTQDSMTVEDVETIISET 615
hClC-6      YDIHVGLRGVPLLEWET-------EVEMDKLRASDIMEPNLTYVYPHTRIQSLVSILRTT 628
hClC-7      YDMHIQLQSVPFLHWEA-------PVTSHSLTAREVMSTPVTCLRRREKVGVIVDVLSDT 654
hClC-Ka     YDGTIIVKKLPYLPRIL-----GRNIGSHHVRVEHFMNHSITTLAKDTPLEEVVKVVTST 574
hClC-Kb     YDGTVIVKKLPYLPRIL-----GRNIGSHRVRVEHFMNHSITTLAKDTPLEEVVKVVTST 574
EcClC       YS----------------------------AILARTLAKQEAEQLARSKAASASENT---- 473
StClC       YS----------------------------TILARTLAKQDAEQAEKNQNAPADENT---- 473
            *.  : :     :                  :                    :
Topology
```

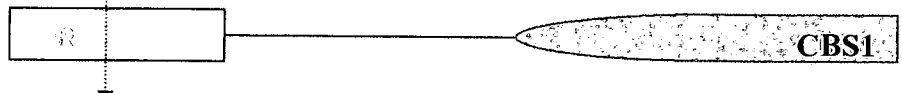

```
hClC-1          T--VKTLPLVDSKDSMILLGSVERSELQALLQRHLCPERRLRAAQEMARKLSELPYDGKA 690
rClC-1          T--VKTLPLVDSKDSMILLGSVERSELQSLLQRHLCAERRLKAAQDMARKLSELPYNGQA 690
gClC-1          T--VKTLPLVESKDSMILLGSVERSELQSLLQRHLCPERXLRLAQDMARKLSELPFDGKV 678
TmClC-0         K--LKFFPFVDTPDTNTLLGSIDRTEVEGLLQRRISAYRRQPAAAAEADE------EGRN 618
TcClC-0         K--LKFFPFVDTPETNTLLGSIERTEVEGLLQRRISAYRRQPATAAEAEE------EGRN 618
hClC-2          K--GRMLALVESPESMILLGSIERSQVVALLGAQLSPARRRQHMQERRATQTSPLSDQEG 665
hClC-3          S--YNGFPVIMS---------------------------------------------- 641
hClC-4          D--YNGFPVVVS---------------------------------------------- 639
hClC-5          T--YSGFPVVVS---------------------------------------------- 625
hClC-6          V--HHAFPVVTENRGNEKEFMKGNQLISNNIKFKKSSILTRAGEQRKRSQSMKSYPSSEL 686
hClC-7          ASNHNGFPVV------------------------------------------------ 664
hClC-Ka         D--VTEYPLVESTESQILVGIVQRAQLVQALQ-------------------------- 604
hClC-Kb         D--VAEYPLVESTESQILVGIVRRAQLVQALK-------------------------- 604
EcClC           ------------------------------------------------------------
StClC           ------------------------------------------------------------

                         .:              :   :
Topology
```



```
hClC-1          RLAGEGPPGAPP-GRPESFAFVDEDEDEDLSGKSELPPSLALHPSTTAPLS--------- 740
rClC-1          QLAGEWHPG----GRPESFAFVDEDEDEDVSRKTELPQTPTPPPPPPPPLPPQFPIAPSY 746
gClC-1          RPAGVGRSGVWPQGRPESFAFVDEDEDEDLYGKPEMPPLHPPHPLPTDPLP--------- 729
TmClC-0         GETGASFT----GEAESSFAYIDQEDAEGQQ-REGLEAVKVQTEDPRPPSP--------- 664
TcClC-0         GERGASFTGDVPGEAETSFAYIDQEEAEGQQQREGLEAVKVQTEDPRPPSP--------- 669
hClC-2          PPSPEASVCFQVNTEDSAFPAARGETHKPLKPALKRGPSVTRNLGESPTGS--------- 716
hClC-3          ----------KESQR------------------------------------------- 646
hClC-4          ----------RDSER------------------------------------------- 644
hClC-5          ----------RESQR------------------------------------------- 630
hClC-6          RNMCDEHIASEEPAEKEDLLQQMLERRYTPYPNLYPDQSPSEDWTMEERFR--------- 737
hClC-7          -----EHADDTQPAR------------------------------------------- 674
hClC-Ka         ------------------------------------------------------------
hClC-Kb         ------------------------------------------------------------
EcClC           ------------------------------------------------------------
StClC           ------------------------------------------------------------

                                  :
Topology
```



```
hClC-1          PEEPNGPLPGHKQQPEAPEPAGQRPSIFQSLLHCLLGRARPTKKKTTQDSTDLVDNMSPE 800
rClC-1          PEEPNGPLPSHKQPPEASDSADQRSSIFQRLLHCLLGKAHSTKKKITQDSTDLVDNMSPE 806
gClC-1          PEEPNGPLPSHKQQLEALASTGPRPSIFRSLLHCLLGRARPKKKKMTQDSTDLVDNMSPE 789
TmClC-0         ---------------VPAEEPTQTSGIYQ----------KKQKGTGQVASRFEEMLTLE 698
TcClC-0         ---------------VPAEEPTQTSGIYQ----------KKHKGTGQVASRFEEMLTLE 703
hClC-2          AESAGIALRSLFCGSPPPEAASEKLESCEK-------RKLKRVRISLASDADLEGEMSPE 769
hClC-3          --------------LVGFALRRDLTIAIESARKKQEGIVGS-----SRVCFAQHTPSLPA 687
hClC-4          --------------LIGFAQRRELILAIKNARQRQEGIVSN-----SIMYFTEEPPELPA 685
hClC-5          --------------LVGFVLRRDLIISIENARKKQDGVVST-----SIIYFTEHSPPLPP 671
hClC-6          -----------PLTFHGLILRSQLVTLLVRGVCYSESQSSASQPRLSYAEMAEDYPRYPD 786
hClC-7          --------------LQGLILRSQLIVLLKHKVFVERSNLGLVQRRLRLKDFRDAYPRFPP 720
hClC-Ka         ----------------AEPPSRAP---------------------------------- 612
hClC-Kb         ----------------AEPPSWAP---------------------------------- 612
EcClC           ------------------------------------------------------------
StClC           ------------------------------------------------------------

                       :

Topology
```

```
hClC-1          EIEAWEQEQLSQPVCFDSCCIDQSPFQLVEQTTLHKTHTLFSLLGLHLAYVTSM-GKLRG 859
rClC-1          EIEAWEREQLSQPVCFDFCCIDQSPFQLVEQTTLHKTHTLFSLLGLHLAYVTSM-GKLRG 865
gClC-1          EIEAWEQEQLGQPVCFDSCCIDQSPFQLVEQTTLQQTHTLFSLLGLHLAYVTSM-GKLRG 848
TmClC-0         EIYRWEQREKNVVVNFETCRIDQSPFQLVEGTSLQKTHTLFSLLGLDRAYVTSM-GKLVG 757
TcClC-0         EIYQWEQREKNVVVNFETCRIDQSPFQLVEGTSLQKTHTLFSLLGLDRAYVTSM-GKLVG 762
hClC-2          EILEWEEQQLDEPVNFSDCKIDPAPFQLVERTSLHKTHTIFSLLGVDHAYVTSI-GRLIG 828
hClC-3          ESPRPLKLRS---------ILDMSPFTVTDHTPMEIVVDIFRKLGLRQCLVTHN-GRLLG 737
hClC-4          NSPHPLKLRR---------ILNLSPFTVTDHTPMETVVDIFRKLGLRQCLVTRS-GRLLG 735
hClC-5          YTPPTLKLRN---------ILDLSPFTVTDLTPMEIVVDIFRKLGLRQCLVTHN-GRLLG 721
hClC-6          IHDLDLTLLNPRMIVDVTPYMNPSPFTVSPNTHVSQVFNLFRTMGLRHLPVVNAVGEIVG 846
hClC-7          IQSIHVSQDERECTMDLSEFMNPSPYTVPQEASLPRVFKLFRALGLRHLVVVDNRNQVVG 780
hClC-Ka         -----GHQQCLQDILARGCPTEPVTLTLFSETTLHQAQNLFKLLNLQSLFVTSR-GRAVG 666
hClC-Kb         -----GHQQCLQDILAAGCPTEPVTLKLSPETSLHEAHNLFELLNLHSLFVTSR-GRAVG 666
EcClC           ------------------------------------------------------------
StClC           ------------------------------------------------------------
                                      :     :     ::  : :    :

Topology        ──────────────────────────────────────────────────────────────
                                                          CBS2
                                                    D13
```

```
hClC-1          VLALEELQKAIEG-HTKSGVQLRPPLASFRNTTSTRKSTGAPPSSAENWNLPEDRPGATG 918
rClC-1          VLALEELQKAIKG-HTKSGVQLRPPLASFRNTTSIRKTPGGPPPPAESWNVPEGEDGAPE 924
gClC-1          VLALEELQKAIEG-NTKSGVQLRPPLASFRSTTSTRKNTGVLLPPAEGWSLPEDGAGATG 907
TmClC-0         VVALAEIQAAIEG-SYQKGFRLPPPLASFRDVKHARNS---------GRTATSNSSGK-- 805
TcClC-0         VVALAEIQAAIEG-SYQKGFRLPPPLASFRDAKNARNS---------GRTATSNSSGK-- 810
hClC-2          IVTLKELRKAIEGSVTAQGVKVRPPLASFRDSATSSSD----------TETTEVHALWG 877
hClC-3          IITKKDILRHMAQ------TANQDPASIMFN---------------------------- 762
hClC-4          IITKKDVLRHMAQ------MANQDPESIMFN---------------------------- 760
hClC-5          IITKKDVLKHIAQ------MANQDPDSILFN---------------------------- 746
hClC-6          IITRHNLTYEFLQ------ARLRQHYQTI------------------------------ 869
hClC-7          LVTRKDLARYRLG------KRGLEELSLAQT------------------------------ 805
hClC-Ka         CVSWVEMKKAISN-------LTNPPAPK---------------------------- 687
hClC-Kb         CVSWVEMKKAISN-------LTNPPAPK---------------------------- 687
EcClC           ------------------------------------------------------------
StClC           ------------------------------------------------------------
                 :    :

Topology        ──────────────────────────────────────────────────────────────
```

Peptide proposed to be cleaved from C_{721}-tail during purification (Section 5.4.4)

```
hClC-1          TGDVIAASPETPVPSPSPEPPLSLAPGKVEGELEELELVESPGLEEELADILQGPSLRST 978
rClC-1          REVMVPTMPETPVPPPSPEVPSCLAPARVEGELEELEMVGNLGPEEDLADILHGPSLRST 984
gClC-1          AGDMTPASPETPVPFPFPEHPLSQAPAKAESELEELELVEGPGPEEELADILQGPSLRST 967
TmClC-0         ------------------------------------------------------------
TcClC-0         ------------------------------------------------------------
hClC-2          ----------PHSRHGLPREGSPSDSDDKCQ------------------------- 898
hClC-3          ------------------------------------------------------------
hClC-4          ------------------------------------------------------------
hClC-5          ------------------------------------------------------------
hClC-6          ------------------------------------------------------------
hClC-7          ------------------------------------------------------------
hClC-Ka         ------------------------------------------------------------
hClC-Kb         ------------------------------------------------------------
EcClC           ------------------------------------------------------------
StClC           ------------------------------------------------------------
                   :        :                    : ::        :  ::    :

Topology        ──────────────────────────────────────────────────────────────
```

```
hClC-1          DEEDEDELIL 988
rClC-1          DEEDEDELIL 994
gClC-1          DEEDGDELVL 977
TmClC-0         ----------
TcClC-0         ----------
hClC-2          ----------
hClC-3          ----------
hClC-4          ----------
hClC-5          ----------
hClC-6          ----------
hClC-7          ----------
hClC-Ka         ----------
hClC-Kb         ----------
EcClC           ----------
StClC           ----------
                      :::
Topology        ----------
```

Annotation

The sequences were aligned using the default setting of the CLUSTAL W version 1.83 program which can be accessed via the European Bioinformatics Institute website (www.ebi.ac.uk/clustalw/). The colours of amino acids are default setting from this program. Red, blue, magenta, green and grey coloured amino acids represent small and hydrophobic amino acids (AVFPMILW), acidic (DE), basic (RHK), hydroxyl with amine and basic (STYHCNGQ) and other, respectively. The sequences included ClC-1 from human (h), rat (r) and goat (g); ClC-0 from *Torpedo marmorata* (Tm) and *Torpedo californica* (Tc), transporter members of ClC from *Escherichia coli* (Ec) and *Salmonella typhimurium* (St) and the other members of ClC from human (ClC-2, 3, 4, 5, 7, Ka and Kb).

Topology:
There is a one-dimensional cartoon topology picture underneath the sequences. This picture can be referenced to the 2-dimension topology model shown in Figure 1.3 of Chapter 1. The lime and aqua boxes represent the 17 transmembrane α-helices identified from bacterial ClC X-ray structure (Dutzler *et al.* 2002). The light green cylinders represent the thirteen hydrophobic stretches determined by hydropathy analysis (Steinmeyer, Ortland & Jentsch 1991). The purple ovals represent the CBS domains in the cytoplasmic C-terminus.

The highly conserved sequences/amino acid located at the N-terminus of the α-helices D, F, N and R are highlighted in yellow. These regions are proposed to stabilize Cl^- ions inside the pore by helix dipole positive charge (Dutzler *et al.* 2002).

APPENDIX B: List of Suppliers, Distributors and Manufacturers

Supplier	Address / email
AGFA	Agfa Healthcare Offices on the Park, 8 Greenhill Road, Wayville SA 5034, Australia www.agfa.com
Amersham	Amersham Biosciences Unit 1, Number 22, Hudson Avenue, Castle Hill, NSW 2154, Australia www.amershambiosciences.com
Applied Biosystems	Applied Biosystems 52 Rocco Drive, Scoresby VIC 3179, Australia www.appliedbiosystems.com
Axon Instruments	Axon Instruments *Distributor: Molecular Devices Corporation* 107 Union Road, Unit 3, Surrey Hills VIC 3127, Australia www.axon.com
BioLabs	New England BioLabs Inc *Distributor: Genesearch Pty Ltd* 14 Technology Drive Arundel, Queensland 4214, Australia www.neb.com
Bio-Rad	Bio-Rad Laboratories Unit 1, Block Y, Regents Park Industrial Estate, 391 Park Road, Regents Park, NSW 2143, Australia www.bio-rad.com
Cell Signaling	Cell Signaling Technology, Inc www.cellsignaling.com
Clontech	BD Biosciences 4 Research Park Drive, Macquarie University, Research Park, North Ryde, NSW 2113, Australia www.bdbiosciences.com
Diploma	Bonlac Foods Ltd PO Box 4313, Melbourne VIC 3001, Australia www.bonlacfoods.com
Dow Corning	Dow Corning Australia Pty Ltd Dow Corning Building, Macquarie University Research Park, 3 Innovation Road, NORTH RYDE NSW 2113, Australia www.dowcorning.com
FUSA	SouthPath & Flinders Sequencing Facility Dept. of Haematology, Flinders Medical Centre http://som.flinders.edu.au/FUSA/Haematology/DNA.htm.
Gibco	Invitrogen Australia Pty Ltd 2A/14 Lionel Road, Mount Waverly, VIC 3149, Australia www.invitrogen.com
GraphPad	GraphPad Software Inc 11452 El Camino Real, #215, San Diego, CA 92130, USA www.graphpad.com

Eppendorf	Eppendorf South Pacific Pty Ltd 4 Research Park Drive, Macquarie University, North Ryde, NSW 2113, Australia www.eppendorf.com.au
Hycor	Hycor Biomedical Inc *Distributor: Vital Diagnostics Pty* 34/7 Salixbury Road, Castile Hill, New South Wales www.hycorbiomedical.com
IMVS	Institute of Medical and Veterinary Science Frome Rd, Adelaide SA 5000 www.imvs.sa.gov.au/molpath/geneseq/
Invitrogen	Invitrogen Australia Pty Ltd 2A/14 Lionel Road, Mount Waverly, VIC 3149, Australia www.invitrogen.com
Millipore	Millipore Australia Pty Ltd 9A Byfield Street, North Ryde, NSW 2113, Australia www.millipore.com
Nalge Nunc	Nalge Nunc International www.nalgenunc.com
Newport	NewSpec Pty Ltd 83 King William Road, Unley SA 5061, Australia www.newport.com
Novagen	Merck Pty 207 Colchester Road, Kilsth, VIC 3137, Australia www.merckbiosciences.com
Olympus	Olympus Imaging Australia Pty Ltd 82 Waterloo Rd, North Ryde NSW 2113 www.olympus.com.au
Oxoid	Oxoid Australia Pty Ltd 20 Dalgleish Street, Thebarton, Adelaide SA 5031 www.oxoid.com
Pall	Pall Corporation (Melbourne Office) 1-2 Wandarri Court, Cheltenham VIC 3192 www.pall.com
Pierce	Quantum Scientific Pty Ltd P.O. Box 164, Paddington QLD, 4064 www.quantum-scientific.com.au
Promega	Promega Corporation 37 Nelson Street, Annandale NSW 2038, Australia www.promega.com/au/
Qiagen	QIAGEN Pty Ltd PO Box 641, Doncaster VIC 3108, Australia www.qiagen.com
Roche	Roche Diagnostics Australia Pty Ltd PO Box 955, 31 Victoria Avenue, Castle Hill, NSW 2154, Australia www.roche-applied-science.com

Sartorius	Sartorius Australia Pty Ltd Unit 17/104 Ferntree Gully Road, Waverley Business Park, East Oakleigh, Victoria 3166 www.sartorius.com
Sigma Sigma-Genosys	Sigma-Aldrich Pty Ltd Sydney, Australia www.sigmaaldrich.com
Sanyo	SANYO Oceania Pty Ltd PO Box 947, NORTH RYDE BC, NSW 1670 www.sanyo.com.au
Sony	Sony Australia Ltd 14 Lum St, Export Park SA 5950 www.sony.com.au
Sutter	Sutter Instrument Co 51 Digital Drive, Novato, CA 94949, USA www.sutter.com
Stratagene	Stratagene *Distributor: Integrated Sciences* PO Box 196, East Kew VIC 3102, Australia www.stratagene.com
Thermo	Thermo Electron Corporation 11 West Thebarton Road, Thebarton, SA5030, Australia www.thermo.com
Ulead	Ulead Systems Inc 2F, 358 Neihu Rd., Section 1, Taipei 114, Taiwan, ROC www.ulead.com
UltraLum	Ultra Lum Inc *Distributor: Scitech Pty Ltd* Unit 4, 72-74 Chifley Drive, Preston, VIC 3072, Australia www.ultralum.com
Zymed	Zymed Laboratories Inc *Distributor: Invitrogen Australia Pty Ltd* www.zymed.com

APPENDIX C: Sequencing results of the recombinant DNAs in BEpMIG

a. BEpMIG

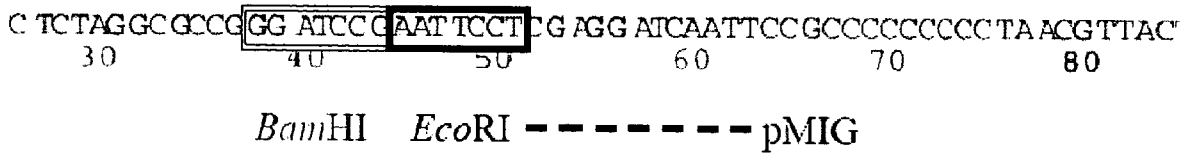



b. $C_{863\text{-}886}$/BEpMIG

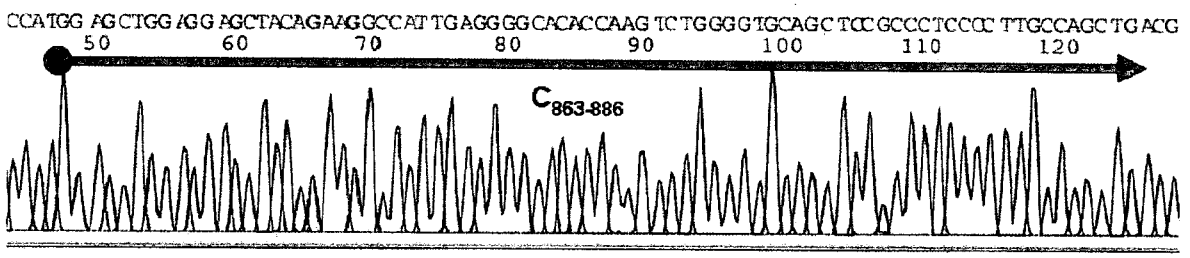

c. $C_{863\text{-}887}$/BEpMIG

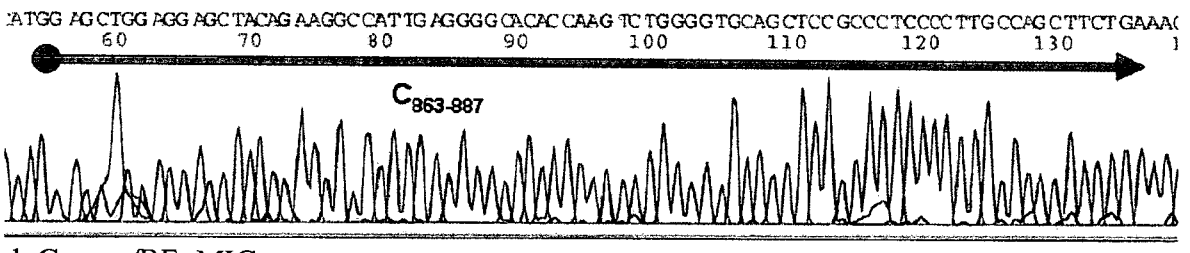

d. $C_{864\text{-}888}$/BEpMIG

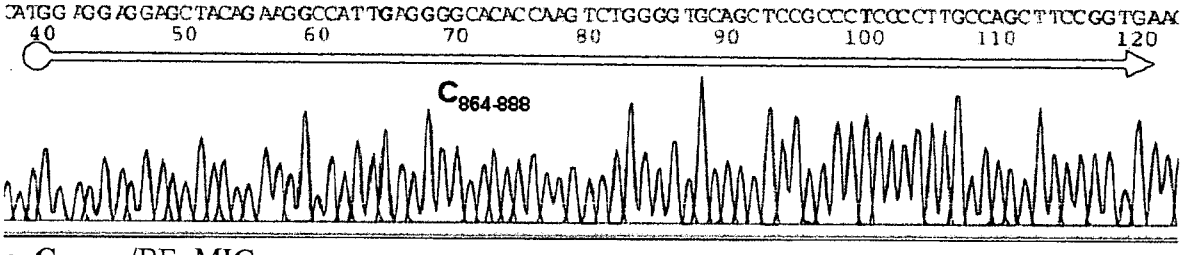

e. $C_{865\text{-}888}$/BEpMIG

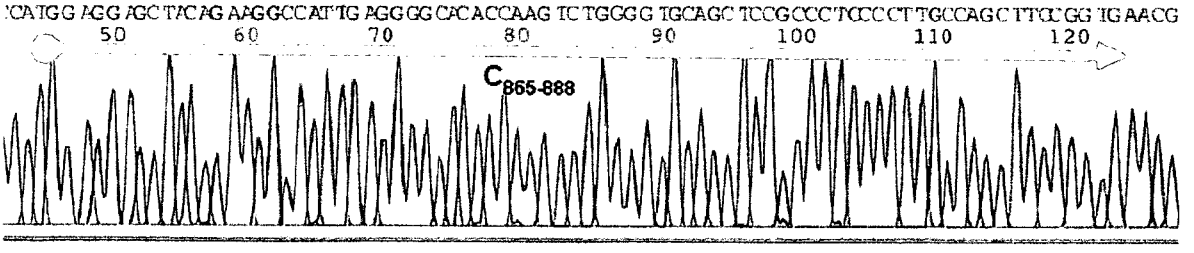

f. $C_{866\text{-}888}$/BEpMIG

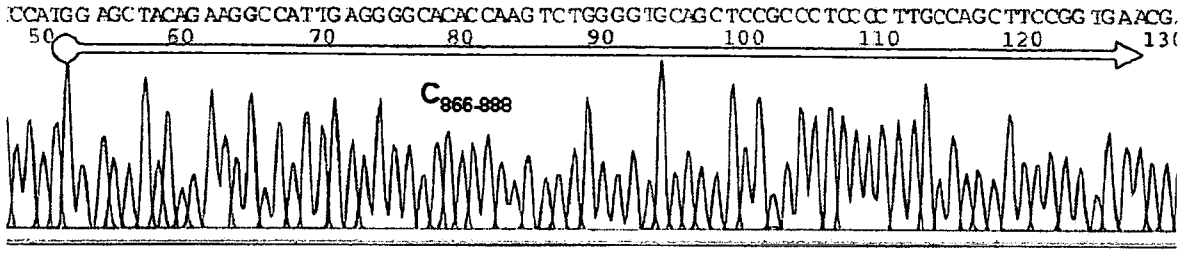

g. $C_{721\text{-}988}$/BEpMIG

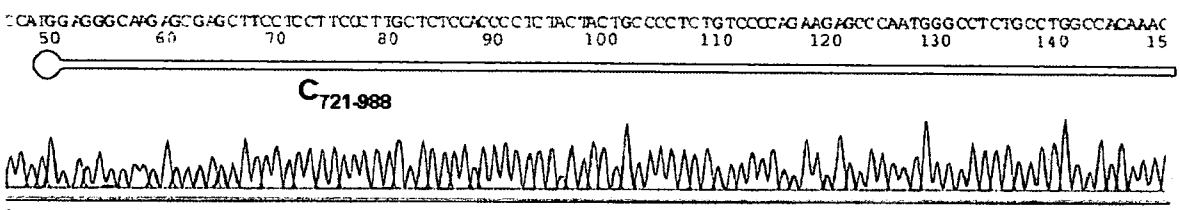

h. $C_{863\text{-}988}$/BEpMIG

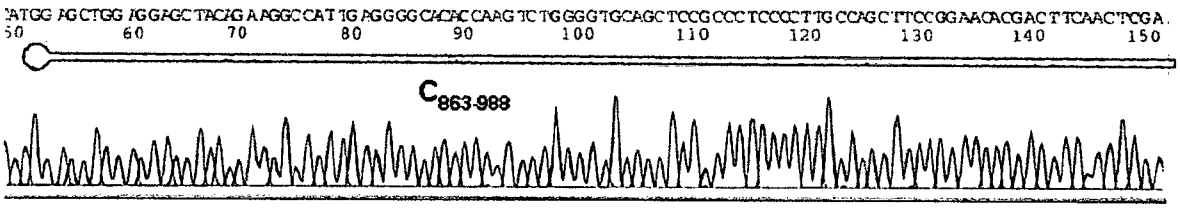

i. $C_{575\text{-}988}$/BEpMIG

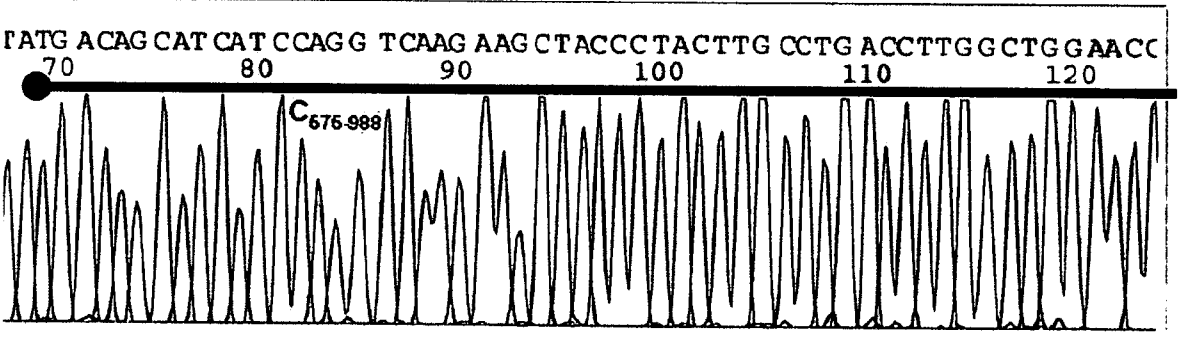

Annotation

The sequences (a) with pink and blue squares are introduced *Bam*HI and *Eco*RI sites in the multi-cloning site of pMIG vector, respectively. The mutated vector is called BEpMIG.

The probe head arrows (b-f) indicate sequence region that codes for the peptides, $C_{863\text{-}886}$, $C_{863\text{-}887}$, $C_{864\text{-}888}$, $C_{865\text{-}888}$, and $C_{866\text{-}888}$ cloned in BEpMIG vector.

The probe lines (g-i) indicate the N-terminal sequence of the truncated ClC-1 mutants, $C_{721\text{-}988}$, $C_{863\text{-}988}$ and $C_{575\text{-}988}$. The circular head is to the start codon region.

APPENDIX D: Methodology of constructing shortened $C_{863-888}$ peptide in pTLN

D-1. DNA templates for construction of shortened $C_{863-888}$ shortened peptides in site-directed mutagenesis

Two DNA plasmids synthesized by Dr. Wu in our laboratory were used as DNA templates in the Site-directed mutagenesis method for generation of the amino acid deletion peptides. They are illustrated as N_{1-888}/pTLN and $C_{863-988}$/pTLN in **Figure D.1**.

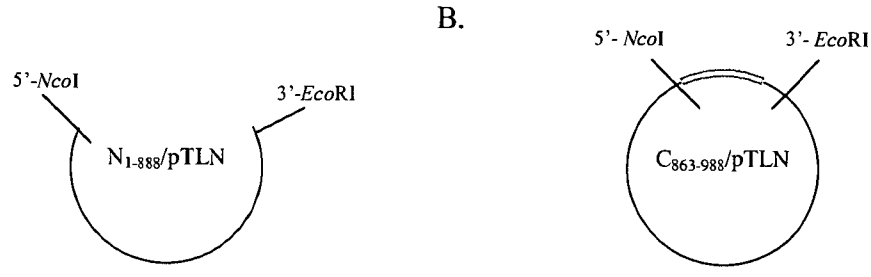

Figure D.1 Cartoon pictures of N_{1-888}/pTLN (A) and $C_{863-988}$/pTLN (B) plasmid maps

The N-terminal fragment, N_{1-888} in light green, and C-tail fragment, $C_{863-988}$ in pink, of ClC-1 were cloned in frame with *Nco*I and *Eco*RI restriction sites into the pTLN vector. These were used as DNA templates in the subsequent site-directed mutagenesis.

D-2. Primers used for generating deletion mutants of $C_{863-888}$ peptides in pTLN

In order to create consecutive amino acid deletions of the $C_{863-888}$ peptides at either the 5' or 3' end, five pairs of primers were designed. The 5' end amino acid deletion primers were labeled hE864 (Fw: 5'-G GGG AAG CTC AGG GGC GTC CCC ATG GAG **GAG** GAG CTA CAG AAG G- 3', Rv: 3'-C CTT CTG TAG CTC CTC CTC CAT GGG GAC GCC CCT GAG CTT CCC C-5'), hE865 (Fw: 5'G CTC AGG GGC GTC CCC ATG GAG **GAG** CTA CAG AAG GCC ATT GAG GGG-3', Rv: 3'CCC CTC AAT GGC CTT CTG TAG CTC CTC CAT GGG GAC GCC CCT GAG C-5') and hL866 (Fw: 5'-G CTC AGG GGC GTC CCC ATG GAG **CTA** CAG AAG GCC ATT GAG GGG-3', Rv: 3'-CCC CTC AAT GGC CTT CTG TAG CTC CAT GGG GAG GCC CCT GAG C-5') for creating one, two and three amino acid deletions at the 5'end of $C_{863-888}$, respectively by using N_{1-888}/pTLN as the DNA template in site-directed mutagenesis. The mutation sequence was set in the middle of the primers. A sequence CCATGGAG was introduced immediately before the amino acid residue (bolded) defined by each primer label, in this case E864, E865 and L866. It consequently incorporated an *Nco*I site, (CCATGG), and the first two

amino acids in hClC-1 DNA, Methionine (ATG) and Glycine (GAG). The other two pairs of primers creating 3' end amino acid deletions labeled hF887X (Fw: 5'-CT CCC CTT GCC AGC **TTC** TGA AAC ACG ACT TCA AC-3', Rv: 3'-GT TGA AGT CGT GTT TCA GAA GCT GGC AAG GGG AG-5') and hS886X (Fw: 5'-CGC CCT CCC CTT GCC **AGC** TGA CGG AAC ACG AC-3', Rv: 3'-GT CGT GTT CCG TCA GCT GGC AAG GGG AGG GCG-5'), introduced a stop codon (TGA) after the respective amino acid residue (bolded) number in the primer label. During the site-directed mutagenesis, $C_{863-988}$/pTLN was used as DNA template.

D-3. Sub-cloning of the of 5' end deletion fragment into pTLN

The site-directed mutagenesis products generated by 5' end deletion primers hE864, hE865 and hL866, were digested by *Nco*I restriction enzyme. Two fragments were generated and separated by agarose gel electrophoresis. In each case the small fragment containing the sequence upstream of the newly introduced *Nco*I site was discarded and the large fragment containing the modified peptide and the pTLN vector sequences were extracted from agarose gel (Section 2.5.3). Purified linear DNA was ligated back as a circular DNA (Section 2.7.2). Schematic diagrams for the sub-cloning steps are shown in **Figure D.2**.

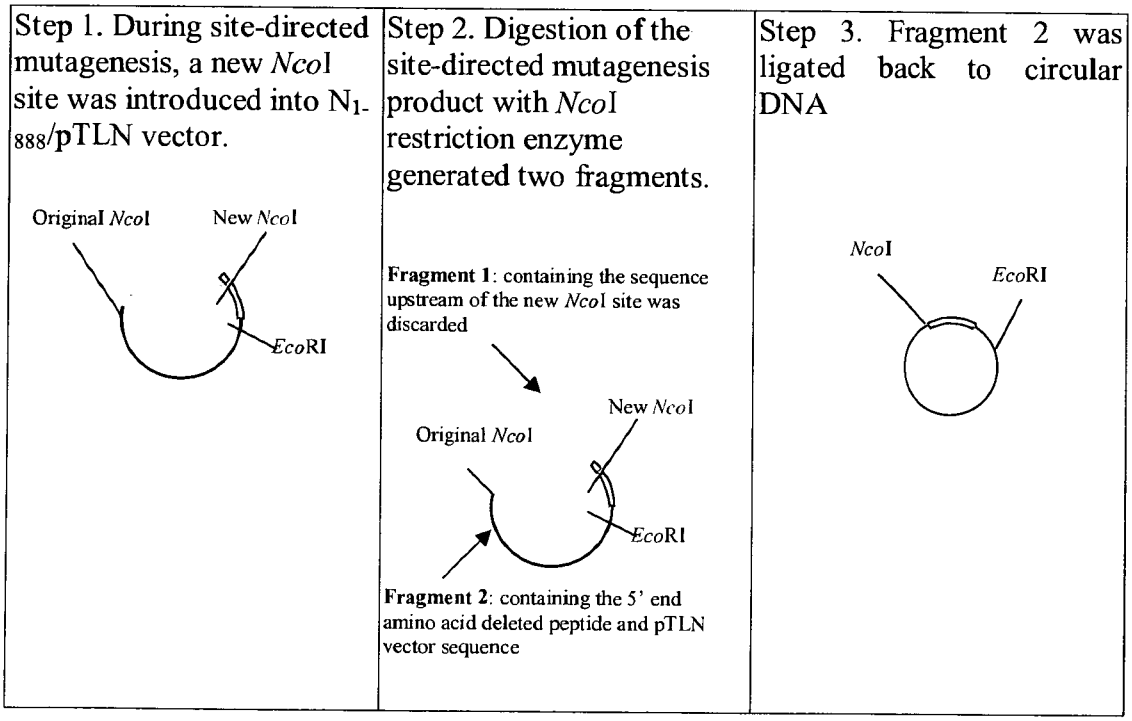

Figure D.2 Schematic diagrams showing steps involved in sub-cloning the mutated 5'end deletion fragment into the pTLN vector

D-4. Verifying the site-directed mutagenesis products by DNA sequencing

Both the 3' and sub-cloned 5' deletion mutants were subjected to DNA sequencing reactions to verify the mutated sequence. Sequencing primer, Sp6-F (5'ATT TAG GTG ACA CTA TAG AA), framed upstream of the start codon of the construct was used in the reaction. Sequencing results are shown in following chromatograms.

a. $C_{863\text{-}886}$/pTLN

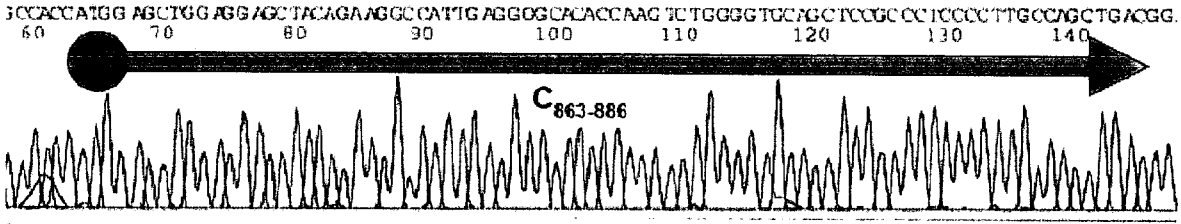

b. $C_{863\text{-}887}$/pTLN

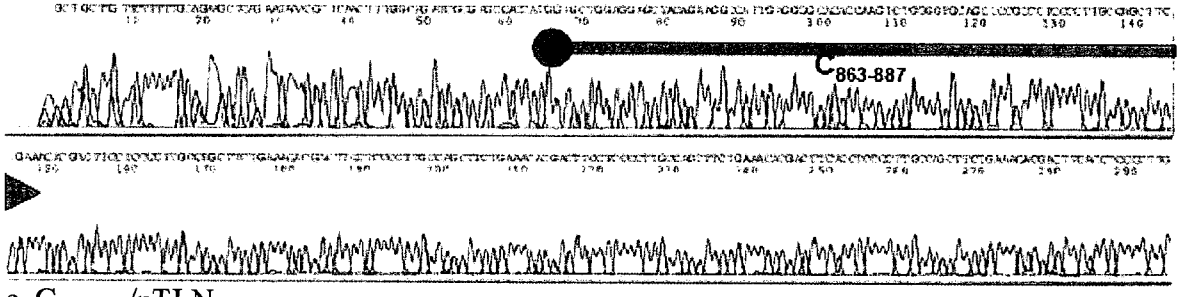

c. $C_{864\text{-}888}$/pTLN

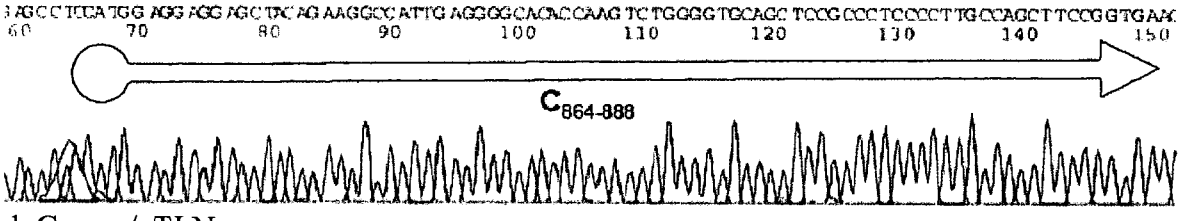

d. $C_{865\text{-}888}$/pTLN

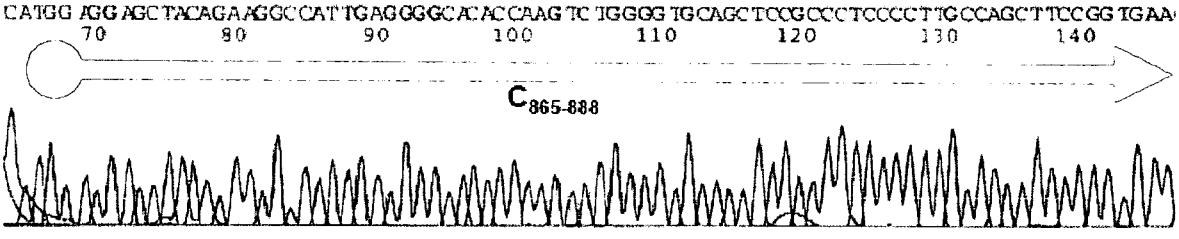

e. $C_{866\text{-}888}$/pTLN

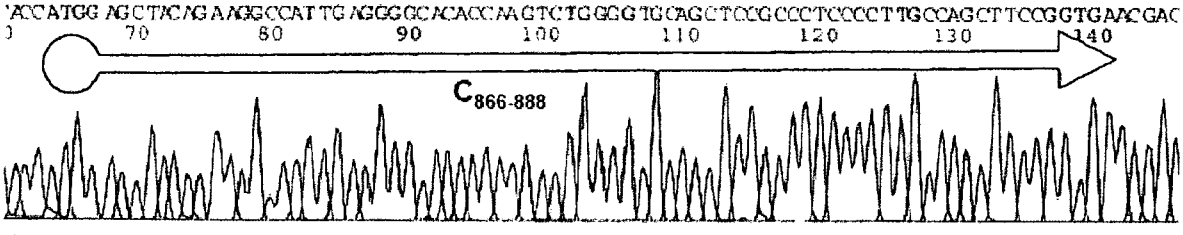

Annotation

The probe head arrows (a-e) indicate sequence region that codes for the peptides, $C_{863\text{-}886}$, $C_{863\text{-}887}$, $C_{864\text{-}888}$, $C_{865\text{-}888}$ and $C_{866\text{-}888}$, cloned in pTLN vector. The circular head and arrow head indicate the start codon (ATG) and the stop codon (TGA) position, respectively.

APPENDIX E: Sequencing results of missense mutants of hClC-1

V851M

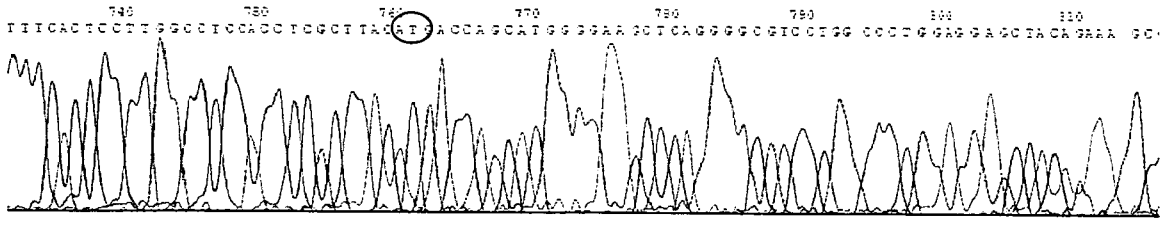

E724A

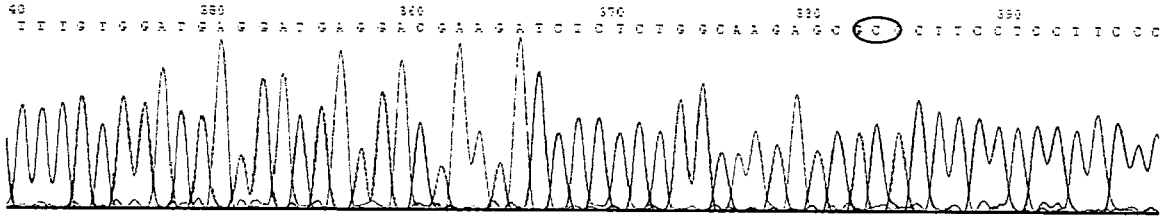

R691S

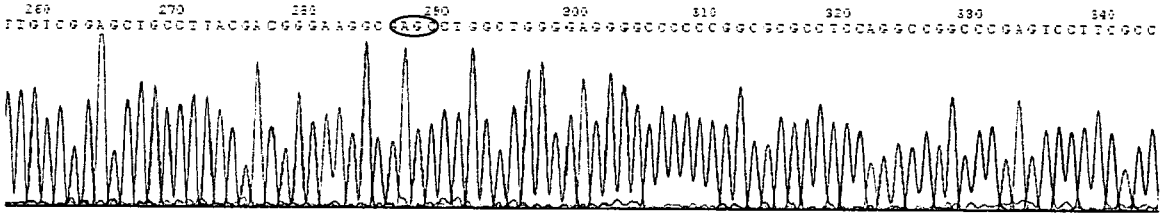

G551D

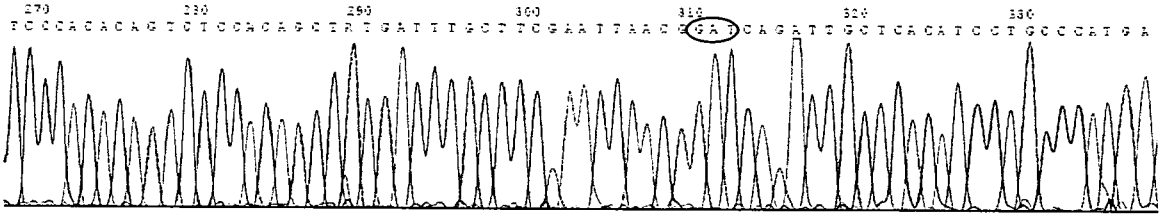

Annotation

The circled triple nucleotides in the above sequencing chromatogram are the corresponding amino acid mutation region. The following table shows the original sequence of hClC-1 on that region at the left hand side of the arrow and mutated sequence at the right hand side of the arrow. Underlined nucleotides have been mutated.

V851M	GTG→<u>A</u>TG	E724A	GAG→G<u>C</u>G
R691S	CGG→<u>A</u>G<u>C</u>	G551D	GGT→G<u>A</u>T

T550R

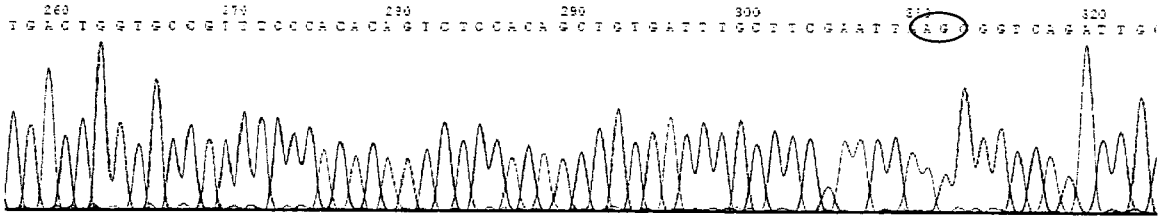

P480S

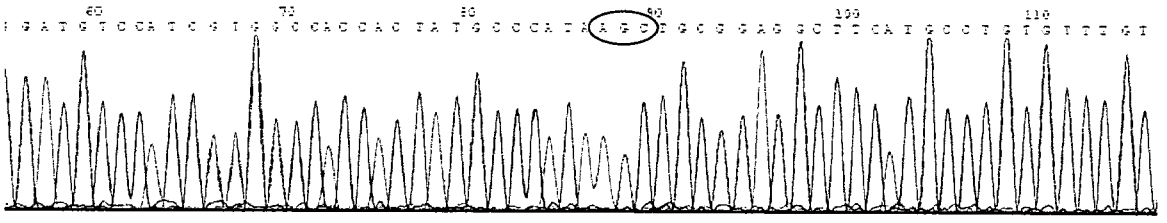

W433R

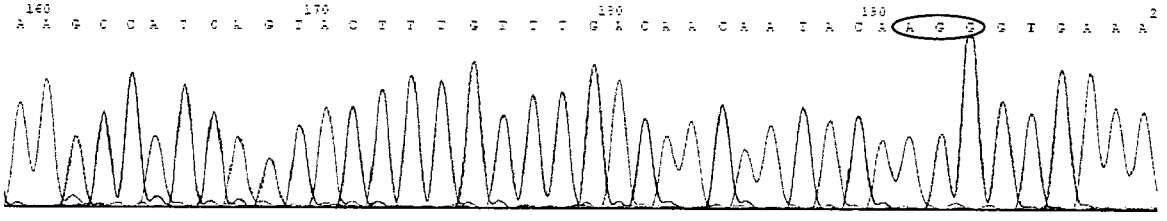

M373L

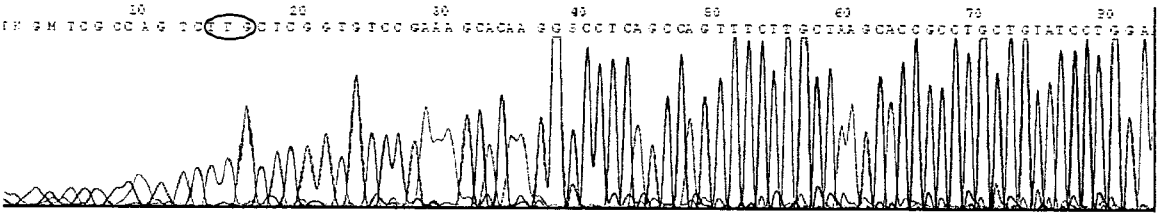

A298T

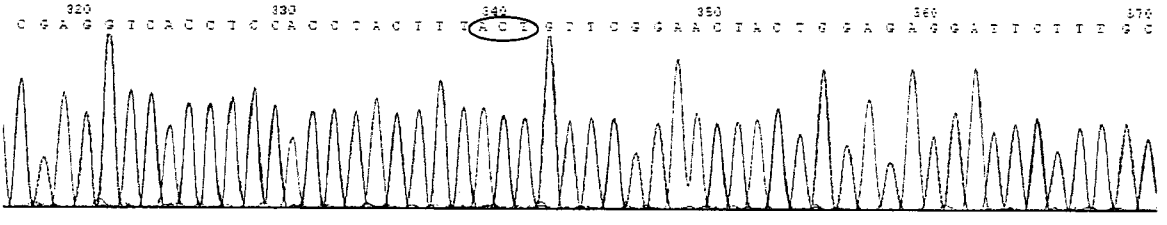

Annotation

The circled triple nucleotides in the above sequencing chromatogram are the corresponding amino acid mutation region. The following table shows the original sequence of hClC-1 on that region at the left hand side of the arrow and mutated sequence at the right hand side of the arrow. Underlined nucleotides have been mutated.

T550R	ACG→A<u>G</u>G	P480S	CCC→A<u>G</u>C	W433R	TGG→<u>A</u>GG
M373L	ATG→<u>T</u>TG	A298T	GCT→<u>A</u>CT		

F297S

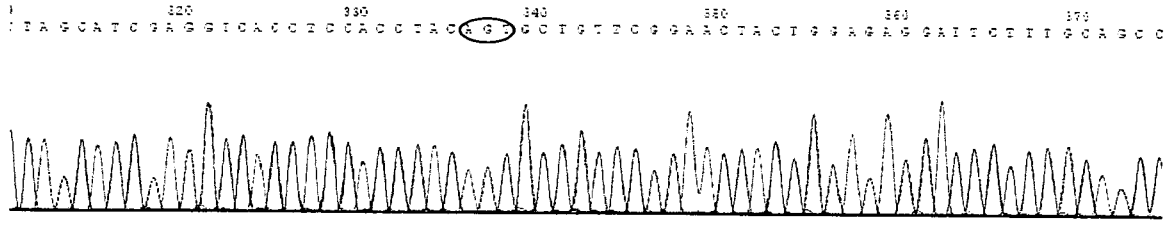

K215R

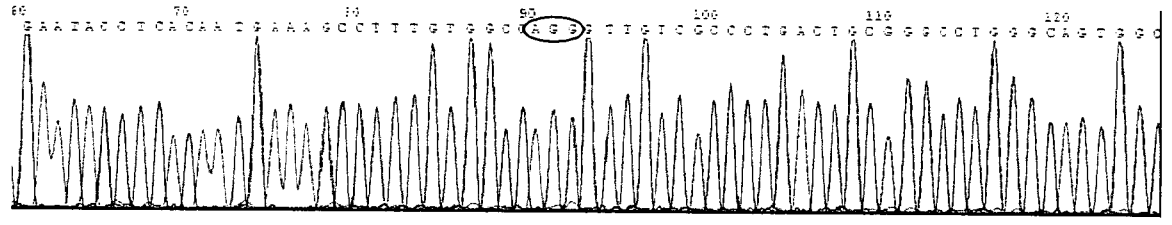

S189C

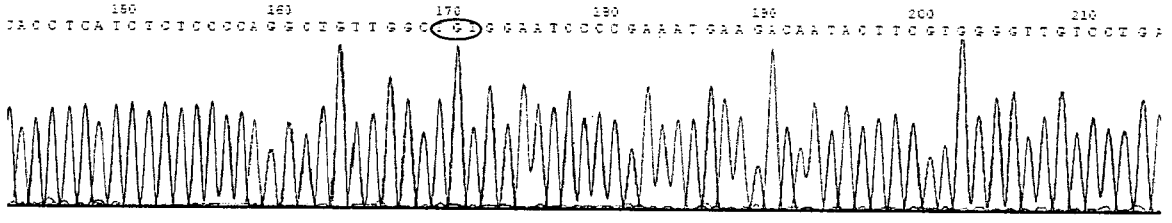

R47W

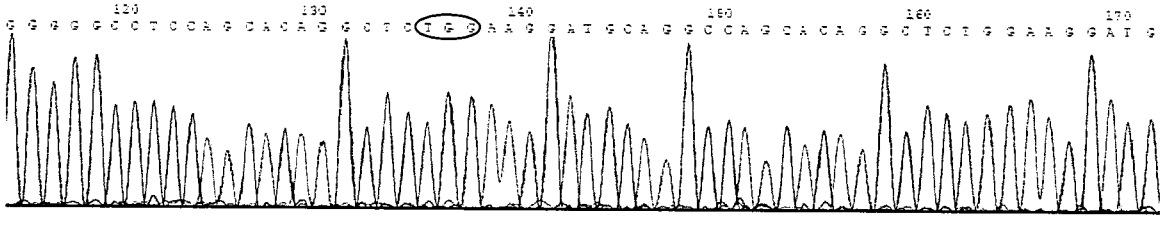

Annotation

The circled triple nucleotides in the above sequencing chromatogram are the corresponding amino acid mutation region. The following table shows the original sequence of hClC-1 on that region at the left hand side of the arrow and mutated sequence at the right hand side of the arrow. Underlined nucleotides have been mutated.

F297S	TTT→AGT	K215R	AAG→AGG
S189C	TGT→TCT	R47W	CGG→TGG

APPENDIX F: Sequencing results of the C-tail cDNAs in Thx/pET32a

a. Thx-$C_{721\text{-}988}$/pET32a

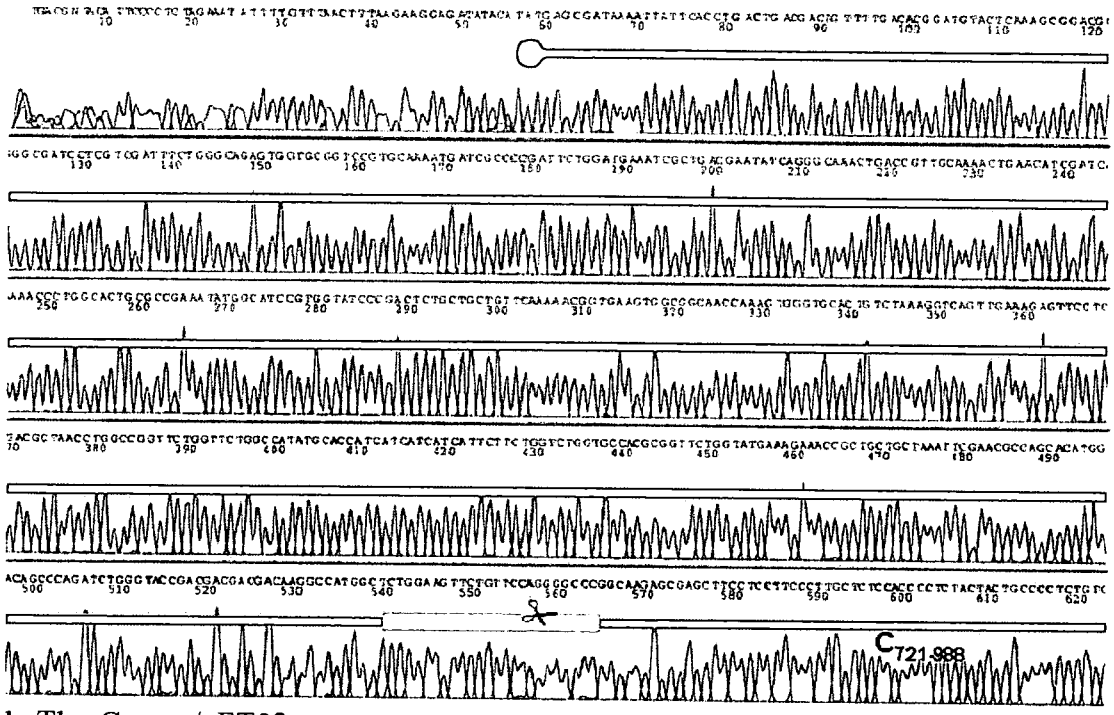

b. Thx-$C_{575\text{-}988}$/pET32a

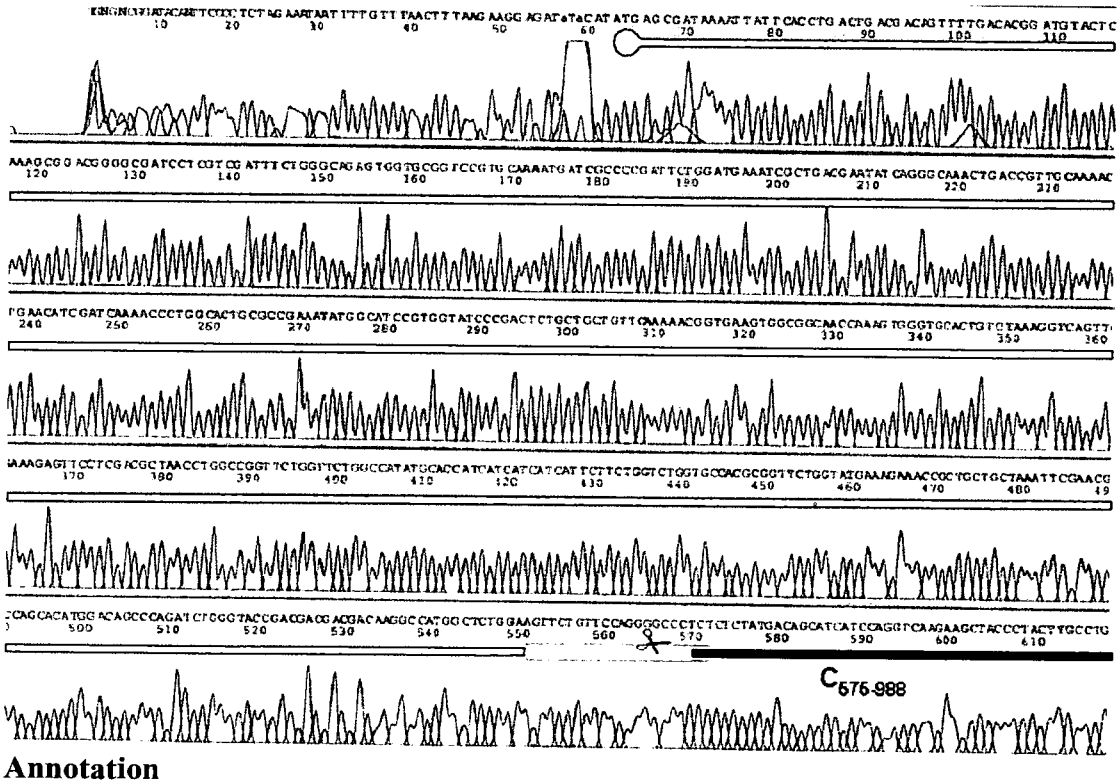

Annotation

Thx-tag sequences are underlined by pink lines and the start codons are indicated by a circular head. PreScission protease cleavage sequences are underlined by a yellow line. Scissor symbol indicates the cleavage point. Beginning of the C_{721}-tail sequences and C_{575}-tail sequence are underlined by green (a) and blue (b) lines, respectively.

APPENDIX G: Publications

Results of Chapters 4 and 7 have been presented in conferences and the abstracts were published and listed in Acta Myologica and in the Proceedings of the Australian Society for Biochemistry and Molecular Biology.

Bretag A. H., **Fung P. L. Y.** Human ClC-1 channel function restored by co-expression of a C-tail fragment with otherwise non-functional, myotonia-causing, truncation mutants. Acta Myologica 25,137 (2006), Abstracts of the Eighth Mediterranean Society of Myology Congress, Djerba, Tunisia (2007).

Fung P. and Bretag A. ATP induces a conformational change in the C-terminus domain of the voltage gated skeletal muscle chloride channel (ClC-1). *The Proceedings of the Australian Society for Biochemistry and Molecular Biology*, 38, 117, 2006

Fung P., Bartley P., Rychkov G., Bagley C., Cederholm J., Kwok F., Hughes B. and Bretag A. The function of truncated skeletal muscle chloride channels mutants restored by co-expression with carboxyl-tail fragments containing the second CBS domain. *The Proceedings of the Australian Society for Biochemistry and Molecular Biology*, 37, 109, 2005

Fung P. Wu W. and Bretag A. Expression of the Cytoplasmic C-Tail of the CLC-1 chloride Channel. *The Proceedings of Australian Society for Biochemistry and Molecular Biology*, 36, 144, 2004